Oxidative Medicine and Cellular Longevity

Harnessing Oxidative Stress as an Innovative Target for Cancer Therapy

Lead Guest Editor: Spencer Gibson
Guest Editors: Lynne Postovit, Peng Huang, and Christian Widmann

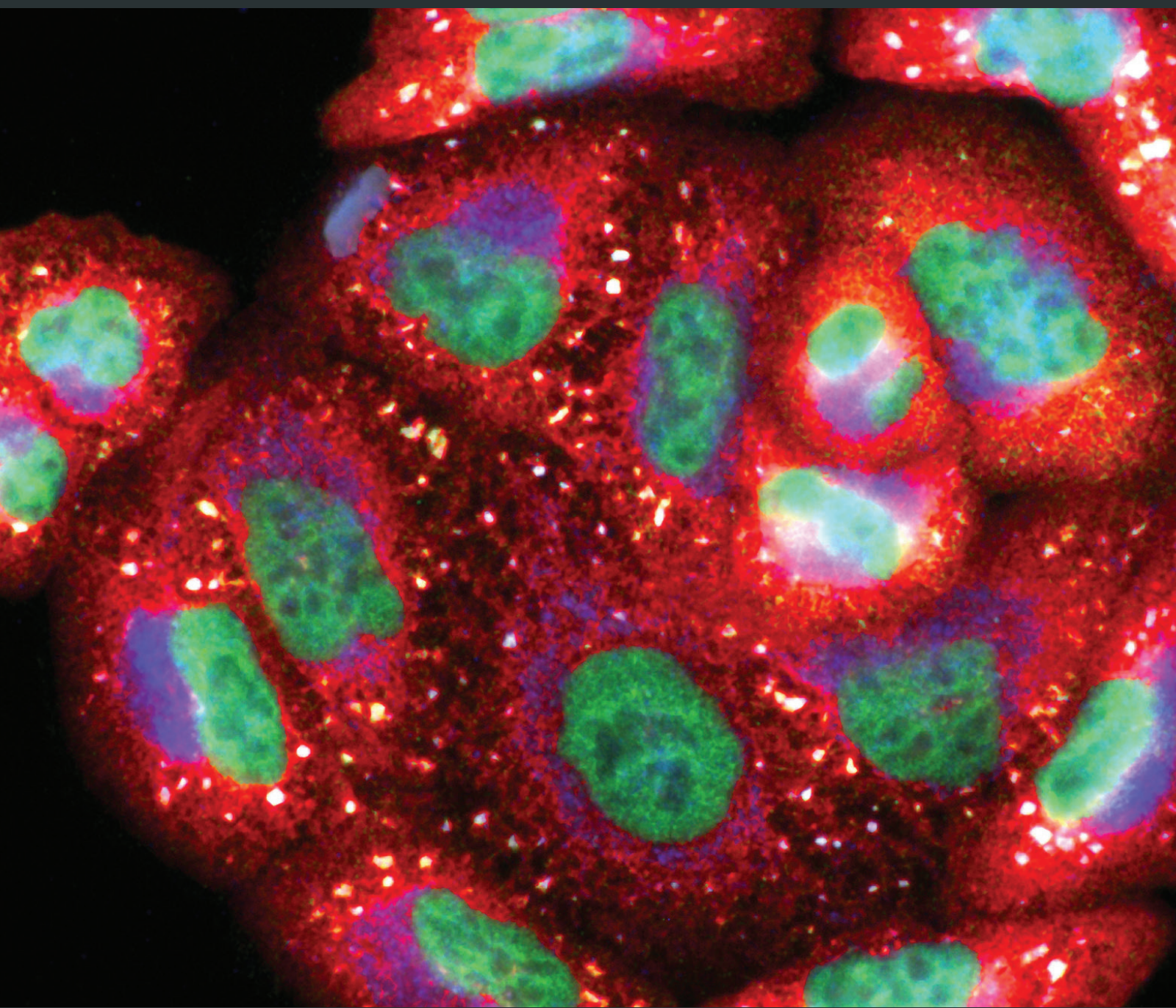

Harnessing Oxidative Stress as an Innovative Target for Cancer Therapy

Oxidative Medicine and Cellular Longevity

Harnessing Oxidative Stress as an Innovative Target for Cancer Therapy

Lead Guest Editor: Spencer Gibson
Guest Editors: Lynne Postovit, Peng Huang, and Christian Widmann

Editorial Board

Contents

Harnessing Oxidative Stress as an Innovative Target for Cancer Therapy
Lynne Postovit, Christian Widmann, Peng Huang, and Spencer B. Gibson
Editorial (2 pages), Article ID 6135739, Volume 2018 (2018)

Targeting Mitochondrial Bioenergetics as a Therapeutic Strategy for Chronic Lymphocytic Leukemia
Subir Roy Chowdhury and Versha Banerji
Review Article (10 pages), Article ID 2426712, Volume 2018 (2018)

UVA Irradiation Enhances Brusatol-Mediated Inhibition of Melanoma Growth by Downregulation of the Nrf2-Mediated Antioxidant Response
Mei Wang, Guangwei Shi, Chunxiang Bian, Muhammad Farrukh Nisar, Yingying Guo, Yan Wu, Wei Li, Xiao Huang, Xuemei Jiang, Jörg W. Bartsch, Ping Ji, and Julia Li Zhong
Research Article (15 pages), Article ID 9742154, Volume 2018 (2018)

Evaluation of Potential Mechanisms Controlling the Catalase Expression in Breast Cancer Cells
Christophe Glorieux, Juan Marcelo Sandoval, Nicolas Dejeans, Sandrine Nonckreman, Khadija Bahloula, Hélène A. Poirel, and Pedro Buc Calderon
Research Article (10 pages), Article ID 5351967, Volume 2018 (2018)

Xylopine Induces Oxidative Stress and Causes G_2/M Phase Arrest, Triggering Caspase-Mediated Apoptosis by p53-Independent Pathway in HCT116 Cells
Luciano de Souza Santos, Valdenizia Rodrigues Silva, Leociley Rocha Alencar Menezes, Milena Botelho Pereira Soares, Emmanoel Vilaça Costa, and Daniel Pereira Bezerra
Research Article (13 pages), Article ID 7126872, Volume 2017 (2018)

The eIF4E2-Directed Hypoxic Cap-Dependent Translation Machinery Reveals Novel Therapeutic Potential for Cancer Treatment
Gaelan Melanson, Sara Timpano, and James Uniacke
Review Article (12 pages), Article ID 6098107, Volume 2017 (2018)

The Role of Redox-Regulating Enzymes in Inoperable Breast Cancers Treated with Neoadjuvant Chemotherapy
Nelli Roininen, Kirsi-Maria Haapasaari, and Peeter Karihtala
Clinical Study (9 pages), Article ID 2908039, Volume 2017 (2018)

Cytotoxicity, Oxidative Stress, Cell Cycle Arrest, and Mitochondrial Apoptosis after Combined Treatment of Hepatocarcinoma Cells with Maleic Anhydride Derivatives and Quercetin
Gabriela Carrasco-Torres, Rafael Baltiérrez-Hoyos, Erik Andrade-Jorge, Saúl Villa-Treviño, José Guadalupe Trujillo-Ferrara, and Verónica Rocío Vásquez-Garzón
Research Article (16 pages), Article ID 2734976, Volume 2017 (2018)

Lysosomes as Oxidative Targets for Cancer Therapy
Rebecca F. Dielschneider, Elizabeth S. Henson, and Spencer B. Gibson
Review Article (8 pages), Article ID 3749157, Volume 2017 (2018)

Reactive Oxygen Species-Mediated Mechanisms of Action of Targeted Cancer Therapy
Hanna-Riikka Teppo, Ylermi Soini, and Peeter Karihtala
Review Article (11 pages), Article ID 1485283, Volume 2017 (2018)

Cellular Preoxygenation Partially Attenuates the Antitumoral Effect of Cisplatin despite Highly Protective Effects on Renal Epithelial Cells
Bahram Rasoulian, Ayat Kaeidi, Maryam Rezaei, and Zahra Hajializadeh
Research Article (11 pages), Article ID 7203758, Volume 2017 (2018)

Triethylenetetramine Synergizes with Pharmacologic Ascorbic Acid in Hydrogen Peroxide Mediated Selective Toxicity to Breast Cancer Cell
Lianlian Wang, Xiaofang Luo, Cong Li, Yubing Huang, Ping Xu, Laetitia H. Lloyd-Davies, Thibaut Delplancke, Chuan Peng, Rufei Gao, Hongbo Qi, Chao Tong, and Philip Baker
Research Article (13 pages), Article ID 3481710, Volume 2017 (2018)

Hindawi
Oxidative Medicine and Cellular Longevity
Volume 2018, Article ID 6135739, 2 pages
https://doi.org/10.1155/2018/6135739

Editorial

Harnessing Oxidative Stress as an Innovative Target for Cancer Therapy

Lynne Postovit,[1] Christian Widmann,[2] Peng Huang,[3] and Spencer B. Gibson [4,5]

[1]*Department of Oncology, University of Alberta, Edmonton, AB, Canada*
[2]*Department of Physiology, University of Lausanne, Lausanne, Switzerland*
[3]*Department of Translational Molecular Pathology, University of Texas MD Anderson Cancer Center, Houston, TX, USA*
[4]*Department of Biochemistry and Medical Genetics, University of Manitoba, Winnipeg, MB, Canada*
[5]*Research Institute in Oncology and Hematology, CancerCare Manitoba, Winnipeg, MB, Canada*

Correspondence should be addressed to Spencer B. Gibson; spencer.gibson@umanitoba.ca

Received 18 December 2017; Accepted 20 December 2017; Published 24 May 2018

One of the hallmarks of cancer is the deregulation of cellular energetics [1]. This allows cancer cells to proliferate and survive in microenvironments that would lead to the death of a normal cell. As a consequence of deregulated cellular energetics, cells produce higher levels of reactive oxygen species (ROS) concomitant with alterations in antioxidant pathways [2]. ROS contributes to cell survival, proliferation, and metastasis in a variety of cancers but left uncontrolled leads to cell death [3]. Cancer cells have adapted to this oxidative stress through various mechanisms allowing them to survive in hypoxia and to become drug resistant [4]. This has given rise to different treatment strategies aiming to enhance ROS production in cancer cells leading to the selective killing of these cells when compared to normal cells.

This special issue on harnessing oxidative stress as an innovative target for cancer therapy focuses both on understanding how cancer cells alter their antioxidant signaling pathways causing drug resistance as well as utilizing alterations in ROS regulation to target cancer cells with novel treatment strategies.

The manuscripts submitted to this special issue were reviewed by at least 2 external reviewers and one guest editor. All the papers were selected on the basis of scientific significance, relevance to topic of oxidative stress and novelty. Mentioned below are the highlights of the manuscripts published in this special issue.

Adaptation to oxidative stress leads to drug resistance [2]. C. Glorieux et al. have shown that chromatin remodeling of the catalase gene leads to increased catalase activation in breast cancer cell lines. The increased expression appeared to be independent of the activation of DNA damage signaling, blockage of protein degradation, or increased mRNA stability. Other redox regulation proteins are also increased in breast cancer. N. Roininen et al. have shown that redox-regulating proteins Nrf2, Keap1, Trx, and Prx1 were increased in breast cancer patients undergoing neoadjuvant chemotherapy. Before chemotherapy, the lower expression levels of these redox regulatory proteins in breast tumors correlated with reduced disease-free survival of patients. This suggests that redox-regulating enzymes might be able to prognosticate cancers and that they may also be excellent targets for treatment.

In addition to drug resistance, cytotoxicity of chemotherapy on normal tissue in patients is a major limitation in treatments [5]. It has been suggested that oxygen pretreatment of tissue could reduce cisplatin cytotoxicity in renal tubular cells of the kidney [6]. However, B. Rasoulian et al. have demonstrated that oxygen pretreatment also reduces the cytotoxicity of cisplatin in malignant cells suggesting that oxygen pretreatment might not be a successful strategy to reduce toxicity in patients treated with cisplatin.

Hypoxia is a poor prognostic factor in cancer, and adaptations to low oxygen levels help drive tumor progression, causing cancer cells to become more aggressive and resistant to chemotherapy [7]. A major mechanism for this adaptation involves the stabilization and activation of the transcription

factor, HIF-1. However, recent studies suggest that the regulation of mRNA translation may also play an important role in this process [8]. Indeed, some alterations in translation may occur via an elF4E2-depedendent pathway, leading to increased migration, invasion, and tumor growth. G. Melanson et al. have reviewed the potential for elF4E2 inhibitors to be an effective therapy for hypoxic tumors.

Adaptations to oxidative stress are being explored as novel treatment targets in cancer [2]. Two review articles by S. R. Chowdhury and V. Banerji and R. F. Dielschneider et al. have illustrated that targeting mitochondrial bioenergetics and alterations in lysosomes is an effective strategy to selectively kill cancer cells. Both of these targets in cancer cells utilize elevated ROS levels to induce cell death.

Novel drugs are also being investigated to induce oxidative stress in cancer cells leading to cell death. L. Wang et al. showed that the combination of triethylenetetramine and ascorbic acid leads to synergistic cell death mediated by elevated levels of hydrogen peroxide. Similarly, L. D. Santos et al. showed that xylopine (an aporphine alkaloid agent) induced apoptosis dependent upon increased ROS levels in cancer cells. Using an inhibitor of the redox-regulating protein Nrf2, M. Wang et al. showed that this inhibitor effectively induces apoptosis in combination with UVA irradiation and reduced tumor growth in mouse models. These innovative drugs could provide novel treatment strategies to target ROS adaptations in cancer cells leading to cell death while sparing normal cells.

Novel drugs given as monotherapies are unlikely to be effective due to cellular adaptations leading to drug resistance. Rational drug combination needs to be developed to combat drug resistance in cancer. G. Carrasco-Torres et al. showed that a combination of maleic anhydride derivatives (prooxidant) and quercetin (antioxidant) could induce cell death in cancer cells but not normal human epithelial cells. This suggests that using drugs that first give an oxidative response followed by an antioxidant drug might be a potential new treatment strategy.

Taken together, this special issue gives insight into the potential of targeting the oxidative stress response in cancer cells that could overcome drug resistance and spare normal tissue. This will provide patients with more therapeutic strategies to combat cancer utilizing the cancers' alterations in the redox defense systems. This will hopefully lead to longer disease-free survival of the cancer patient.

Lynne Postovit
Christian Widmann
Peng Huang
Spencer B. Gibson

References

[1] D. Hanahan and R. A. Weinberg, "Hallmarks of cancer: the next generation," *Cell*, vol. 144, no. 5, pp. 646–674, 2011.

[2] M. B. Azad, Y. Chen, and S. B. Gibson, "Regulation of autophagy by reactive oxygen species (ROS): implications for cancer progression and treatment," *Antioxidants & Redox Signaling*, vol. 11, no. 4, pp. 777–790, 2009.

[3] J. N. Moloney and T. G. Cotter, "ROS signalling in the biology of cancer," *Seminars in Cell & Developmental Biology*, no. 16, pp. 30383-30384, 2017.

[4] H. Xie and M. C. Simon, "Oxygen availability and metabolic reprogramming in cancer," *Journal of Biological Chemistry*, vol. 292, no. 41, pp. 16825–16832, 2017.

[5] M. K. L. Fung and G. C.-F. Chan, "Drug-induced amino acid deprivation as strategy for cancer therapy," *Journal of Hematology & Oncology*, vol. 10, no. 1, p. 144, 2017.

[6] A. Kaeidi, B. Rasoulian, Z. Hajializadeh, S. Pourkhodadad, and M. Rezaei, "Cisplatin toxicity reduced in human cultured renal tubular cells by oxygen pretreatment," *Renal Failure*, vol. 35, no. 10, pp. 1382–1386, 2013.

[7] A. Monteiro, R. Hill, G. Pilkington, and P. Madureira, "The role of hypoxia in glioblastoma invasion," *Cell*, vol. 6, no. 4, 2017.

[8] L. K. Brady, H. Wang, C. M. Radens et al., "Transcriptome analysis of hypoxic cancer cells uncovers intron retention in EIF2B5 as a mechanism to inhibit translation," *PLoS Biology*, vol. 15, no. 9, article e2002623, 2017.

Hindawi
Oxidative Medicine and Cellular Longevity
Volume 2018, Article ID 2426712, 10 pages
https://doi.org/10.1155/2018/2426712

Review Article

Targeting Mitochondrial Bioenergetics as a Therapeutic Strategy for Chronic Lymphocytic Leukemia

Subir Roy Chowdhury[1] and Versha Banerji[1,2,3]

[1]*Research Institute in Oncology and Hematology, CancerCare Manitoba, Winnipeg, Canada*
[2]*Department of Biochemistry and Medical Genetics, Max Rady College of Medicine, Rady Faculty of Health Sciences, University of Manitoba, Winnipeg, MB, Canada*
[3]*Department of Internal Medicine, Max Rady College of Medicine, Rady Faculty of Health Sciences, University of Manitoba, Winnipeg, MB, Canada*

Correspondence should be addressed to Versha Banerji; vbanerji1@cancercare.mb.ca

Received 24 June 2017; Accepted 6 November 2017; Published 28 February 2018

Academic Editor: Peng Huang

Altered cellular metabolism is considered a hallmark of cancer and is fast becoming an avenue for therapeutic intervention. Mitochondria have recently been viewed as an important cellular compartment that fuels the metabolic demands of cancer cells. Mitochondria are the major source of ATP and metabolites necessary to fulfill the bioenergetics and biosynthetic demands of cancer cells. Furthermore, mitochondria are central to cell death and the main source for generation of reactive oxygen species (ROS). Overall, the growing evidence now suggests that mitochondrial bioenergetics, biogenesis, ROS production, and adaptation to intrinsic oxidative stress are elevated in chronic lymphocytic leukemia (CLL). Hence, recent studies have shown that mitochondrial metabolism could be targeted for cancer therapy. This review focuses the recent advancements in targeting mitochondrial metabolism for the treatment of CLL.

1. Introduction to CLL and Its Treatment

Chronic lymphocytic leukemia (CLL) is part of a spectrum of lymphoproliferative disorders that include monoclonal B-cell lymphocytosis (MBL) and small lymphocytic lymphoma (SLL) which are defined by the aberrant accumulation of mature CD19-/CD5-positive monoclonal B-lymphocytes in peripheral blood [1]. In CLL, monoclonal B-lymphocytes must achieve a threshold of $>5 \times 10^9$/L in the peripheral blood, whereas in SLL and MBL, they remain lower [1]. The lymph nodes, spleen, and bone marrow may be affected in CLL or SLL. In MBL, there is no evidence of enlarged lymph nodes or spleen and blood counts are normal [2]. The progression rate of MBL to CLL is approximately 1% per year requiring treatment [2]. For the purpose of this review, CLL and SLL will be considered as one entity.

CLL is the most common leukemia in the Western world affecting adult patients, and the true incidence is underestimated [3]. The clinical course of CLL is highly variable, ranging from a long-lasting stable disease requiring observation to a one that rapidly progresses requiring treatment [4]. The natural history of this indolent lymphoproliferative disorder is most patients relapse and require retreatment [5]. Treatments have exploited cell proliferation or DNA replication to target cells within the peripheral blood, lymph nodes, and bone marrow [6]. Common treatments include nucleoside analogues (fludarabine), alkylating agents (cyclophosphamide, chlorambucil, and bendamustine) in combination with monoclonal antibodies directed against CD 20 (rituximab or obinutuzimab) in the front line setting [4]. Within the relapse setting or in high-risk patients harboring a deletion of 17p chromosome, targeted agents such as tyrosine kinase inhibitors, ibrutinib, a BTK (Bruton's tyrosine kinase) inhibitor, and idelalisib, a PI3Kdelta (phosphoinositide-3-kinase) inhibitor, as well as small molecules, specifically venetoclax, a BCL-2 (B-cell lymphoma gene)

inhibitor, are currently available [4]. The sites of disease relapse are often within the lymph nodes and bone marrow microenvironments. This is in part due to acquired tumor suppressor loss specifically ATM (ataxia telangiectasia mutated gene) and/or TP53 or the development of clonal evolution [7, 8]. These CLL cells are resilient based on their ability to escape apoptosis and furthermore protected by the tumor microenvironment. This may be as a result of alterations in cellular metabolism which represent a hallmark of cancer [9]. Certain metabolic changes in cells are essential in order for them to be transformed to cancerous cells, and as a consequence, the metabolic framework is substantially altered [10]. Thus, nutrients, cytokines, and signaling molecules within the cancer cell and its microenvironment promote cell and promote drug resistance mainly by crosstalk from the stromal microenvironment or tissue niche that enhances leukemia cell viability [11]. Signaling through direct cell-cell contact, secretion of stromal factors and metabolic interactions of the tissue microenvironment also results in the protection of leukemia cells [12, 13].

Although altered cellular metabolism was recognized as a characteristic of cancer cells by Otto Warburg almost a century ago, it was popularized in the 1950s, only to recently have actual functional links been established between oncogenic pathways and cellular metabolism [14]. Mitochondria play an important role in cellular metabolism. Mitochondria are involved in cell death, cell differentiation, innate immunity, hypoxia, and the metabolism of amino acids, calcium, iron-sulphur clusters including heme biosynthesis [15]. In addition, altered mitochondrial bioenergetics, the redox balance of cells, and proapoptotic factors are controlled by mitochondria that may lead to cell death. Thus, crucial roles of mitochondria in the neoplastic phenotype notably are resistance to apoptosis, uncontrolled proliferation, and metabolic reprogramming [16, 17]. The increasing data eventually indicate that mitochondria may be the prime target for cancer therapy rather than simple bystanders for cancer maintenance.

2. Mitochondrial DNA

Mitochondria are important bioenergetics and biosynthetic factories critical for normal cell function and human health [18]. Unlike any other organelle, the mitochondrion has its own DNA which can be altered and result in disease conditions. The human mitochondrial genome is a double-stranded circular structure that is about 16.6 kb pairs in length. It contains 37 genes that code 2 rRNAs, 22 tRNAs, and 13 mitochondrial proteins of the respiratory chain [19, 20]. One of main features that differentiate mitochondrial genome from nuclear genome is the intrinsic susceptibility to damage. Mitochondrial DNA (mtDNA) is substantially more susceptible to mutations than nuclear DNA (nDNA) as it is less protected due to its complex chromatin organization, limited repair capacity, and also ROS generated by the electron transport chain being close to its proximity; however, this remains controversial [21]. Given that there are multiple copies of mtDNA in each cell, mutations can affect either all of them (this is termed as homoplasmy) or a proportion (termed as heteroplasmy). This becomes important when thinking of reasons for why CLL occurs and how this may contribute to the physiology of the disease. However, it is important to point out that mitochondrial proteins involved in oxidative phosphorylation (OXPHOS) and ATP production are vastly encoded by nuclear DNA.

3. Mitochondrial Physiology and ROS

The main physiological function of mitochondria is the production of ATP by OXPHOS and the essential metabolites to accomplish the bioenergetics and biosynthetic demands of normal and cancer cells [22]. Three major and important aspects of OXPHOS involved in mitochondrial pathogenesis are (i) energy production, (ii) ROS production, and (iii) apoptosis [21]. Carbon fuels are utilized by mitochondria to produce ATP. The sources of carbon pools are pyruvate generated from glycolysis, amino acids like glutamine, and fatty acids. The Krebs cycle in the mitochondrial matrix uses these carbon fuels to generate the reducing equivalents NADH and $FADH_2$, which subsequently pass their electrons to the electron transport chain (ETC). The transfer of electrons is coupled to the efflux of hydrogen ions from the matrix to the intermembrane space by mitochondrial complexes I, III, and IV (Figure 1). The two main components generated by the proton-motive force are the membrane potential that occurs from the net movement of positive charges across the inner mitochondrial membrane and the pH gradient. Most of the energy largely supplied by the membrane potential (cca 150–180 mV) is reserved in the gradient. Complex V uses this proton-motive force to generate ATP from ADP and P_i. Thus, the mitochondrial membrane potential is crucial to maintain the physiological function of the ETC in order to produce ATP. A significant loss of mitochondrial membrane potential renders cells depleted of energy with subsequent death. Besides, the generation of NADH and $FADH_2$, the Krebs cycle also produces intermediates that can fuel into multiple biosynthetic ways to synthesize glucose, amino acids, lipids, heme, and nucleotides. Hence, mitochondria serve as a center for both catabolic and anabolic metabolism.

ROS is a byproduct of the mitochondrial electron transport chain. Free radicals are mainly generated in the inner mitochondrial membrane during the process of OXPHOS. The leakage of electrons primarily occurs at complexes I and III that leads to partial reduction of oxygen and forms superoxide. Superoxide anions are subsequently and rapidly dismutated to hydrogen peroxide by superoxide dismutases 1 and 2 (SOD1, Cu-Zn superoxide dismutase, and SOD2, Mn-superoxide dismutase). SOD1 is located in the inner mitochondrial membrane space and SOD2 in the mitochondrial matrix. H_2O_2 is then converted to water by glutathione peroxidase (Figure 1). The important role of ROS has been implicated in the regulation of growth and survival of cancer as well as structural damages to cells along with lipids, membranes, and DNA [23].

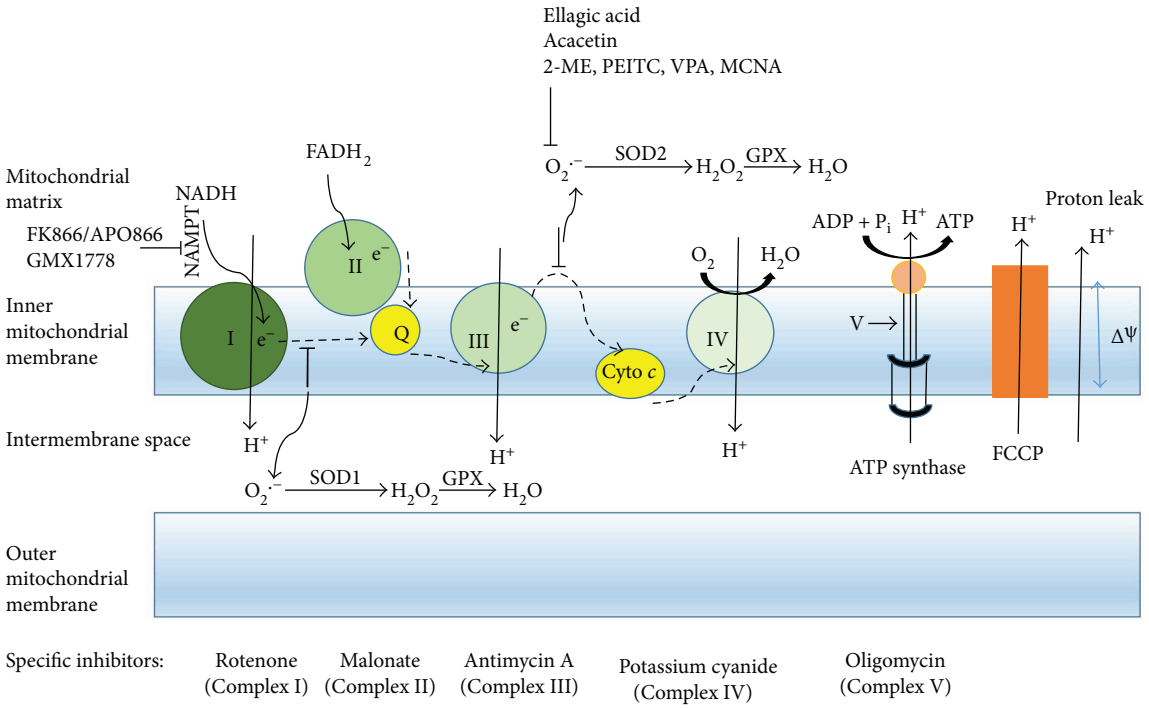

Figure 1: Scheme of the mitochondrial electron transport chain. During the respiration process in mitochondria, electrons from the oxidized state of substrates are transported through a series of electron transport carriers (dashed arrows) located in the inner mitochondrial membrane. Electrons (e^-) raised from NADH and $FADH_2$ enter the electron transport chain at Complexes I and II, respectively. The free energy is released from Complexes I, III, and IV by the gradual decrease of redox potential while electrons are passing and translocating protons (H^+) from the matrix into the intermembrane space of mitochondria. The proton electrochemical potential gradient generated across the inner mitochondrial membrane is referred as the proton-motive force (pmf). The pmf is used to generate ATP by ATP synthase and also allows the return of protons into the matrix. The redox state of mitochondrial complexes is shown in green. Several chemical compounds (ellagic acid; acacetin; 2-ME, 2-methoxiestradiol; PEITC, β-phenylethyl isothiocyanate; VPA, valproic acid; and MCNA, metal-containing nucleoside analogues) alter the ROS generation in CLL. The comparatively darker carrier indicates a more reduced state and vice versa. Cyto *c*: cytochrome *c*; NADH: nicotinamide-adenine dinucleotide (reduced); $FADH_2$: flavin-adenine dinucleotide (reduced); Q: ubiquinone; $\Delta\Psi$: mitochondrial membrane potential; FCCP: carbonyl cyanide-*p*-trifluoromethoxyphenylhydrazone; I, II, III, and IV attribute to mitochondrial complexes; NAMPT: nicotinamide phosphoribosyltransferase; SOD1 or SOD2: superoxide dismutase 1 or 2; GPX: glutathione peroxidase.

4. Mitochondrial Bioenergetics

Mitochondrial bioenergetics is important to evaluate the pathogenesis of mitochondrial diseases including cancer. Recently developed new techniques are implemented to quantify mitochondrial function and cellular bioenergetics in order to avoid issues associated with mitochondrial isolation or cell permeabilization [24]. The most commonly utilized bioenergetics parameters (Figure 2), basal respiration, proton leak, coupling efficiency, maximal respiration, respiratory control ratio, reserve respiratory capacity, and nonmitochondrial respirations, are defined herein in intact cells to further understand the bioenergetics profile of mitochondria and its importance [24, 25]. Routine respiration in intact cells is termed as basal respiration, especially by the Seahorse analyzer users. This artificially so-called basal respiration depends on the cellular activity and substrate supplied. Under physiological conditions, cells usually at basal level require only a part of their total bioenergetics capability. The portion of basal respiration inhibited by oligomycin, the ATP synthase inhibitor, can be referred as coupled respiration. The fraction of basal respiration that is not coupled to ATP production is referred to proton leak. Proton leak may forecast mitochondrial injury and may be involved in the regulation of ATP production. The coupling efficiency is calculated by the fraction of oxygen consumption rates driven to produce ATP related to basal respiration. The coupling efficiency varies with ATP demand. The maximal oxygen consumption rate can be achieved by an uncoupler (e.g., FCCP: carbonyl cyanide-*p*-trifluoromethoxyphenylhydrazone). An uncoupler stimulates the respiratory chain to operate at maximum capacity and causes prompt oxidation of substrates from sugar, fat, to amino acid. A titration of an uncoupler is highly recommended in order to achieve the optimum concentration necessary for the maximal stimulation. Single dose of uncoupler in experiments may fail to yield the estimation of maximal respiratory capacity. Respiratory control ratio is defined as the ratio of uncoupled respiration and oligomycin-treated respiration rates. This ratio depends on the substrate oxidation and proton leak; it is not affected by ATP turnover. One of the most important bioenergetics parameters is "reserve respiratory capacity" or

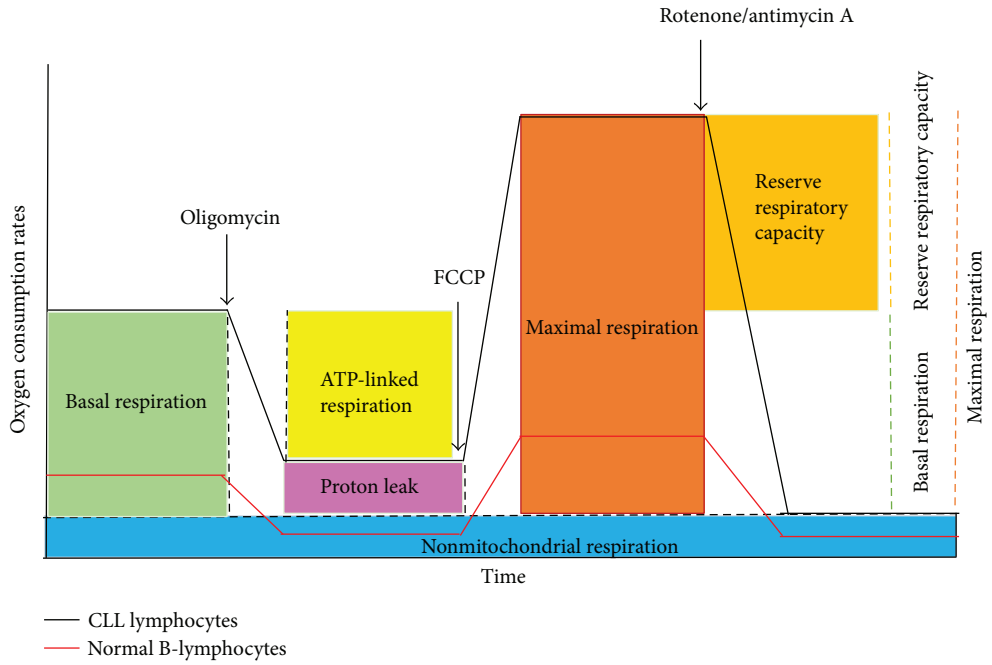

Figure 2: Bioenergetics profile in normal B lymphocytes and primary CLL cells. General scheme of bioenergetics parameters during mitochondrial stress test is shown. Sequential injections of oligomycin, FCCP, rotenone, and antimycin A measure basal respiration (green), ATP-linked oxygen consumption (yellow), proton leak (pink), maximal respiration (orange), reserve respiratory capacity (gold: maximal respiration—basal respiration), and nonmitochondrial respiration (blue). Dashed lines indicate OCR for the portion of each defined parameter. CLL, chronic lymphocytic leukemia lymphocytes, (black line) and normal B-lymphocytes (red line). The comparison of mitochondrial of bioenergetics between CLL and normal B-lymphocytes shown in this figure is adapted based on the results demonstrated by Jitschin et al. [29].

"spare respiratory capacity" to evaluate potential respiratory capacity to scope the stressed conditions. It is calculated by the difference between the maximal respiration achieved by an uncoupler and the basal respiration. The respiration rate after the addition of specific inhibitors of mitochondrial complexes I and III, rotenone and antimycin A, respectively, is nonmitochondrial respiration. It is subtracted from other respiration rates in order to evaluate the accurate measure of mitochondrial respiration.

5. Mitochondrial DNA and CLL

Through GWAS (genome-wide association studies), susceptibility genes were associated with apoptosis and the mitochondrial outer membrane which are important factors in CLL pathophysiology [26]. Environmental exposure may also play a role in its development [27], yet no true causative agents have been identified. Interestingly, the mtDNA structure of patients with CLL is no different from that of normal individuals; however, it has been shown that an increase in mtDNA copy number is associated with an increased risk for the development of CLL [28]. Treatments may also interfere with mtDNA. The mtDNA analysis of 20 CLL patients revealed that heteroplasmic mutations are significantly more frequent in CLL cells of treated patients compared to untreated [19]. The findings in this study suggest that heteroplasmy mutations caused by the chemotherapy in primary CLL cells are associated with increased ROS generation. This may lead to further development of chemoresistance and frequent relapses given the role of ROS in CLL.

6. Mitochondria-Derived ROS and Oxidative Stress in CLL

Tumor cells as well as tumor-associated cells can generate abundant ROS. However, the underlying mechanisms of oxidative stress in cancer patients often remain ambiguous. Mitochondrial respiration rate is increased in CLL cells, and as a result, the levels of mitochondria-derived ROS are higher in CLL cells than in normal B cells, and increased oxidative stress can lead to chemotherapy resistance in CLL cells [29]. A variety of antioxidant defenses, for example, intracellular glutathione, glutathione peroxidase, glutathione transferases, catalase, and superoxide dismutases: cytosolic copper-zinc superoxide dismutase (Cu-Zn SOD) and mitochondrial Manganese superoxide dismutase (MnSOD) control ROS levels which enables cells to regulate normal oxidative stress and to avoid excessive oxidative stress [30]. MnSOD plays an important role in metabolizing superoxides; therefore, the reduced MnSOD expression contributes to increase mitochondrial ROS in CLL cells [29]. Increased ROS through the inhibition of MnSOD was shown to induce CLL cell death [31], while elevated ROS levels promote genetic instability and mobilize cell-signaling [32, 33]. Oxidative stress also attenuates immune responses which in CLL may lead to progressive infectious complications and second malignancies [34]. Numerous recent studies

suggested an interrelationship between tumor-specific metabolism and excess of ROS. Tumor cells learn to adapt to permanent oxidative stress. They sustain protective pathways [35] that favor resistance towards anticancer agents [36, 37]. This is key in the behavior of CLL cells and their ability to escape the benefits of current chemotherapeutics. It also enables novel strategies to be employed in the treatment of this incurable disease [10]. Recent studies suggest that CLL cells adjust to their increased energy demands by increasing their mitochondrial activity. Jitschin et al. found that the number of mitochondria (demonstrated by electron microscopy), the total mitochondrial mass, mitochondrial biogenesis, mitochondrial bioenergetics (basal, maximal, and ATP-linked respiration rates), mitochondrial membrane potential, and mitochondria-derived ROS and oxidative stress are increased in CLL cells compared to normal B-lymphocytes [29]. There is possibility that certain drugs can further enhance mitochondrial ROS and thereby overwhelm the cancer cells' protective systems that could selectively impact CLL cells opposed to normal B-lymphocytes.

7. Importance of Mitochondria in CLL Cell Survival and Microenvironment

The survival of a cell depends on its ability to meet its energy requirements. Metabolic imbalances and augmented resistance to mitochondrial apoptosis are characteristics of cancer cells. Even though there has been recent progress in the understanding of molecular mechanisms in CLL, this disease still remains incurable. Therefore, it is necessary to pinpoint more elements that exclusively favor cell survival in order to target them. The importance of mitochondrial biogenesis and OXPHOS system has not been fully assessed yet. Subunits of mitochondrial complexes encoded by mtDNA are crucial to maintain function of OXPHOS. Otto Warburg, the famous German scientist, introduced the hypothesis that cancer cells depend overwhelmingly on glycolysis rather than OXPHOS for survival [38]. The glycolytic inhibitors as a therapeutic target to control cell proliferation in various cancers were not successful, even though malignant cells are highly glycolytic. These findings suggest that the Warburg hypothesis is not applicable to all malignancies. However, recent findings revealed that some tumors remarkably rely on OXPHOS for survival including CLL [29, 39, 40]. Therefore, OXPHOS may be the potential therapeutic target in order to arrest the uncontrolled proliferation of malignant cells.

The microenvironment for CLL cells is defined as the interactions between stromal cells and matrix [41]. The communication between CLL and the microenvironment affects survival and proliferation of CLL cells and drug resistance that may be conferred by the remaining disease after treatment. Even though drugs for CLL therapy available in the market are efficient in killing cells *in vitro*, the therapeutic efficacy rapidly declines *in vivo* due to the presence of stromal cells [11]. Since the survival of CLL cells is affected by mitochondrial metabolism, mitochondria may have a role on the conditions of the microenvironment in CLL cells and contribute to drug resistance. The study performed by Li et al. identified perhexiline, a carnitine palmitoyltransferase inhibitor that abolishes the transport of fatty acid into mitochondria and selectively kills CLL cells in the presence of bone marrow stromal cells and *in vivo* [42]. This demonstrates that by altering mitochondrial metabolism, one can impact CLL cell survival and its interactions within the microenvironment.

8. List of Therapeutic Compounds Targeting Mitochondrial Bioenergetics, Redox Pathways, and Cell Survival in CLL

Since CLL cells have an increased mitochondrial biogenesis, such as increased mitochondrial mass and number, membrane potential, ATP production, mitochondrial DNA copy numbers, mitochondrial bioenergetics profile, and ROS, these changes provide a possibility to preferentially target CLL cell mitochondria to improve therapeutic selectivity [19, 28]. Recent findings are described below (Table 1).

The polyphenolic compound, *ellagic acid* selectively leads to apoptosis mediated by ROS overproduction in CLL cells that directly targets mitochondria [43]. The antioxidant and antiproliferative properties have been found in several *in vitro* and small animal models [44, 45]. Ellagic acid can induce apoptosis while increasing ROS production, mitochondria swelling, decrease in MMP resulting in cytochrome *c* release, caspase 3 cleavage, and apoptosis in CLL cells.

Sodium dichloroacetate (DCA) exhibits anti-CLL activity and is synergistic with the p53 activator nutlin-3 [46]. DCA showed a dose-dependent anti-CLL effect in both primary CLL and CLL-like cell lines with a functional p53. At the molecular level, DCA, via posttranscriptional modifications of p53 protein and in the presence of nutlin-3, increased expression of p53-target genes, particularly p21. Genetic silencing of p21 significantly rescued the DCA + nutlin3-induced cell death phenotype. This study substantiates that DCA needs to be further evaluated as a potential therapeutic agent for CLL, likely in combination with other compounds. CLL cells often acquire defects in p53 status and this becomes a common mechanism of drug resistance, and the ability to enhance and maintain p53 function would enable standard chemotherapeutics, a continued role in CLL.

Acacetin (4′-methoxy-5,7-dihydroxyflavone), a natural flavone, can selectively induce apoptosis in CLL cells by directly targeting mitochondria through increased ROS production, loss of MMP, mitochondrial permeability transition pore, release of cytochrome *c*, and caspase 3 activation, while non-CLL lymphocytes remain unaffected [47]. Oral administration of acacetin showed potent anticancer activity in CLL xenograft mouse models. This compound is attractive because it does not belong to other classes of drugs that are currently utilized in CLL therapy, and as a result, it may be beneficial as mechanisms of resistance emerge with novel agents in CLL.

The antidiabetic drug *metformin* was found to inhibit the mitochondrial respiratory chain and consequent OXPHOS in human epithelial type 2 (HeP2) cells originated from human laryngeal carcinoma and 143B cells from human

Table 1: List of compounds targeting mitochondrial metabolism in CLL.

Compound	Target	Possible mechanism	References
Ellagic acid (EA, 2,3,7,8-tetrahydroxy-chromeno[5,4,3-cde]chromene-5,10-dione)	Antioxidant and antiproliferative properties (inhibition of DNA binding of certain carcinogens)	↓ MMP, ↑ cytochrome *c* release, caspase 3 activation, and apoptosis	[43]
Sodium dichloroacetate	Pyruvate dehydrogenase kinase	P53 activity	[46]
Acacetin (4′-methoxy-5,7-dihydroxyflavone)	Unknown	↓ MMP, ↑ cytochrome *c* release, caspase 3 activation, and apoptosis	[47]
Metformin (1,1-dimethylbiguanide hydrochloride)	Energetic metabolism, cell proliferation through AMPK-dependent and independent mechanism	Apoptosis, inhibition of cell cycle entry	[54]
2-Methoxiestradiol (2-ME)	Superoxide dismutase inhibition	Apoptosis	[55]
β-phenylethyl isothiocyanate (PEITC)	Glutathione antioxidant system	↓ Glutathione, ↑ ROS, oxidation of cardiolipin	[56]
FK866/APO866	NAMPT inhibition	NAD depletion, ↓ cell viability, ↑ ROS	[57, 58]
Valproic acid (VPA)	Histone deacetylase inhibition	↓ AKT and ATM activation ↑ ROS, ↑ Cytochrome *c* release, activation of caspases	[59]
Venetoclax (ABT-199)	BH3 mimetic, BCL-2-selective inhibitor	Apoptosis	[61]
ZGDHu-1 [N,N′-di-(m-methylphenyi)-3,6-dimethyl-1,4-dihydro-1,2,4,5-tetrazine-1,4-dicarboamide]	Proteasome inhibitor	Apoptosis	[66]
MCNA, metal-containing nucleoside analogues	PARP-mediated cell death	↓ OCR, rapid membrane depolarization	[67]
ROS inducible DNA crosslinking agents	DNA crosslinking coupled with H_2O_2	Cytotoxic, tumor-specific damage	[69]

↓: decreased; ↑: increased; MMP: mitochondrial membrane potential; ROS: reactive oxygen species; NAMPT: nicotinamide phosphoribosyl transferase; AMPK: 5′ adenosine monophosphate-activated protein kinase; AKT: RAC-alpha serine/threonine-protein kinase; ATM: ataxia telangiectasia mutated; BCL2: B-cell lymphoma gene 2; BH3: BCL2 homology domain 3; PARP: poly (ADP-ribose) polymerase; OCR: oxygen consumption rate.

bone osteosarcoma [48, 49]. Metformin decreases tumor growth indirectly, that is, systematic effect; it lowers glucose and insulin or directly inhibits energetic metabolism and cellular pathways involved in proliferation through AMPK-dependent [50, 51] or AMPK-independent mechanisms [52, 53]. This has also been studied in CLL, where metformin-induced apoptosis in resting CLL cells and inhibition of cell cycle entry when CLL cells were stimulated by CD40-CD40L ligation (a mimic of the CLL microenvironment), while non-CLL lymphocytes remained unaffected at the same doses [54]. This arrest in cell cycle was accompanied by decreased expression of proteins associated with survival and proliferation and inhibition of signal transduction pathways responsible for CLL progression as well as loss of intracellular glucose available for glycolysis. Given the common use of metformin in patients in general, metformin alone would not be effective as a treatment for CLL in doses that would be tolerable by patients. However, in drug combination experiments with fludarabine or the BCL2 inhibitor ABT-737, metformin enabled lower doses of each agent studied to decrease the apoptotic threshold and potentiate CLL cell death [54].

2-methoxiestradiol (2-ME), a reagent that inhibits superoxide dismutase, induces apoptosis in leukemia cells by free radical-mediated mechanism [55]. The cellular production of O_2^- is necessary for the antileukemia activity of 2-ME *in vitro*. Primary patient CLL cells demonstrate heterogeneous levels of cellular O_2^-; however, leukemia cells from previously treated patients had higher O_2 levels. As newer mechanisms of resistance and challenging tocxicities evolve with some of the newer agents, alternative mechanisms of cell death need to be explored. Interestingly, CLL cells with high levels of superoxide were more sensitive to 2-ME, and thus this may be an attractive option for those patients who have failed previous therapies. In addition, CLL cells could be sensitized by the use of exogenous ROS-generating agents, such as arsenic trioxide in CLL cells with a low level of endogenous superoxide which were resistant to 2-ME to significantly enhance antileukemia activity. Thus, combination of ROS-producing agents and SOD inhibitors may provide a new strategy to enhance therapeutic activity and overcome drug resistance in CLL patients who have or have not been previously treated.

Fludarabine is the standard treatment for younger patients with CLL. At the same time, fludarabine resistance is a common clinical dilemma. Fludarabine-resistant CLL cells can be eliminated by *β-phenylethyl isothiocyanate (PEITC)* through a redox-mediated mechanism [56]. However, sensitivity to PEITC was observed in fludarabine-resistant and fludarabine-sensitive cells while non-CLL lymphocytes were not. Exposure of CLL cells to PEITC causes severe glutathione depletion, increased ROS, and oxidation of mitochondrial cardiolipin leading to cell death.

This study demonstrates that PEITC via a redox-mediated mechanism eliminates fludarabine resistance with minimal toxicity to normal lymphocytes. Given that current fludarabine-based treatments remain the standard of care in young, fit, low-risk patients, this agent warrants further clinical evaluation to reduce toxicity and improve efficacy of fludarabine-based regimes.

FK866/*APO866*, a nicotinamide phosphoribosyltransferase (NAMPT) inhibitor, mediates apoptosis in CLL cells [57]. NAMPT is overexpressed in CLL cells versus non-CLL lymphocytes and thus an attractive target for CLL-specific cell death. FK866 induces CLL cell death by depleting cellular NAD^+ content at 24 hours along with loss of MMP, ROS increase, and induction of apoptotic signaling within 48 hours. These on-target effects were confirmed by NAD-mediated rescue of NAD and ATP loss, apoptotic signaling, and viability. Patients who had previously been treated with fludarabine were sensitive to FK866, and fludarabine and FK866 were synergistic at clinically relevant concentrations. This paper suggests that FK866 enhance efficacy and/or allow dose reduction of standard chemotherapeutics for improved tolerability. APO866 increases leukemia cell death of cyclosporine-A by inducing mitochondrial and endoplasmic reticulum stress [58]. The combination of APO866 with Pgp (P-glycoprotein-1) inhibitors resulted in a synergistic combination in leukemia cells, while sparing normal blood cells. Combining Pgp inhibitors with APO866 lead to increased intracellular APO866 levels, compounded NAD^+ and ATP storage, and induced $\Delta\Psi m$ dissipation. This suggests that selectively targeting NAMPT, an enzyme upregulated in malignant B cells, offers an avenue to utilize and repurpose current treatment strategies and potentially reduce toxicities for patients. The challenge with NAMPT inhibitors in patients has been drug delivery by intravenous infusion opposed to oral ingestion. A second oral NAMPT inhibitor, GMX1778 is depicted along with FK866/APO866 at the site of complex I in Figure 1. This may improve the uptake of this agent moving forward.

Valproic acid (VPA), a HDAC (histone deacetylase) inhibitor, increases cell death in CLL-like cell lines. VPA improves fludarabine-induced apoptosis mediated by ROS and involved decreasing AKT and ATM activation in B-cell lymphoid neoplastic cells [59]. This increased apoptosis resulted in the release of cytochrome *c*, activation of caspases, and increased ROS generation. Combination of VPA with fludarabine treatment decreased both phosphorylated and total levels of AKT and ATM both key proteins in CLL signaling and DNA damage, respectively. VPA reduces ATM levels and induced ROS-dependent cell death via the mitochondrial apoptotic pathway when combined with fludarabine. This suggests that HDAC inhibitors could potentiate fludarabine-based treatments while limiting toxicity.

Venetoclax (ABT-199) is a BH3 mimetic and a specific inhibitor to BCL2 that is currently approved for treatment of CLL by the U.S. Food and Drug Administration (FDA) for use in CLL patients who have received prior therapy [60, 61]. Since BCL-2 is overexpressed in CLL, it blunts activation of the mitochondrial pathway to apoptosis and is thus required for CLL survival [62]. Venetoclax binds to BCL2, thereby dislodging proapoptotic proteins, BAX and BAK from their binding to BCL-2. This recently approved drug further demonstrates the importance of mitochondrial metabolism. This agent also has high rate of complete responses, and 5% of study patients achieved minimal residual disease negativity [63]. This occurs rarely with tyrosine kinase inhibitors, further pointing to the importance of the mitochondria in CLL.

ZGDHu-1 [N,N′-di-(m-methylphenyi)-3,6-dimethyl-1,4-dihydro-1,2,4,5-tetrazine-1,4-dicarboamide] is a proteasome inhibitor and has been reported to exhibit antitumor activity [64, 65]. A study has recently been conducted to assess whether this drug has a synergistic effect with fludarabine and mediates apoptosis in CLL cells [66]. CLL cell-specific apoptosis occurred through the mitochondrial pathway as normal cells remained unaffected. Most importantly, a combination of ZGDHu-1 and a sublethal dose of fludarabine led to synergy. Notably, the rate of apoptosis caused by ZGDHu-1 alone or in combination with fludarabine did not correlate with high-risk disease features. Therefore, the use of ZGDHu-1 alone or in combination with fludarabine may further enhance treatment options for CLL patients. This becomes important when thinking of fludarabine-based therapies as it may improve the efficacy and lower the toxicity profile of this drug.

Increased oxidative stress and altered mitochondrial metabolism in CLL cells are associated with the lymphoid oncogene TCL-1 (T cell leukemia 1). Prinz et al. demonstrated that organometallic nucleosides *(MCNA, metal-containing nucleoside analogues)* induce nonclassical cell death that is mitochondrial ROS dependent and facilitated by TCL1 oncogene overexpression [67]. MCNA induced cell death through PARP that was nonautophagic and nonnecrotic as well as caspase- and P53-independent. The authors investigated how these aberrant redox characteristics and bioenergetics of CLL are impacted by TCL1 and how targeting it could be exploited for therapy in the future. The TCL-1 transgenic mice have been characterized by Johnson et al. as a suitable animal model for preclinical drug assessment tool in human CLL [68]. These animals expressed relevant therapeutic targeted proteins with wild-type p53 status and showed sensitivity *in vitro* to therapeutic agents generally used in the treatment of CLL. This also enables a suitable model for mitochondrial targeting in CLL.

ROS inducible *DNA crosslinking agents* are activated aromatic nitrogen mustards, the ability to crosslink DNA. DNA inter-strand crosslinks are identified as one of principle mechanisms for the cytotoxic effect of many antitumor drugs. These compounds exhibit very powerful crosslinking abilities in the presence of H_2O_2 and provide a novel strategy for tumor-specific damage. Primary CLL samples were more sensitive (40–80% apoptosis) than non-CLL lymphocytes from healthy donors [69]. They further demonstrated that these compounds function through ROS-dependent mechanisms as NAC rescued the viability effect and decreased ROS generated in primary CLL cells. The data described in this study provide an additional selective agent for development in CLL.

9. Conclusion

Mitochondrial metabolism has only now become of interest in the realm of cancer therapy. CLL is a disease that has many mitochondrial metabolic dependencies. However, the nature of metabolic networks that enable abhorrent cell proliferation, cell-cell communication, evasion of apoptosis, and drug resistance remains poorly understood. The list of therapeutic compounds described in this review implements a strong suggestion that targeting mitochondrial bioenergetics and metabolic alterations may provide a mechanistic explanation for the growth advantage and apoptotic resistance of tumor cells. In CLL patients, standard chemi-immunotherapy and novel targeted agents continue to lead to treatment failures. In order to best target this cancer, a multipronged treatment strategy such as combinations with mitochondrial targeting agents and currently approved treatments may enable a chance at cure for a currently incurable cancer.

Conflicts of Interest

The authors declare that there are no conflicts of interest.

Acknowledgments

The authors thank CancerCare Manitoba Foundation and Research Manitoba for continued funding support.

References

[1] M. Hallek, B. D. Cheson, D. Catovsky et al., "Guidelines for the diagnosis and treatment of chronic lymphocytic leukemia: a report from the international workshop on chronic lymphocytic leukemia updating the national cancer institute-working group 1996 guidelines," *Blood*, vol. 111, no. 12, pp. 5446–5456, 2008.

[2] T. D. Shanafelt, N. E. Kay, K. G. Rabe et al., "Survival of patients with clinically identified monoclonal B-cell lymphocytosis (MBL) relative to the age- and sex-matched general population," *Leukemia*, vol. 26, no. 2, pp. 373–376, 2012.

[3] M. D. Seftel, A. A. Demers, V. Banerji et al., "High incidence of chronic lymphocytic leukemia (CLL) diagnosed by immunophenotyping: a population-based Canadian cohort," *Leukemia Research*, vol. 33, no. 11, pp. 1463–1468, 2009.

[4] S. Stilgenbauer, "Prognostic markers and standard management of chronic lymphocytic leukemia," *Hematology*, vol. 2015, pp. 368–377, 2015.

[5] K. R. Rai and P. Jain, "Chronic lymphocytic leukemia (CLL)—then and now," *American Journal of Hematology*, vol. 91, pp. 330–340, 2015.

[6] M. Hallek, "Chronic lymphocytic leukemia: 2015 update on diagnosis, risk stratification, and treatment," *American Journal of Hematology*, vol. 90, no. 5, pp. 446–460, 2015.

[7] E. Wawrzyniak, A. Kotkowska, J. Z. Blonski et al., "Clonal evolution in CLL patients as detected by FISH versus chromosome banding analysis, and its clinical significance," *European Journal of Haematology*, vol. 92, no. 2, pp. 91–101, 2014.

[8] N. E. Kay, E. A. Ranheim, and L. C. Peterson, "Tumor suppressor genes and clonal evolution in B-CLL," *Leukemia & Lymphoma*, vol. 18, no. 1-2, pp. 41–49, 2009.

[9] D. Hanahan and R. A. Weinberg, "Hallmarks of cancer: the next generation," *Cell*, vol. 144, no. 5, pp. 646–674, 2011.

[10] H. Cheong, C. Lu, T. Lindsten, and C. B. Thompson, "Therapeutic targets in cancer cell metabolism and autophagy," *Nature Biotechnology*, vol. 30, no. 7, pp. 671–678, 2012.

[11] W. Zhang, D. Trachootham, J. Liu et al., "Stromal control of cystine metabolism promotes cancer cell survival in chronic lymphocytic leukaemia," *Nature Cell Biology*, vol. 14, no. 3, pp. 276–286, 2012.

[12] L. Lagneaux, A. Delforge, D. Bron, C. de Bruyn, and P. Stryckmans, "Chronic lymphocytic leukemic B cells but not normal B cells are rescued from apoptosis by contact with normal bone marrow stromal cells," *Blood*, vol. 91, no. 7, pp. 2387–2396, 1998.

[13] M. Grdisa, "Influence of CD40 ligation on survival and apoptosis of B-CLL cells in vitro," *Leukemia Research*, vol. 27, no. 10, pp. 951–956, 2003.

[14] R. A. Cairns, I. S. Harris, and T. W. Mak, "Regulation of cancer cell metabolism," *Nature Reviews Cancer*, vol. 11, no. 2, pp. 85–95, 2011.

[15] P. Vandenabeele, L. Galluzzi, T. vanden Berghe, and G. Kroemer, "Molecular mechanisms of necroptosis: an ordered cellular explosion," *Nature Reviews Molecular Cell Biology*, vol. 11, no. 10, pp. 700–714, 2010.

[16] D. A. Tennant, R. V. Duran, and E. Gottlieb, "Targeting metabolic transformation for cancer therapy," *Nature Reviews Cancer*, vol. 10, no. 4, pp. 267–277, 2010.

[17] G. Kroemer, "Mitochondria in cancer," *Oncogene*, vol. 25, no. 34, pp. 4630–4632, 2006.

[18] W. X. Zong, J. D. Rabinowitz, and E. White, "Mitochondria and cancer," *Molecular Cell*, vol. 61, no. 5, pp. 667–676, 2016.

[19] J. S. Carew, Y. Zhou, M. Albitar, J. D. Carew, M. J. Keating, and P. Huang, "Mitochondrial DNA mutations in primary leukemia cells after chemotherapy: clinical significance and therapeutic implications," *Leukemia*, vol. 17, no. 8, pp. 1437–1447, 2003.

[20] S. Anderson, A. T. Bankier, B. G. Barrell et al., "Sequence and organization of the human mitochondrial genome," *Nature*, vol. 290, no. 5806, pp. 457–465, 1981.

[21] D. C. Wallace, "Mitochondrial diseases in man and mouse," *Science*, vol. 283, no. 5407, pp. 1482–1488, 1999.

[22] S. E. Weinberg and N. S. Chandel, "Targeting mitochondria metabolism for cancer therapy," *Nature Chemical Biology*, vol. 11, no. 1, pp. 9–15, 2015.

[23] P. L. Pedersen, "Mitochondrial events in the life and death of animal cells: a brief overview," *Journal of Bioenergetics and Biomembranes*, vol. 31, no. 4, pp. 291–304, 1999.

[24] M. D. Brand and D. G. Nicholls, "Assessing mitochondrial dysfunction in cells," *The Biochemical Journal*, vol. 435, no. 2, pp. 297–312, 2011.

[25] S. K. Roy Chowdhury, D. R. Smith, A. Saleh et al., "Impaired adenosine monophosphate-activated protein kinase signalling in dorsal root ganglia neurons is linked to mitochondrial dysfunction and peripheral neuropathy in diabetes," *Brain*, vol. 135, no. 6, pp. 1751–1766, 2012.

[26] H. E. Speedy, M. C. di Bernardo, G. P. Sava et al., "A genome-wide association study identifies multiple susceptibility loci for chronic lymphocytic leukemia," *Nature Genetics*, vol. 46, no. 1, pp. 56–60, 2014.

[27] S. I. Berndt, N. J. Camp, C. F. Skibola et al., "Meta-analysis of genome-wide association studies discovers multiple loci for

chronic lymphocytic leukemia," *Nature Communications*, vol. 7, article 10933, 2016.

[28] F. S. Hosnijeh, Q. Lan, N. Rothman et al., "Mitochondrial DNA copy number and future risk of B-cell lymphoma in a nested case-control study in the prospective EPIC cohort," *Blood*, vol. 124, no. 4, pp. 530–535, 2014.

[29] R. Jitschin, A. D. Hofmann, H. Bruns et al., "Mitochondrial metabolism contributes to oxidative stress and reveals therapeutic targets in chronic lymphocytic leukemia," *Blood*, vol. 123, no. 17, pp. 2663–2672, 2014.

[30] J. B. Stewart and P. F. Chinnery, "The dynamics of mitochondrial DNA heteroplasmy: implications for human health and disease," *Nature Reviews Genetics*, vol. 16, no. 9, pp. 530–542, 2015.

[31] J. F. Zhou, P. Chen, Y. H. Zhou, L. Zhang, and H. H. Chen, "3,4-Methylenedioxymethamphetamine (MDMA) abuse may cause oxidative stress and potential free radical damage," *Free Radical Research*, vol. 37, no. 5, pp. 491–497, 2003.

[32] D. Trachootham, J. Alexandre, and P. Huang, "Targeting cancer cells by ROS-mediated mechanisms: a radical therapeutic approach?," *Nature Reviews Drug Discovery*, vol. 8, no. 7, pp. 579–591, 2009.

[33] B. D'Autreaux and M. B. Toledano, "ROS as signalling molecules: mechanisms that generate specificity in ROS homeostasis," *Nature Reviews Molecular Cell Biology*, vol. 8, no. 10, pp. 813–824, 2007.

[34] A. Takahashi, M. G. V. Hanson, H. R. Norell et al., "Preferential cell death of $CD8^+$ effector memory ($CCR7^-CD45RA^-$) T cells by hydrogen peroxide-induced oxidative stress," *Journal of Immunology*, vol. 174, no. 10, pp. 6080–6087, 2005.

[35] G. M. DeNicola, F. A. Karreth, T. J. Humpton et al., "Oncogene-induced Nrf2 transcription promotes ROS detoxification and tumorigenesis," *Nature*, vol. 475, no. 7354, pp. 106–109, 2011.

[36] S. Pervaiz and M. V. Clement, "Tumor intracellular redox status and drug resistance-serendipity or a causal relationship?," *Current Pharmaceutical Design*, vol. 10, no. 16, pp. 1969–1977, 2004.

[37] R. P. Wu, T. Hayashi, H. B. Cottam et al., "Nrf2 responses and the therapeutic selectivity of electrophilic compounds in chronic lymphocytic leukemia," *Proceedings of the National Academy of Sciences of the United States of America*, vol. 107, no. 16, pp. 7479–7484, 2010.

[38] R. Fukuda, H. Zhang, J.w. Kim, L. Shimoda, C. V. Dang, and G. L. Semenza, "HIF-1 regulates cytochrome oxidase subunits to optimize efficiency of respiration in hypoxic cells," *Cell*, vol. 129, no. 1, pp. 111–122, 2007.

[39] J. M. Funes, M. Quintero, S. Henderson et al., "Transformation of human mesenchymal stem cells increases their dependency on oxidative phosphorylation for energy production," *Proceedings of the National Academy of Sciences of the United States of America*, vol. 104, no. 15, pp. 6223–6228, 2007.

[40] S. Rodriguez-Enriquez, P. A. Vital-González, F. L. Flores-Rodríguez, A. Marín-Hernández, L. Ruiz-Azuara, and R. Moreno-Sánchez, "Control of cellular proliferation by modulation of oxidative phosphorylation in human and rodent fast-growing tumor cells," *Toxicology and Applied Pharmacology*, vol. 215, no. 2, pp. 208–217, 2006.

[41] J. A. Burger, "Nurture versus nature: the microenvironment in chronic lymphocytic leukemia," *Hematology*, vol. 2011, pp. 96–103, 2011.

[42] P. P. Liu, J. Liu, W. Q. Jiang et al., "Elimination of chronic lymphocytic leukemia cells in stromal microenvironment by targeting CPT with an antiangina drug perhexiline," *Oncogene*, vol. 35, no. 43, pp. 5663–5673, 2016.

[43] A. Salimi, M. H. Roudkenar, L. Sadeghi et al., "Ellagic acid, a polyphenolic compound, selectively induces ROS-mediated apoptosis in cancerous B-lymphocytes of CLL patients by directly targeting mitochondria," *Redox Biology*, vol. 6, pp. 461–471, 2015.

[44] N. P. Seeram, L. S. Adams, S. M. Henning et al., "In vitro antiproliferative, apoptotic and antioxidant activities of punicalagin, ellagic acid and a total pomegranate tannin extract are enhanced in combination with other polyphenols as found in pomegranate juice," *The Journal of Nutritional Biochemistry*, vol. 16, no. 6, pp. 360–367, 2005.

[45] B. A. Narayanan, O. Geoffroy, M. C. Willingham, G. G. Re, and D. W. Nixon, "p53/p21(WAF1/CIP1) expression and its possible role in G1 arrest and apoptosis in ellagic acid treated cancer cells," *Cancer Letters*, vol. 136, no. 2, pp. 215–221, 1999.

[46] C. Agnoletto, E. Melloni, F. Casciano et al., "Sodium dichloroacetate exhibits anti-leukemic activity in B-chronic lymphocytic leukemia (B-CLL) and synergizes with the p53 activator Nutlin-3," *Oncotarget*, vol. 5, no. 12, pp. 4347–4360, 2014.

[47] A. Salimi, M. H. Roudkenar, L. Sadeghi et al., "Selective anticancer activity of acacetin against chronic lymphocytic leukemia using both in vivo and in vitro methods: key role of oxidative stress and cancerous mitochondria," *Nutrition and Cancer*, vol. 68, no. 8, pp. 1404–1416, 2016.

[48] B. Viollet, B. Guigas, N. S. Garcia, J. Leclerc, M. Foretz, and F. Andreelli, "Cellular and molecular mechanisms of metformin: an overview," *Clinical Science*, vol. 122, no. 6, pp. 253–270, 2012.

[49] H. R. Bridges, A. J. Y. Jones, M. N. Pollak, and J. Hirst, "Effects of metformin and other biguanides on oxidative phosphorylation in mitochondria," *The Biochemical Journal*, vol. 462, no. 3, pp. 475–487, 2014.

[50] M. Y. El-Mir, V. Nogueira, E. Fontaine, N. Avéret, M. Rigoulet, and X. Leverve, "Dimethylbiguanide inhibits cell respiration via an indirect effect targeted on the respiratory chain complex I," *The Journal of Biological Chemistry*, vol. 275, no. 1, pp. 223–228, 2000.

[51] G. Zhou, R. Myers, Y. Li et al., "Role of AMP-activated protein kinase in mechanism of metformin action," *The Journal of Clinical Investigation*, vol. 108, no. 8, pp. 1167–1174, 2001.

[52] B. N. Zordoky, D. Bark, C. L. Soltys, M. M. Sung, and J. R. Dyck, "The anti-proliferative effect of metformin in triple-negative MDA-MB-231 breast cancer cells is highly dependent on glucose concentration: implications for cancer therapy and prevention," *Biochimica et Biophysica Acta (BBA) - General Subjects*, vol. 1840, no. 6, pp. 1943–1957, 2014.

[53] L. A. Cantrell, C. Zhou, A. Mendivil, K. M. Malloy, P. A. Gehrig, and V. L. Bae-Jump, "Metformin is a potent inhibitor of endometrial cancer cell proliferation—implications for a novel treatment strategy," *Gynecologic Oncology*, vol. 116, no. 1, pp. 92–98, 2010.

[54] S. Bruno, B. Ledda, C. Tenca et al., "Metformin inhibits cell cycle progression of B-cell chronic lymphocytic leukemia cells," *Oncotarget*, vol. 6, no. 26, pp. 22624–22640, 2015.

[55] Y. Zhou, E. O. Hileman, W. Plunkett, M. J. Keating, and P. Huang, "Free radical stress in chronic lymphocytic leukemia cells and its role in cellular sensitivity to ROS-generating anticancer agents," *Blood*, vol. 101, no. 10, pp. 4098–4104, 2003.

[56] D. Trachootham, H. Zhang, W. Zhang et al., "Effective elimination of fludarabine-resistant CLL cells by PEITC through a redox-mediated mechanism," *Blood*, vol. 112, no. 5, pp. 1912–1922, 2008.

[57] I. Gehrke, E. D. J. Bouchard, S. Beiggi et al., "On-target effect of FK866, a nicotinamide phosphoribosyl transferase inhibitor, by apoptosis-mediated death in chronic lymphocytic leukemia cells," *Clinical Cancer Research*, vol. 20, no. 18, pp. 4861–4872, 2014.

[58] A. Cagnetta, I. Caffa, C. Acharya et al., "APO866 increases antitumor activity of cyclosporin-a by inducing mitochondrial and endoplasmic reticulum stress in leukemia cells," *Clinical Cancer Research*, vol. 21, no. 17, pp. 3934–3945, 2015.

[59] J. Y. Yoon, G. Ishdorj, B. A. Graham, J. B. Johnston, and S. B. Gibson, "Valproic acid enhances fludarabine-induced apoptosis mediated by ROS and involving decreased AKT and ATM activation in B-cell-lymphoid neoplastic cells," *Apoptosis*, vol. 19, no. 1, pp. 191–200, 2014.

[60] V. A. Pullarkat and E. M. Newman, "BCL2 inhibition by venetoclax: targeting the Achilles' heel of the acute myeloid leukemia stem cell?," *Cancer Discovery*, vol. 6, no. 10, pp. 1082-1083, 2016.

[61] S. K. Tahir, M. L. Smith, P. Hessler et al., "Potential mechanisms of resistance to venetoclax and strategies to circumvent it," *BMC Cancer*, vol. 17, no. 1, p. 399, 2017.

[62] M. A. Anderson, J. Deng, J. F. Seymour et al., "The BCL2 selective inhibitor venetoclax induces rapid onset apoptosis of CLL cells in patients via a TP53-independent mechanism," *Blood*, vol. 127, no. 25, pp. 3215–3224, 2016.

[63] A. W. Roberts, M. S. Davids, J. M. Pagel et al., "Targeting BCL2 with venetoclax in relapsed chronic lymphocytic leukemia," *The New England Journal of Medicine*, vol. 374, no. 4, pp. 311–322, 2016.

[64] G. W. Rao and W. X. Hu, "Synthesis, structure analysis, and antitumor activity of 3,6-disubstituted-1,4-dihydro-1,2,4,5-tetrazine derivatives," *Bioorganic & Medicinal Chemistry Letters*, vol. 16, no. 14, pp. 3702–3705, 2006.

[65] L. N. Qiu, Y. L. Zhou, Z. N. Wang, Q. Huang, and W. X. Hu, "ZGDHu-1 promotes apoptosis of chronic lymphocytic leukemia cells," *International Journal of Oncology*, vol. 41, no. 2, pp. 533–540, 2012.

[66] L. Qiu, J. Liu, Z. Wang, W. Hu, Q. Huang, and Y. Zhou, "ZGDHu-1 and fludarabine have a synergistic effect on apoptosis of chronic lymphocytic leukemia cells," *Oncology Reports*, vol. 34, no. 3, pp. 1239–1248, 2015.

[67] C. Prinz, E. Vasyutina, G. Lohmann et al., "Organometallic nucleosides induce non-classical leukemic cell death that is mitochondrial-ROS dependent and facilitated by TCL1-oncogene burden," *Molecular Cancer*, vol. 14, no. 1, p. 114, 2015.

[68] A. J. Johnson, D. M. Lucas, N. Muthusamy et al., "Characterization of the TCL-1 transgenic mouse as a preclinical drug development tool for human chronic lymphocytic leukemia," *Blood*, vol. 108, no. 4, pp. 1334–1338, 2006.

[69] W. Chen, K. Balakrishnan, Y. Kuang et al., "Reactive oxygen species (ROS) inducible DNA cross-linking agents and their effect on cancer cells and normal lymphocytes," *Journal of Medicinal Chemistry*, vol. 57, no. 11, pp. 4498–4510, 2014.

Hindawi
Oxidative Medicine and Cellular Longevity
Volume 2018, Article ID 9742154, 15 pages
https://doi.org/10.1155/2018/9742154

Research Article

UVA Irradiation Enhances Brusatol-Mediated Inhibition of Melanoma Growth by Downregulation of the Nrf2-Mediated Antioxidant Response

Mei Wang,[1] Guangwei Shi,[1] Chunxiang Bian,[1,2] Muhammad Farrukh Nisar,[1,3] Yingying Guo,[1] Yan Wu,[1,2] Wei Li,[1] Xiao Huang,[1] Xuemei Jiang,[1] Jörg W. Bartsch,[4] Ping Ji,[2] and Julia Li Zhong[1,2]

[1]*Key Laboratory of Biorheological Science and Technology, Ministry of Education, Chongqing University, Chongqing 400044, China*
[2]*Stomatological Hospital of Chongqing Medical University, Chongqing Municipal Key Laboratory of Oral Biomedical Engineering of Higher Education, Chongqing Key Laboratory of Oral Diseases and Biomedical Sciences, Chongqing 401147, China*
[3]*Interdisciplinary Research Center in Biomedical Materials (IRCBM), COMSATS Institute of Information Technology, Lahore 54000, Pakistan*
[4]*Department of Neurosurgery, Philipps-University Marburg, Baldingerstrasse, 35033 Marburg, Germany*

Correspondence should be addressed to Ping Ji; pingji1962@163.com and Julia Li Zhong; jlzhong@cqu.edu.cn

Received 15 May 2017; Revised 9 November 2017; Accepted 27 November 2017; Published 18 February 2018

Academic Editor: Peng Huang

Brusatol (BR) is a potent inhibitor of Nrf2, a transcription factor that is highly expressed in cancer tissues and confers chemoresistance. UVA-generated reactive oxygen species (ROS) can damage both normal and cancer cells and may be of potential use in phototherapy. In order to provide an alternative method to treat the aggressive melanoma, we sought to investigate whether low-dose UVA with BR is more effective in eliminating melanoma cells than the respective single treatments. We found that BR combined with UVA led to inhibition of A375 melanoma cell proliferation by cell cycle arrest in the G1 phase and triggers cell apoptosis. Furthermore, inhibition of Nrf2 expression attenuated colony formation and tumor development from A375 cells in heterotopic mouse models. In addition, cotreatment of UVA and BR partially suppressed Nrf2 and its downstream target genes such as HO-1 along with the PI3K/AKT pathway. We propose that cotreatment increased ROS-induced cell cycle arrest and cellular apoptosis and inhibits melanoma growth by regulating the AKT-Nrf2 pathway in A375 cells which offers a possible therapeutic intervention strategy for the treatment of human melanoma.

1. Introduction

Malignant melanoma (MM) is one of the most prevalent cancers in the Western world and is a highly aggressive dermatological malignancy associated with poor patient prognosis. The majority of MM arise from congenital melanocytic nevi or are due to a family history of MM; however, in some cases, 50% MM can also be associated with repeated intermittent sporadic ultraviolet (UV) exposure [1, 2], mostly UVB radiation plays a dominant role in the development of malignant melanoma, but the role of UVA is still unclear and controversial [3].

The progressive accumulation of genetic and environmental alterations causes disruption of homeostatic pathways, resulting in tumor cell invasion and lymphatic or haematogenous dissemination to distant sites [4]. In addition, B-Raf gene mutations are activated in 70% of human malignant melanomas [4, 5]. Over the past decades, the incidence of malignant melanoma is steadily rising [6]. Although significant advances have been made in diagnosis and treatment of MM, therapy resistance and metastasis are still the major reasons for mortality of patients [7]. Recently, some reports showed that Nrf2 expression in melanoma is related to invasion thereby worsening melanoma-specific

survival [8]. Furthermore, aberrant activation of Nrf2 has been shown to be involved in chemoresistance and radioresistance of various malignant tumors, such as glioma and gastric cancer [9–11]. Thus, it is highly desirable to investigate novel therapeutic strategies capable to enhance the efficacy of metastatic melanoma treatments with fewer side effects. Nrf2 suppression and subsequent low-dose UVA irradiation might be a potential auxiliary regimen for melanoma (low dose of UVA has no carcinogenesis).

Nuclear factor E2-related factor 2 (Nrf2), a transcription factor belonging to the cap'n'collar family of leucine-zipper (b-ZIP) proteins, has been reported to play an essential role in regulation of the cellular defense against chemicals and oxidative stress [12, 13]. However, Nrf2 is highly expressed in many cancer tissues, thereby increasing an unwanted resistance against chemotherapy, and might activate cell proliferation and suppress apoptosis [14, 15]. In addition, Nrf2 is activated by numerous oncogenic signaling pathways such as the PI3K/protein kinase B (Akt) pathway [16].

Under oxidative stress conditions including chemicals, UV irradiation, and heat shock, Nrf2 binding to its upstream keap1 (Kelch-like erythroid cell-derived protein with CNC homology- (ECH-) associated protein 1) is disrupted and leads to Nrf2 nuclear translocation and consequently activates expression of cytoprotective genes such as heme oxygenase 1 (HO-1), NAD(P)H:quinone oxidoreductase-1 (NQO1), and glutathione S-transferase (GST) drug transporters to dissipate redox homoeostasis [17, 18]. Stable activation of Nrf2 increased the resistance of human breast adenocarcinoma and neuroblastoma against tert-butylhydroquinone (tBHQ) [19]. Conversely, suppression of the Nrf2-mediated antioxidant defense system sensitizes cancer cell to ionizing radiation and chemotherapeutic drugs [17, 20, 21]. Furthermore, Nrf2 knockout mice significantly enhance the sensitivity to acetaminophen hepatotoxicity [22], cisplatin-induced nephrotoxicity [23], and bleomycin-induced pulmonary injury and fibrosis [24]. Since Nrf2 hampers cancer cell treatment, it has been analyzed as a promising drug target to combat chemoresistance [14, 19] and, up to now, a few effective Nrf2 inhibitors have been reported [25].

BR is a quassinoid isolated from *Brucea javanica* plant and has extensive pharmacological activities such as antimalarial, anti-inflammatory, and ant-tumor activity [26], primarily due to induction of proliferation arrest and activation of cell differentiation [27–29]. Recently, it was reported that BR is a potent inhibitor of Nrf2 activation thereby leading ultimately to tumor growth inhibition and ameliorated chemoresistance as in case of cisplatin [30–33]. We have found that RNA interference of Nrf2 in human skin fibroblasts increases long wave UVA- (320–400 nm) mediated damage [34], while Hirota et al. showed that $Nrf2^{-/-}$ 3T3 mouse fibroblasts exert increased UVA-mediated apoptosis and necrosis [35].

Medium and high doses of UVA irradiation cause oxidative stress, penetrate deeply into the dermis and subcutaneous layer [36, 37], and mediate oxidative damage to biomolecules such as proteins, lipids, carbohydrates, and nucleic acids (DNA and RNA) through reactive oxygen species (ROS) triggered by endogenous photosensitization [38].

UVA exposure following 4-thiothymidine treatment markedly increased cancer cell death [39], and reactive oxidative stress inhibits distant metastasis of human melanoma cells [40]. Thus, UVA-mediated oxidative stress offers a potential source for a novel photochemotherapy. Since BR is a specific inhibitor of Nrf2, downregulation of its expression may potentiate the therapeutic effect of phototherapy in combination with an Nrf2-inhibiting drug such as BR. We therefore speculated that cotreatment of UVA radiation and BR may have synergistic effects in the treatment of melanoma.

Using BR and low-dose UVA irradiation in A375 melanoma cells, we found that cotreatment (UVA + BR) inhibited melanoma cell growth and proliferation both *in vitro* and *in vivo* and induces cell apoptosis. Suppression of Nrf2 expression causes further accumulation of cellular ROS following UVA irradiation, which in turn inhibits AKT signaling. Our experiments revealed that cotreatment of UVA and BR caused an inhibition of AKT-Nrf2 cascades and reduced melanoma growth. Thus, this cotreatment can be a novel therapeutic attempt to enhance the effectiveness of melanoma treatment with less or no side effect compared to existing treatment options.

2. Materials and Methods

2.1. Chemicals and Reagents. Dulbecco's Modified Eagle Medium (DMEM) high glucose, DMEM without phenol red, and RPMI 1640 medium were obtained from Life Technologies (Gibco, USA). Fetal calf serum was purchased from Biological Industries (BI, Israel). Penicillin and streptomycin were obtained from North China Pharmaceutical Co. Ltd. (NCPC, China). Dimethyl sulfoxide (DMSO) and 4,6-diamidino-2-phenylindole dihydrochloride (DAPI) were obtained from Sigma. CellTiter 96 Aqueous One Solution Cell Proliferation Assay was obtained from Promega (USA). Nrf2 and NQO1 primary antibodies were purchased from Santa Cruz Biotechnology Inc. (USA). HO-1, GSTP, Bcl-2, Bcl-xL, Bax, IκBα, COX2, caspase-3, caspase-7, caspase-8, caspase-9, and PARP primary antibodies were obtained from Cell Signaling Technology (CST, USA). β-Actin antibody was purchased from Beijing Zhongshan-Golden Bridge Biological Technology (China). Annexin V-FITC Apoptosis Detection Kit was obtained from Beyotime Institute of Biotechnology (China). BR was purchased from Dingchen Technology (China).

2.2. Irradiation of Cells with UVA. UV light therapy system (Lifotronic) 365 nm (peak) spectrum lamp was used to irradiate cells (in PBS) following standard procedures, while nonirradiated cells were used as a background control (control = 0 kJ/m^2). Following UVA irradiation, cells were incubated in conditional medium for the required time.

2.3. Cell Lines and Cell Culture. Human malignant melanoma A375 cell line was bought from Shanghai Cell Resource Center (Chinese Academy of Sciences, China). HaCaT cells were kindly provided by Dr. Rex M. Tyrrell (University of

Bath, UK). Cells were cultured in DMEM (Gibco) high glucose or RPMI 1640 (Gibco) supplemented with 10% FBS (Biological Industries), 100 U/ml penicillin, and 150 U/ml streptomycin. Cell cultures were incubated in a humidified cell incubation chamber adjusted at 37°C with 5% CO_2. BR was dissolved in DMSO and further diluted by triple distilled sterilized water, so that the DMSO content in cell culture medium was not higher than 3%.

2.4. Cell Viability Assay. Cell viability was measured by the 3-(4,5-dimethylthiazol-2-yl)-5-(3-carboxymethoxyphenyl)-2-(4-sulfophenyl)-2H-tetrazolium, inner salt (MTS, 3582, Promega), which monitors cell growth in response to treatment at certain time points. A375 cells (3000 per well) were seeded into 96-well plates and incubated overnight. Cells were then treated with various concentrations of BR and UVA alone or in combinations for times indicated. After that, cells were washed twice with PBS and 100 μL MTS prepared in 10% DMEM was added and incubated for 2 hours to read the OD values at 490 nm.

2.5. Western Blot Assay. A375 cells were cultured for 24–30 h and treated with either UVA or BR or both for the indicated times. After specific time points, treated/nontreated cells were lysed in RIPA lysis buffer (Beyotime, P0013B). To detect the phosphorylation status of various proteins, cell lysates were prepared and extracted with SDS lysis buffer (Beyotime, P0013G), in the presence of 1 mM phenylmethylsulfonyl fluoride (Beyotime, ST506). Protein concentrations were measured by using the BCA protein assay kit (Beyotime, P0010), and 50 μg protein per lane was separated by SDS-PAGE and transferred to polyvinylidene difluoride membranes (PVDF). After transfer, membranes were blocked with 5% nonfat milk in TBST for 1 hour at 37°C and incubated with the respective primary antibodies overnight at 4°C. Membranes were washed three times with 1X-TBST and incubated with horseradish peroxidase-conjugated secondary antibodies. The signals were recorded by ECL reagent (Thermo Scientific) and visualized by VersaDoc imaging system (Bio-Rad, USA).

2.6. Immunofluorescence Staining with FITC and Costaining with DAPI. Cells cultured in 24-well plates were washed three times with PBS and fixed with 4% formaldehyde for 20 minutes, followed by permeabilization using 0.1% Triton X-100 in PBS for 10 minutes. After washing with PBS, cells were blocked with 1% BSA 20 minutes at room temperature. The following operations were carried out in the dark: to each well, 200 μl FITC (diluted to 1 : 30) was added and incubated for 1 hour at room temperature. After washing with PBS three times, 1 mg/ml DAPI (in 200 μl) was incubated for 20 minutes. After washing with PBS twice, cells were mounted and analyzed under a fluorescence microscope.

2.7. Flow Cytometry and Cell Cycle Analysis. A375 cells were treated with BR and UVA, and apoptotic cells were detected using an Annexin V-FITC Apoptosis Detection Kit (Beyotime), followed by flow cytometry. For cell cycle analysis, A375 cells were treated with either BR or UVA or both, fixed with 70% ethanol, incubated with propidium iodide (PI) and RNase A mixture, and analyzed by flow cytometry (Becton Dickinson, USA).

2.8. Xenograft Assay in Nude Mice. Athymic nude (*nu*/*nu*) mice were obtained from Chongqing Medical University. 4-week-old male mice were injected with A375 cells (3×10^6 cells) in the right flanks into the subdermal space. Tumor volumes were estimated every other day by caliper measurements, and tumor volumes were calculated by the formula (volume = tumor length in mm $\times$ width^2 in mm $\times$ 0.5236). Once tumors reached a mean volume of 30–50 mm^3, mice were randomly allocated into four groups and treated with either DMSO or BR (2 mg/kg) or UVA (75 kJ/m^2) and in combination of BR and UVA every other day for seven days. Mice were sacrificed, and tumors were dissected. Formalin-fixed, paraffin-embedded tumor tissue sections were used for IHC, whereas snap-frozen tissues were subjected to Western blot analysis.

2.9. qRT-PCR. Incubation of A375 cells was performed with UVA, BR, or both for times indicated. Treated cells were lysed with TRIzol (Takara) for total RNA purification. Reverse transcription was performed using Go Script™ Reverse Transcription System (Promega). The qPCR analysis was performed by using a RT^2 SYBR Green/Fluorescein PCR Master Mix (Promega) on an iQ5 real-time PCR system (Bio-Rad) with oligonucleotide primer pairs to detect various genes. All samples were normalized to GAPDH mRNA levels, and relative mRNA expressions were analyzed using $2-^{\triangle\triangle Ct}$ method as described previously [41].

2.10. Colony Formation Assay. A375 cells were plated at densities of 500 cells per well in 6-well plates. After 24 hours of incubation, cells were exposed to UVA (75 kJ/m^2) and/or BR (50 nM) and the colonies formed were photographed after one week. Colonies were confirmed only if a single clone contained more than 50 cells. Fresh DMEM (10% FBS) was replaced every 72 hours.

2.11. Statistical Analysis. All experiments were performed three times in independent experiments to obtain reproducible results. Statistical data were subjected to analysis of variance (ANOVA) following Tukey's test to analyze the differences. A P value of <0.05 was considered as statistically significant.

3. Results

3.1. Low-Dose UVA Modulates the Expression of Phase II Detoxification Enzyme. To explore the effect of UVA on growth of melanoma cells, A375 melanoma cells were treated with different doses of UVA. Low dose of UVA irradiation did not significantly affect survival of cells at UVA doses of up to 100 kJ/m^2 (Figure 1(a)). Western blot results showed that these doses of UVA irradiation induced the expression of Nrf2, HO-1, and GSTP1 proteins, with slight induction of NQO1 protein (Figure 1(b)). We chose the low dose of 75 kJ/m^2 for the following experiments since cell survival at this dose was not affected but caused an increase in the

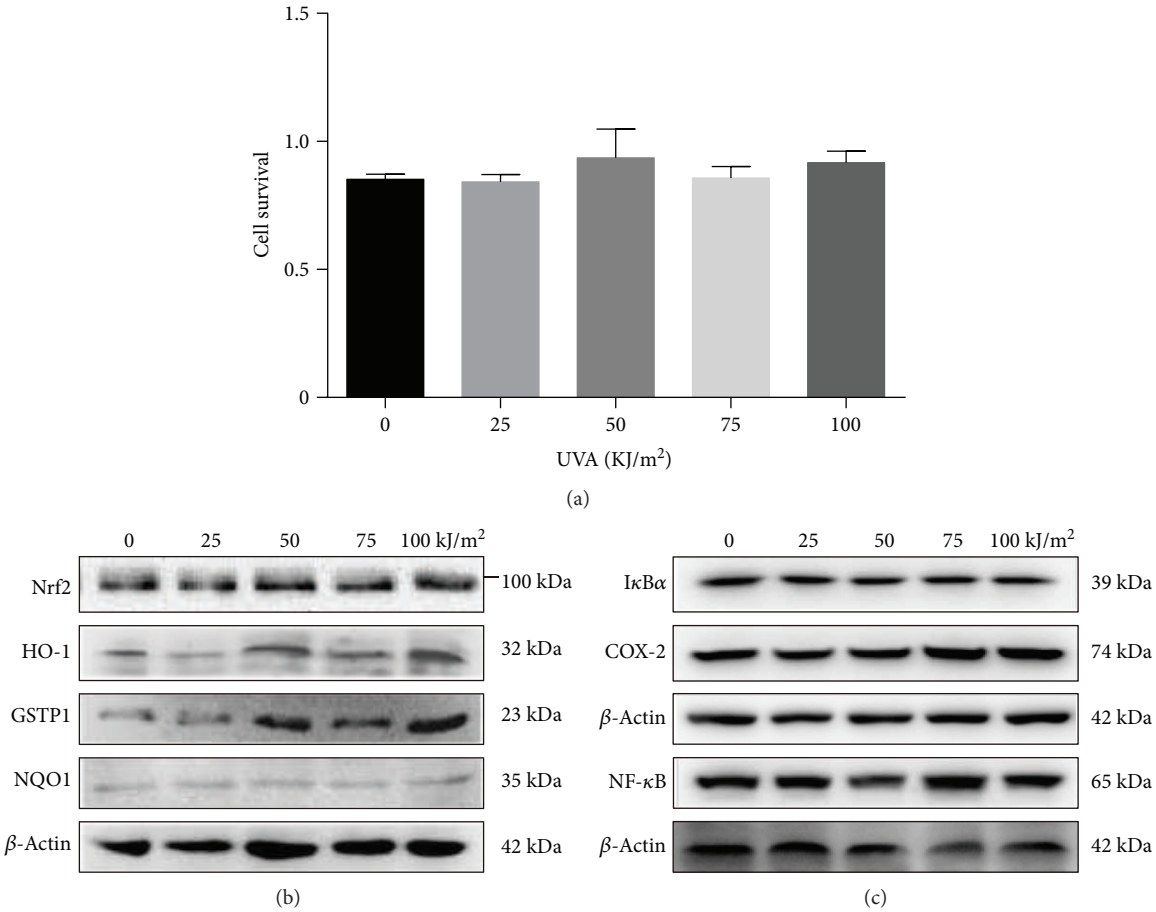

Figure 1: Low-dose UVA can modulate the expression of phase II detoxification enzymes. (a) A375 cells were plated overnight and irradiated with different doses of UVA, and cell survival was determined 24 hours after UVA irradiation. (b and c) Cells were treated with UVA in the range of 0–100 kJ/m^2 for 24 hours. Total cell extracts were prepared for 24 hours following UVA irradiation and subjected to Western blot using antibodies for Nrf2, HO-1, NQO1, GSTP1, IκBα, COX2, NF-κB, and actin. We received a similar result in three independent experiments.

protein levels of HO-1 and a slight increase of the GSTP1 and NQO1 (Figure 1(b)).

Nrf2 and NF-κB are transcription factors. It was previously reported that Nrf2 and NF-κB simultaneously accumulate in the cell nucleus and NF-κB (p65) antagonizes Nrf2-induced gene transcription [42]. Conversely, some phase II-inducers (enzyme) activate the signaling and inhibit NF-κB pathway [43]. To understand the relationship between Nrf2 and NF-κB in our experimental setup, we analyzed the NF-κB signaling pathway by Western blot assay. NF-κB and COX2 expression were slightly increased following UVA irradiation in a dose-dependent manner (Figure 1(c)). However, the levels of IκBα as NF-κB target proteins were not affected by UVA irradiation (Figure 1(c)), indicating that this low-dose UVA irradiation does not significantly affect the NF-κB signaling pathway.

3.2. BR Potentially Inhibits the Nrf2 Signaling Pathway. First, we examined the effect of BR on cell viability. A375 cells were treated with a concentration range of BR (0–100 nM), and the proliferation rates of A375 cell were slightly reduced in a dose-dependent manner (Figure 2(a)). To confirm that BR inhibits the Nrf2 pathway in A375 cells, whole-cell lysates were collected and protein expression levels were determined by Western blotting after treatment with BR. After 24 hours, BR caused a reduction of Nrf2 and GSTP1 protein levels in a concentration-dependent manner, whereas the levels of NQO1 remained relatively unchanged (Figure 2(b), right).

A time course of BR (50 nM) treatment of A375 cells showed an effect on the Nrf2 pathway and revealed that Nrf2 protein levels were significantly decreased at 2, 4, and 24 hours following the addition of BR, with maximal reduction at 4 hours (Figure 2(b), left). Significant changes in downstream targets of Nrf2, that is, HO-1 and NQO1, were not observed over the time course, whereas only a slight reduction in GSTP1 was observed (Figure 2(b), left). Further, we did not find that 50 nM BR had an effect on NF-κB and IκBα, whereas the COX2 protein levels were slightly increased compared to controls (Figure 2(c)). A previous study demonstrated that BR induces activation of NF-κB in HL-60 cell [44]. This difference in NF-κB activation is most likely due to a cell line-specific effect, and a concentration of 50 nM BR is required for this effect. These results suggest

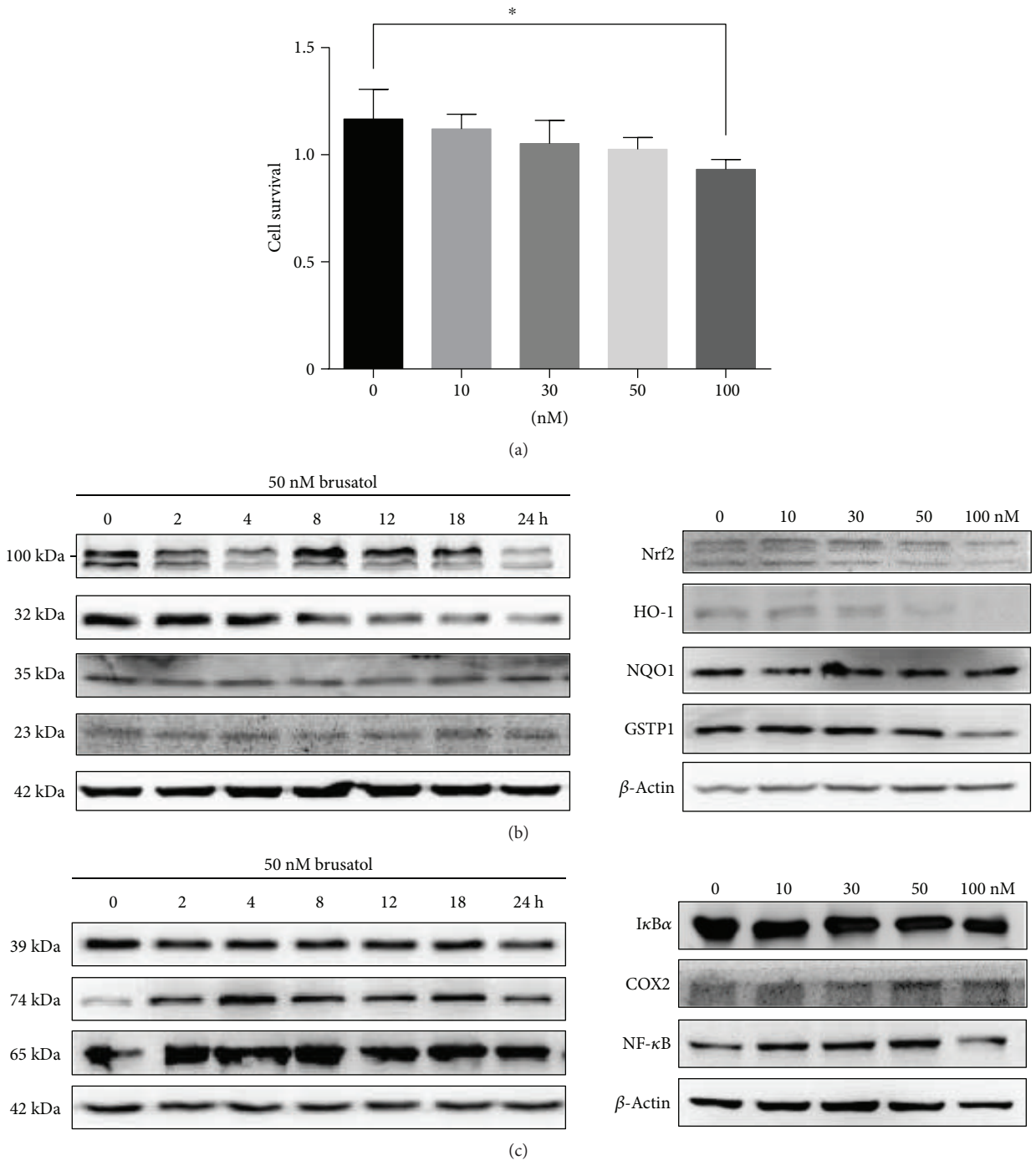

FIGURE 2: BR specifically inhibits the Nrf2 signaling pathway. A375 cells were treated with BR for 24 hours. (a) Cell survival was assessed using an MTS assay. (b and c) Cells were treated with various concentrations of BR for 24 hours ((b), right; (c) right) or with 50 nM BR for different time interval as indicated ((b), left; (c) left). Total cell extracts were prepared and subjected to Western blot using antibodies for Nrf2, HO-1, NQO1, GSTP1, IκBα, COX2, NF-κB, and actin. Data in (a) are shown as mean ± SD; $^*P < 0.032$. P values are based on control versus treatment.

that the predominant effect of BR in A375 cells is a potential inhibition of the Nrf2 signaling pathway.

3.3. Cotreatment Increases Intracellular ROS Level and Inhibits A375 Cell Growth and Proliferation. We hypothesize that a relatively low-dose UVA irradiation of 75 kJ/m^2 combined with 50 nM BR can affect cell survival in A375 cells. Therefore, we addressed the question whether cotreatment with UVA and BR resulted in lower cell survival in conjunction with elevated intracellular ROS levels and hence an increased sensitivity to BR treatment. Intracellular ROS levels were measured in A375 cells using flow cytometry. Low-dose

UVA-treated A375 cells displayed slightly increased ROS levels compared to nontreated cells. Likewise, BR treatment increased intracellular ROS levels slightly, so that cotreatment further increased ROS levels (Figure 3(c)). To determine the efficacy of BR and UVA on cell growth, A375 cells were treated with BR or UVA and cell proliferation were counted by MTS. As shown in Figures 3(a) and 3(b), combination treatment significantly suppressed cell proliferation. We also check the proliferation marker Ki67 in BR- or UVA-treated cells, and the results were similar as that for cell survival (Supplementary Figure 1).

Furthermore, the cell cycle of A375 cells was analyzed by flow cytometry to examine whether cotreatment inhibits cell proliferation by inducing a cell cycle arrest. UVA treatment plus BR resulted in a marked increase in the percentage of A375 cells in the G1 phase (Figures 3(d) and 3(e)). To confirm these results, we analyzed the mRNA levels of cyclinD1, cyclinE2, CDK2, CDK4, and CDK6 which could promote A375 cells to pass the G1 to S phase checkpoint. We found that cyclinD1, cyclinE2, CDK4, and CDK6 were reduced following UVA/BR cotreatment, while CDK2 expression was increased (Figure 3(f)) at gene expression level, but this gene expression was different in translational level. Immunoblot assays revealed that cylinE2 and CDK2 were slightly decreased following UVA/BR cotreatment, but no significant change was seen in cyclinD1 expression (Figure 3(g)). Collectively, these results suggest that UVA is able to enhance BR-induced ROS levels and affects cell survival and the regulation of cell cycle-related proteins.

3.4. Cotreatment Blocks Nrf2 and AKT Signaling through Enhanced Cell Apoptosis. To explore whether the observed reduced cell viability of A375 cells was due to apoptosis, A375 melanoma cells and HaCaT skin keratinocytes were stained with Annexin V-FITC and PI and analyzed by flow cytometry. The results showed that HaCaT cells do not exert significant apoptosis after treatment with either BR alone or cotreatment under this condition (Supplementary Figure 2). In contrast, BR or cotreatment in A375 cells leads to significant apoptosis detected 24 hours post treatment, with a higher apoptosis rate in A375 cells after cotreatment (Figures 4(a) and 4(b)). Furthermore, UVA/BR cotreatment markedly suppressed protein levels of Bcl-2 and Bcl-xl and increased the expression levels of Bax. Consistent with these findings, UVA/BR cotreatment causes cleavage and activation of caspase-3, clearly indicating a marked increase in apoptosis rate (Figures 4(c) and 4(d)).

To evaluate the effect of cotreatment on the Nrf2 pathway in the presence of UVA, we performed immunoblot assays to detect protein levels of Nrf2 and its downstream genes. The expression levels of Nrf2, HO-1, and GSTP1 were decreased 24 hours following cotreatment compared with UVA or BR single treatment (Figure 4(e)). In addition, we found that AKT phosphorylation at position Ser473 was markedly reduced 24 hours after application of UVA/BR, whereas total AKT was not significantly changed (Figure 4(e)). These results indicate that cotreatment in A375 inhibits/AKT signaling while inhibiting Nrf2 expression. Similar results were obtained with camptothecin as another potential inhibitor of Nrf2 (data not shown) [45, 46].

3.5. Combination Treatment Inhibited Tumor Growth in Mice. Since the observed apoptosis induction by combined treatment with UVA/BR occurs in melanoma cells, but not in skin keratinocytes (HaCaT cells) under these conditions (data not show), we addressed the question whether a combination of UVA and BR can affect cell proliferation in melanoma-derived tumors *in vitro* and *in vivo* (Figure 5). For assessment of tumor growth in vitro, a colony formation assay was performed. Both BR alone and in combination with UVA reduced the number of colonies formed, while UVA has no significant effect on colony formation (Figures 5(a) and 5(b)). To explore the effect of UVA/BR cotreatment on tumor growth *in vivo*, A375 xenografts were grown in NOD/SCID mice as a heterotopic tumor model. NOD/SCID mice were injected with A375 cells (3×10^6 per injection site) to form a tumor. After 18 days, tumors reached volumes of about 30 to 50 mm^3 and UVA (75 KJ/m^2) irradiation or BR (2 mg/kg) was administered intraperitoneally every other day for 10 days [47]. Mice were covered with silver paper, contact and irradiate the tumors using a UVA lamp, and tumor growth was observed for 5 days after cessation of treatment. We observed a significant inhibition of tumor growth *in vivo* after cotreatment (Figures 5(c) and 5(d)) that was significantly higher than after single treatments of the tumors. Moreover, in one out of four cases treated with BR alone, a complete remission of the tumor and in two cases after UVA/BR cotreatment was observed. These observations demonstrate that cotreatment of melanoma-derived tumors reduced the tumor growth *in vivo*.

3.6. UVA Enhances Nrf2 Knockout-Mediated Cell Suppression. In addition to the pharmacological inhibition of Nrf2 using BR, we examined the effect of a genetic knockout of Nrf2 in A375 cells using the CRISPR/Cas9 method. Cas9 plasmids that expressed Nrf2 gRNA sequences against Nrf2 were used, and the clone number 1 identified bearing the knockdown, and $Nrf2^{-/-}$ clone number 2 exhibited the most significant reduction of Nrf2 protein expression (Figure 6(a)). Therefore, subsequent experiments were performed with this cell clone named $Nrf2^{-/-}$ while Cas9 clones of A375 cells were used as a control cell line for the knockout cell line. First, we determined whether UVA enhances intracellular ROS in A375 Nrf2 knockout cells leading to increased sensitivity against UVA treatment. Furthermore, we investigated intracellular ROS levels in $Nrf2^{-/-}$ cells following UVA irradiation and observed increased ROS levels compared to $Nrf2^{-/-}$ cells (Figure 6(b)).

To determine the efficacy of UVA on cell growth in $Nrf2^{-/-}$ cells, cells were treated with UVA (75 kJ/m^2) and cell proliferation was quantified by MTS (Figure 6(c)). UVA irradiation suppressed proliferation of $Nrf2^{-/-}$ cells at 48 hours when compared to sham control, and the result of $Nrf2^{-/-}$ number 1 similar to $Nrf2^{-/-}$ number 2 (Supplementary Figures 3A and 3C). Furthermore, flow cytometry was used to examine whether UVA irradiation inhibits proliferation

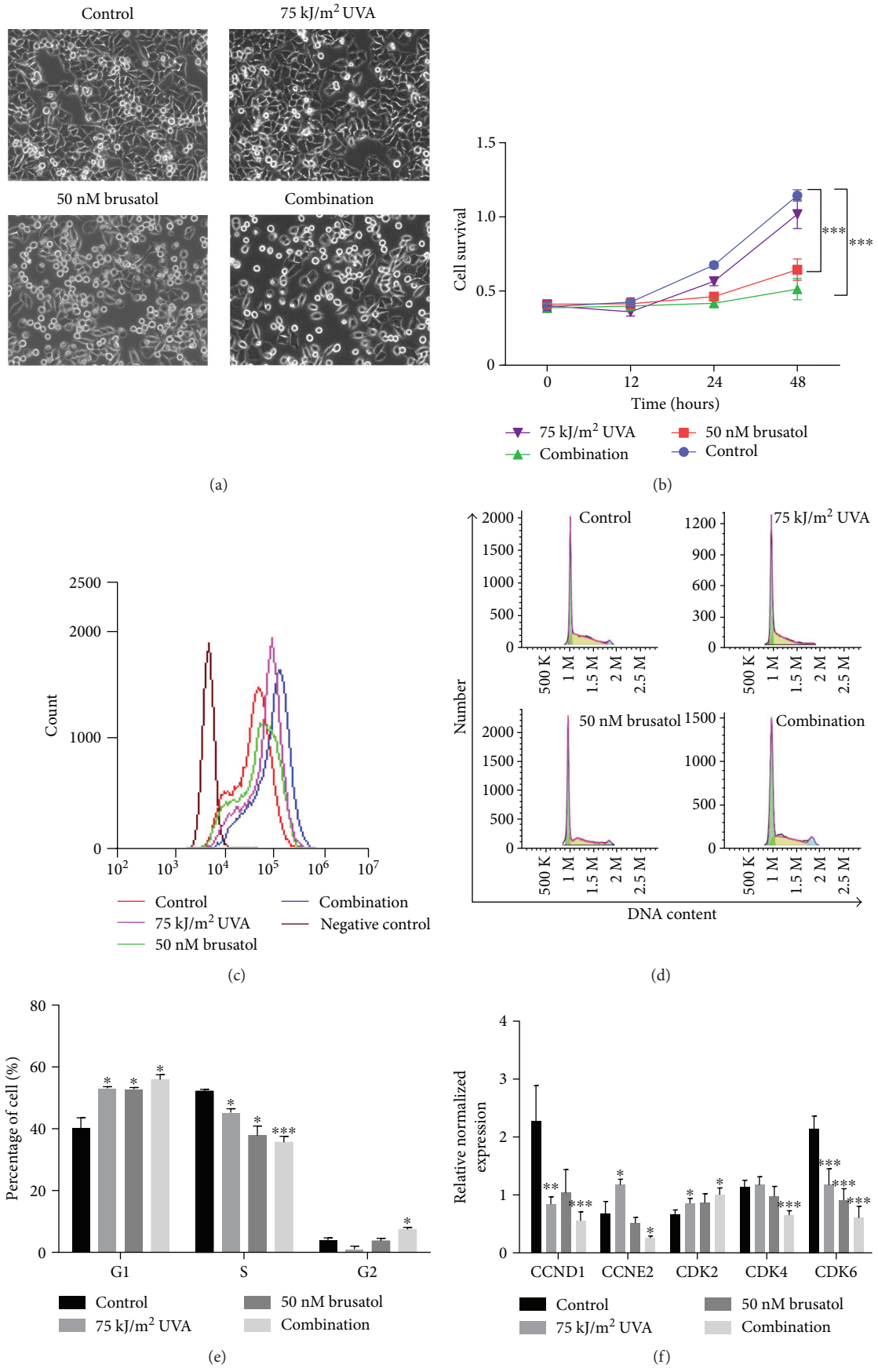

Figure 3: Continued.

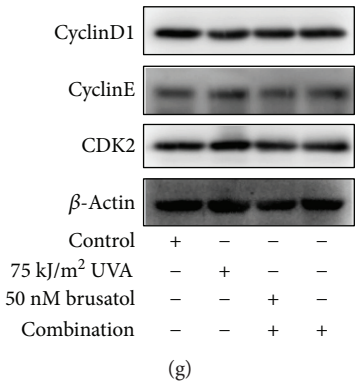

(g)

Figure 3: Cotreatment increases intracellular ROS level and inhibits A375 cell growth and proliferation. (a) A375 cells were treated with UVA and BR for 24 hours. Cell morphology was observed, and cell survival analyses were performed by an MTS assay (b). Cell cycle analysis by PI staining (d and e) and cell cycle-related genes cyclinD1, cyclinE2, CDK2, CDK4, and CDK6 were performed by qRT-PCR assay (f). (c) A375 cells were pretreated with BR for 2 hours prior to UVA exposure and were then irradiated with low-dose UVA (75 kJ/m^2). ROS levels were determined by flow cytometry immediately following UVA irradiation. All data are shown as the mean ± SD; $^*P < 0.05$, $^{**}P < 0.01$, and $^{***}P < 0.001$. All P values are based on analysis control versus treatment.

of Nrf2$^{-/-}$ cells by inducing cell cycle arrest. Representative histograms and combined results are summarized (Figures 6(d) and 6(e)). UVA treatment resulted in a marked increase of the percentage of G1 phase in Nrf2$^{-/-}$ cells at 48 hours (Figures 6(d) and 6(e)). To explore whether the reduced cell viability was due to apoptosis, Nrf2$^{-/-}$ cells were irradiated with UVA and flow cytometer analysis revealed no increase in apoptosis in Nrf2$^{-/-}$ cells (Figure 6(f)). To further assess the effect of UVA irradiation on Nrf2$^{-/-}$ cell proliferation, a colony formation assay was conducted. UVA irradiation has no effect on colony formation in Nrf2$^{-/-}$ cells (Figure 6(g)), and we also get the similar results in Nrf2$^{-/-}$ number 1 cell (Supplementary Figure 3B). These results demonstrate that this dose of UVA mediates cell suppression, but not apoptosis in Nrf2$^{-/-}$ cells. Previous studies suggested that 150 kJ/m^2 UVA irradiation induced cell death in Nrf2-deficient murine dermal fibroblasts [33]. The different results may due to a difference in UVA dose (75 kJ/m^2) applied in our study and to the variable UVA response in different cell lines.

4. Discussion

Nrf2 is a key player of the cellular defense against endogenous and exogenous chemical and oxidative insults. Exposure to chemicals may cause organ damage, so that the lung, liver, and kidney are significantly more affected in Nrf2 knockout mice than in their latter controls [48], hence made them highly prone to develop oxidative damage-related diseases and cancers. Moreover, Nrf2 has been proposed as an effective target for cancer chemoprevention and chemoresistance due to its linkage to pathways such as NF-κB pathway [49]. Recently, some studies reported that BR provokes a rapid and transient inhibition of Nrf2 signaling and sensitizes hepatoma cells to chemical toxicity [13]. As demonstrated, increased levels of Nrf2 contribute to resistance in therapies (radio- and chemotherapy) in breast and lung cancer [49]; on the contrary, inhibition of Nrf2 may lead to enhanced efficacy of photo- or chemotherapy. In this study, we have shown that UVA enhances BR chemosensitivity in an additive fashion and that cotreatment inhibits cell proliferation and induces apoptosis *in vitro* and ameliorates melanoma growth *in vivo*.

BR is a broad spectrum anti-inflammatory agent that stabilizes lysosomal membranes, thereby reducing the release of hydrolytic enzymes that cause damage to surrounding tissues [50]. The anticancer properties of BR were demonstrated in lymphocytic leukemia, Ehrlich carcinoma, and hepatoma [51–53] and are mainly due to a significant inhibition of chemoresistance-mediating Nrf2 gene and the resulting downstream target genes, thereby sensitizing tumor cells to chemo- and phototherapy [30, 31, 37]. Previously, it was reported that low concentrations of BR may inhibit general protein synthesis, but more recently, it was shown that BR acts as a Nrf2 pathway-specific inhibitor when used in an upper nanomolar range [19, 48, 53]. Here, we also demonstrated that BR when used in A375 melanoma cells in a range of 10–100 nM, specifically downregulated the protein level of Nrf2 and its target genes. Despite a moderate reduction of HO-1 and NQO1, we did not find a significant effect on the NF-κB and its target genes.

UVA can penetrate deeply into the subcutaneous layer and primarily induces cellular responses through oxidative stress (ROS) triggered by endogenous photosensitization of the drug. UVA alone or in combination with photoreactive drugs can lead to ROS-mediated damage of biomolecules including DNA [54]. For instance, psoralen plus UVA (PUVA), a nontoxic photoreactive drug, is activated by subsequent exposure to UVA light, which causes extensive DNA damage leading to extensive tumor cell death, and clinically used to treat psoriasis as well as head and neck cancers [39, 55]. Recently, berberine has been reported to be a photosensitive drug and can be used in photodynamic therapy (PDT) to treat cancer cells, where the photosensitive drug is activated upon exposure to UVA, causing massive DNA strand breaks in tumor cells [56]. In addition, low concentration of S^{4}TdR when combined with nonlethal doses of UVA kills hyperproliferative or cancerous skin cells [39].

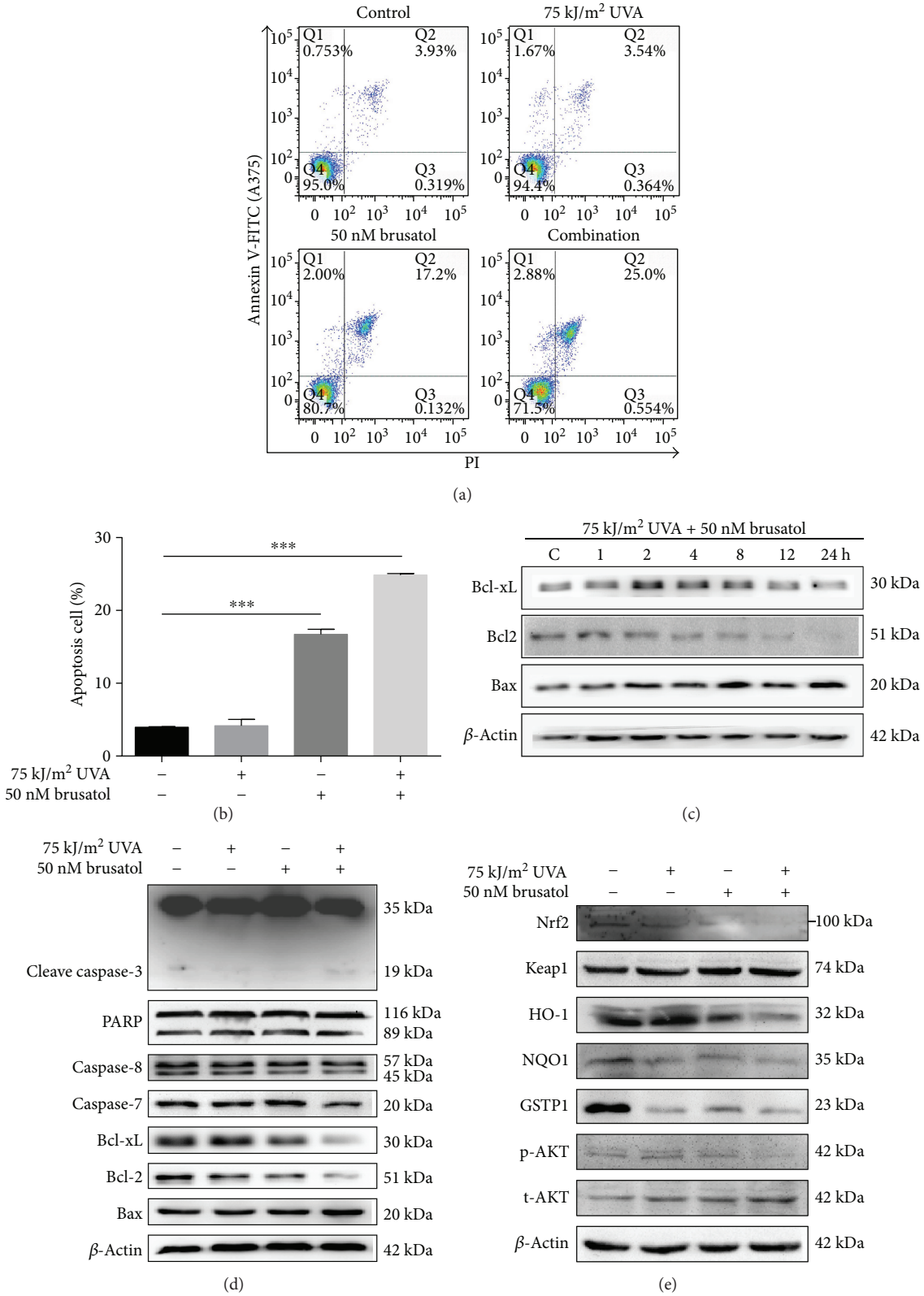

Figure 4: Cotreatment inhibits Nrf2 and AKT pathways and leads to apoptosis in A375 cells. (a and b) A375 cells were treated with UVA and BR for 24 hours before measuring apoptosis using Annexin V and PI in conjunction with flow cytometry. (c and d) Whole-cell lysates from A375 cells were prepared and subjected to immunoblotting using antibodies against Bcl-2 family proteins, PARP, cleaved caspase-3 (C-caspase3), caspase7, caspase8, and actin. Cells were treated with UVA, BR, or both for 24 hours or different time intervals as indicated. (e) Immunoblot analysis using antibody against Nrf2 pathway proteins, AKT and p-AKT protein from A375 cell lysates. $^{*}P < 0.05$, $^{**}P < 0.01$, and $^{***}P < 0.001$. All P values are based on analysis control versus treatment.

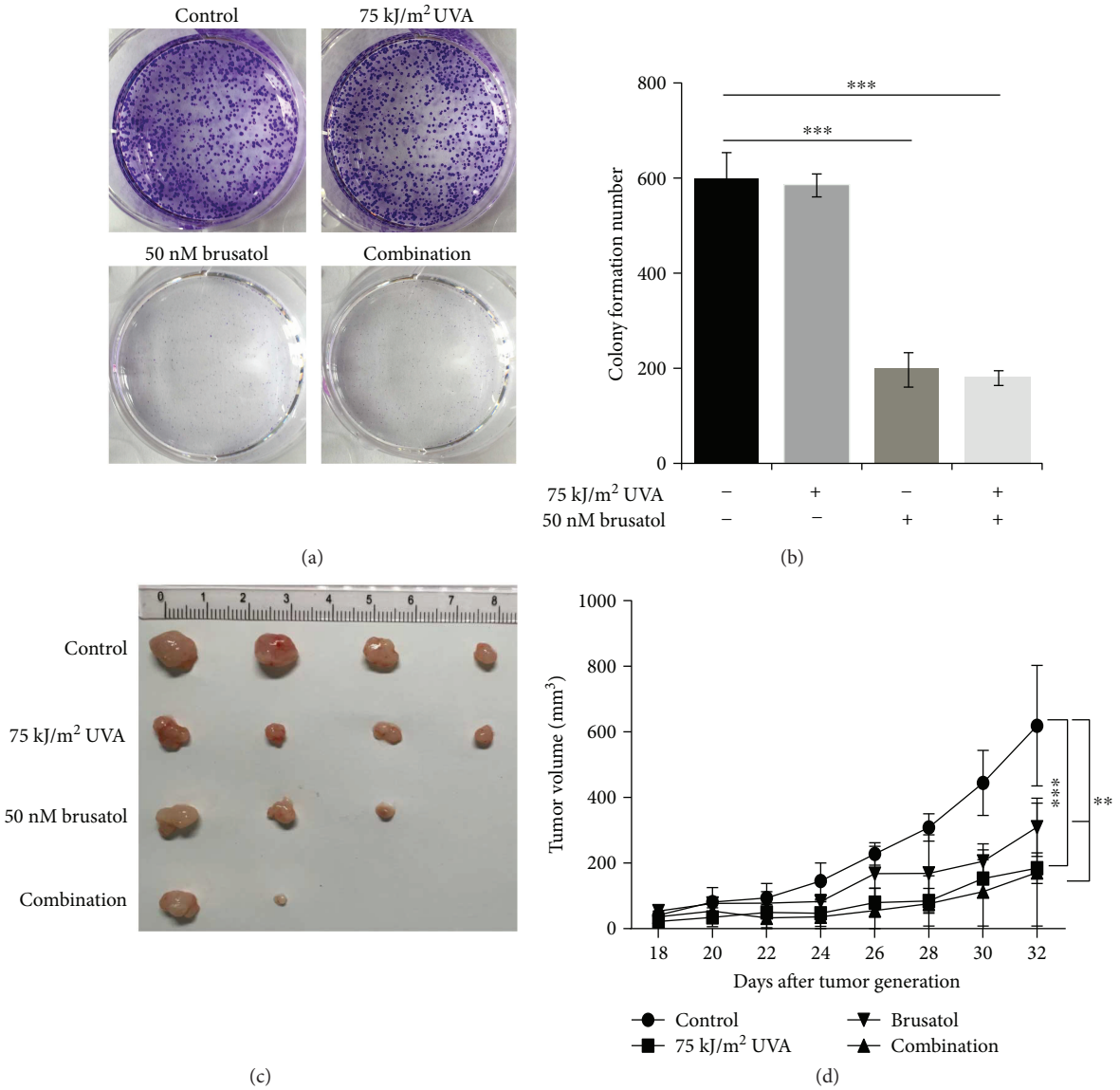

Figure 5: Cotreatment causes reduction of melanoma cell-derived tumors *in vivo*. (a and b) A375 cells were treated with UVA and BR for 7 days. At days 2, 4, and 6, UVA and BR treatment was repeated. After 7 days, colony formation was examined by staining the resulting colonies with crystal violet. Colonies with more than 50 cells were counted ($n = 3$). (c) A375 cells (3.0×10^6) were injected subcutaneously into the right flank of 4-week-old male nude mice ($n = 4$ for each group). When tumor size reached 30~50 mm^3, intraperitoneal injections of BR (2 mg/kg) or irradiation with UVA (75 kJ/m^2) or with both were administered every other day for five times. (d) Xenograft tumor sizes were measured after mice bearing tumors were treated with either vehicle (control), UVA alone, BR (2 mg/kg), or with a combination of UVA and BR for 10 days ($n = 4$). All data are shown as the mean ± SD; $^{**}P < 0.01$ and $^{***}P < 0.001$. All P values are based on the analysis of control tumors versus treated ones.

In this study, we found that cotreatment (UVA + BR) elevated intracellular ROS and induced the Akt pathway by inhibition of Akt phosphorylation at Ser473 [57]. The Akt/PI3K pathway forms an important component of cell survival mechanisms [58, 59], and previous reports demonstrated functional interactions with Nrf2 activation [60–62]. Similarly, our results revealed that Akt phosphorylation was decreased with Nrf2 suppression in A375 cells with cotreatment.

Previously, it was demonstrated that a decrease in Nrf2 activity is associated with chemotherapeutic efficacy in mice after chronic administration of BR [30, 31]. We found that either BR alone or in a regimen with UVA and BR abolished the clonogenicity of melanoma cells. The tumor xenograft experiments in nude mice revealed that unlike cotreatment, treatment of either UVA or BR alone has an inhibitory effect on melanoma growth. However, Zhang and colleagues found that cisplatin or BR alone showed no significant inhibition of tumor growth in A549 xenografts. The difference in our results may be due to the experimental conditions or in the cell lines used.

We conclude that UVA/BR cotreatment inhibited melanoma cell growth and proliferation both *in vitro* and

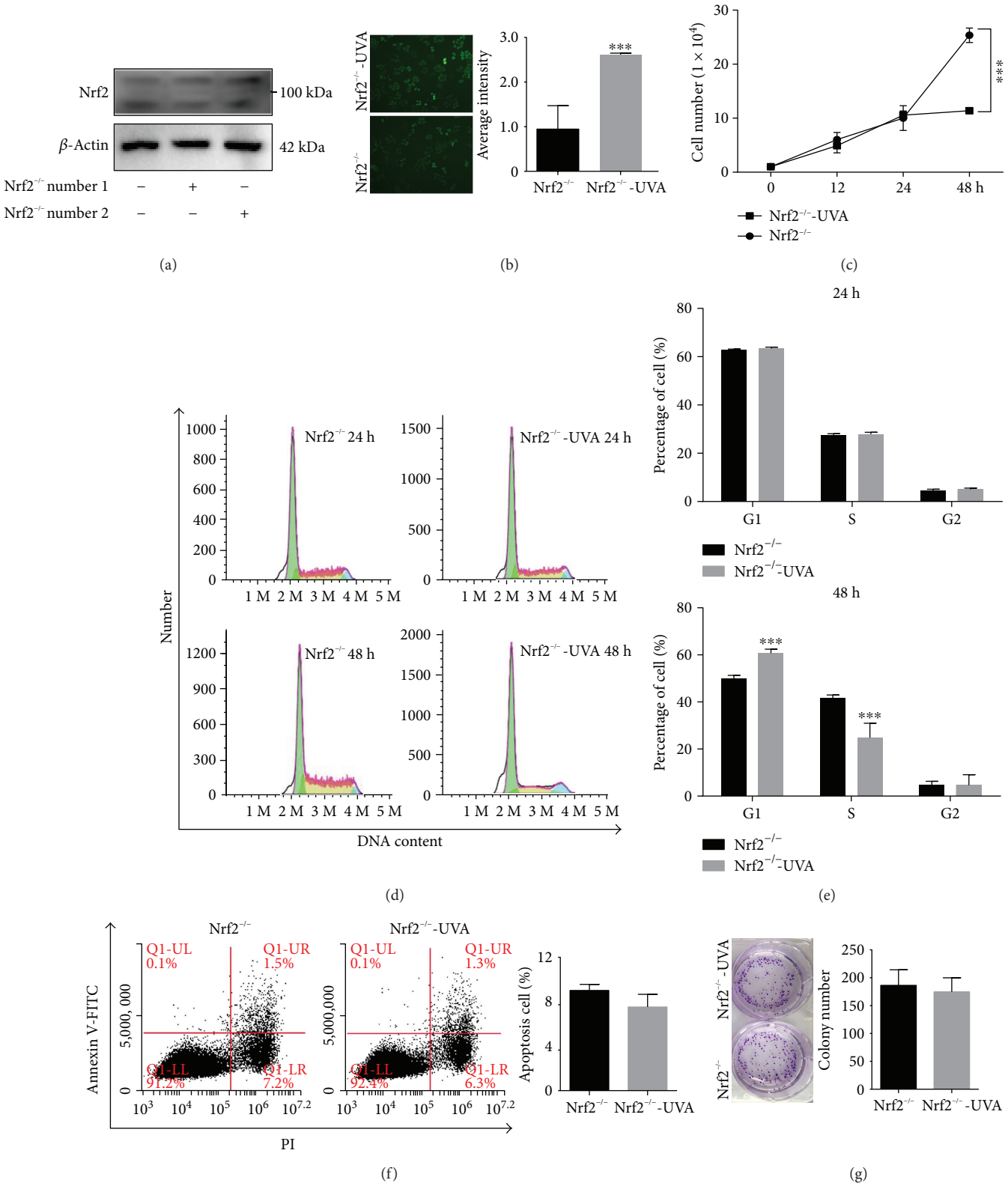

Figure 6: UVA irradiation leads to suppression of A375 Nrf2 knockout cells. (a) Western blot assay was used to analyze protein expression levels of Nrf2 in A375 cells. (b) DCFH-DA-based ROS quantification. (c) A375 $Nrf2^{-/-}$ irradiated with 75 kJ/m^2 UVA, followed by MTS assay (d) cell cycle analysis by PI staining after 24 and 48 hours. (f) Apoptosis assay using Annexin V and PI to analyzed $Nrf2^{-/-}$ cells after 48 hours irradiation. (g) Colony formation was examined by staining colonies with crystal violet. Colonies with more than 50 cells were counted ($n = 3$). $^{***}P < 0.001$.

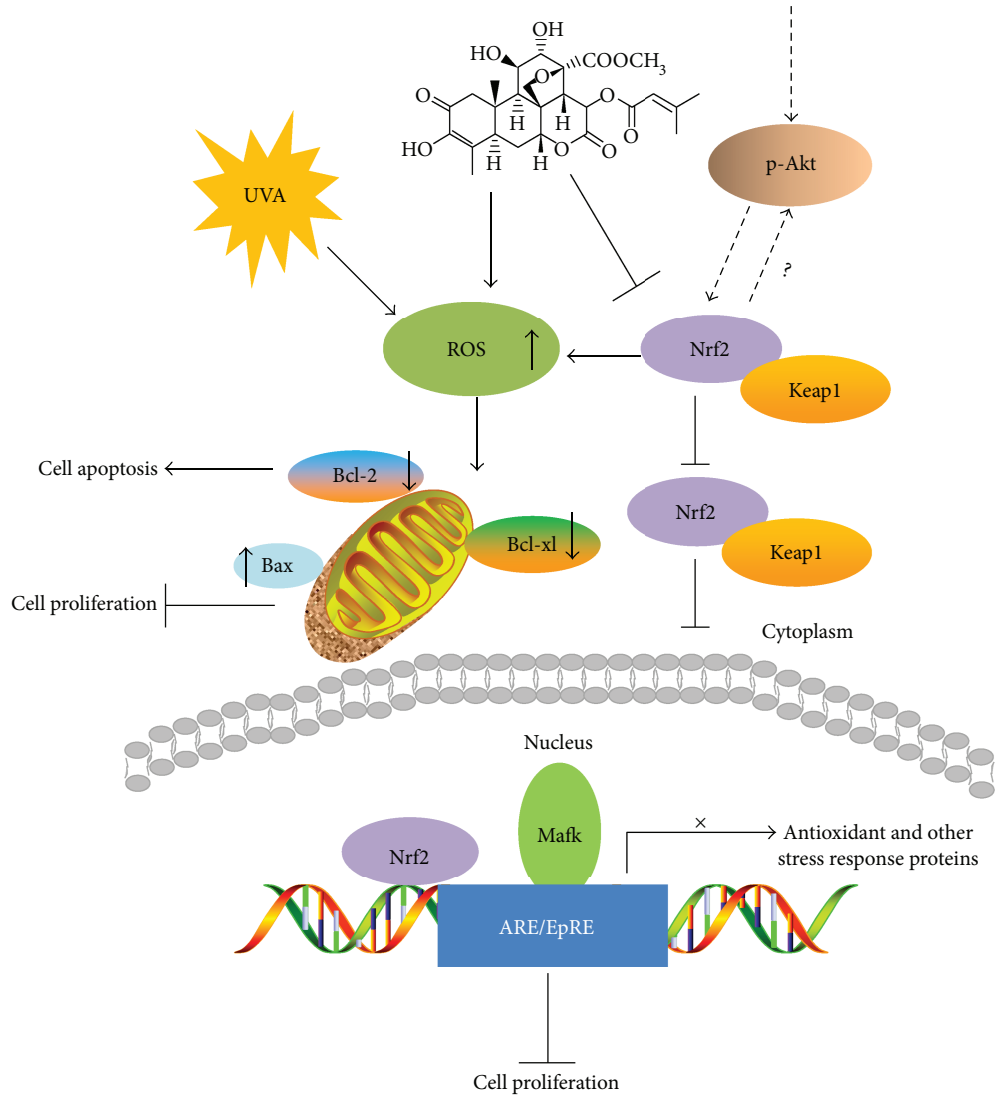

Figure 7: Schematic representation of combination- (UVA and brusatol) induced Nrf2 suppression in A375 cells.

in vivo. Furthermore, we identified the AKT-Nrf2 pathway as mechanistically relevant for the observed antitumor effect of UVA and BR when both are combined. Therefore, we propose the usage of UVA and BR in combination as a novel treatment regimen for malignant melanomas thereby causing a prominent antitumor effect via regulation of AKT-Nrf2 pathway (summarized in Figure 7).

Conflicts of Interest

The authors declare no conflict of interest.

Acknowledgments

This work was supported by the National Natural Science Foundation of China (81271776 and 81573073), Chongqing Municipal Key Laboratory of Oral Biomedical Engineering of Higher Education (ODBS-2014-004), and Graduate Student Research Innovation Project (CYB16040). The authors thank Professor Xianjun Qu, Capital Medical University, for the useful discussion.

Supplementary Materials

Supplementary Figure 1: cotreatment inhibited Ki67 expression. Immunofluorescence assay was used to analyze cell proliferation marker Ki67 and its expression in UVA- and BR-treated cells for 48 hours. Supplementary Figure 2: cotreatment has no effect on keratinocyte apoptosis. (A and B) Keratinocyte HaCaT cells were treated with UVA and BR for 24 hours before measuring apoptosis using Annexin V and PI in conjunction with flow cytometry. Supplementary Figure 3: UVA irradiation inhibited $Nrf2^{-/-}$ number 1 A375 cell proliferation. (A) A375 $Nrf2^{-/-}$ number 1 irradiated with 75 kJ/m2 UVA, followed by MTS assay. (B) Cell cycle-related genes cyclinE2, CDK4, and CDK6 were performed by qRT-PCR assay. (C) Colony formation was examined by staining colonies with crystal violet. Colonies with more than 50 cells were counted ($n = 3$). *(Supplementary Materials)*

References

[1] J. Mounessa, T. Buntinx-Krieg, R. Qin, C. A. Dunnick, and R. P. Dellavalle, "Primary and secondary chemoprevention of malignant melanoma," *American Journal of Clinical Dermatology*, vol. 17, no. 6, pp. 625–634, 2016.

[2] M. Constantinou, "Melanoma genomics and immunotherapy," *Rhode Island Medical Journal*, vol. 98, no. 11, pp. 31–34, 2015.

[3] H. Swalwell, J. Latimer, R. M. Haywood, and M. A. Birch-Machin, "Investigating the role of melanin in UVA/UVB- and hydrogen peroxide-induced cellular and mitochondrial ROS production and mitochondrial DNA damage in human melanoma cells," *Free Radical Biology & Medicine*, vol. 52, no. 3, pp. 626–634, 2012.

[4] G. Merlino, M. Herlyn, D. E. Fisher et al., "The state of melanoma: challenges and opportunities," *Pigment Cell & Melanoma Research*, vol. 29, no. 4, pp. 404–416, 2016.

[5] K. E. Mercer and C. A. Pritchard, "Raf proteins and cancer: B-Raf is identified as a mutational target," *Biochimica et Biophysica Acta (BBA) - Reviews on Cancer*, vol. 1653, no. 1, pp. 25–40, 2003.

[6] M. Maroti, E. Ulff, J. Lyth, and U. Falkmer, "A prospective population-based study, aiming to support decision-making in a follow-up programme for patients with cutaneous malignant melanoma, based on patterns of recurrence," *European Journal of Dermatology*, vol. 26, no. 6, pp. 586–591, 2016.

[7] S. Mourah and C. Lebbe, "Molecular alterations in melanoma and targeted therapies," *Bulletin du Cancer*, vol. 101, Supplement 2, pp. S5–S11, 2014.

[8] H. R. Hintsala, E. Jokinen, K. M. Haapasaari et al., "Nrf2/Keap1 pathway and expression of oxidative stress lesions 8-hydroxy-2′-deoxyguanosine and nitrotyrosine in melanoma," *Anticancer Research*, vol. 36, no. 4, pp. 1497–1506, 2016.

[9] S. Reuter, S. C. Gupta, M. M. Chaturvedi, and B. B. Aggarwal, "Oxidative stress, inflammation, and cancer: how are they linked?," *Free Radical Biology & Medicine*, vol. 49, no. 11, pp. 1603–1616, 2010.

[10] X. F. Hu, J. Yao, S. G. Gao et al., "Nrf2 overexpression predicts prognosis and 5-FU resistance in gastric cancer," *Asian Pacific Journal of Cancer Prevention*, vol. 14, no. 9, pp. 5231–5235, 2013.

[11] S. Sukumari-Ramesh, N. Prasad, C. H. Alleyne, J. R. Vender, and K. M. Dhandapani, "Overexpression of Nrf2 attenuates carmustine-induced cytotoxicity in U87MG human glioma cells," *BMC Cancer*, vol. 15, no. 1, 2015.

[12] I. Gañán-Gómez, Y. Wei, H. Yang, M. C. Boyano-Adánez, and G. García-Manero, "Oncogenic functions of the transcription factor Nrf2," *Free Radical Biology & Medicine*, vol. 65, pp. 750–764, 2013.

[13] A. Olayanju, I. M. Copple, H. K. Bryan et al., "Brusatol provokes a rapid and transient inhibition of Nrf2 signaling and sensitizes mammalian cells to chemical toxicity—implications for therapeutic targeting of Nrf2," *Free Radical Biology & Medicine*, vol. 78, pp. 202–212, 2015.

[14] J. H. No, Y. B. Kim, and Y. S. Song, "Targeting Nrf2 signaling to combat chemoresistance," *Journal of Cancer Prevention*, vol. 19, no. 2, pp. 111–117, 2014.

[15] A. Uruno and H. Motohashi, "The Keap1-Nrf2 system as an *in vivo* sensor for electrophiles," *Nitric Oxide*, vol. 25, no. 2, pp. 153–160, 2011.

[16] M. K. Kwak, N. Wakabayashi, and T. W. Kensler, "Chemoprevention through the Keap1–Nrf2 signaling pathway by phase 2 enzyme inducers," *Mutation Research/Fundamental and Molecular Mechanisms of Mutagenesis*, vol. 555, no. 1-2, pp. 133–148, 2004.

[17] T. Shibata, T. Ohta, K. I. Tong et al., "Cancer related mutations in *NRF2* impair its recognition by Keap1-Cul3 E3 ligase and promote malignancy," *Proceedings of the National Academy of Sciences of the United States of America*, vol. 105, no. 36, pp. 13568–13573, 2008.

[18] T. Suzuki, H. Motohashi, and M. Yamamoto, "Toward clinical application of the Keap1-Nrf2 pathway," *Trends in Pharmacological Sciences*, vol. 34, no. 6, pp. 340–6, 2013.

[19] X. J. Wang, Z. Sun, N. F. Villeneuve et al., "Nrf2 enhances resistance of cancer cells to chemotherapeutic drugs, the dark side of Nrf2," *Carcinogenesis*, vol. 29, no. 6, pp. 1235–1243, 2008.

[20] S. Lee, M. J. Lim, M. H. Kim et al., "An effective strategy for increasing the radiosensitivity of human lung cancer cells by blocking Nrf2-dependent antioxidant responses," *Free Radical Biology & Medicine*, vol. 53, no. 4, pp. 807–816, 2012.

[21] P. Zhang, A. Singh, S. Yegnasubramanian et al., "Loss of Kelch-like ECH-associated protein 1 function in prostate cancer cells causes chemoresistance and radioresistance and promotes tumor growth," *Molecular Cancer Therapeutics*, vol. 9, no. 2, pp. 336–346, 2010.

[22] K. Chan, X. D. Han, and Y. W. Kan, "An important function of Nrf2 in combating oxidative stress: detoxification of acetaminophen," *Proceedings of the National Academy of Sciences of the United States of America*, vol. 98, no. 8, pp. 4611–4616, 2001.

[23] L. M. Aleksunes, M. J. Goedken, C. E. Rockwell, J. Thomale, J. E. Manautou, and C. D. Klaassen, "Transcriptional regulation of renal cytoprotective genes by Nrf2 and its potential use as a therapeutic target to mitigate cisplatin-induced nephrotoxicity," *The Journal of Pharmacology and Experimental Therapeutics*, vol. 335, no. 1, pp. 2–12, 2010.

[24] H. Y. Cho, S. P. Reddy, M. Yamamoto, and S. R. Kleeberger, "The transcription factor NRF2 protects against pulmonary fibrosis," *FASEB Journal*, vol. 18, no. 9, pp. 1258–1260, 2004.

[25] J. Zhu, H. Wang, F. Chen et al., "An overview of chemical inhibitors of the Nrf2-ARE signaling pathway and their potential applications in cancer therapy," *Free Radical Biology & Medicine*, vol. 99, pp. 544–556, 2016.

[26] W. Tang, J. Xie, S. Xu et al., "Novel nitric oxide-releasing derivatives of brusatol as anti-inflammatory agents: design, synthesis, biological evaluation, and nitric oxide release studies," *Journal of Medicinal Chemistry*, vol. 57, no. 18, pp. 7600–7612, 2014.

[27] S. T. Lau, Z. X. Lin, Y. Liao, M. Zhao, C. H. K. Cheng, and P. S. Leung, "Bruceine D induces apoptosis in pancreatic adenocarcinoma cell line PANC-1 through the activation of p38-mitogen activated protein kinase," *Cancer Letters*, vol. 281, no. 1, pp. 42–52, 2009.

[28] S. T. Lau, Z. X. Lin, M. Zhao, and P. S. Leung, "*Brucea javanica* fruit induces cytotoxicity and apoptosis in pancreatic adenocarcinoma cell lines," *Phytotherapy Research*, vol. 22, no. 4, pp. 477–486, 2008.

[29] E. Mata-Greenwood, M. Cuendet, D. Sher, D. Gustin, W. Stock, and J. M. Pezzuto, "Brusatol-mediated induction of leukemic cell differentiation and G_1 arrest is associated

with down-regulation of c-*myc*," *Leukemia*, vol. 16, no. 11, pp. 2275–2284, 2002.

[30] D. Ren, N. F. Villeneuve, T. Jiang et al., "Brusatol enhances the efficacy of chemotherapy by inhibiting the Nrf2-mediated defense mechanism," *Proceedings of the National Academy of Sciences of the United States of America*, vol. 108, no. 4, pp. 1433–1438, 2011.

[31] S. Tao, S. Wang, S. J. Moghaddam et al., "Oncogenic KRAS confers chemoresistance by upregulating NRF2," *Cancer Research*, vol. 74, no. 24, pp. 7430–7441, 2014.

[32] T. Wu, B. G. Harder, P. K. Wong, J. E. Lang, and D. D. Zhang, "Oxidative stress, mammospheres and Nrf2-new implication for breast cancer therapy?," *Molecular Carcinogenesis*, vol. 54, no. 11, pp. 1494–1502, 2015.

[33] B. Harder, W. Tian, J. J. la Clair et al., "Brusatol overcomes chemoresistance through inhibition of protein translation," *Molecular Carcinogenesis*, vol. 56, no. 5, pp. 1493–1500, 2017.

[34] J. L. Zhong, C. M. Raval, M. F. Nisar et al., "Development of refractoriness of HO-1 induction to a second treatment with UVA radiation and the involvement of Nrf2 in human skin fibroblasts," *Photochemistry and Photobiology*, vol. 90, no. 6, pp. 1340–1348, 2014.

[35] A. Hirota, Y. Kawachi, K. Itoh et al., "Ultraviolet A irradiation induces NF-E2-related factor 2 activation in dermal fibroblasts: protective role in UVA-induced apoptosis," *The Journal of Investigative Dermatology*, vol. 124, no. 4, pp. 825–832, 2005.

[36] G. J. Clydesdale, G. W. Dandie, and H. K. Muller, "Ultraviolet light induced injury: immunological and inflammatory effects," *Immunology and Cell Biology*, vol. 79, no. 6, pp. 547–568, 2001.

[37] F. R. de Gruijl, "[33] photocarcinogenesis: UVA vs UVB," *Methods in Enzymology*, vol. 319, pp. 359–366, 2000.

[38] A. Svobodova, D. Walterova, and J. Vostalova, "Ultraviolet light induced alteration to the skin," *Biomedical Papers*, vol. 150, no. 1, pp. 25–38, 2006.

[39] O. Reelfs, Y. Z. Xu, A. Massey, P. Karran, and A. Storey, "Thiothymidine plus low-dose UVA kills hyperproliferative human skin cells independently of their human papilloma virus status," *Molecular Cancer Therapeutics*, vol. 6, no. 9, pp. 2487–2495, 2007.

[40] E. Piskounova, M. Agathocleous, M. M. Murphy et al., "Oxidative stress inhibits distant metastasis by human melanoma cells," *Nature*, vol. 527, no. 7577, pp. 186–191, 2015.

[41] K. J. Livak and T. D. Schmittgen, "Analysis of relative gene expression data using real-time quantitative PCR and the $2^{-\Delta\Delta C}$T method," *Methods*, vol. 25, no. 4, pp. 402–408, 2001.

[42] W. Li, T. O. Khor, C. Xu et al., "Activation of Nrf2-antioxidant signaling attenuates NFκB-inflammatory response and elicits apoptosis," *Biochemical Pharmacology*, vol. 76, no. 11, pp. 1485–1489, 2008.

[43] M. Buelna-Chontal and C. Zazueta, "Redox activation of Nrf2 & NF-κB: a double end sword?," *Cellular Signalling*, vol. 25, no. 12, pp. 2548–2557, 2013.

[44] M. Cuendet, J. J. Gills, and J. M. Pezzuto, "Brusatol-induced HL-60 cell differentiation involves NF-κB activation," *Cancer Letters*, vol. 206, no. 1, pp. 43–50, 2004.

[45] F. Chen, H. Wang, J. Zhu et al., "Camptothecin suppresses NRF2-ARE activity and sensitises hepatocellular carcinoma cells to anticancer drugs," *British Journal of Cancer*, vol. 117, no. 10, pp. 1495–1506, 2017.

[46] R. P. Verma and C. Hansch, "Camptothecins: a SAR/QSAR study," *Chemical Reviews*, vol. 109, no. 1, pp. 213–235, 2009.

[47] Y. Ma, X. Li, A. Li, P. Yang, C. Zhang, and B. Tang, "H_2S-Activable MOF nanoparticle photosensitizer for effective photodynamic therapy against cancer with controllable singlet-oxygen release," *Angewandte Chemie*, vol. 56, no. 44, pp. 13752–13756, 2017.

[48] H. Y. Cho and S. R. Kleeberger, "Nrf2 protects against airway disorders," *Toxicology and Applied Pharmacology*, vol. 244, no. 1, pp. 43–56, 2010.

[49] S. Zhou, W. Ye, Q. Shao, M. Zhang, and J. Liang, "Nrf2 is a potential therapeutic target in radioresistance in human cancer," *Critical Reviews in Oncology Hematology*, vol. 88, no. 3, pp. 706–715, 2013.

[50] I. H. Hall, K. H. Lee, Y. Imakura, M. Okano, and A. Johnson, "Anti-inflammatory agents III: structure-activity relationships of brusatol and related quassinoids," *Journal of Pharmaceutical Sciences*, vol. 72, no. 11, pp. 1282–1284, 1983.

[51] K. H. Lee, M. Okano, I. H. Hall, D. A. Brent, and B. Soltmann, "Antitumor agents XLV: bisbrusatolyl and brusatolyl esters and related compounds as novel potent antileukemic agents," *Journal of Pharmaceutical Sciences*, vol. 71, no. 3, pp. 338–345, 1982.

[52] Y. F. Liou, I. H. Hall, M. Okano, K. H. Lee, and S. G. Chaney, "Antitumor agents XLVIII: structure-activity relationships of quassinoids as in vitro protein synthesis inhibitors of P-388 lymphocytic leukemia tumor cell metabolism," *Journal of Pharmaceutical Sciences*, vol. 71, no. 4, pp. 430–435, 1982.

[53] I. H. Hall, Y. F. Liou, K. H. Lee, S. G. Chaney, and W. Willingham Jr., "Antitumor agents LIX: effects of quassinoids on protein synthesis of a number of murine tumors and normal cells," *Journal of Pharmaceutical Sciences*, vol. 72, no. 6, pp. 626–630, 1983.

[54] O. Reelfs, V. Abbate, R. C. Hider, and C. Pourzand, "A powerful mitochondria-targeted iron chelator affords high photoprotection against solar ultraviolet a radiation," *The Journal of Investigative Dermatology*, vol. 136, no. 8, pp. 1692–1700, 2016.

[55] S. Hackenberg, A. Scherzed, M. Kessler et al., "Zinc oxide nanoparticles induce photocatalytic cell death in human head and neck squamous cell carcinoma cell lines in vitro," *International Journal of Oncology*, vol. 37, no. 6, pp. 1583–1590, 2010.

[56] N. Luiza Andreazza, C. Vevert-Bizet, G. Bourg-Heckly, F. Sureau, M. José Salvador, and S. Bonneau, "Berberine as a photosensitizing agent for antitumoral photodynamic therapy: insights into its association to low density lipoproteins," *International Journal of Pharmaceutics*, vol. 510, no. 1, pp. 240–249, 2016.

[57] Y. Y. He, S. E. Council, L. Feng, and C. F. Chignell, "UVA-induced cell cycle progression is mediated by a disintegrin and metalloprotease/epidermal growth factor receptor/AKT/cyclin D1 pathways in keratinocytes," *Cancer Research*, vol. 68, no. 10, pp. 3752–3758, 2008.

[58] B. D. Manning and L. C. Cantley, "AKT/PKB signaling: navigating downstream," *Cell*, vol. 129, no. 7, pp. 1261–1274, 2007.

[59] R. M. Uranga, S. Katz, and G. A. Salvador, "Enhanced phosphatidylinositol 3-kinase (PI3K)/Akt signaling has pleiotropic

targets in hippocampal neurons exposed to iron-induced oxidative stress," *The Journal of Biological Chemistry*, vol. 288, no. 27, pp. 19773–19784, 2013.

[60] M. H. Li, Y. N. Cha, and Y. J. Surh, "Peroxynitrite induces HO-1 expression via PI3K/Akt-dependent activation of NF-E2-related factor 2 in PC12 cells," *Free Radical Biology & Medicine*, vol. 41, no. 7, pp. 1079–1091, 2006.

[61] F. Rizvi, S. Shukla, and P. Kakkar, "Essential role of PH domain and leucine-rich repeat protein phosphatase 2 in Nrf2 suppression via modulation of Akt/GSK3β/Fyn kinase axis during oxidative hepatocellular toxicity," *Cell Death & Disease*, vol. 5, article e1153, 2014.

[62] L. Wang, Y. Chen, P. Sternberg, and J. Cai, "Essential roles of the PI3 kinase/Akt pathway in regulating Nrf2-dependent antioxidant functions in the RPE," *Investigative Ophthalmology & Visual Science*, vol. 49, no. 4, pp. 1671–1678, 2008.

Hindawi
Oxidative Medicine and Cellular Longevity
Volume 2018, Article ID 5351967, 10 pages
https://doi.org/10.1155/2018/5351967

Research Article

Evaluation of Potential Mechanisms Controlling the Catalase Expression in Breast Cancer Cells

Christophe Glorieux,[1] Juan Marcelo Sandoval,[2] Nicolas Dejeans,[1] Sandrine Nonckreman,[3] Khadija Bahloula,[3] Hélène A. Poirel,[3] and Pedro Buc Calderon[1,2]

[1]*Metabolism and Nutrition Research Group, Louvain Drug Research Institute, Université catholique de Louvain, 1200 Brussels, Belgium*
[2]*Facultad de Ciencias de la Salud, Universidad Arturo Prat, 1100000 Iquique, Chile*
[3]*Centre de Génétique Humaine, Cliniques Universitaires Saint-Luc & de Duve Institute, Université catholique de Louvain, 1200 Brussels, Belgium*

Correspondence should be addressed to Pedro Buc Calderon; pedro.buccalderon@uclouvain.be

Received 30 August 2017; Accepted 9 November 2017; Published 28 January 2018

Academic Editor: Spencer Gibson

Development of cancer cell resistance against prooxidant drugs limits its potential clinical use. MCF-7 breast cancer cells chronically exposed to ascorbate/menadione became resistant (Resox cells) by increasing mainly catalase activity. Since catalase appears as an anticancer target, the elucidation of mechanisms regulating its expression is an important issue. In MCF-7 and Resox cells, karyotype analysis showed that chromosome 11 is not altered compared to healthy mammary epithelial cells. The genomic gain of *catalase* locus observed in MCF-7 and Resox cells cannot explain the differential catalase expression. Since ROS cause DNA lesions, the activation of DNA damage signaling pathways may influence catalase expression. However, none of the related proteins (i.e., p53, ChK) was activated in Resox cells compared to MCF-7. The c-abl kinase may lead to catalase protein degradation via posttranslational modifications, but neither ubiquitination nor phosphorylation of catalase was detected after catalase immunoprecipitation. Catalase mRNA levels did not decrease after actinomycin D treatment in both cell lines. DNMT inhibitor (5-aza-2′-deoxycytidine) increased catalase protein level in MCF-7 and its resistance to prooxidant drugs. In line with our previous report, chromatin remodeling appears as the main regulator of catalase expression in breast cancer after chronic exposure to an oxidative stress.

1. Introduction

Catalase mainly catalyzes the dismutation of hydrogen peroxide (H_2O_2) into water and molecular oxygen. This antioxidant enzyme is expressed in all major body organs especially in the liver, kidney, and erythrocytes. In these organs, catalase plays an essential role in cell defense against oxidative stress [1, 2]. A decrease in catalase activity is thus frequently associated with several diseases. For instance, some polymorphisms into the promoter or introns of the *catalase* gene are involved in diabetes, hypertension, vitiligo, Alzheimer's disease, and acatalasemia [3, 4]. Interestingly, catalase is also frequently downregulated in tumor tissues compared to normal tissues of the same origin [5–7]. In this context, when compared to their normal healthy counterparts, we have reported a severe decrease of catalase activity in TLT cells, a murine hepatocarcinoma cell line [8]; in K562 cells, a human chronic myeloid leukemia cell line [9]; and in MCF-7 cells, a human breast carcinoma cell line [10]. These observations are consistent with the study of Sun et al., who showed that immortalization and transformation of mouse liver cells with SV40 virus results in a decrease in catalase activity, which contributes to oncogenesis by increasing reactive oxygen species (ROS) level in transformed cells [11]. The mechanisms

controlling the transcription of *catalase* gene are poorly understood, and diverse mechanisms have also been proposed to regulate catalase expression [3].

We explored a potential role of catalase during the acquisition of cancer cell resistance to chemotherapeutic agents. To this end, we overexpressed human catalase in MCF-7 breast cancer cells. No particular resistance against conventional chemotherapies like doxorubicin, cisplatin, and paclitaxel was observed in cells overexpressing catalase, but they were more resistant to prooxidant therapies [12]. Furthermore, we generated a resistant cell line by chronic exposure of MCF-7 cells to an H_2O_2-generating system, namely, the ascorbate/menadione (Asc/Men) combination. Catalase was overexpressed in resistant-Resox cells when compared to parental MCF-7 cells [13, 14]. In these cells, transcription factors (i.e., RARα and JunB) and other proteins belonging to coactivator or corepressor complexes (i.e., HDACs) affect chromatin remodelling and lead to the activation or repression of *catalase* gene [10].

Additional regulatory levels clarifying this altered catalase expression in cancer cells were also explored. Since ROS induce DNA lesions, we were interested to know whether a potential role of DNA repair pathways may have an impact on the regulation of catalase expression. Genetic alterations such as loss of heterozygosity or amplification of the *catalase* gene locus, although very rare, were investigated. Both posttranscriptional and posttranslational catalase modifications were also analysed regarding putative alterations of protein stability. Finally, since gene transcription is also regulated by chromatin modulation due to histone acetylation or DNA methylation, these epigenetic marks were also investigated as potential modulators of altered catalase expression in breast cancer cells.

2. Materials and Methods

2.1. Cell Lines and Chemicals. MCF-7 cells were purchased at ATCC (Manassas, VA, United States). An MCF-7 cell line resistant to oxidative stress (namely Resox cells) was generated by chronic exposure of cells to increasing concentrations of the prooxidant combination of ascorbate/menadione (Asc/Men) for 6 months, starting with 0.5 mM ascorbate/5 μM menadione to a final concentration of 1.5 mM ascorbate/15 μM menadione. Cells were first treated at 50% confluence by replacing their media with fresh media containing Asc/Men. When surviving cells reached 50% confluence, they were washed with warm PBS and treated again [13]. To avoid the development of islets of resistance, which could arise from cooperation between cells, the cells were trypsinized every 2 weeks and subcultured into new flasks. After selection, the cell line was stabilized in drug-free medium for 1 month. Cells were kept in DMEM medium supplemented with 10% foetal calf serum, in the presence of penicillin (100 U/ml) and streptomycin (100 μg/ml) from Gibco (Grand Island, NY, USA). Human mammary epithelial cells 250MK were provided by Dr. M. Stampfer and Dr. J.C. Garbe (Lawrence Berkeley National Laboratory, Berkeley, California, USA). They were maintained in a M87A + CT + X medium and used between passages 8 and 10 [15].

Sodium ascorbate, menadione sodium bisulfite, MG132, actinomycin D, and 5-aza-2′-deoxycytidine were purchased from Sigma (St. Louis, MO, USA).

2.2. Conventional Cytogenetic Analysis. Metaphase chromosomes were obtained according to standard protocols from the different cell lines [16]. Briefly, cultured cells, in exponential growth phase, were treated for 4 h with 0.02 μg/ml of Colcemid (Invitrogen). Harvested cells from the flasks after trypsinization were incubated for 30 minutes at 37°C in hypotonic 0.055 M KCl and fixed in a 3 : 1 methanol : glacial acetic acid solution. Chromosome harvesting and metaphase slide preparation were performed according to standard procedures [16–18]. Twenty Reverse Trypsin Wright (RTW) banded metaphases were analysed and karyotypes were reported according to the last 2013 International System for Human Cytogenetics Nomenclature (ISCN 2013).

2.3. Fluorescence In Situ Hybridization (FISH). Specific BAC RP11-964L11 (catalase/11p13; stained with Cy3: red spots) and RP11-90K17 (control/11q14; stained with FITC: green spots) probes from the UCSC (http://genome.ucsc.edu) databases were obtained from the BACPAC Resources Centre at the Children's Hospital Oakland Research Institute (Oakland, CA, USA).

The FISH (fluorescence in situ hybridization) assay was carried out on nuclei and metaphases from fixed pellet of cell as previously described [19]. All hybridized metaphases were captured on a Zeiss Axioplan 2 microscope (Zeiss, Zaventem, Belgium) and analysed using the Isis software (Metasystems, Altlussheim, Germany).

2.4. Immunoblotting. The procedures for protein sample preparation from cell cultures, protein quantification, immunoblotting, and data analyses were performed as previously described [12, 14]. Antibody against catalase (#AB1212) was obtained from Millipore (Merck KGaA, Darmstadt, Germany); antibodies against c-abl (#sc-23) and p53 (#sc-126) were from Santa Cruz Biotechnology (Santa Cruz, CA, USA); antibodies against phosphocatalase Y385 (#ab59429) and β-actin (#ab6276) were from Abcam (Cambridge, UK); antibodies against phospho-Chk2 T68 (#2661) and phospho-p53 S15 (#9284) were from Cell signaling (Beverly, MA, USA); and antibody against Flag (#F3165) was from Sigma (St. Louis, MO, USA). Protein bands were then detected by chemiluminescence, using the ECL detection kit (Pierce, Thermo Scientific, Rockford, IL, USA). When appropriate, bands obtained via Western blot analysis were quantified, using ImageJ software (http://rsb.info.nih.gov/ij/). Protein expression was normalized to that of β-actin.

2.5. Real-Time PCR. Total RNA was extracted with the Tri-Pure reagent from Roche Applied Science Diagnostics (Mannheim, Germany). Reverse transcription was performed using SuperScript II RNase H- reverse transcriptase and random hexamer primers (Invitrogen, Grand Island, NY, USA). Sybr Green Supermix (BioRad, Hercules, CA, USA) was used for qRT-PCR. All Primers sequences were

designed from Sigma (St. Louis, MO, USA) and provided in Table S1. The samples were incubated 5 min at 95°C, 40 cycles of 10 s at 95°C and 30 s at 60°C, and followed by a melting curve. The fluorescence in the samples was measured after each cycle in a Bio-Rad IQ5 thermocycler (Bio-Rad, Hercules, CA, USA). The results were calculated from the following calculation: $2^{-(\text{Ct target gene} - \text{Ct EF1})}$ and matched to the control samples.

2.6. Ubiquitination and Phosphorylation Assays. Cells were transiently transfected, at 50% confluence, with 1 μg of plasmid pcDNA3 coding an ubiquitin-Flag fusion protein, a kind gift from Prof. J-B. Demoulin (UCL, Brussels, Belgium). Twenty-four hours posttransfection, cells were treated with 25 μM MG132 for 5 h. Cells were washed twice with ice-cold PBS and then resuspended in the lysis buffer in the presence of proteases (Protease Inhibitor Cocktail, Sigma, St. Louis, MO, USA) and phosphatase inhibitors (Phosphatase Inhibitor Cocktail, Calbiochem, Merck KGaA, Darmstadt, Germany). Cell lysates were immunoprecipitated in columns containing catalase antibody (AB1212, Millipore), using coimmunoprecipitation kit from Pierce (Rockford, IL, USA). Eluates were then tested by immunoblotting.

2.7. MTT Assay. The effects of Asc/Men after incubation with DNMT inhibitor on cell metabolic status were assessed by following the reduction of MTT (3-(4,5-dimethylthiazolyl-2)-2,5-diphenyltetrazolium bromide) to blue formazan [20]. Blue formazan crystals were solubilized with DMSO and the coloured solution was subsequently read at 550 nm. Results are expressed as % of MTT reduction compared to untreated control conditions.

2.8. Statistics. All experiments were performed at least in triplicates. Groups were analysed using unpaired *t*-test performed with GraphPad Prism software (San Diego, CA, USA). The level of significance was set at $p < 0.05$.

3. Results and Discussion

3.1. Is a Genomic Gain of Catalase Locus in Breast Cancer Cell Lines Responsible for Catalase Overexpression in Resistant Cells? Since the human *catalase* gene is located on the short arm of chromosome 11 (11p13) [21] and deletion of this chromosomal region is generally associated with a decrease of catalase activity, we first focused on genetic alterations, an important hallmark of cancer. Interestingly, the deletion of chromosome 11p is frequently observed in later passages of SV40-transformed human fibroblasts and correlated with a low catalase activity [22]. Such alteration may occur in children affected by WAGR syndrome, a rare genetic disease in which the affected children are predisposed to develop Wilms' tumor (tumor of the kidney), aniridia (absence of the iris), gonadoblastoma, and mental retardation [23–29]. This chromosomal region was altered in the breast cancer cell lines, but karyotypes showed that chromosome 11 was not altered in MCF-7 and Resox cells compared to healthy 250MK, a human epithelial mammary cell line (Figure 1(a)). The complete karyotype analyses of these three cell lines have been previously published [13].

Loss of alleles (i.e., loss of heterozygosity) of *catalase* gene was also observed in non-small-cell lung cancer and was associated with a decrease of catalase activity [30–32]. On the contrary, gain of *catalase* gene copy number and amplification of chromosome 11p can also explain an increased expression of catalase. This phenomenon has been observed in HL-60 cell lines rendered resistant to H_2O_2. These cells were more resistant because they have an enhanced catalase activity that correlated with an increase of gene copy number from two to eight times higher than in parental cell line [33].

We have thus investigated a potential loss of heterozygosity or a genomic gain by performing hybridization of catalase and control FISH probes on metaphases. The catalase and control FISH probes were controlled in human lymphocytes (data not shown) and normal mammary epithelial 250MK cells (Figure 1(b)). We observed two red (*catalase* locus) and two green spots (control) localized on the two chromosome 11. A genomic gain of *catalase* locus was observed in MCF-7 and Resox cell lines compared to 250MK cells: we counted 3 *catalase* spots, two localized on the two normal chromosome 11 and one localized on an unidentified chromosome (Figures 1(c) and 1(d)). However, the number of *catalase* loci remained similar in these two cell lines. For Resox cells, one subclonal population was characterized by 6 red spots and two-fold chromosome number (not shown) corresponding to 20% of total Resox population. We can conclude that this genomic gain of chromosome 11p13 is not involved in mechanisms leading to catalase overexpression in Resox cells.

3.2. Are Proteins of DNA Damage Pathway Involved in Catalase Expression of Breast Cancer Cells? Since the karyotypes were altered in breast cancer cell lines [13] and ROS induce DNA damage, we investigated whether the activation of DNA repair system may influence the regulation of catalase expression. To our knowledge, a putative link between this repair system and antioxidant enzyme expression as a possible response against ROS-mediated DNA damage has not yet been investigated.

Three different kinases, namely, DNA-PK (DNA-activated protein kinase), ATM (ataxia telangiectasia mutated), and ATR (ataxia telangiectasia and Rad3 related), are activated when the DNA is damaged leading to the activation of proteins involved in DNA repair [34, 35]. These pathways induced a cascade of protein kinases such as Chk1 and Chk2 (checkpoint kinases), which activate protein p53 inducing γ-histone H2AX phosphorylation. Neither p53 nor ChK2 proteins appeared activated in Resox cells (Figures 2(a) and 2(b)), whereas a strong activation was observed in control MCF-7 cells incubated with Asc/Men (Figure 2(a)). Moreover, among the mRNA levels of the different kinases involved in the signaling cascade, only a slight increase of Chk1 mRNA level was observed in Resox cells (Figure 2(c)).

The protein c-abl (Abelson murine leukemia viral oncogene homolog 1) is also induced during the activation of DNA damage pathway [36]. Cao et al. demonstrated that c-abl is capable of phosphorylating catalase leading to its subsequent ubiquitination and degradation by the

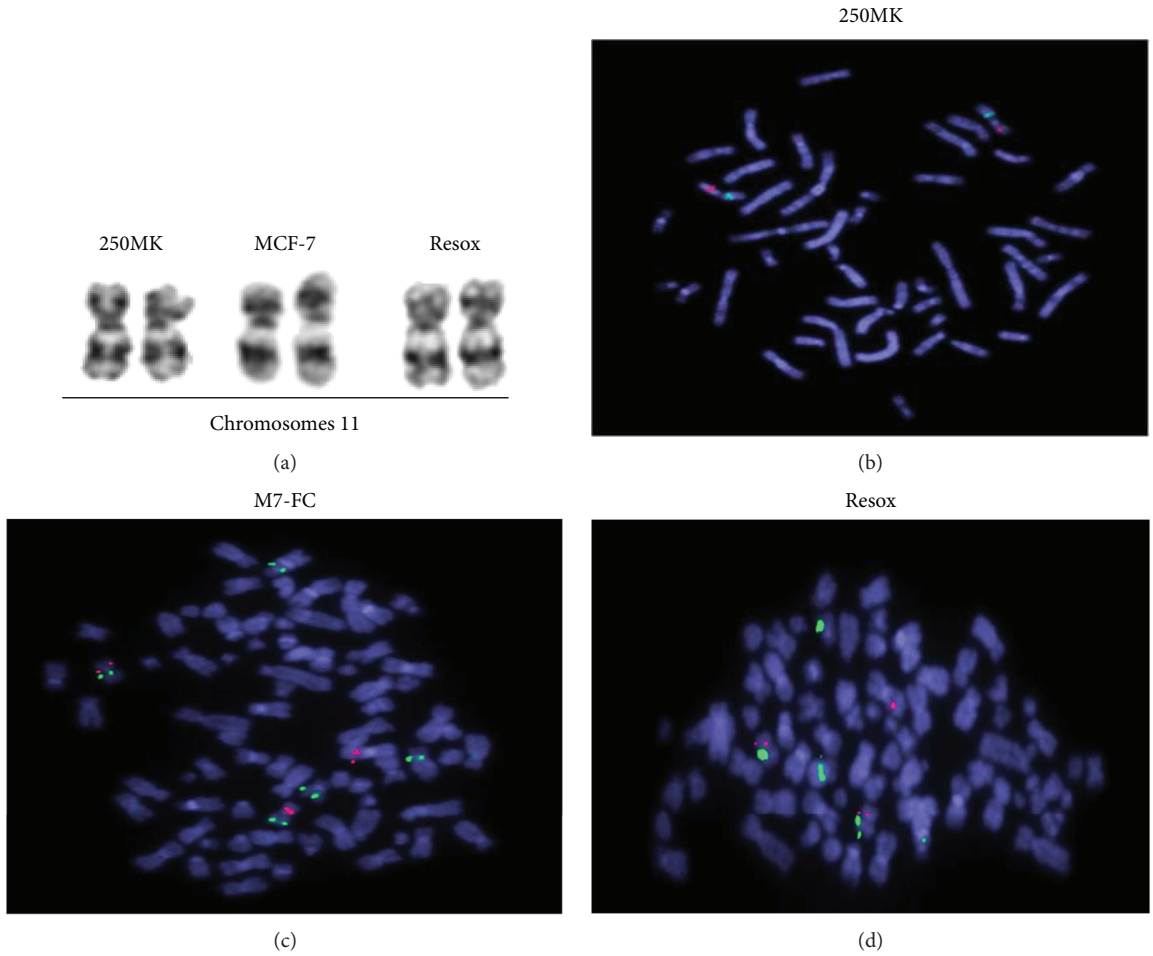

Figure 1: Genomic gain of *catalase* locus in breast cancer cell lines is not responsible for catalase overexpression in resistant cells. (a) Karyotypes: chromosome 11 of human normal epithelial cells (250MK) and breast cancer cell lines. (b) Hybridization of catalase (red spots) and control (green spots) FISH probes on metaphases of 250 MK cells. (c) MCF-7 and (d) Resox cells.

proteasome [37, 38]. Interestingly, c-abl mRNA and protein levels were decreased in Resox cells compared to MCF-7 cells (Figures 2(d)–2(f)).

Altogether, these results show that DNA damage pathway is not the cause of catalase overexpression in Resox cells, but posttranslational modifications mediated by c-abl might occur on catalase protein.

3.3. Are Catalase Covalent Modifications Occurring in Breast Cancer Cells? Various posttranslational modifications such as phosphorylation, ubiquitination, acetylation, glycosylation, and covalent binding with other proteins (i.e., p53, Atm) have been reported to modulate both catalase expression and activity at different levels [37–43]. The half-life of catalase is generally high, reaching more than 3 days [44–46]. When cells are under oxidative stress conditions, c-abl and c-abl-related gene (Arg) tyrosine kinases are able to phosphorylate catalase at Tyr231 and Tyr386 [37, 38]. The phosphorylated enzyme is subsequently ubiquitinated and degraded by the proteasome. It appears that a physical interaction exists between these kinases and catalase, as demonstrated by immunoprecipitation assays performed in cancer cells and KO MEF (mouse embryonic fibroblast) for the kinases. Furthermore, two proteasome inhibitors, namely, MG132 and lactacystin, also restored catalase expression in these cells [37, 38].

Catalase posttranslational modifications were analysed in our breast cancer cells model. The MG132 proteasome inhibitor did not modify catalase expression in MCF-7 and Resox cells (Figure 3(a)). Finally, catalase phosphorylation did not appear to play a role as a main covalent modification. Indeed, neither ubiquitination nor phosphorylation of catalase was detected after catalase immunoprecipitation (Figure 3(b)), although c-abl protein level was decreased in Resox cell line (Figure 2(e)).

3.4. Are Posttranscriptional Modifications Playing a Role in Catalase Overexpression in Resox Cells? The expression of catalase expression can also be regulated at the RNA level. The *catalase* gene possesses a 3′ flanking region with T-rich clusters and CA repeats that are susceptible to be regulated by some redox-sensitive proteins, which bind catalase mRNA and enhances translation [47]. Some unidentified proteins could bind to the 5′UTR (untranslated region) of the catalase mRNA to accelerate the transcriptional rate, as has been observed in cancer PC12 cells exposed to H_2O_2 [48].

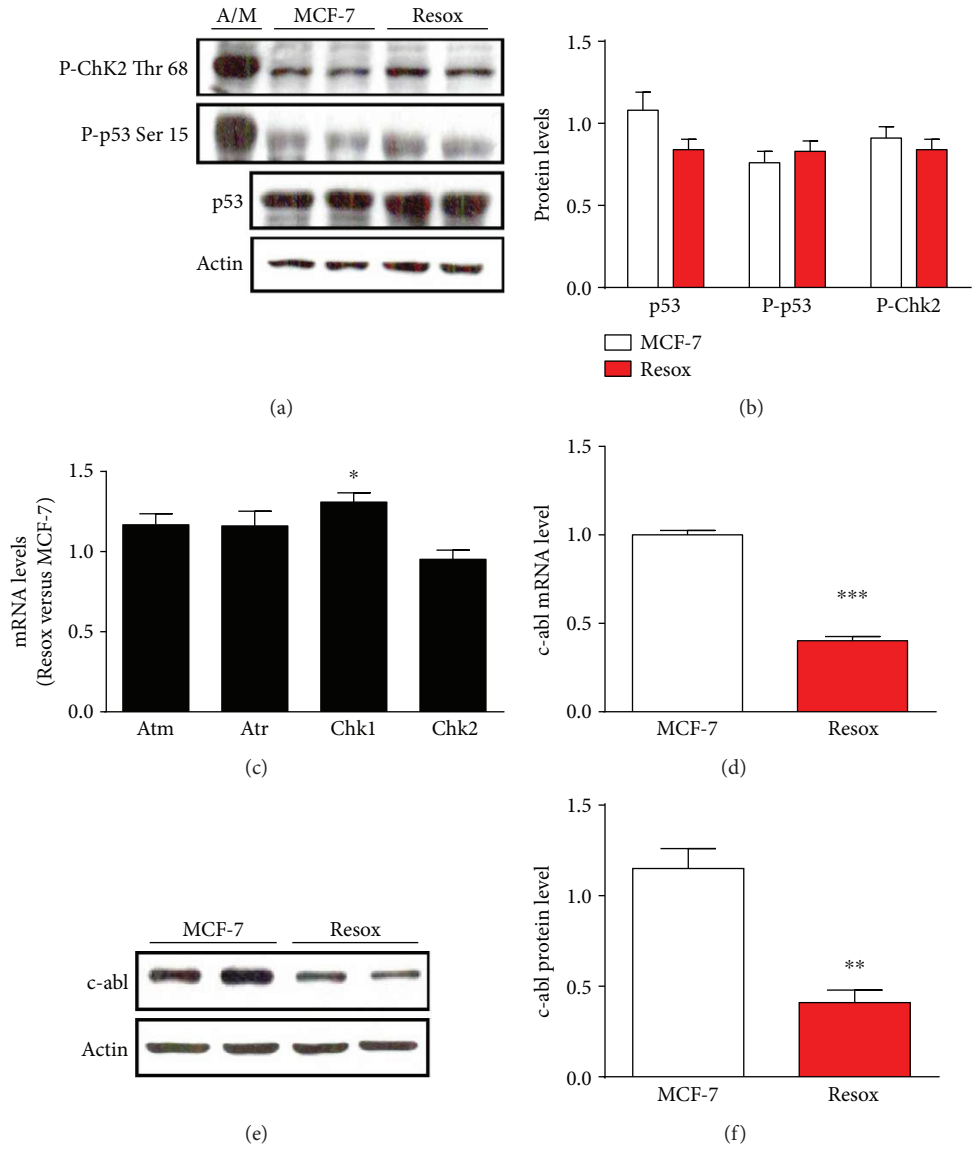

Figure 2: DNA damage pathway did not enhance catalase expression in breast cancer cell lines. (a and b) Immunoblotting and protein quantification of p53, P-p53, and P-Chk2 in breast cancer cells. Ascorbate 1 mM/menadione 10 μM (A/M) for 2 h is used as a positive control to induce DNA damage. (c) mRNA levels of the different kinases activated during the DNA damage pathway. (d) c-abl mRNA level in both MCF-7 and Resox cells. (e and f) Immunoblotting and protein quantification of c-abl in breast cancer cells. Data are mean ± s.e.m. Groups were compared using unpaired *t*-test. $^{*}p$ value <0.05; $^{**}p$ value <0.01; $^{***}p$ value <0.001.

The microRNA miR-451 can also modulate and enhance catalase expression by suppressing the protein 14-3-3ξ, an inhibitor of the FoxO3a (forkhead box O3a) pathway, thereby protecting cells against oxidant drugs [49], but this transcription factor appears to not play a critical role in our models [14]. Moreover, microRNA miR-30b can bind directly to the 3′UTR region of the catalase mRNA, on a conserved site across several species. Mimics of miR-30b can drastically decrease the catalase protein level in human retinal pigment epithelial cell ARPE-19 [50].

In a MCF-7 cell line rendered resistant to H_2O_2 and as a result overexpressed catalase, a treatment with actinomycin D (an inhibitor of the transcription) induces a delay in the degradation of catalase mRNA [51]. As previously shown, Resox cells have more mRNA than MCF-7 suggesting that mRNA stability in the former cells might be higher than in MCF-7 cells [10]. However, the levels of catalase mRNA did not decrease after 6 hours of actinomycin D incubation in both cells (Figure 4(a)).

3.5. DNA Methyltransferase Inhibitor Increases Catalase Protein Level in MCF-7 Cells. Since the transcription of a gene can be regulated by chromatin remodelling due to histone acetylation or DNA methylation, the importance of these mechanisms for the expression of catalase in cancer cells has been raised. In this context, epigenetic changes were proposed to regulate catalase expression in acute myelogenous leukaemia resistant to doxorubicin (AML-2/

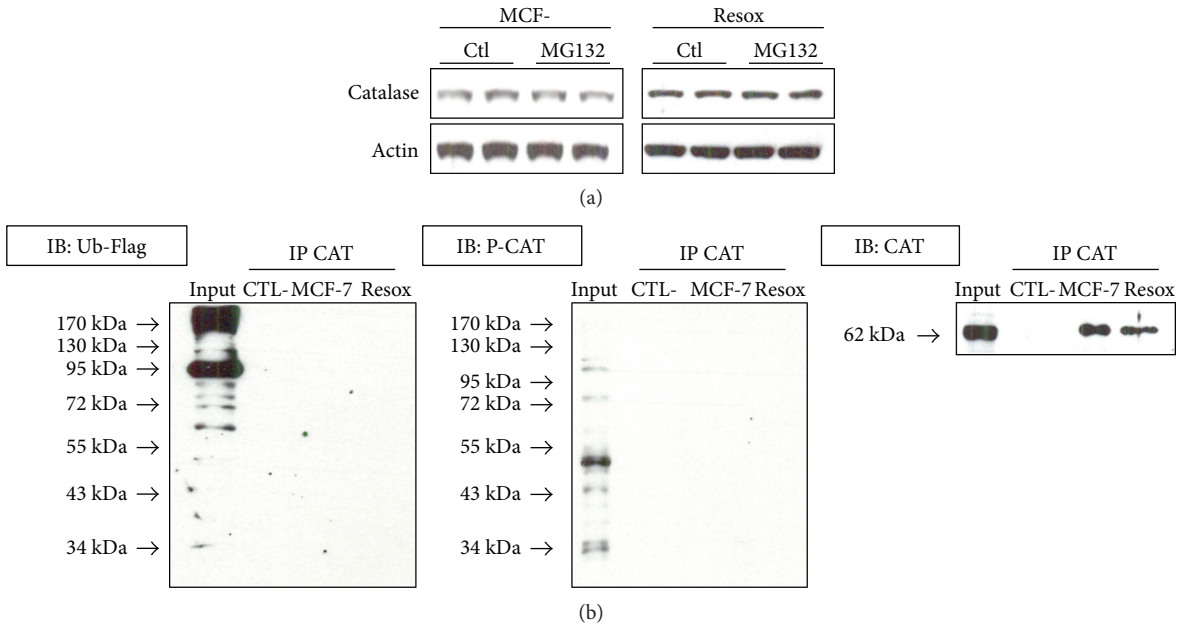

Figure 3: Catalase is neither phosphorylated nor ubiquitinated in breast cancer cells. (a) Catalase protein levels were measured after 5 h incubation with proteasome inhibitor MG132 in both MCF-7 and Resox cells. (b) Immunoprecipitation (IP) with anticatalase antibody and immunoblotting (IB) with anti-Flag, antiphosphocatalase, and catalase antibodies. Prior IP, cells were transfected with a plasmid pcDNA3 (1 μg) coding an ubiquitin-Flag for 72 h.

DX100 cells), which exhibit less catalase activity compared to their parental cell lines [52]. Indeed, both Trichostatin A (TSA), an inhibitor of histone deacetylases (HDAC), and 5-aza-2′-deoxycytidine, an inhibitor of DNA methylation, increase the protein levels of catalase in the AML-2/DX100 cells. These data were then confirmed by chromatin immunoprecipitation and sodium bisulfite sequencing assays. The results suggested a hypoacetylation of histones H4 but not H3. DNA hypermethylation on the catalase promoter in AML-2/DX100 cells was also observed [52]. We have also described the acetylation of histones (at least histone H4), leading to an opening repression of chromatin structures near −1518/−1201 promoter region in MCF-7 cells [10], as shown by ChIP (chromatin precipitation) assays.

DNA methylation is also involved in the regulation of catalase. Indeed, specific CpG islands in the human promoters of *catalase* and *Oct-1* (octamer-binding transcription factor 1: an inducer of *catalase* gene transcription) genes were methylated in human hepatocellular carcinoma cell line after H_2O_2 treatment. This is in good correlation with a decreasing catalase expression in this model [53, 54]. In this particular type of cancer, the catalase promoter is hypermethylated in the tumor itself but not in the neighbouring tissues [55]. On the contrary, DNA hypomethylation of the *catalase* gene is frequently observed in colon tumors whereas few modifications of DNA methylation are observed in breast adenocarcinoma compared to normal breast tissues. In the studies where a change in the DNA methylation pattern was observed, DNA hypomethylation and hypermethylation occurred only around the exon 2 of the *catalase* gene [55, 56].

We have thus explored the possibility that DNA methylation may regulate catalase expression in our cellular models. The DNA methyltransferase (DNMT) inhibitor, 5-aza-2′-deoxycytidine, tends to increase catalase protein level in MCF-7 and not significantly in Resox cells (Figures 4(b) and 4(c)). Moreover, MCF-7 cells became more resistant to prooxidant drugs (Asc/Men) after preincubation with the DNMT inhibitor (Figures 4(d) and 4(e)). Once again, our results demonstrate a potential role of chromatin remodelling in the regulation of catalase expression during cancer cell resistance acquisition to a chronic prooxidant treatment. Consistent with our previous study, methyl CpG-binding proteins (i.e., MECP2) and DNMT (i.e., DNMT1) were identified by AP-MS (affinity purification followed by mass spectrometry) analyses and interact with −1518/−1200 promoter region of *catalase* gene in MCF-7 cells [10]. Altogether, it suggests that DNA methylation and post-translational modifications of histones are events associated to repress the transcription of *catalase* gene. In a panel of 12 cancer cell lines treated with TSA, we confirmed that chromatin remodelling is not a general regulatory mechanism in cancer cells but another breast cancer cell line, an estrogen receptor-negative MDA-MB-231 cell line, also showed increased catalase protein level when incubated with HDAC or RARα (retinoic acid receptor alpha) inhibitors [10]. Moreover, RARα overexpression decreased drastically the expression of catalase and histone acetylation was not detected on the catalase promoter by ChIP assay in MDA-MB-231 cells [data not shown], suggesting a similar mechanism regulating catalase expression in these breast cancer cells. In this context, we have recently reported that targeting the redox status of cancer cells by modulating catalase expression is emerging as a novel approach to potentiate chemotherapy [57]. Modifying epigenetic changes such as histone acetylation or DNA methylation in breast cancer cells

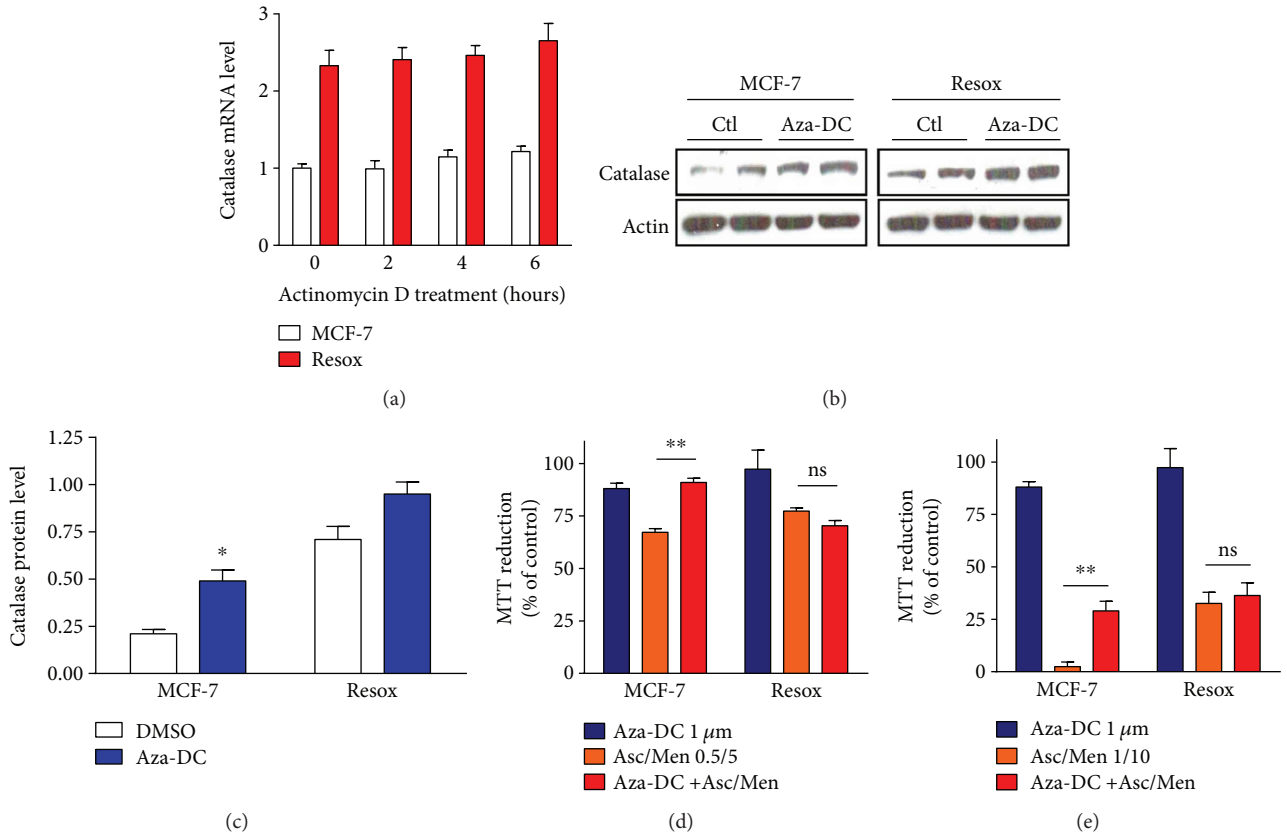

FIGURE 4: Evaluation of mRNA stability in MCF-7 and Resox cells. DNA methyltransferase inhibitor 5-aza-2′-deoxycytidine tends to increase the levels of catalase protein level in MCF-7 cells. (a) Catalase mRNA levels were measured in MCF-7 and Resox cells after 2, 4, and 6 h of actinomycin D treatment (10 μg/ml). (b and c) Immunoblotting and protein quantification of catalase, after 72 h incubation with 1 μM of 5-aza-2′-deoxycytidine (Aza-DC). (d and e) Cells were prior incubated with 1 μM of 5-aza-2′-deoxycytidine for 72 h, then with various concentrations of ascorbate (Asc, mM) and menadione (Men, μM). Cell survival was measured by MTT assay. Data are mean ± s.e.m. Groups were compared using unpaired t-test. $^{*}p$ value <0.05; $^{**}p$ value <0.01.

will thus dramatically alter the expression of various genes including catalase, thus sensitizing cells to prooxidant chemotherapies [3, 10, 57].

4. Final Concluding Remarks

Regulatory mechanisms involved in catalase expression occur at different levels from genetic to posttranscriptional modifications including epigenetic and transcriptional processes [3]. Loss of heterozygosity or gene amplification may contribute to an altered expression of catalase but data obtained in this study indicate a minor role as compared to other regulatory mechanisms such as *catalase* gene transcription as we have recently reported [10, 14]. Meanwhile, although ROS induce DNA damage, the activation of the DNA repair system did not lead to a conclusive role of these pathways on regulation of catalase expression either in MCF-7 or Resox cells. Neither posttranscriptional nor posttranslational modifications are likely involved in the different catalase protein levels in both cell lines. Instead, we have already shown that histones H4 were acetylated around the promoter region −1518/+16 in Resox cells, explaining the catalase overexpression in these cells. In this study, we have demonstrated that DNA hypo/hypermethylation also plays a pivotal role in this regulation and resistance to prooxidant drugs.

Since catalase expression is sensitive to redox modulation, a therapeutic strategy may be developed in the context of cancer, taking in mind the level of catalase expression. For instance, if catalase is downregulated and the clinical option is to get increased amounts of catalase, an interesting approach would be the use of epigenetic agents (DNMT or HDAC inhibitors) in order to promote a change in chromatin remodelling. Another possibility would be the use of antagonists of RARα, leading to a pharmacological inhibition of this nuclear receptor and consequently to a loss of catalase repression. Indeed, we recently showed that both compounds, TSA and Ro 41-5255 (HDAC and RARα inhibitor, resp.), enhance catalase expression not only in MCF-7 cells but also, as previously mentioned, in other mammary cell lines such as the highly aggressive and metastatic MDA-MB-231 cells [10]. Conversely, in case of catalase overexpression, a therapeutic option would be the use of siRNA against catalase coupled to nanoparticles or, as we have recently shown, the use of arsenic trioxide (Trisenox) which decreases catalase expression likely by activating the Akt/PKB (protein kinase B) signalling pathway and/or inducing the expression of RARα [57, unpublished results]. It should be noted that

the hypothesis suggesting that chromatin remodelling as the main event controlling catalase expression requires both activating and inhibitory factors. Indeed, we have recently shown that the transcription factors JunB and RARα are involved in the positive and negative expression of catalase by recruiting coactivators and corepressors leading to chromatin remodelling [10].

Taking together, these findings and previous results obtained in our laboratory [10, 12, 14, 57] suggest that chromatin remodelling is a major regulatory process controlling catalase expression in breast cancer cells during resistance acquisition against an oxidative stress.

Abbreviations

Akt/PKB: Protein kinase B
AP-MS: Affinity purification followed by mass spectrometry
Arg: c-abl-related gene
ATM: Ataxia telangiectasia mutated
ATR: Ataxia telangiectasia and Rad3 related
Asc/Men: Ascorbate/menadione
c-abl: Abelson murine leukemia viral oncogene homolog 1
ChIP: Chromatin precipitation
Chk: Checkpoint kinase
DNA-PK: DNA-activated protein kinase
DNMT: DNA methyltransferase
FISH: Fluorescence in situ hybridization
FoxO3: Forkhead box O3
HDAC: Histone deacetylase
MEF: Mouse embryonic fibroblast
Oct-1: Octamer-binding transcription factor 1
RARα: Retinoic acid receptor alpha
ROS: Reactive oxygen species
TSA: Trichostatin A
UTR: Untranslated region
WAGR: Wilms' tumor
Aniridia: Gonadoblastoma and mental retardation (syndrome).

Disclosure

Christophe Glorieux current address is Sun Yat-Sen University Cancer Center, State Key Laboratory of Oncology in South China, Collaborative Innovation Center of Cancer Medicine, 510275 Guangzhou, China. Nicolas Dejeans current address is Université Bordeaux-Segalen, Inserm U1053, 33000 Bordeaux, France.

Conflicts of Interest

The authors declare that there are no conflicts of interest.

Acknowledgments

This project was funded by FNRS-Télévie Grant (Grant no. 7.4575.12F). The authors thank Dr. Anabelle Decottignies (UCL, Brussels, Belgium) for her kind gift of phospho-p53 and Chk2 antibodies. The authors are also grateful to Dr. Martha Stampfer and Dr. James Garbe (Lawrence Berkeley National Laboratory, Berkeley, CA, USA) for the 250MK cells and to Dr. Jean-Baptiste Demoulin (UCL, Brussels, Belgium) for supplying the authors with the plasmid pcDNA3 coding an ubiquitin-Flag.

Supplementary Materials

Table S1: Oligonucleotides (qRT-PCR). *(Supplementary Materials)*

References

[1] M. Nishikawa, M. Hashida, and Y. Takakura, "Catalase delivery for inhibiting ROS-mediated tissue injury and tumor metastasis," *Advanced Drug Delivery Reviews*, vol. 61, no. 4, pp. 319–326, 2009.

[2] M. C. Winternitz and C. R. Meloy, "On the occurrence of catalase in human tissues and its variations in diseases," *The Journal of Experimental Medicine*, vol. 10, no. 6, pp. 759–781, 1908.

[3] C. Glorieux, M. Zamocky, J. M. Sandoval, J. Verrax, and P. B. Calderon, "Regulation of catalase expression in healthy and cancerous cells," *Free Radical Biology & Medicine*, vol. 87, pp. 84–97, 2015.

[4] L. Goth, P. Rass, and A. Pay, "Catalase enzyme mutations and their association with diseases," *Molecular Diagnosis*, vol. 8, no. 3, pp. 141–149, 2004.

[5] D. G. Bostwick, E. E. Alexander, R. Singh et al., "Antioxidant enzyme expression and reactive oxygen species damage in prostatic intraepithelial neoplasia and cancer," *Cancer*, vol. 89, no. 1, pp. 123–134, 2000.

[6] J. Chung-man Ho, S. Zheng, S. A. Comhair, C. Farver, and S. C. Erzurum, "Differential expression of manganese superoxide dismutase and catalase in lung cancer," *Cancer Research*, vol. 61, no. 23, pp. 8578–8585, 2001.

[7] C. Lauer, A. Volkl, S. Riedl, H. D. Fahimi, and K. Beier, "Impairment of peroxisomal biogenesis in human colon carcinoma," *Carcinogenesis*, vol. 20, no. 6, pp. 985–989, 1999.

[8] J. Verrax, R. Pedrosa, R. Beck, N. Dejeans, H. Taper, and P. Calderon, "In situ modulation of oxidative stress: a novel and efficient strategy to kill cancer cells," *Current Medicinal Chemistry*, vol. 16, no. 15, pp. 1821–1830, 2009.

[9] R. Beck, R. C. Pedrosa, N. Dejeans et al., "Ascorbate/menadione-induced oxidative stress kills cancer cells that express normal or mutated forms of the oncogenic protein Bcr-Abl. An in vitro and in vivo mechanistic study," *Investigational New Drugs*, vol. 29, no. 5, pp. 891–900, 2011.

[10] C. Glorieux, J. M. Sandoval, A. Fattaccioli et al., "Chromatin remodeling regulates catalase expression during cancer cells adaptation to chronic oxidative stress," *Free Radical Biology & Medicine*, vol. 99, pp. 436–450, 2016.

[11] Y. Sun, N. H. Colburn, and L. W. Oberley, "Depression of catalase gene expression after immortalization and transformation of mouse liver cells," *Carcinogenesis*, vol. 14, no. 8, pp. 1505–1510, 1993.

[12] C. Glorieux, N. Dejeans, B. Sid, R. Beck, P. B. Calderon, and J. Verrax, "Catalase overexpression in mammary cancer cells leads to a less aggressive phenotype and an altered response to chemotherapy," *Biochemical Pharmacology*, vol. 82, no. 10, pp. 1384–1390, 2011.

[13] N. Dejeans, C. Glorieux, S. Guenin et al., "Overexpression of GRP94 in breast cancer cells resistant to oxidative stress promotes high levels of cancer cell proliferation and migration: implications for tumor recurrence," *Free Radical Biology & Medicine*, vol. 52, no. 6, pp. 993–1002, 2012.

[14] C. Glorieux, J. Auquier, N. Dejeans et al., "Catalase expression in MCF-7 breast cancer cells is mainly controlled by PI3K/Akt/mTor signaling pathway," *Biochemical Pharmacology*, vol. 89, no. 2, pp. 217–223, 2014.

[15] J. C. Garbe, S. Bhattacharya, B. Merchant et al., "Molecular distinctions between stasis and telomere attrition senescence barriers shown by long-term culture of normal human mammary epithelial cells," *Cancer Research*, vol. 69, no. 19, pp. 7557–7568, 2009.

[16] B. Marquez, G. Ameye, C. M. Vallet, P. M. Tulkens, H. A. Poirel, and F. van Bambeke, "Characterization of *Abcc4* gene amplification in stepwise-selected mouse J774 macrophages resistant to the topoisomerase II inhibitor ciprofloxacin," *PLoS One*, vol. 6, no. 12, article e28368, 2011.

[17] F. P. Duhoux, G. Ameye, C. P. Montano-Almendras et al., "*PRDM16* (1p36) translocations define a distinct entity of myeloid malignancies with poor prognosis but may also occur in lymphoid malignancies," *British Journal of Haematology*, vol. 156, no. 1, pp. 76–88, 2012.

[18] S. Medves, F. P. Duhoux, A. Ferrant et al., "KANK1, a candidate tumor suppressor gene, is fused to PDGFRB in an imatinib-responsive myeloid neoplasm with severe thrombocythemia," *Leukemia*, vol. 24, no. 5, pp. 1052–1055, 2010.

[19] C. Glorieux, J. M. Sandoval, N. Dejeans et al., "Overexpression of NAD(P)H:quinone oxidoreductase 1 (NQO1) and genomic gain of the *NQO1* locus modulates breast cancer cell sensitivity to quinones," *Life Sciences*, vol. 145, pp. 57–65, 2016.

[20] T. Mosmann, "Rapid colorimetric assay for cellular growth and survival: application to proliferation and cytotoxicity assays," *Journal of Immunological Methods*, vol. 65, no. 1-2, pp. 55–63, 1983.

[21] P. Wieacker, C. R. Mueller, A. Mayerova, K. H. Grzeschik, and H. H. Ropers, "Assignment of the gene coding for human catalase to the short arm of chromosome 11," *Annales de Génétique*, vol. 23, no. 2, pp. 73–77, 1980.

[22] F. Hoffschir, M. Vuillaume, L. Sabatier et al., "Decrease in catalase activity and loss of the 11p chromosome arm in the course of SV40 transformation of human fibroblasts," *Carcinogenesis*, vol. 14, no. 8, pp. 1569–1572, 1993.

[23] C. Barletta, M. A. Castello, E. Ferrante et al., "11p13 deletion and reduced RBC catalase in a patient with aniridia, glaucoma and bilateral Wilms' tumor," *Tumori*, vol. 71, no. 2, pp. 119–121, 1985.

[24] J. L. Dufier, L. H. Phug, P. Schmelck et al., "Intercalary deletion of the short arm of chromosome 11: aniridia, glaucoma, staturoponderal and mental retardation, sexual ambiguity, gonadoblastoma and catalase deficiency," *Bulletin des Sociétés d'Ophtalmologie de France*, vol. 81, no. 10, pp. 747–749, 1981.

[25] M. J. Gregoire, C. Pernot, F. Himont, M. Pierson, and S. Gilgenkrantz, "Chromosome 11 and cancer," *Journal de Génétique Humaine*, vol. 31, no. 1, pp. 31–36, 1983.

[26] E. E. Michalopoulos, P. J. Bevilacqua, N. Stokoe, V. E. Powers, H. F. Willard, and W. H. Lewis, "Molecular analysis of gene deletion in aniridia-Wilms tumor association," *Human Genetics*, vol. 70, no. 2, pp. 157–162, 1985.

[27] L. Sabatier, F. Hoffschir, W. A. al Achkar, C. Turleau, J. de Grouchy, and B. Dutrillaux, "The decrease of catalase or esterase D activity in patients with microdeletions of 11p or 13q does not increase their radiosensitivity," *Annales de Génétique*, vol. 32, no. 3, pp. 144–148, 1989.

[28] E. N. Sotnikova, L. A. Durnov, R. V. Zhordania, R. F. Gar'kavtseva, and A. F. Bukhny, "Changes in the hemoglobin fractions of nephroblastoma patients," *Genetika*, vol. 20, no. 2, pp. 357–361, 1984.

[29] V. van Heyningen, P. A. Boyd, A. Seawright et al., "Molecular analysis of chromosome 11 deletions in aniridia-Wilms tumor syndrome," *Proceedings of the National Academy of Sciences of the United States of America*, vol. 82, no. 24, pp. 8592–8596, 1985.

[30] K. M. Fong, P. V. Zimmerman, and P. J. Smith, "Correlation of loss of heterozygosity at 11p with tumour progression and survival in non-small cell lung cancer," *Genes, Chromosomes & Cancer*, vol. 10, no. 3, pp. 183–189, 1994.

[31] C. U. Ludwig, G. Raefle, P. Dalquen, P. Stulz, R. Stahel, and J. P. Obrecht, "Allelic loss on the short arm of chromosome 11 in non-small-cell lung cancer," *International Journal of Cancer*, vol. 49, no. 5, pp. 661–665, 1991.

[32] R. Shipman, P. Schraml, M. Colombi, and C. U. Ludwig, "Allelic deletion at chromosome 11p13 defines a tumour suppressor region between the catalase gene and D11S935 in human non-small cell lung carcinoma," *International Journal of Oncology*, vol. 12, no. 1, pp. 107–111, 1998.

[33] M. Yamada, K. Hashinaka, J. Inazawa, and T. Abe, "Expression of catalase and myeloperoxidase genes in hydrogen peroxide-resistant HL-60 cells," *DNA and Cell Biology*, vol. 10, no. 10, pp. 735–742, 1991.

[34] J. Rouse and S. P. Jackson, "Interfaces between the detection, signaling, and repair of DNA damage," *Science*, vol. 297, no. 5581, pp. 547–551, 2002.

[35] B. B. Zhou and S. J. Elledge, "The DNA damage response: putting checkpoints in perspective," *Nature*, vol. 408, no. 6811, pp. 433–439, 2000.

[36] E. Maiani, M. Diederich, and S. Gonfloni, "DNA damage response: the emerging role of c-Abl as a regulatory switch?," *Biochemical Pharmacology*, vol. 82, no. 10, pp. 1269–1276, 2011.

[37] C. Cao, Y. Leng, and D. Kufe, "Catalase activity is regulated by c-Abl and Arg in the oxidative stress response," *The Journal of Biological Chemistry*, vol. 278, no. 32, pp. 29667–29675, 2003.

[38] C. Cao, Y. Leng, X. Liu, Y. Yi, P. Li, and D. Kufe, "Catalase is regulated by ubiquitination and proteosomal degradation. Role of the c-Abl and Arg tyrosine kinases," *Biochemistry*, vol. 42, no. 35, pp. 10348–10353, 2003.

[39] H. Furuta, A. Hachimori, Y. Ota, and T. Samejima, "Dissociation of bovine liver catalase into subunits on acetylation," *The Journal of Biochemistry*, vol. 76, no. 3, pp. 481–491, 1974.

[40] M. Y. Kang, H. B. Kim, C. Piao et al., "The critical role of catalase in prooxidant and antioxidant function of p53," *Cell Death & Differentiation*, vol. 20, no. 1, pp. 117–129, 2013.

[41] R. Rafikov, S. Kumar, S. Aggarwal et al., "Endothelin-1 stimulates catalase activity through the PKCδ-mediated phosphorylation of serine 167," *Free Radical Biology & Medicine*, vol. 67, pp. 255–264, 2014.

[42] D. Watters, P. Kedar, K. Spring et al., "Localization of a portion of extranuclear ATM to peroxisomes," *The Journal of Biological Chemistry*, vol. 274, no. 48, pp. 34277–34282, 1999.

[43] H. Yan and J. J. Harding, "Glycation-induced inactivation and loss of antigenicity of catalase and superoxide dismutase," *The Biochemical Journal*, vol. 328, no. 2, pp. 599–605, 1997.

[44] A. Geerts, B. De Prest, and F. Roels, "On the topology of the catalase biosynthesis and -degradation in the guinea pig liver. A cytochemical study," *Histochemistry*, vol. 80, no. 4, pp. 339–345, 1984.

[45] B. Poole, "The kinetics of disappearance of labeled leucine from the free leucine pool of rat liver and its effect on the apparent turnover of catalase and other hepatic proteins," *The Journal of Biological Chemistry*, vol. 246, no. 21, pp. 6587–6591, 1971.

[46] B. Poole, F. Leighton, and C. De Duve, "The synthesis and turnover of rat liver peroxisomes," *The Journal of Cell Biology*, vol. 41, no. 2, pp. 536–546, 1969.

[47] B. Ghosh, E. Barbosa, and I. Singh, "Characterization of fibroblast cytoplasmic proteins that bind to the 3′ UTR of human catalase mRNA," *Molecular and Cellular Biochemistry*, vol. 209, no. 1-2, pp. 9–15, 2000.

[48] D. Sampath and R. Perez-Polo, "Regulation of antioxidant enzyme expression by NGF," *Neurochemical Research*, vol. 22, no. 4, pp. 351–362, 1997.

[49] D. Yu, C. O. dos Santos, G. Zhao et al., "miR-451 protects against erythroid oxidant stress by repressing 14-3-3ζ," *Genes & Development*, vol. 24, no. 15, pp. 1620–1633, 2010.

[50] R. Haque, E. Chun, J. C. Howell, T. Sengupta, D. Chen, and H. Kim, "MicroRNA-30b-mediated regulation of catalase expression in human ARPE-19 cells," *PLoS One*, vol. 7, no. 8, article e42542, 2012.

[51] S. A. Akman, G. Forrest, F. F. Chu, and J. H. Doroshow, "Resistance to hydrogen peroxide associated with altered catalase mRNA stability in MCF7 breast cancer cells," *Biochimica et Biophysica Acta (BBA) - Gene Structure and Expression*, vol. 1009, no. 1, pp. 70–74, 1989.

[52] T. B. Lee, Y. S. Moon, and C. H. Choi, "Histone H4 deacetylation down-regulates catalase gene expression in doxorubicin-resistant AML subline," *Cell Biology and Toxicology*, vol. 28, no. 1, pp. 11–18, 2012.

[53] J. Y. Min, S. O. Lim, and G. Jung, "Downregulation of catalase by reactive oxygen species via hypermethylation of CpG island II on the catalase promoter," *FEBS Letters*, vol. 584, no. 11, pp. 2427–2432, 2010.

[54] X. Quan, S. O. Lim, and G. Jung, "Reactive oxygen species downregulate catalase expression via methylation of a CpG island in the Oct-1 promoter," *FEBS Letters*, vol. 585, no. 21, pp. 3436–3441, 2011.

[55] S. Ding, B. D. Gong, J. Yu et al., "Methylation profile of the promoter CpG islands of 14 "drug-resistance" genes in hepatocellular carcinoma," *World Journal of Gastroenterology*, vol. 10, no. 23, pp. 3433–3440, 2004.

[56] S. Ribieras, X. G. Song-Wang, V. Martin, P. Lointier, L. Frappart, and R. Dante, "Human breast and colon cancers exhibit alterations of DNA methylation patterns at several DNA segments on chromosomes 11p and 17p," *Journal of Cellular Biochemistry*, vol. 56, no. 1, pp. 86–96, 1994.

[57] C. Glorieux and P. B. Calderon, "Catalase, a remarkable enzyme: targeting the oldest antioxidant enzyme to find a new cancer treatment approach," *Biological Chemistry*, vol. 398, no. 10, pp. 1095–1108, 2017.

Hindawi
Oxidative Medicine and Cellular Longevity
Volume 2017, Article ID 7126872, 13 pages
https://doi.org/10.1155/2017/7126872

Research Article

Xylopine Induces Oxidative Stress and Causes G_2/M Phase Arrest, Triggering Caspase-Mediated Apoptosis by p53-Independent Pathway in HCT116 Cells

Luciano de Souza Santos,[1] Valdenizia Rodrigues Silva,[1] Leociley Rocha Alencar Menezes,[2] Milena Botelho Pereira Soares,[1,3] Emmanoel Vilaça Costa,[4] and Daniel Pereira Bezerra[1]

[1]*Gonçalo Moniz Institute, Oswaldo Cruz Foundation (IGM-FIOCRUZ/BA), Salvador, BA, Brazil*
[2]*Department of Chemistry, Federal University of Sergipe, São Cristóvão, SE, Brazil*
[3]*Center of Biotechnology and Cell Therapy, Hospital São Rafael, 41253-190 Salvador, BA, Brazil*
[4]*Department of Chemistry, Federal University of Amazonas, Manaus, AM, Brazil*

Correspondence should be addressed to Daniel Pereira Bezerra; danielpbezerra@gmail.com

Received 6 August 2017; Revised 12 September 2017; Accepted 20 September 2017; Published 6 December 2017

Academic Editor: Spencer Gibson

Xylopine is an aporphine alkaloid that has cytotoxic activity to cancer cells. In this study, the underlying mechanism of xylopine cytotoxicity was assessed in human colon carcinoma HCT116 cells. Xylopine displayed potent cytotoxicity in different cancer cell lines in monolayer cultures and in a 3D model of cancer multicellular spheroids formed from HCT116 cells. Typical morphology of apoptosis, cell cycle arrest in the G_2/M phase, increased internucleosomal DNA fragmentation, loss of the mitochondrial transmembrane potential, and increased phosphatidylserine externalization and caspase-3 activation were observed in xylopine-treated HCT116 cells. Moreover, pretreatment with a caspase-3 inhibitor (Z-DEVD-FMK), but not with a p53 inhibitor (cyclic pifithrin-α), reduced xylopine-induced apoptosis, indicating induction of caspase-mediated apoptosis by the p53-independent pathway. Treatment with xylopine also caused an increase in the production of reactive oxygen/nitrogen species (ROS/RNS), including hydrogen peroxide and nitric oxide, but not superoxide anion, and reduced glutathione levels were decreased in xylopine-treated HCT116 cells. Application of the antioxidant N-acetylcysteine reduced the ROS levels and xylopine-induced apoptosis, indicating activation of ROS-mediated apoptosis pathway. In conclusion, xylopine has potent cytotoxicity to different cancer cell lines and is able to induce oxidative stress and G_2/M phase arrest, triggering caspase-mediated apoptosis by the p53-independent pathway in HCT116 cells.

1. Introduction

Colon and rectal carcinoma is a major public health problem with the third highest incidence and the fourth highest mortality worldwide [1]. The most common chemotherapy used for colon and rectal carcinoma treatment include 5-fluorouracil (5-FU, combined with folinic acid), capecitabine, irinotecan, oxaliplatin, and trifluridine (combined with tipiracil); however, resistance development and severe side effects are limitations commonly associated with the use of these drugs [2].

Aporphine alkaloids are plant-derived compounds that belong to the isoquinoline class of alkaloids and possess diverse therapeutical potential, including cancer treatment, with potent cytotoxic activity to cancer cells and the ability to prevent cell proliferation and induce apoptosis and inhibition of DNA topoisomerase and epidermal growth factor receptor [3]. Moreover, the 1,2-methylenedioxy and methylation of nitrogen have been reported as important pharmacophoric groups for the cytotoxicity of aporphine alkaloids [4, 5].

Xylopine (Figure 1) is an aporphine alkaloid found in the stem of *Xylopia laevigata* (Annonaceae). In our previous

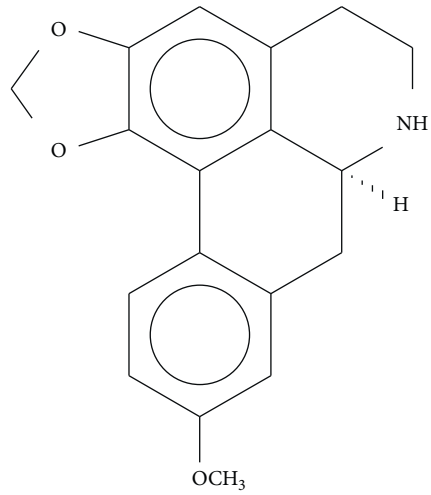

Figure 1: Chemical structure of xylopine.

studies, we identified xylopine as a potent cytotoxic agent that causes G_2/M cell cycle arrest and apoptosis in human hepatocellular carcinoma HepG2 cells [6]. However, the mechanisms of action of xylopine in cancer cells have not been clearly demonstrated. In this study, the underlying mechanism of xylopine cytotoxicity was assessed in human colon carcinoma (HCT116) cells.

2. Material and Methods

2.1. Xylopine Isolation. The stem of *X. laevigata* was collected in "Serra de Itabaiana" between Itabaiana and Areia Branca cities (coordinates: 10°44′50″S, 37°20′24″W), Sergipe, Brazil, in February 2013. The identity of the plant was confirmed by Dr. Ana Paula do N. Prata, Department of Biology, Federal University of Sergipe, Brazil, and a voucher specimen (number 26805) has been deposited in the Herbarium of the Federal University of Sergipe. The dried and powdered stem of *X. laevigata* (1.4 kg) was successively extracted with hexane followed by methanol, to yield hexane (18.8 g) and methanol (87.8 g) extracts. Xylopine was isolated from the methanol extract as previously described [6].

2.2. Cells. MCF7 (human breast carcinoma), HCT116 (human colon carcinoma), HepG2 (human hepatocellular carcinoma), SCC-9 (human oral squamous cell carcinoma), HSC-3 (human oral squamous cell carcinoma), HL-60 (human promyelocytic leukemia), K-562 (human chronic myelogenous leukemia), B16-F10 (murine melanoma), MRC-5 (human lung fibroblast), WT SV40 MEF (wild-type immortalized mouse embryonic fibroblast), and BAD KO SV40 MEF (BAD gene knockout immortalized mouse embryonic fibroblast) cell lines were obtained from the American Type Culture Collection (ATCC, Manassas, VA, USA). Cells were cultured in complete medium with appropriate supplements as recommended by ATCC. All cell lines were tested for mycoplasma using the Mycoplasma Stain Kit (Sigma-Aldrich) to validate the use of cells free from contamination. Primary cell culture of peripheral blood mononuclear cells (PBMC) was obtained by standard Ficoll density protocol. The Research Ethics Committee of the Oswaldo Cruz Foundation (Salvador, BA, Brazil) approved the experimental protocol (number 031019/2013). Cell viability was examined using trypan blue exclusion assay for all experiments.

2.3. Cytotoxic Activity Assay. Cell viability was quantified using the alamarBlue assay according to Ahmed et al. [7]. Cells were inserted in 96-well plates for all experiments (7×10^4 cells/mL for adherent cells or 3×10^5 cells/mL for suspended cells in 100 μL of medium). After 24 h, xylopine was dissolved in dimethyl sulfoxide (DMSO) and added to each well and incubated for 72 h. Doxorubicin (purity ≥ 95%, doxorubicin hydrochloride, Laboratory IMA S.A.I.C., Buenos Aires, Argentina) and oxaliplatin (Sigma-Aldrich Co., Saint Louis, MO, USA) were used as positive controls. Four (for cell lines) or 24 h (for PBMCs) before the end of incubation, 20 μL of a stock solution (0.312 mg/mL) of the alamarBlue (resazurin, Sigma-Aldrich Co., Saint Louis, MO, USA) was added to each well. Absorbance at 570 nm and 600 nm was measured using the SpectraMax 190 Microplate Reader (Molecular Devices, Sunnyvale, CA, USA), and the drug effect was quantified as the percentage of control absorbance.

2.4. 3D Multicellular Spheroids Culture. HCT116 cells were cultivated in three-dimensional (3D) multicellular spheroids. Briefly, 100 μL of a solution of cells (0.5×10^6 cells/mL) was inserted in 96-well plates with a cell-repellent surface (Greiner Bio-One, Kremsmünster, Austria) and cultured in complete medium plus 3% Matrigel (BD Biosciences, San Jose, CA, USA). Spheroids with stable structures had formed after three days. Then, the spheroids were exposed to a range of drug concentrations for 72 h, after which the cell viability was quantified by alamarBlue assay as described above.

2.5. Morphological Analysis. To evaluate alterations in morphology, cells were cultured under coverslip and stained with May-Grünwald-Giemsa. Morphological changes were examined by light microscopy using Image-Pro software.

2.6. Internucleosomal DNA Fragmentation and Cell Cycle Distribution. Cells were harvested in a permeabilization solution containing 0.1% Triton X-100 (Sigma Chemical Co., St Louis, MO, USA), 2 μg/mL propidium iodide (Sigma Chemical Co.), 0.1% sodium citrate, and 100 μg/mL RNAse (Sigma Chemical Co.) and incubated in the dark for 15 min at room temperature [8]. Finally, cell fluorescence was measured by flow cytometry on a BD LSRFortessa cytometer using the BD FACSDiva software (BD Biosciences) and FlowJo software 10 (FlowJo, LCC, Ashland, OR, USA).

2.7. Annexin V/PI Staining Assay. For apoptosis detection, we used the FITC Annexin V Apoptosis Detection Kit I (BD Biosciences), and the analysis was performed according to the manufacturer's instructions. The cell fluorescence was determined by flow cytometry as described above. The protection assays using a caspase-3 inhibitor (Z-DEVD-FMK, BD Biosciences), a p53 inhibitor (cyclic pifithrin-α, Cayman

Table 1: Cytotoxic activity of xylopine (XYL).

Cells	Histological type	IC_{50} in μM		
		DOX	OXA	XYL
Cancer cells				
MCF7	Human breast carcinoma	1.1 0.3–3.5	5.9 3.5–9.9	12.0 6.1–23.6
HCT116	Human colon carcinoma	0.1 0.04–0.11	4.1 2.7–6.4	6.4 5.1–8.2
HepG2	Human hepatocellular carcinoma	0.1 0.04–0.11	1.0 0.2-3.9	9.4 6.0–14.8
SCC9	Human oral squamous cell carcinoma	0.5 0.4–0.7	N.d.	26.6 21.9–32.1
HSC3	Human oral squamous cell carcinoma	0.3 0.2–0.4	3.3 1.4–7.8	15.7 10.2–24.3
HL-60	Human promyelocytic leukemia	0.3 0.3–0.4	0.4 0.1–3.8	18.5 16.0–21.3
K562	Human chronic myelogenous leukemia	0.3 0.2–0.5	0.9 0.1–9.7	7.8 6.1–9.9
B16-F10	Murine melanoma	0.03 0.02–0.07	0.1 0.03–1.3	9.6 8.0–11.4
Noncancer cells				
MRC5	Human lung fibroblast	1.5 1.2–2.0	1.5 0.9–2.8	24.1 20.8–28.3
PBMC	Human peripheral blood mononuclear cells	5.2 2.4–11.4	14.9 8.9–24.8	18.3 11.0–29.0

Data are presented as IC_{50} values in μM and their respective 95% confidence interval obtained by nonlinear regression from at the least three independent experiments performed in duplicate and measured by alamarBlue assay after 72 h incubation. Doxorubicin (DOX) and oxaliplatin (OXA) were used as positive controls. N.d.: not determined.

Table 2: Selectivity index of xylopine (XYL).

Cancer cells	Noncancer cells					
	MRC5			PBMC		
	DOX	OXA	XYL	DOX	OXA	XYL
MCF7	1.4	0.3	2	4.7	2.5	1.5
HCT116	15	0.4	3.8	52	3.6	2.9
HepG2	15	1.5	2.6	52	14.9	2
SCC-9	3	N.d.	0.9	10.4	N.d.	0.7
HSC-3	5	0.5	1.5	17.3	4.5	1.2
HL-60	5	3.8	1.3	17.3	37.3	1
K-562	5	1.7	3.1	17.3	16.6	2.4
B16-F10	50	15	2.5	173.3	149	1.9

Data are presented the selectivity index (SI) calculated using the following formula: SI = IC_{50}(noncancer cells)/IC_{50}(cancer cells). Cancer cells: MCF7 (human breast carcinoma), HCT116 (human colon carcinoma), HepG2 (human hepatocellular carcinoma), SCC-9 (human oral squamous cell carcinoma), HSC-3 (human oral squamous cell carcinoma), HL-60 (human promyelocytic leukemia), K-562 (human chronic myelogenous leukemia), and B16-F10 murine melanoma. Noncancer cells: MRC-5 (human lung fibroblast) and PBMC human peripheral blood mononuclear cells. Doxorubicin (DOX) and oxaliplatin (OXA) were used as positive controls. N.d.: not determined.

Chemical, Ann Arbor, MI, USA), and an antioxidant N-acetyl-L-cysteine (NAC, Sigma-Aldrich Co.) were performed. In brief, the cells were pretreated for 2 h with 50 μM Z-DEVD-FMK and 10 μM cyclic pifithrin-α and for 1 h with 5 mM NAC, followed by incubation with 14 μM xylopine for 48 h. The cells were then trypsinized and the FITC Annexin V Apoptosis Detection assay was conducted as described above.

2.8. Measurement of the Mitochondrial Transmembrane Potential. Mitochondrial transmembrane potential was determined by the retention of the dye rhodamine 123 [9]. Cells were incubated with rhodamine 123 (5 μg/mL, Sigma-Aldrich Co.) at room temperature for 15 min in the dark and washed with saline. The cells were then incubated again in saline for 30 min in the dark and cell fluorescence was determined by flow cytometry as described above.

2.9. Caspase-3 Activation Assay. A Caspase-3 Colorimetric Assay Kit (Sigma-Aldrich Co.) was used to investigate caspase-3 activation in xylopine-treated HCT116 cells based on the cleavage of Ac-DEVD-pNA and the analysis was performed according to the manufacturer's instructions.

2.10. Measurement of Cellular Reactive Oxygen Species Levels. The levels of reactive oxygen species (ROS) were measured

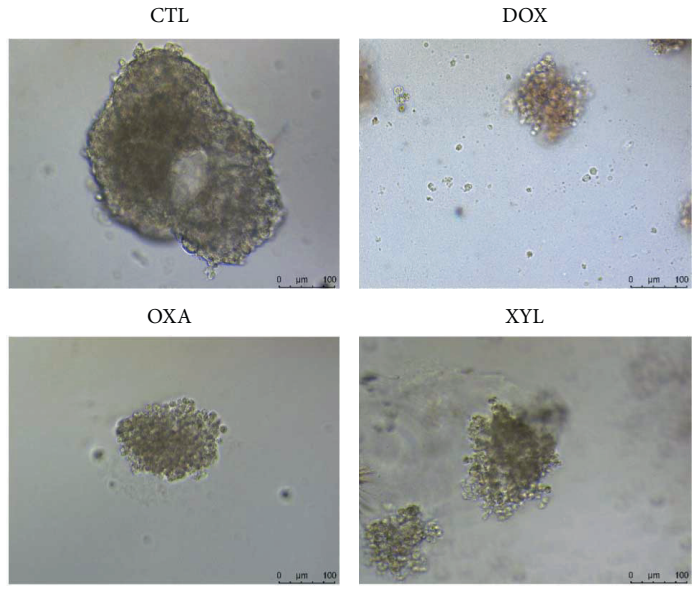

(a)

Spheroids	IC_{50} in μM		
	DOX	OXA	XYL
HCT116	4.5	6.0	24.6
	2.5–8.2	3.5–10.5	17.9–34.0

(b)

Figure 2: Effect of xylopine (XYL) in 3D in vitro model of cancer multicellular spheroids formed from HCT116 cells. (a) Cells examined by light microscopy (bar = 100 μm). (b) IC_{50} values in μM and their respective 95% confidence interval obtained by nonlinear regression from three independent experiments performed in duplicate and measured by alamarBlue assay after 72 h of incubation. The negative control (CTL) was treated with the vehicle used for diluting the compound tested. Doxorubicin (DOX) and oxaliplatin (OXA) were used as positive controls.

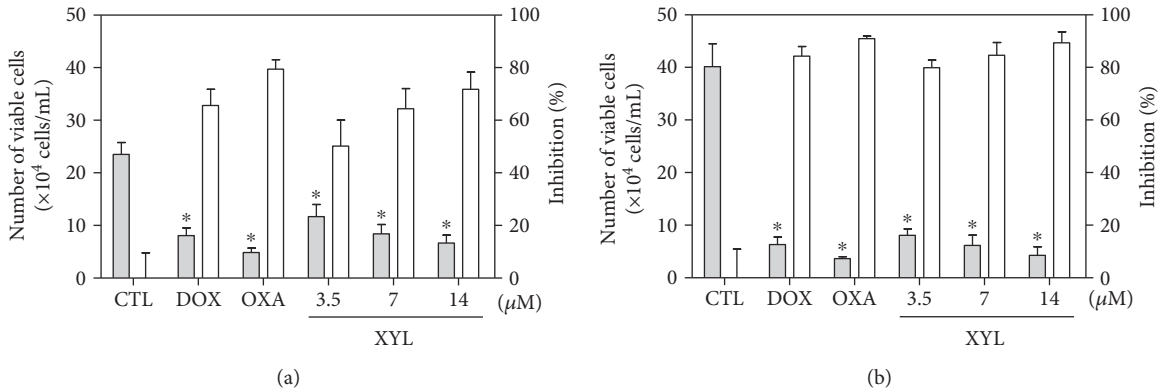

Figure 3: Effect of xylopine (XYL) in the cell viability of HCT116 cells determined by trypan blue staining after 24 h (a) and 48 h (b) of incubation. The gray bars represent the number of viable cells ($\times 10^4$cells/mL), and the white bars represent cell inhibition (%). The negative control (CTL) was treated with the vehicle (0.1% DMSO) used for diluting the compound tested. Doxorubicin (DOX, 1 μM) and oxaliplatin (OXA, 2.5 μM) were used as positive controls. Data are presented as the mean ± S.E.M. of three independent experiments performed in duplicate. $^*p < 0.05$ compared with the negative control by ANOVA followed by Student–Newman–Keuls test.

Table 3: Effect of xylopine (XYL) in the cell cycle distribution of HCT116 cells.

Treatment	Concentration (μM)	DNA content (%)			
		Sub-G_0/G_1	G_0/G_1	S	G_2/M
24 h incubation					
CTL	—	3.9 ± 1.0	42.0 ± 2.5	12.6 ± 2.8	30.7 ± 4.1
DOX	1	9.7 ± 2.5	28.0 ± 6.3	10.0 ± 2.5	44.1 ± 3.4*
OXA	2.5	8.8 ± 3.5	32.4 ± 3.7	13.5 ± 3.1	39.9 ± 1.5
XYL	3.5	6.2 ± 1.9	17.0 ± 7.0*	24.7 ± 4.8	57.2 ± 3.5*
	7	5.1 ± 1.6	14.9 ± 4.2*	23.3 ± 3.7	58.5 ± 2.9*
	14	11.3 ± 1.4	30.5 ± 6.0	11.1 ± 1.6	54.0 ± 6.1*
48 h incubation					
CTL	—	3.3 ± 0.7	44.8 ± 1.1	13.5 ± 2.4	23.8 ± 2.8
DOX	1	18.3 ± 2.5	22.5 ± 4.0*	14.9 ± 2.5	44.2 ± 4.4*
OXA	2.5	17.7 ± 1.9	36.2 ± 2.6	7.6 ± 0.4	32.2 ± 4.4
XYL	3.5	15.2 ± 1.9	17.0 ± 6.3*	11.1 ± 2.2	52.0 ± 6.8*
	7	25.9 ± 2.5*	10.3 ± 1.3*	6.8 ± 2.0	52.7 ± 3.6*
	14	33.4 ± 6.2*	14.6 ± 2.6*	9.3 ± 1.7	40.8 ± 5.7*

Data are presented as the mean ± S.E.M. of three independent experiments performed in duplicate. The negative control (CTL) was treated with the vehicle (0.1% DMSO) used for diluting the compound tested. Doxorubicin (DOX) and oxaliplatin (OXA) were used as positive controls. Ten thousand events were evaluated per experiment, and cellular debris was omitted from the analysis. *$p < 0.05$ compared with the negative control by ANOVA followed by Student–Newman–Keuls test.

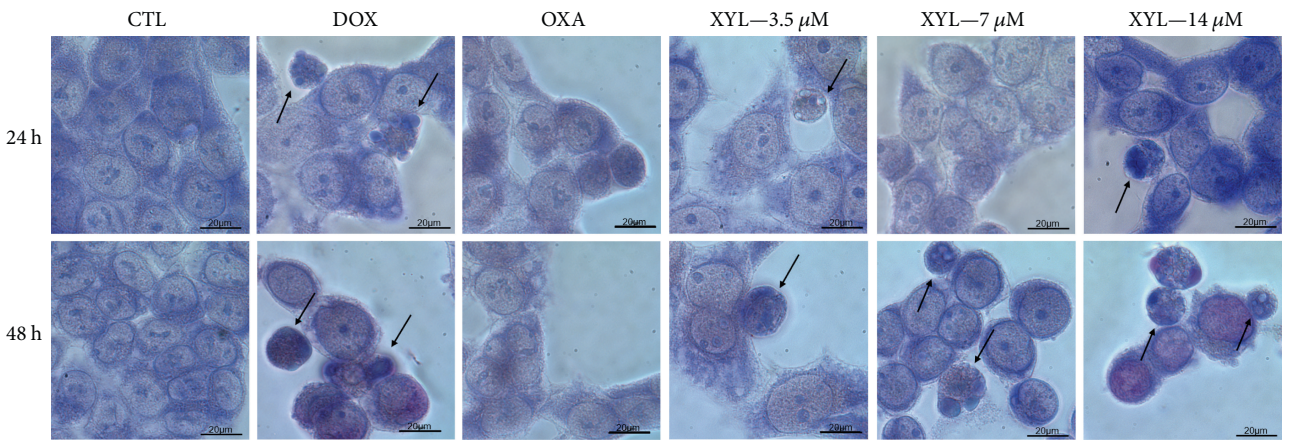

Figure 4: Effect of xylopine (XYL) in the morphologic analysis of HCT116 cells after 24 and 48 h incubation. The cells were stained with May-Grünwald-Giemsa and examined by light microscopy (bar = 20 μm). Arrows indicated cells with a reduction in the cell volume, chromatin condensation, or fragmented DNA. The negative control (CTL) was treated with the vehicle (0.1% DMSO) used for diluting the compound tested. Doxorubicin (DOX, 1 μM) and oxaliplatin (OXA, 2.5 μM) were used as positive controls.

according to previously described [10] using 2′,7′-dichlorofluorescin diacetate (DCF-DA) (Sigma-Aldrich Co.). In brief, cells were treated with xylopine for 1 and 3 h. Then, the cells were collected, washed with saline, and resuspended in FACS tubes with saline containing 5 μM DCF-DA for 30 min. Finally, the cells were washed with saline and the cell fluorescence was determined by flow cytometry as described above. The protection assay using the antioxidant NAC and catalase (Sigma-Aldrich Co.) was performed. In brief, the cells were pretreated for 1 h with 5 mM NAC or 2000 UI catalase and then incubated with xylopine in the established concentration for 1 h. The cells were then trypsinized and the ROS levels were measured as described above.

2.11. Measurement of Cellular Superoxide Anion Level. Hydroethidine (Sigma-Aldrich Co.) was used to detect cellular superoxide levels after 1 h of treatment with xylopine [11]. The cells were labeled with 10 μM of hydroethidine for 30 min. Finally, the cells were washed with saline and the cell fluorescence was determined by flow cytometry as described above.

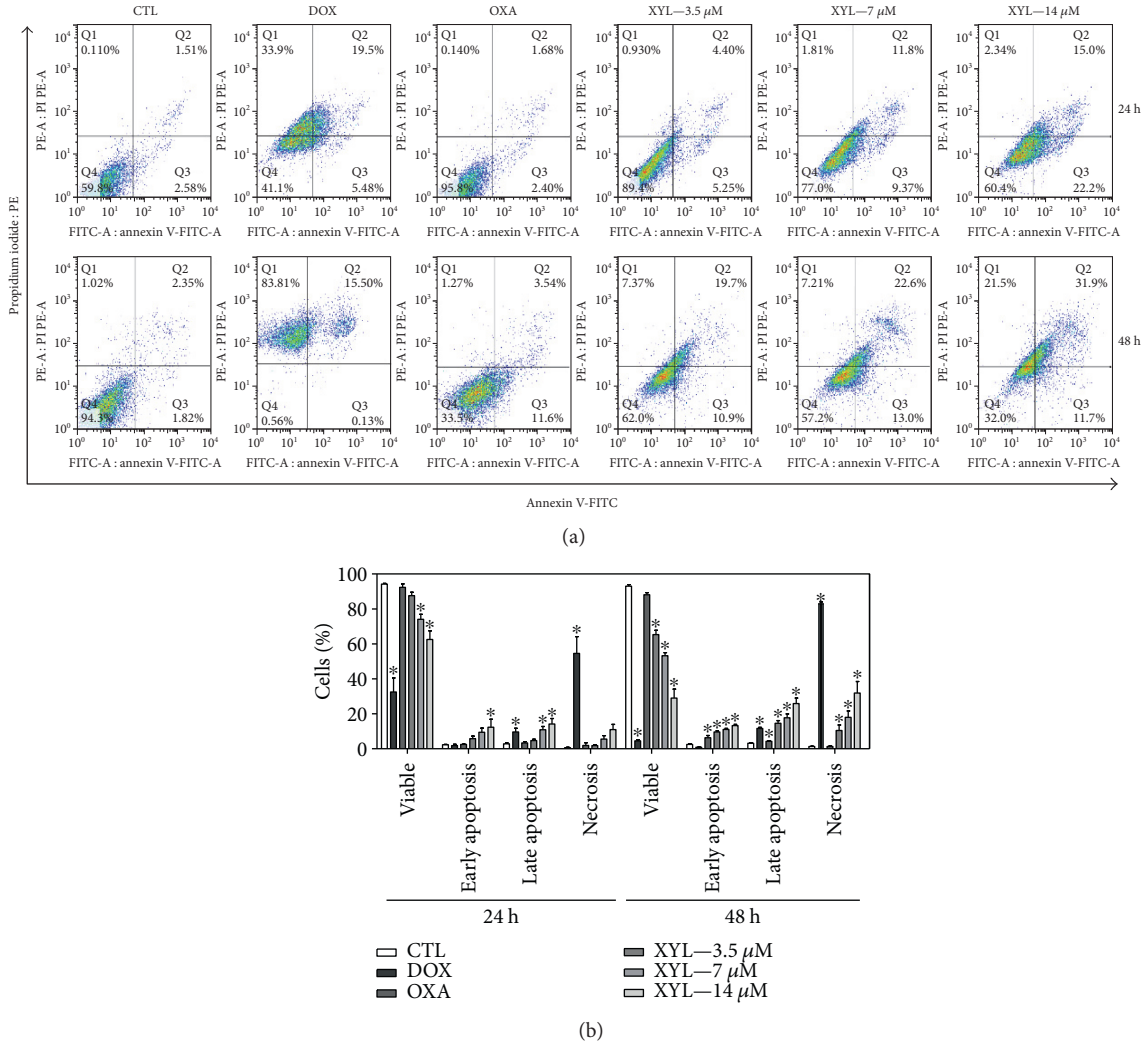

Figure 5: Effect of xylopine (XYL) in the induction of apoptosis in HCT116 cells determined by flow cytometry using annexin V-FITC/PI staining after 24 and 48 h incubation. (a) Representative flow cytometric dot plots showing the percentage of cells in viable, early apoptotic, late apoptotic, and necrotic stages. (b) Quantification of the cell viability. The negative control (CTL) was treated with the vehicle (0.1% DMSO) used for diluting the compound tested. Doxorubicin (DOX, 1 μM) and oxaliplatin (OXA, 2.5 μM) were used as positive controls. Data are presented as the mean ± S.E.M. of three independent experiments performed in duplicate. Ten thousand events were evaluated per experiment and cellular debris was omitted from the analysis. $^*p < 0.05$ compared with the negative control by ANOVA followed by Student–Newman–Keuls test.

2.12. Measurement of Nitric Oxide Production. Nitric oxide generation was detected with 4-amino-5-methylamino-2′-,7′-difluofluorescein diacetate (DAF-FM diacetate) (Molecular Probes, Eugene, OR, USA) [12]. The cells were labeled with 3 μM of DAF-FM diacetate for 60 minutes at 37°C. Following staining cells were washed with saline and incubated for an additional 15 minutes at 37°C to allow for complete deesterification of the intracellular diacatates. Then, the nitric oxide radical was measured by flow cytometry as described above.

2.13. Measurement of Cellular GSH Level. A quantification kit for reduced glutathione (L-γ-glutamyl-L-cysteinyl-glycine, GSH, Sigma-Aldrich Co.) was used to investigate cellular GSH level in xylopine-treated HCT116 cells and the analysis was performed according to the manufacturer's instructions.

2.14. DNA Intercalation Assay. DNA intercalation was assessed by examining the ability of xylopine to displace ethidium bromide from calf thymus DNA (ctDNA, Sigma-Aldrich Co.) [13]. The assay was conducted in 96-well plates and contained 15 μg/mL ctDNA, 1.5 μM ethidium bromide, and 10 or 20 μM xylopine in 100 μL saline solution. Doxorubicin (10 μM) was used as positive control. Fluorescence was measured using excitation and emission wavelengths of 320 and 600 nm, respectively.

2.15. Statistical Analysis. Data are presented as mean ± S.E.M. or IC_{50} values and their 95% confidence intervals (CI 95%)

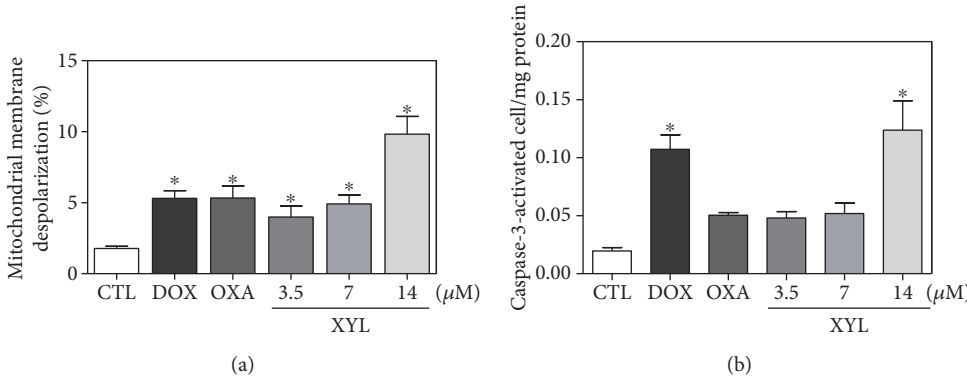

Figure 6: Effect of xylopine (XYL) in the caspase-3 activity and mitochondrial membrane potential in HCT116 cells. (a) Mitochondrial membrane potential determined by flow cytometry using rhodamine 123 staining after 24 h incubation. (b) Caspase-3 activity determined by colorimetric assay after 48 h incubation. The negative control (CTL) was treated with the vehicle (0.1% DMSO) used for diluting the compound tested. Doxorubicin (DOX, 1 μM) and oxaliplatin (OXA, 2.5 μM) were used as positive controls. Data are presented as the mean ± S.E.M. of three independent experiments performed in duplicate. For flow cytometry analysis, 10,000 events were evaluated per experiment and cellular debris was omitted from the analysis. $^*p < 0.05$ compared with the negative control by ANOVA followed by Student–Newman–Keuls test.

obtained by nonlinear regression. Differences between experimental groups were compared using analysis of variance (ANOVA) followed by the Student–Newman–Keuls test ($p < 0.05$). All statistical analyses were performed using GraphPad (Intuitive Software for Science, San Diego, CA, USA).

3. Results

3.1. Xylopine Displays Potent Cytotoxicity in Different Cancer Cell Lines. The cytotoxicity of xylopine was assessed in eight different cancer cell lines (MCF7, HCT116, HepG2, SCC-9, HSC-3, HL-60, K-562, and B16-F10) and in two noncancer cells (MRC-5 and PBMC) using the alamarBlue assay after 72 h incubation. Table 1 shows the results obtained. Xylopine presented IC_{50} values ranging from 6.4 to 26.6 μM for cancer cells HCT116 and SCC9, respectively. Doxorubicin presented IC_{50} values ranging from 0.03 to 1.1 μM for cancer cell lines B16-F10 and MCF7, respectively. Oxaliplatin presented IC_{50} values ranging from 0.1 to 5.9 μM for cancer cell lines B16-F10 and MCF7, respectively. The IC_{50} value for noncancer cells was 24.1 and 18.3 μM for xylopine, 1.5 and 5.2 μM for doxorubicin, and 1.5 and 14.9 μM for oxaliplatin for MRC5 and PBMC cells, respectively. Table 2 shows the selectivity index obtained. For the most cancer cell lines, xylopine exhibited selectivity index similar to positive controls doxorubicin and oxaliplatin.

HCT116 was the most sensitive cell line to xylopine-induced cytotoxicity and was used as a cellular model in a new set of experiment. Furthermore, the cytotoxic effect of xylopine was then evaluated in an in vitro 3D model of cancer multicellular spheroids formed from HCT116 cells. Xylopine-treated spheroids presented morphological alterations that indicate drug permeability and cytotoxicity in the 3D culture (Figure 2(a)). The IC_{50} value of xylopine was 24.6 μM after 72 h incubation (Figure 2(b)). Doxorubicin and oxaliplatin showed IC_{50} values of 4.5 and 6.0 μM, respectively.

Cell viability of HCT116 cell treated with xylopine was also determined by trypan blue exclusion assay after 24 and 48 h incubation. Xylopine significantly reduced ($p < 0.05$) the number of viable cells (Figure 3). At concentrations of 3.5, 7, and 14 μM, xylopine reduced the number of viable cells by 50.2, 64.4, and 71.8% after 24 h and 79.9, 84.6, and 89.4% after 48 h, respectively. No significant increase in the number of nonviable cells was observed ($p > 0.05$). Doxorubicin and oxaliplatin also reduced the number of viable cells after 24 and 48 h incubation.

3.2. Xylopine Induces G_2/M Phase Arrest and Caspase-Mediated Apoptosis in HCT116 Cells. The cell cycle distribution in xylopine-treated HCT116 cells was investigated by flow cytometry after 24 and 48 h incubation. Table 3 shows the obtained cell cycle distribution. All DNA that was subdiploid in size (sub-G_0/G_1) was considered fragmented. At all concentrations, xylopine treatment resulted in a significant increase in the number of cells in G_2/M phase compared to the negative control (30.7% at control against 57.2, 58.5, and 54.0% at 3.5, 7, and 14 μM xylopine after 24 h incubation and 23.8% at control against 52.0, 52.7, and 40.8% at the same concentration of xylopine after 48 h incubation, resp.). The G_2/M phase block was followed by an increase in the internucleosomal DNA fragmentation ($p < 0.05$). Doxorubicin and oxaliplatin also caused cell cycle block at the phase G_2/M, which was also followed by internucleosomal DNA fragmentation.

Cell morphology of xylopine-treated HCT116 cells presented a reduction in the cell volume, chromatin condensation, and fragmentation of the nuclei (Figure 4). Doxorubicin and oxaliplatin also induced cell shrinkage, chromatin condensation, and nuclear fragmentation. Apoptosis induction was assessed using the annexin V/PI double stain by flow cytometry in xylopine-treated HCT116

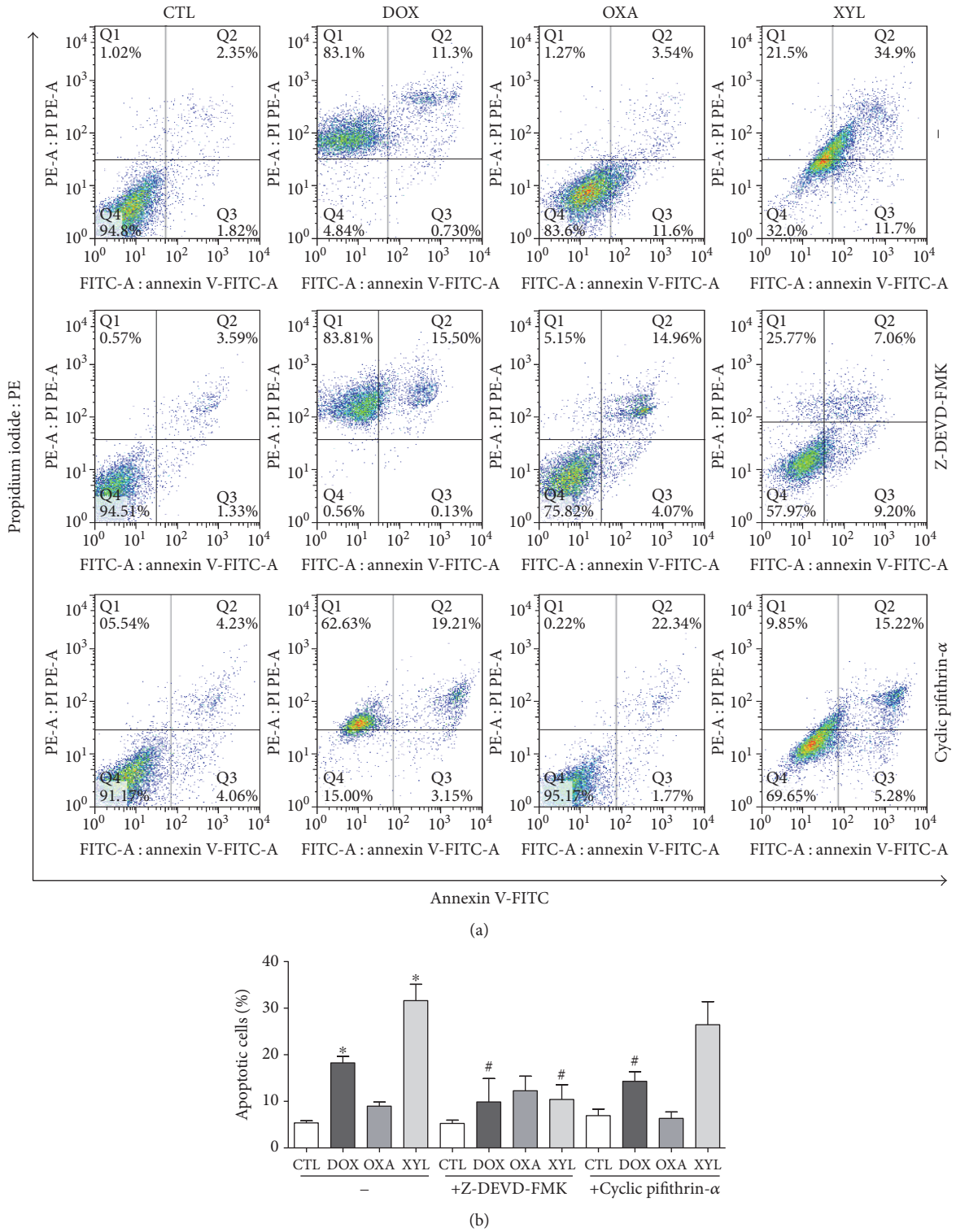

Figure 7: Effect of the caspase-3 inhibitor (Z-DEVD-FMK) and p53 inhibitor (cyclic pifithrin-α) in xylopine-induced apoptosis in HCT116 cells determined by flow cytometry using annexin V-FITC/PI staining. (a) Representative flow cytometric dot plots showing the percentage of cells in viable, early apoptotic, late apoptotic, and necrotic stages. (b) Quantification of apoptotic cells. The cells were pretreated for 2 h with 50 μM Z-DEVD-FMK and 10 μM cyclic pifithrin-α and then incubated with 14 μM xylopine (XYL) for 48 h. The negative control (CTL) was treated with the vehicle (0.1% DMSO) used for diluting the compound tested. Doxorubicin (DOX, 1 μM) and oxaliplatin (OXA, 2.5 μM) were used as positive controls. Data are presented as the mean ± S.E.M. of three independent experiments performed in duplicate. Ten thousand events were evaluated per experiment, and cellular debris was omitted from the analysis. $^{*}p < 0.05$ compared with the negative control by ANOVA followed by Student–Newman–Keuls test. $^{\#}p < 0.05$ compared with the respective treatment without inhibitor by ANOVA followed by Student–Newman–Keuls test.

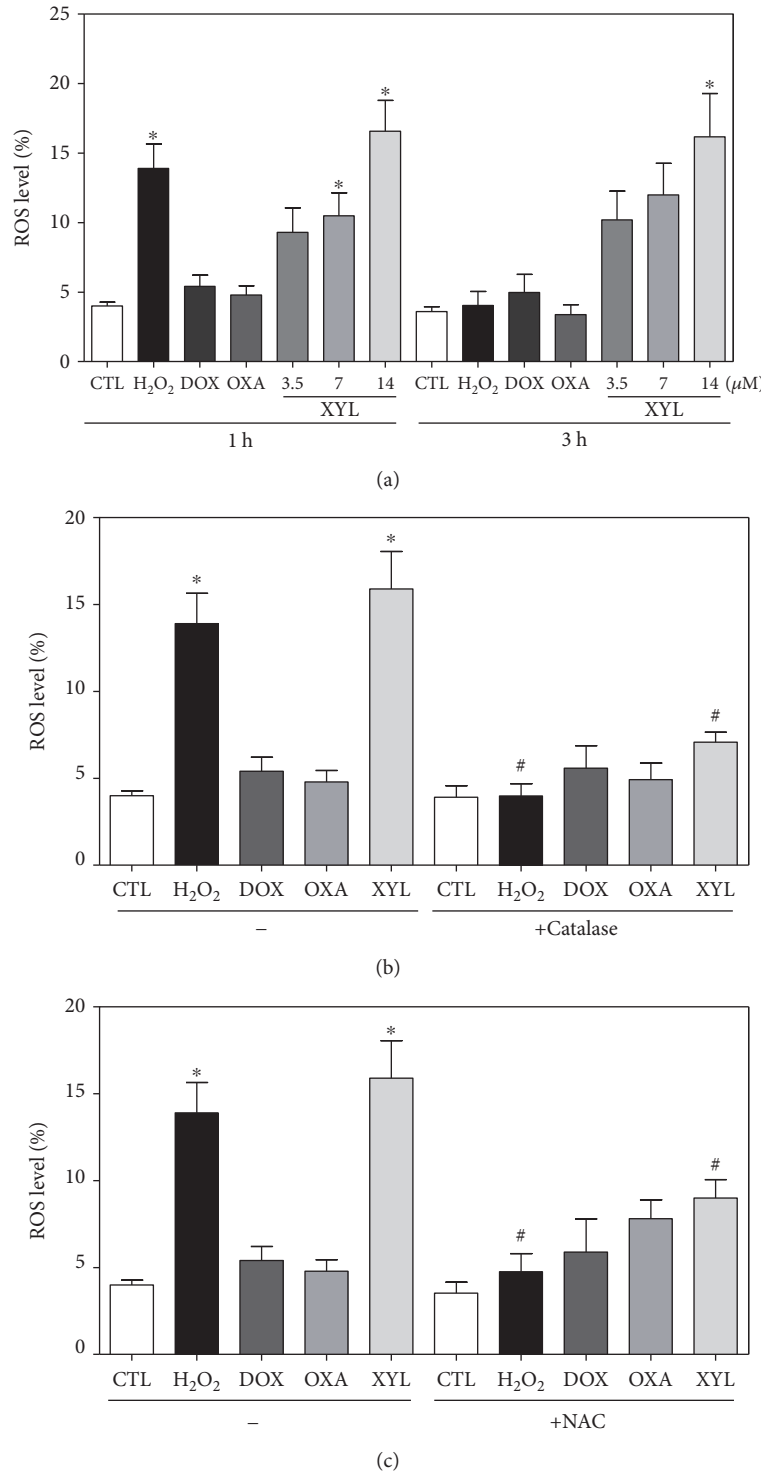

Figure 8: Effect of xylopine (XYL) in the levels of reactive oxygen species (ROS) of HCT116 cells and protection by N-acetyl-L-cysteine (NAC) and catalase determined by flow cytometry using DCF-DA staining. (a) ROS levels of HCT116 cells after 1 and 3 h incubation. (b) ROS levels of HCT116 cells pretreated with the antioxidant NAC and then treated with xylopine. (c) ROS levels of HCT116 cells pretreated with the antioxidant catalase and then treated with xylopine. For the protection assay, the cells were pretreated for 1 h with 5 mM NAC or 2000 UI catalase and then incubated with 14 μM xylopine for 1 h. The negative control (CTL) was treated with the vehicle (0.1% DMSO) used for diluting the compound tested. Hydrogen peroxide (H_2O_2, 200 μM), doxorubicin (DOX, 1 μM), and oxaliplatin (OXA, 2.5 μM) were used as positive controls. Data are presented as the mean ± S.E.M. of three independent experiments performed in duplicate or triplicate. Ten thousand events were evaluated per experiment, and cellular debris was omitted from the analysis. $^{*}p < 0.05$ compared with the negative control by ANOVA followed by Student–Newman–Keuls test. $^{\#}p < 0.05$ compared with the respective treatment without inhibitor by ANOVA followed by Student–Newman–Keuls test.

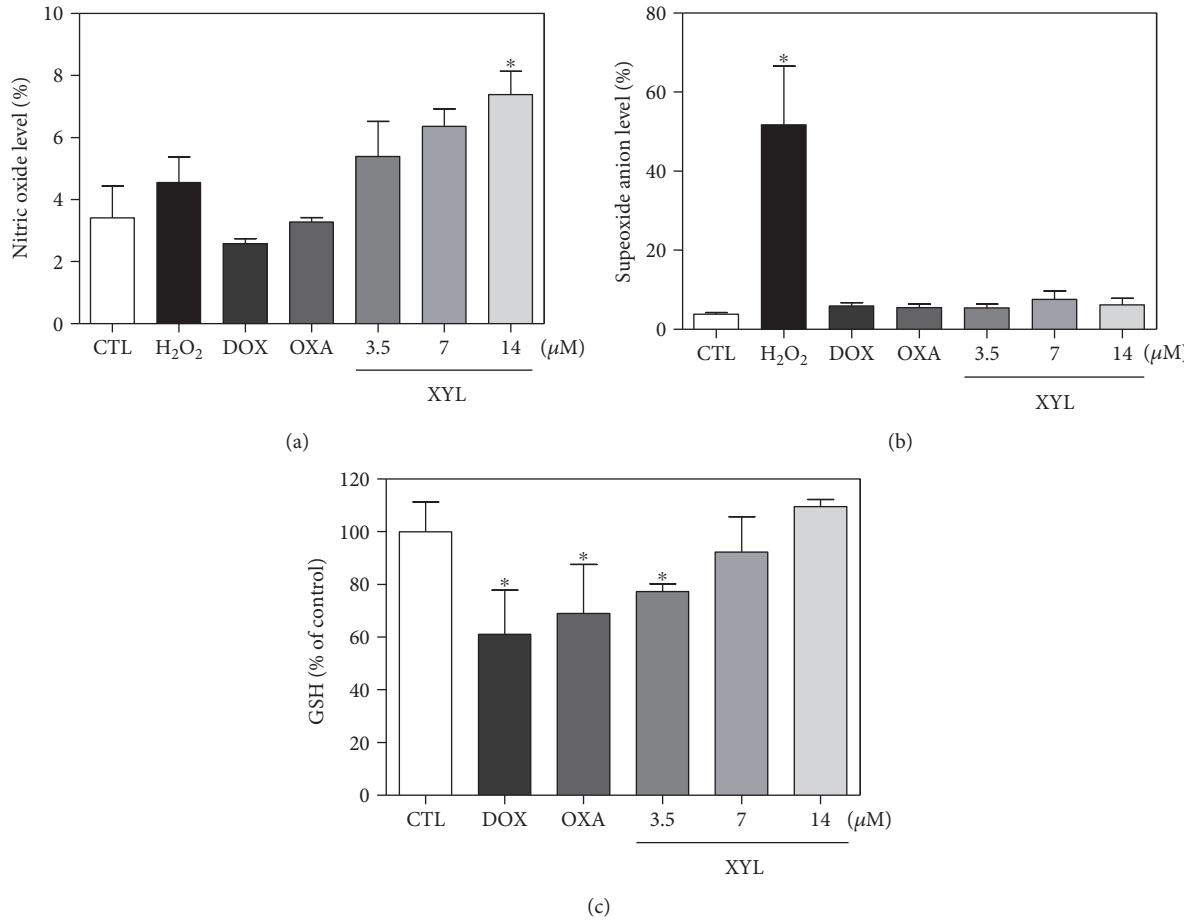

Figure 9: Effect of xylopine (XYL) in the levels of reactive oxygen species (ROS) and reduced glutathione (GSH) of HCT116 cells after 1 h incubation. (a) Nitric oxide level of HCT116 cells determined by flow cytometry using DAF-FM diacetate staining. (b) Superoxide anion level of HCT116 cells determined by flow cytometry using hydroethidine staining. (c) GSH level of HCT116 cells determined by colorimetric assay. The negative control (CTL) was treated with the vehicle (0.1% DMSO) used for diluting the compound tested. Hydrogen peroxide (H_2O_2, 200 μM), doxorubicin (DOX, 1 μM), and oxaliplatin (OXA, 2.5 μM) were used as positive controls. Data are presented as the mean ± S.E.M. of three independent experiments performed in duplicate. For flow cytometry analysis, 10,000 events were evaluated per experiment and cellular debris was omitted from the analysis. $^*p < 0.05$ compared with the negative control by ANOVA followed by Student–Newman–Keuls test.

cells (Figure 5). Xylopine significantly increased the early and late apoptosis ($p < 0.05$). A significant increase in necrotic cells was observed in xylopine-treated HCT116 cells after 48 h incubation ($p < 0.05$). Xylopine also induced mitochondrial depolarization ($p < 0.05$) in HCT116 cells after 24 h incubation (Figure 6(a)) and increased caspase-3 activation ($p < 0.05$) after 48 h incubation (Figure 6(b)). Moreover, cotreatment with a caspase-3 inhibitor (Z-DEVD-FMK), but not with a p53 inhibitor (cyclic pifithrin-α), prevented the xylopine-induced increasing apoptosis (Figures 7(a) and 7(b)). On the other hand, the IC_{50} values for xylopine were 6.4 μM for the BAD gene knockout immortalized mouse embryonic fibroblast (BAD KO SV40 MEF) cell line, while 8.0 μM was for wild-type immortalized mouse embryonic fibroblast (WT SV40 MEF) cell line, suggesting that BAD gene is not essential for xylopine-induced cytotoxicity. Doxorubicin presents IC_{50} values of 0.4 and 0.03 μM, while 5-FU presents IC_{50} values of 7.3 and 1.7 μM on BAD KO SV40 MEF and WT SV40 MEF cell lines, respectively.

3.3. Xylopine Causes ROS-Mediated Apoptosis in HCT116 Cells. The effect of xylopine in intracellular reactive oxygen/nitrogen species (ROS/RNS) levels was investigated in HCT116 cells through flow cytometry. Treatment with xylopine for 1 and 3 h caused an increase in the ROS levels (Figure 8(a)), and the cotreatment with the antioxidant NAC prevented the xylopine-induced increase in the intracellular ROS level (Figure 8(b)). Cotreatment with catalase, which induces decomposition of hydrogen peroxide, also prevented xylopine-induced increase in intracellular ROS levels that indicate the production of hydrogen peroxide induced by xylopine (Figure 8(c)). Using fluorescent probe specific for individual ROS/RNS, we found that xylopine increases nitric oxide (Figure 9(b)), but not superoxide anion (Figure 9(a)), in HCT116 cells. Furthermore,

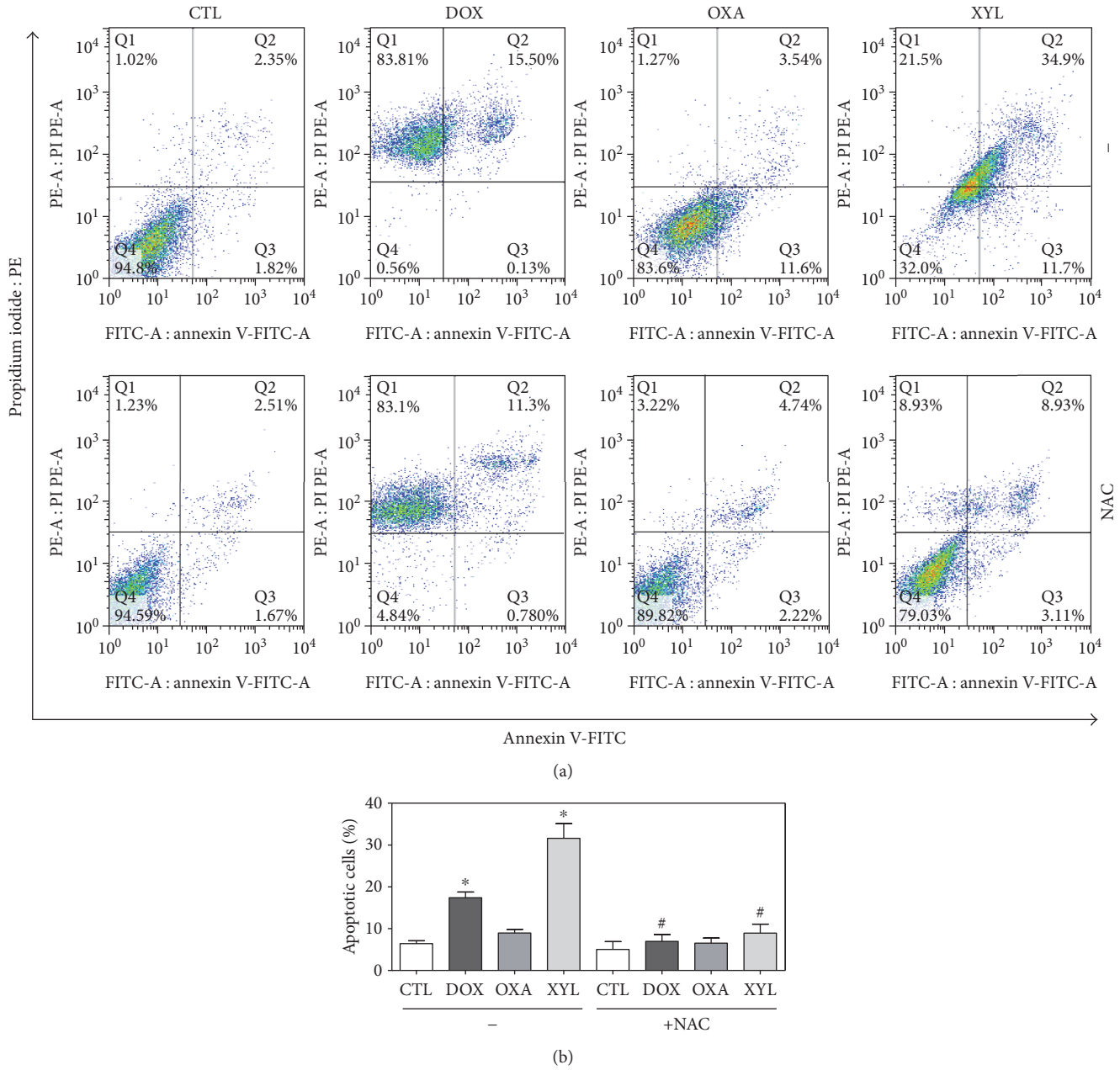

Figure 10: Effect of the antioxidant N-acetyl-L-cysteine (NAC) in xylopine-induced apoptosis in HCT116 cells determined by flow cytometry using annexin V-FITC/PI staining. (a) Representative flow cytometric dot plots showing the percentage of cells in viable, early apoptotic, late apoptotic, and necrotic stages. (b) Quantification of apoptotic cells. The cells were pretreated for 1 h with 5 mM NAC and then incubated with 14 μM xylopine (XYL) for 48 h. The negative control (CTL) was treated with the vehicle (0.1% DMSO) used for diluting the compound tested. Doxorubicin (DOX, 1 μM) and oxaliplatin (OXA, 2.5 μM) were used as positive controls. Data are presented as the mean ± S.E.M. of three independent experiments performed in duplicate. Ten thousand events were evaluated per experiment, and cellular debris was omitted from the analysis. $^{*}p < 0.05$ compared with the negative control by ANOVA followed by Student–Newman–Keuls test. $^{\#}p < 0.05$ compared with the respective treatment without inhibitor by ANOVA followed by Student–Newman–Keuls test.

GSH levels were decreased in xylopine-treated cells (Figure 9(c)). The cotreatment with NAC also prevented the xylopine-induced increase of the cell death by apoptosis (Figures 10(a) and 10(b)).

3.4. Xylopine Does Not Induce DNA Intercalation. DNA intercalation was evaluated by examining the ability of xylopine to displace ethidium bromide from ctDNA and thus decreasing the fluorescence intensity of ethidium bromide. Xylopine was not able to decrease the ethidium bromide fluorescence, indicating that it is not a strong DNA intercalator. Doxorubicin, a potent DNA intercalator, significantly reduced the fluorescence intensity (data not shown).

4. Discussion

In the present study, we report for the first time that xylopine induces oxidative stress and causes G_2/M phase arrest triggering caspase-mediated apoptosis in HCT116 cells. Previous works with xylopine reported that it induces potent cytotoxicity to cancer cells, but its mechanism of action has been not described [6].

Diverse aporphine alkaloids have been reported to exhibit cytotoxic effect on various types of human cancer cells, including acutiaporberine, anonaine, artabotrine, lysicamine, magnoflorine, norglaucine, norpurpureine, calycinine, and liriodenine [6, 14–20]. Acutiaporberine induces apoptosis in human non-small-cell lung cancer PLA-801 cells and human lung cancer 95-D cells, accompanied by downregulation of the bcl-2 gene and upregulation of the bax gene [14, 15]. Liriodenine inhibits human lung adenocarcinoma A549 cell proliferation and blocks the cell cycle progression at the G_2/M phase, accompanied by a reduction of G_1 cyclin D1 and accumulation of G_2 cyclin B1, and the enzymatic activity of the cyclin B1/cyclin-dependent kinase 1 complex was reduced in liriodenine-treated cells. Activation of caspases and induction of apoptosis were also observed in liriodenine-treated A549 cells [16]. Herein, xylopine blocked cell cycle progression at the G_2/M phase and triggered caspase-mediated apoptosis pathway in HCT116 cells, as observed by internucleosomal DNA fragmentation, externalization of phosphatidylserine, loss of mitochondrial transmembrane potential, and activation of caspase-3. Additionally, xylopine-induced apoptosis was prevented by pretreatment with a caspase-3 inhibitor, but not with a p53 inhibitor.

ROS/RNS are toxic products of cellular metabolism and are involved in cellular apoptosis by both the extrinsic cell death receptor pathway and the intrinsic mitochondrial cell death pathway. ROS include free radicals deprived of oxygen, including superoxide anions ($O_2^{\bullet -}$), hydroxyl radicals ($HO^{\bullet}$), peroxyl ($RO_2^{\bullet}$), alkoxyl ($RO^{\bullet}$), and nonradical species deprived of oxygen, including hydrogen peroxide (H_2O_2), whereas RNS include mainly nitric oxide ($^{\bullet}NO$). Moreover, glutathione is usually presented as a reduced form (GSH), but GSH can be converted into an oxidized form (GSSG) by stimulation of oxidative stress, and decreased cellular GSH levels are associated with ROS-mediated apoptosis [21–25]. Xylopine induces oxidative stress, including the increase of the levels of nitric oxide and hydrogen peroxide, but not superoxide anion, in HCT116 cells. Depletion of cellular GSH was also observed in xylopine-treated cells. Moreover, pretreatment with the antioxidant NAC prevented xylopine-induced apoptosis, indicating ROS-mediated apoptosis pathway. The aporphine alkaloids anonaine, glaucine, and norglaucine were previously reported as inductors of oxidative stress [18]. In addition, liriodenine/valproic acid combination treatment enhances ROS production and intracellular GSH depletion [26].

Some aporphine alkaloids are DNA intercalator agents, including liriodenine and dicentrine, which can induce inhibition of DNA topoisomerases as a mechanism of cytotoxicity [27]. Herein, DNA intercalation ability of xylopine was assessed in ctDNA; however, xylopine failed to induce DNA intercalation.

5. Conclusion

In conclusion, xylopine has potent cytotoxicity to different cancer cell lines and induces oxidative stress and causes G_2/M phase arrest triggering caspase-mediated apoptosis by the p53-independent pathway in HCT116 cells.

Abbreviations

3D:	Three-dimensional
5-FU:	5-fluorouracil
ATCC:	American Type Culture Collection
ctDNA:	Calf thymus DNA
DAF-FM diacetate:	4-amino-5-methylamino-2′-,7′-difluofluorescein diacetate
DCF-DA:	2′,7′-dichlorofluorescin diacetate
DMSO:	Dimethyl sulfoxide
GSH:	L-γ-glutamyl-L-cysteinyl-glycine
NAC:	N-acetyl-L-cysteine
PBMC:	Peripheral blood mononuclear cells
RNS:	Reactive nitrogen species
ROS:	Reactive oxygen species.

Conflicts of Interest

The authors have declared that there is no conflict of interest.

Authors' Contributions

Luciano de Souza Santos and Valdenizia Rodrigues Silva contributed equally to this work.

Acknowledgments

The authors are grateful to the flow cytometry platform of FIOCRUZ-Bahia for the performance flow cytometric data acquisition. This work received financial support and fellowships from Brazilian agencies Coordenação de Aperfeiçoamento de Pessoal de Nível Superior (CAPES), Conselho Nacional de Desenvolvimento Científico e Tecnológico (CNPq), Fundação de Amparo à Pesquisa do Estado da Bahia (FAPESB), and Fundação de Amparo à Pesquisa do Estado do Amazonas (FAPEAM).

References

[1] J. Ferlay, I. Soerjomataram, R. Dikshit et al., "Cancer incidence and mortality worldwide: sources, methods and major patterns in GLOBOCAN 2012," *International Journal of Cancer*, vol. 136, no. 5, pp. E359–E386, 2015.

[2] A. Vogel, R. D. Hofheinz, S. Kubicka, and D. Arnold, "Treatment decisions in metastatic colorectal cancer – beyond first and second line combination therapies," *Cancer Treatment Reviews*, vol. 59, pp. 54–60, 2017.

[3] Y. Liu, J. Liu, D. Di, M. Li, and Y. Fen, "Structural and mechanistic bases of the anticancer activity of natural aporphinoid

alkaloids," *Current Topics in Medicinal Chemistry*, vol. 13, no. 17, pp. 2116–2126, 2013.

[4] C. Stevignyl, C. Bailly, and J. Quetin-Leclercq, "Cytotoxic and antitumour potentialities of aporphinoid alkaloids," *Current Medicinal Chemistry - Anti-Cancer Agents*, vol. 5, no. 2, pp. 173–182, 2005.

[5] Q. Z. Zhao and Y. M. Zhao, "Progress in biological activities of aporphinoid alkaloids," *Natural Product Research and Development*, vol. 18, no. 2, pp. 316–324, 2006.

[6] L. R. A. Menezes, C. O. S. Costa, A. C. B. C. Rodrigues et al., "Cytotoxic alkaloids from the stem of *Xylopia laevigata*," *Molecules*, vol. 21, no. 7, article E890, 2016.

[7] S. A. Ahmed, R. M. Gogal Jr., and J. E. Walsh, "A new rapid and simple non-radioactive assay to monitor and determine the proliferation of lymphocytes: an alternative to [^{3}H]thymidine incorporation assay," *Journal of Immunological Methods*, vol. 170, no. 2, pp. 211–224, 1994.

[8] I. Nicoletti, G. Migliorati, M. C. Pagliacci, F. Grignani, and C. Riccardi, "A rapid and simple method for measuring thymocyte apoptosis by propidium iodide staining and flow cytometry," *Journal of Immunological Methods*, vol. 139, no. 2, pp. 271–279, 1991.

[9] F. X. Sureda, E. Escubedo, C. Gabriel, J. Comas, J. Camarasa, and A. Camins, "Mitochondrial membrane potential measurement in rat cerebellar neurons by flow cytometry," *Cytometry*, vol. 28, no. 1, pp. 74–80, 1997.

[10] C. P. LeBel, H. Ischiropoulos, and S. C. Bondy, "Evaluation of the probe 2′,7′-dichlorofluorescin as an indicator of reactive oxygen species formation and oxidative stress," *Chemical Research in Toxicology*, vol. 5, no. 2, pp. 227–231, 1992.

[11] Z. Ni, S. Hou, C. H. Barton, and N. D. Vaziri, "Lead exposure raises superoxide and hydrogen peroxide in human endothelial and vascular smooth muscle cells," *Kidney International*, vol. 66, no. 6, pp. 2329–2336, 2004.

[12] H. Kojima, N. Nakatsubo, K. Kikuchi et al., "Detection and imaging of nitric oxide with novel fluorescent indicators: diaminofluoresceins," *Analytical Chemistry*, vol. 70, no. 13, pp. 2446–2453, 1998.

[13] L. S. Glass, A. Bapat, M. R. Kelley, M. M. Georgiadis, and E. C. Long, "Semi-automated high-throughput fluorescent intercalator displacement-based discovery of cytotoxic DNA binding agents from a large compound library," *Bioorganic & Medicinal Chemistry Letters*, vol. 20, no. 5, pp. 1685–1688, 2010.

[14] Q. Chen, W. Peng, and A. Xu, "Apoptosis of a human non-small cell lung cancer (NSCLC) cell line, PLA-801, induced by acutiaporberine, a novel bisalkaloid derived from *Thalictrum acutifolium* (Hand.-Mazz.) Boivin," *Biochemical Pharmacology*, vol. 63, no. 8, pp. 1389–1396, 2002.

[15] Q. Chen, W. Peng, S. Qi, and A. Xu, "Apoptosis of human highly metastatic lung cancer cell line 95-D induced by acutiaporberine, a novel bisalkaloid derived from *Thalictrum acutifolium*," *Planta Medica*, vol. 68, no. 6, pp. 550–553, 2002.

[16] H. C. Chang, F. R. Chang, Y. C. Wu, and Y. H. Lai, "Anti-cancer effect of liriodenine on human lung cancer cells," *The Kaohsiung Journal of Medical Sciences*, vol. 20, no. 8, pp. 365–371, 2004.

[17] S. M. Mohamed, E. M. Hassan, and N. A. Ibrahim, "Cytotoxic and antiviral activities of aporphine alkaloids of *Magnolia grandiflora* L," *Natural Product Research*, vol. 24, no. 15, pp. 1395–1402, 2010.

[18] C. C. Chiu, H. L. Chou, P. F. Wu, H. L. Chen, H. M. Wang, and C. Y. Chen, "Bio-functional constituents from the stems of *Liriodendron tulipifera*," *Molecules*, vol. 17, no. 4, pp. 4357–4372, 2012.

[19] T. K. Kwan, F. Shipton, N. S. Azman, S. Hossan, K. T. Jin, and C. Wiart, "Cytotoxic aporphines from Artabotrys crassifolius," *Natural Product Communications*, vol. 11, no. 3, pp. 389–392, 2016.

[20] E. V. Costa, M. L. Pinheiro, B. H. Maia et al., "7,7-Dimethylaporphine and other alkaloids from the bark of *Guatteria friesiana*," *Journal of Natural Products*, vol. 79, no. 6, pp. 1524–1531, 2016.

[21] R. S. Balaban, S. Nemoto, and T. Finkel, "Mitochondria, oxidants, and aging," *Cell*, vol. 120, no. 4, pp. 483–495, 2005.

[22] J. Zhao, "Interplay among nitric oxide and reactive oxygen species: a complex network determining cell survival or death," *Plant Signaling & Behavior*, vol. 2, no. 6, pp. 544–547, 2007.

[23] M. L. Circu and T. Y. Aw, "Reactive oxygen species, cellular redox systems, and apoptosis," *Free Radical Biology & Medicine*, vol. 48, no. 6, pp. 749–762, 2010.

[24] K. Sinha, J. Das, P. B. Pal, and P. C. Sil, "Oxidative stress: the mitochondria-dependent and mitochondria-independent pathways of apoptosis," *Archives of Toxicology*, vol. 87, no. 7, pp. 1157–1180, 2013.

[25] T. Kamogashira, C. Fujimoto, and T. Yamasoba, "Reactive oxygen species, apoptosis, and mitochondrial dysfunction in hearing loss," *BioMed Research International*, vol. 2015, Article ID 617207, 7 pages, 2015.

[26] C. Y. Chen, Z. L. Li, K. T. Chung, F. J. Lu, and C. H. Chen, "Process biochemistry liriodenine enhances the apoptosis effect of valproic acid in human colon cancer cells through oxidative stress upregulation and Akt inhibition," *Process Biochemistry*, vol. 49, no. 11, pp. 1990–2000, 2014.

[27] S. H. Woo, N. J. Sun, J. M. Cassady, and R. M. Snapka, "Topoisomerase II inhibition by aporphine alkaloids," *Biochemical Pharmacology*, vol. 57, no. 10, pp. 1141–1145, 1999.

Hindawi
Oxidative Medicine and Cellular Longevity
Volume 2017, Article ID 6098107, 12 pages
https://doi.org/10.1155/2017/6098107

Review Article

The eIF4E2-Directed Hypoxic Cap-Dependent Translation Machinery Reveals Novel Therapeutic Potential for Cancer Treatment

Gaelan Melanson, Sara Timpano, and James Uniacke

Department of Molecular and Cellular Biology, University of Guelph, Guelph, ON, Canada

Correspondence should be addressed to James Uniacke; juniacke@uoguelph.ca

Received 15 August 2017; Accepted 2 November 2017; Published 26 November 2017

Academic Editor: Lynne Postovit

Hypoxia is an aspect of the tumor microenvironment that is linked to radiation and chemotherapy resistance, metastasis, and poor prognosis. The ability of hypoxic tumor cells to achieve these cancer hallmarks is, in part, due to changes in their gene expression profiles. Cancer cells have a high demand for protein synthesis, and translational control is subsequently deregulated. Various mechanisms of translation initiation are active to improve the translation efficiency of select transcripts to drive cancer progression. This review will focus on a noncanonical cap-dependent translation initiation mechanism that utilizes the eIF4E homolog eIF4E2, a hypoxia-activated cap-binding protein that is implicated in hypoxic cancer cell migration, invasion, and tumor growth in mouse xenografts. A historical perspective about eIF4E2 and its various aliases will be provided followed by an evaluation of potential therapeutic strategies. The recent successes of disabling canonical translation and eIF4E with drugs should highlight the novel therapeutic potential of targeting the homologous eIF4E2 in the treatment of hypoxic solid tumors.

1. Introduction

The initiation step of protein synthesis is a focal point of translational control (reviewed in [1]). The mammalian target of rapamycin complex 1 (mTORC1) is a master regulator of this process and senses several external stimuli such as nutrients and oxygen to control cell proliferation [2, 3]. The first step of translation involves the binding of the heterotrimeric eukaryotic initiation factor 4F (eIF4F) complex to the 5′ cap of mRNA. Specifically, it is eIF4E that is the cap-binding component of eIF4F (reviewed in [4]). The mTORC1 regulates the first step of translation by phosphorylating and inactivating the inhibitor of eIF4E, 4E-binding protein (4EBP), under normal conditions [5–7]. When oxygen is low, for example, the kinase activity of mTORC1 is repressed and 4EBP binds to and sequesters eIF4E [8–10]. Several cap-independent mechanisms exist to translate key mRNAs required to overcome a specific stress such as internal ribosomal entry sites (IRES) [11, 12] and upstream open reading frames (uORFs) [13, 14]. It is important to note that the "who's who" of cancer-driving mutations occurs in upstream regulators of mTORC1 (e.g., Akt [15], PTEN [16], PI3K [17], and Ras [18]), which uncouple this master regulator from sensing nutrient and oxygen deprivation. This constitutively active mTORC1 causes eIF4E-driven translation to be hyperactive in most cancers and is currently a major target of cancer therapeutics (reviewed in [19]). This literature review will focus on an alternative cap-dependent translation mechanism that utilizes the eIF4E homolog eIF4E2 [20], a cap-binding protein that is part of a metastatic gene signature [21] and required for tumor growth in mouse xenografts [22]. This pathway is activated by hypoxia [23], a characteristic of the microenvironment common to many solid tumors. A historical perspective about eIF4E2 will be provided followed by an evaluation of potential therapeutic strategies.

2. Translation Initiation

2.1. Canonical Translation Initiation. Eukaryotic translation efficiency is heavily reliant on posttranscriptional

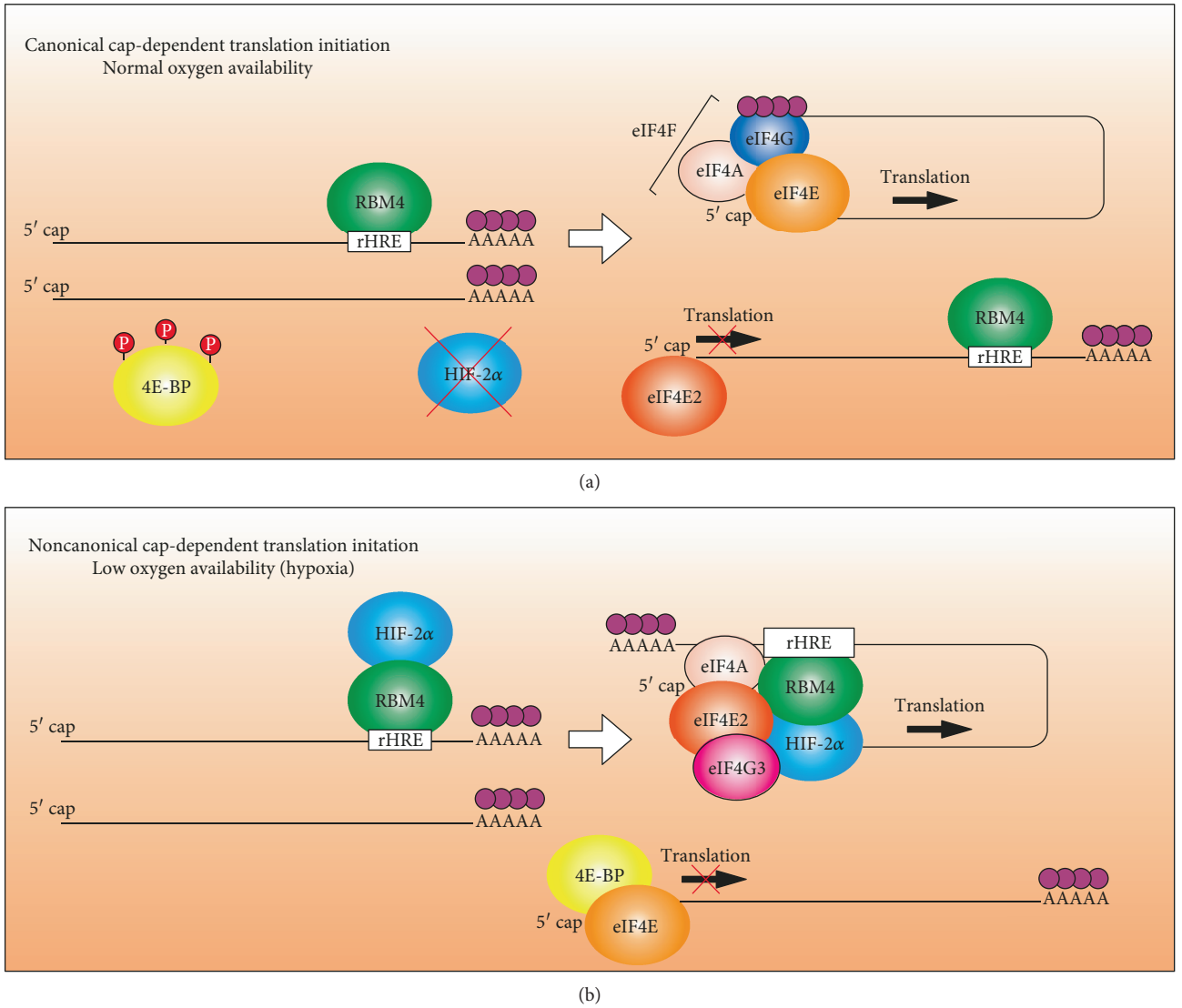

Figure 1: Model of canonical and noncanonical cap-dependent translation initiation. (a) Canonical cap-dependent translation mediated by eIF4E. Under normoxic conditions, the 4E-binding protein (4EBP) is phosphorylated by mTORC1 and repressed, allowing eIF4E to bind the 5′ cap of mRNA, eIF4G, and eIF4A forming the eIF4F complex to initiate translation. HIF-2α is degraded in the presence of oxygen and is unavailable to recruit eIF4E2 to the 5′ cap of transcripts containing RNA hypoxia response elements (rHREs) in their 3′ UTR. RBM4 is an RNA-binding protein that recognizes a motif in the rHRE and is essential for the translation of these transcripts in the presence of HIF-2α. (b) Under hypoxic conditions, HIF-2α is stabilized and interacts with RBM4 to recruit eIF4E2 to the 5′ cap of rHRE-containing transcripts independent of the poly(A)-tail. The eIF4E2 interacts with eIF4G3 and eIF4A to form a hypoxic eIF4F complex ($eIF4F^H$) to initiate the translation of rHRE-containing transcripts. The 4EBP is hypophosphorylated, binds to eIF4E, and blocks the eIF4G binding site to repress canonical cap-dependent translation.

modifications to the mRNA at the 3′ end (poly(A)-tail) and at the 5′ end (7-methyl-guanosine triphosphate cap; m^7GTP) [24, 25]. Canonical cap-dependent translation initiation begins with and can be regulated at two separate events. First, GTP-bound eIF2 binds to the initiator methionyl-tRNA (Met-tRNAi) and then to the 40S ribosomal subunit (reviewed in [4]). The eIF1, eIF3, eIF5, and eIF5B associate followed by the formation of the 43S preinitiation complex (PIC). The other event is the binding of eIF4F onto the 5′ m^7GTP cap of mRNA (Figure 1(a)). eIF4F is a heterotrimeric complex composed of the cap-binding protein eIF4E, the scaffold protein eIF4G, and the RNA helicase eIF4A. The assembly of this complex is the primary target of regulatory proteins such as the 4EBPs, as the cellular availability of eIF4E controls the switch between canonical cap-dependent translation and noncanonical cap-dependent translation or cap-independent mechanisms [26] (Figure 1).

2.2. Cap-Independent Translation Initiation. Hypoxia results in a decreased rate of protein synthesis; yet, de novo proteins are still expressed despite the repression of eIF4F-mediated translation [23]. IRES sequences were first discovered in the

poliovirus and encephalomyocarditis virus RNA genomes [11, 27], but a growing number of cellular IRES-containing transcripts are being identified with the potential to be translated via cap-independent mechanisms [12]. It is important to note, however, that the existence of cellular IRES-containing transcripts remains controversial due to the technical challenges associated with their detection (reviewed in [28, 29]). Some classic examples of cellular IRES-containing transcripts are those encoding the mouse hypoxia-inducible factor- (HIF-) 1α [30] and vascular endothelial growth factor (VEGF) [31]. Both of these proteins are central to the cellular response to hypoxia: HIF-1α is the oxygen-regulated subunit of the HIF-1 heterodimer that mediates the transcriptional response to hypoxia, and VEGF plays a key role in blood vessel formation (angiogenesis). While it is possible for the IRES to independently interact with the 40S and 60S ribosomal subunits, canonical translation factors (e.g., eIF4A and eIF3) and IRES-transacting factors (ITAFs) are usually involved to enhance translation efficiency. To ensure selective translation of the appropriate transcript, many ITAFs are expressed in a tissue-specific manner (reviewed in [32]). Importantly, IRES-mediated translation accounts for less than 1% of hypoxic protein synthesis [33]. This observation may have been, in part, explained through the identification of an alternative noncanonical cap-dependent translation machinery that is activated in hypoxic cells and mediated by the eIF4E homolog, eIF4E2 [23].

3. eIF4E2

3.1. Discovery, Function, and Regulation. eIF4E2 (also known as 4E homologous protein (4EHP)) was first identified in a human fetal brain cDNA library as 30% identical and 60% similar to eIF4E [20]. In humans, the *EIF4E2* gene is located on the long arm of chromosome 2 and its tissue distribution is ubiquitous albeit at 10-fold lower levels than eIF4E [34]. The peptide sequence of eIF4E2 is highly conserved with eIF4E in a core region, possessing two Trp ➔Tyr (Trp43 and Trp56) substitutions within the eight evolutionarily conserved tryptophan residues of eIF4E. eIF4E2 facilitates 5′ cap binding via π–π stacking between the aromatic rings of Tyr78 and Trp124 at 100-fold lower affinity than eIF4E [35]. Structural analysis identified the reduced affinity of eIF4E2 for the 5′ cap resulted from mutation of Arg162 that forms a stabilizing hydrogen bond with the β-phosphate of the mRNA cap in eIF4E [20]. Additionally, eIF4E2 interacts weakly or not at all with 4EBP and eIF4G, respectively [20, 36]. Structural variation around the eIF4G/4E-BP docking sequence, (S/T)VXXFW, impairs the ability of these proteins to associate with eIF4E2. Therefore, due to its inability to bind eIF4G, eIF4E2 inhibits translation when bound to the 5′ cap. Some of the first studies describing the cellular function of eIF4E2 were performed in the developing *Drosophila* embryo. The *Drosophila* homolog of eIF4E2 (d4EHP) inhibits the anterior translation of maternal *caudal* mRNA [37] and represses *belle* mRNA translation in the ovary [38]. Translation repression of *hunchback* mRNA in the posterior of the embryo involves eIF4E2 [39], but it is not obligatory [40]. In mice, eIF4E2 inhibits the translation of *Hoxb4* mRNA in female germ cells [41] and acts as a translation repressor in a complex with GIGYF2 that is essential for normal development in mice [42, 43]. In humans, eIF4E2 also forms a complex with GIGYF2 and/or 4E-T to repress translation initiation [42, 44, 45]. Interestingly, while eIF4E2 binds to the transporter 4E-T, it does not require it to shuttle to the nucleus as does eIF4E suggesting a different role for eIF4E2 in the nucleus [46]. The E3 ubiquitin ligase HHARI interacts to polyubiquitylate eIF4E2, and the authors of this study speculate that this interaction may alter its cap-binding affinity [47].

Several lines of evidence suggest that human eIF4E2 has a distinct cytoplasmic role in the stress response. During periods of arsenite or actinomycin D treatment, eIF4E2 is not sequestered to stress granules or P-bodies, respectively, like its homolog eIF4E [46]. During interferon, genotoxic stress, and pathogen infection, the ubiquitin-like molecule ISG15 is covalently added to eIF4E2 to increase its cap-binding affinity [48]. In mice with defects in glycogen storage, *EIF4E2* (named eIF4EL3 in this study) is one of 44 genes to significantly vary by more than 1.5-fold by increasing 1.57-fold. Conversely, in mice that hyperaccumulate glycogen, *EIF4E2* levels decrease by 2.08-fold [49]. This suggests that eIF4E2 could have an inverse relationship with energy availability, although the biological significance has not been explored. When normal human fibroblasts experience microgravity stress during space flight in cell culture, *EIF4E2* is one of 50 genes that are upregulated [50]. In mice given a 20 min treatment of forebrain ischemia, *EIF4E2* is one of 25 genes in the hippocampus that display a greater than 3-fold transcriptional increase (6-fold) [51]. Finally, eIF4E2 is required for development, a process driven by hypoxia, as knockouts in both *Drosophila* [52] and mouse [42] are embryonic lethal. These data present a theme where eIF4E2 becomes available in the cytoplasm and increases in mRNA and protein abundance in response to various forms of stress.

In 2012, eIF4E2 was identified as an activator of translation initiation during periods of hypoxia [23]. This finding came from the observation of HIF-2α-dependent, but transcription-independent, hypoxic accumulation of the epidermal growth factor receptor (EGFR) [23]. HIF-2α was found to interact with RNA-binding motif 4 (RBM4) in the 3′ UTR of hundreds of transcripts containing RNA hypoxia response elements (rHREs) (Figure 1(b)). The HIF-2α/RBM4 complex joins the 3′ UTR to the 5′ cap via eIF4E2, but not eIF4E, independent of the poly(A)-binding proteins [23]. The eIF4E2 interacts with eIF4A and eIF4G3 to form a hypoxic eIF4F (eIF4F^{H}) complex that increases translation efficiency independent of mRNA abundance [53] (Figure 1(b)). Interestingly, the protein levels of eIF4E2, eIF4G3, and eIF4A do not change in hypoxia relative to normoxia [23, 53] suggesting that posttranslational modifications or compartmentalization may play a role in modifying their activities. On the other hand, HIF-2α is essential for eIF4E2 activity [23]. Therefore, HIF-2α could be the sole activator of eIF4E2 in hypoxia. Since eIF4E2 appears to play a role in the response to other stresses in several eukaryotes, as mentioned above, it is tempting to

speculate that each stress induces unique activators of eIF4E2. However, the role of eIF4E2 in other stresses besides hypoxia has yet to be explored in humans. The eIF4E2 is a strong candidate for a general stress response translation factor that is independent of mTORC1 regulation due to the inability to bind, or weak binding, to 4EBP [20, 36]. Further investigation will be required to elucidate the mechanisms of translation initiation and regulation of $eIF4F^H$ activity.

3.2. Nomenclature and Conservation across Eukaryotes. The protein encoded by the human *EIF4E2* gene can be found in the literature under several aliases including 4E homologous protein (4EHP), 4E-like protein (4E-LP), eIF4EL3, and eIF4E2. This inconsistency in nomenclature for human eIF4E2 may have caused some delays or barriers in data dissemination because of the following: (1) One must know to search through the literature using all of the eIF4E2 aliases to gain access to all the available information. (2) Several studies misleadingly state or imply that eIF4E2 is part of the canonical translation initiation apparatus, especially those where the *EIF4E2* gene that appears in a big data set under a different alias such as microarray or high-throughput sequencing [21, 49–51, 54].

The *EIF4E2* gene is expressed as a divergent homolog of eIF4E in most eukaryotes. This review has already discussed reports of eIF4E2 function in mammals (humans and mice). In addition, several studies have reported functions for eIF4E2 in model organisms such as *Drosophila melanogaster* [37–42, 52], *Caenorhabditis elegans* [55], *Schizosaccharomyces pombe* [56, 57], and *Arabidopsis thaliana* [58]. In *Drosophila*, eIF4E2 is most commonly referred to as 4EHP and is involved in translation repression during the development of the embryo [37–42, 52]. In *C. elegans*, the eIF4E2 homolog is named IFE-4 and is involved in the translation initiation of a subset of mRNAs mostly required for egg laying [55]. In *S. pombe*, the eIF4E2 protein is part of the translation initiation machinery and is required to resist nutrient, salt, and temperature stress, and the eIF4E:eIF4E2 ratio shifts from 2 : 1 at low temperature (15°C) to 1 : 5 at high temperature (42°C) [56, 57]. Similar to human eIF4E2, *S. pombe* eIF4E2 binds very poorly to eIF4G (>100-fold less than eIF4E) [56]. In *A. thaliana*, the eIF4E2 homolog is named novel cap-binding protein (nCBP) and it can initiate the translation of a subset of mRNAs [58]. Therefore, eIF4E2 appears to be conserved across eukaryotes and is often found to be involved in selective translation repression or activation during stress or development. Humans express a third member of the eIF4E family, eIF4E3, albeit with a much more limited tissue distribution [34]. The eIF4E3 binds m^7GTP in an atypical manner [59], marginally suppresses eIF4E-dependent translation in diffuse large B-cell lymphoma [60], and is a tumor suppressor [59]. This review will not discuss eIF4E3 any further as there are much fewer studies relative to eIF4E and eIF4E2.

3.3. eIF4E2 in Cancer. The inconsistency in human eIF4E2 nomenclature has likely played a role in delaying the dissemination of its connection to cancer. In 2003, the metastatic potential of multiple tumor types could be predicted by a six-gene signature that contained *EIF4E2* (named eIF4EL3 in this study) [21]. In 2011, an examination was performed to 105 patients with metastatic non-small-cell lung carcinoma (NSCLC) for single-nucleotide polymorphisms (SNPs) that change the rate of overall survival during treatment with paclitaxel and carboplatin chemotherapeutics [54]. The SNP that produced the biggest effect was in individuals homozygous for an A ➔G mutation in the third exon of *EIF4E2*. These individuals had a significantly lower rate of overall survival ($p = 8.4 \times 10^{-8}$, hazard ratio = 4.22 (confidence interval: 2.32–7.66)) of 7.7 months compared to 18 months for individuals who were heterozygous or homozygous for the A allele. Additionally, expression of *EIF4E2* was found to be significantly increased in metastatic NSCLC tumors. However, the authors incorrectly stated in this study that the *EIF4E2* gene encodes eIF4E. Finally, a detection method for disorders of the lung involving transcriptomic profiling was patented in 2005 that describes changes in *EIF4E2* transcript levels (named eIF4EL3 in the patent) as a marker [61].

It was not until the response of the eIF4E2 protein to hypoxia was described at the molecular level in 2012 [23] that studies began emerging examining its role in tumor growth. The connection to cancer progression was not surprising considering the identity of the eIF4E2 mRNA targets identified through PAR-CLIP [23]. Dozens of eIF4E2 mRNA targets have strong ties to cancer such as a group of receptor tyrosine kinases including EGFR, platelet-derived growth factor receptor-alpha, insulin-like growth factor 1 receptor, and HER-2, which most cancers overexpress at least one. In 2014, several cancer cell lines stably depleted for eIF4E2 (U87MG glioblastoma, 786-O renal cell carcinoma, and HCT116 colorectal carcinoma) displayed impaired proliferation and increased apoptosis only in hypoxia [22]. Moreover, eIF4E2-depleted xenografts in mice displayed significantly less growth than controls. The eIF4E2 was shown to participate in active translation in hypoxic mouse xenografts, and the growth of established tumors in mice could be halted or reversed by treatment with shRNA targeting *EIF4E2* [22]. In 2017, *CDH22* mRNA was identified as a hypoxic eIF4E2 target that encodes cadherin-22, a cell-cell adhesion molecule providing cancer cells with collective migratory and invasive properties specifically in hypoxia [62]. Furthermore, CDH22 expression colocalized with hypoxic regions in human glioma and breast cancer patient tumor specimens and high protein levels significantly correlated with tumor size, cancer stage, and progression-free survival [62]. Thus, proteins synthesized via eIF4E2 offer the possibility of being prognostic markers of hypoxia in cancer patients and eIF4E2, an attractive therapeutic target to disable the adaptation of cells to the hypoxic tumor microenvironment.

4. Hypoxia

4.1. Hypoxia Inducible Factors. HIFs are the master regulators of the transcriptional response to hypoxia in the cell. These heterodimeric transcription factors are strongly tied to cancer progression and consist of an oxygen-regulated α-subunit (HIF-1α or HIF-2α) and a constitutively expressed β-subunit (HIF-1β) (reviewed in [63, 64]). The stabilization of both HIFs leads to angiogenesis, metabolic reprogramming,

immortalization, evasion of apoptosis, migration and invasion, generation of cancer stem cells, and chemo- and radiotherapy resistance. While there is overlap in HIF-1α and HIF-2α structure and function [65, 66], these two α-subunits can have distinct roles in the cell. HIF-1α and HIF-2α share most of their transcription targets but have been shown to bind to distinct targets as well [67]. Interestingly, HIF-α homologs display unexpected suppressive interactions, with enhanced expression of HIF-2α suppressing HIF-1α and vice versa [67]. The α-subunits also display temporal differences in their expression. Analysis of neuroblastoma cell lines showed that HIF-1α protein levels peak within 2 h of hypoxic exposure and then steadily decreased [68]. In contrast, HIF-2α protein expression peaks and remains constant at $\geq$24 h of hypoxia and is more abundant than HIF-1α under physiological oxygen conditions (37 mmHg or 5% O_2) [68]. *In vivo*, HIF-1α is expressed in all mammalian tissues and cell types [69], and HIF-2α expression was initially characterized as restricted to specific cell types, including developing blood vessels and the lung [70]. However, exposure of rats to hypoxia causes HIF-2α to accumulate in all organs investigated, including the brain, heart, lung, kidney, liver, pancreas, and intestine [71]. Therefore, HIF-1α is likely involved in acute responses to *in vitro* hypoxia and HIF-2α with chronic hypoxia. It is important to note that *in vivo*, HIF-1α is expressed in chronically hypoxic tumor regions, which could be partly due to genetic events or oxygen-independent stabilization by several stimuli present in the tumor microenvironment (reviewed in [72]).

The HIF-α-subunits each have nontranscriptional roles in the cell independent of interactions with HIF-1β. HIF-1α inhibits firing of replication origins, decreases DNA replication, and induces cell cycle arrest in various cell types through binding to Cdc6 [73]. HIF-2α binds to RBM4 in the 3′ UTR rHRE of select transcripts as part of the eIF4E2-directed hypoxic translation machinery (Figure 1(b)), while HIF-1α does not play a role in this process [23]. There had been previous reports of HIF-2α, not HIF-1α, becoming trapped in the cytoplasm upon chronic hypoxic exposure [74, 75], which is consistent with a role in translation. It is important to note that HIF-2α does not preferentially bind to mRNAs that are induced by HIF-dependent transcription [23]. This suggests that transcription and translation are distinct layers of regulation for the hypoxic gene expression response.

4.2. Hypoxic Regulation of Translation Initiation. Regulatory proteins are in place to regulate translation initiation by disrupting either the assembly/loading of the PIC complex or the assembly/cap-binding activity of eIF4F (introduced in section 2.1). These two modes of regulation occur as a biphasic response to hypoxia (acute and chronic) mediated through two distinct pathways. Under endoplasmic reticulum stress induced by acute hypoxic conditions, the kinase PERK phosphorylates eIF2α preventing its association with Met-tRNAi and loading of the PIC, thus repressing canonical cap-dependent translation (reviewed in [76]). However, under chronic hypoxia, eIF2α begins to dephosphorylate and a second pathway emerges to maintain translation repression through disruption of eIF4F and sequestration of eIF4E in the cytoplasm by the 4EBPs and in the nucleus by the transporter 4E-T [77]. During chronic hypoxia, mTORC1 is impaired in its ability to phosphorylate the 4EBPs, which allows them to bind to eIF4E using a similar binding motif as eIF4G (YxxxxLϕ) (reviewed in [4, 78]). The binding of the 4E-BPs will not interfere with eIF4E cap-binding ability but will inhibit eIF4G association and canonical cap-dependent mRNA translation (Figure 1). Under chronic hypoxic exposure, cells also induce the expression of REDD1, which decreases the phosphorylation of ribosomal S6 kinase, another mTORC1 phosphotarget, indicating that REDD1 is involved in regulating mTORC1 during hypoxia. Likewise, the presence of the tuberous sclerosis complex heterodimer, which is necessary for down-regulating mTORC1 activity, is induced by REDD1 activity in response to hypoxia [9]. In normal cells under chronic hypoxia, the ability to load the PIC is regained through dephosphorylation of eIF2α (reviewed in [76]). Repression of eIF4E allows for mTORC1-independent mechanisms to take over, such as noncanonical cap-dependent translation (eIF4E2 driven) or cap-independent processes. It is important to note that hypoxic regulation of translation is uncoupled in cancer [79] due to the frequently mutated upstream regulators of mTORC1 (e.g., Akt [15], PTEN [16], PI3K [17], and Ras [18]). Constitutively active mTORC1 causes eIF4E-driven translation to be hyperactive in most cancers and is currently a major target of cancer therapeutics (reviewed in [19]). However, evidence suggests eIF4E2 as a significant contributor for cancer cells to display various cancer hallmarks, for tumor growth, and as a possible predictor of metastasis and poor outcome [21, 22, 54, 62]. Targeting eIF4E2 relative to eIF4E has the potential to be more selective for malignant cells (hypoxic tumor cells) subsequently leading to lower toxicity.

5. Targeting eIF4F and eIF4F^{H} in Cancer

It is evident that an increase in eIF4E activity is oncogenic due to the many ways this is achieved in cancer cells such as gene duplication, increased *EIF4E* transcription, and increased eIF4E availability due to constitutive mTORC1 activation (reviewed in [80]). Phosphorylation of eIF4E via Mnk1 increases its activity [81], and this event is common in various cancers to drive their progression [82–84]. Several therapeutic strategies have been developed that either interfere with mTORC1 or eIF4E (reviewed in [19]). Rapamycin and several analogs are specific inhibitors of mTORC1 that have been extensively used in the clinic or in clinical trials but have shown a lower than expected efficacy [85]. More potent inhibitors of mTORC1 have been developed, such as asTORi [85], but many tumors have displayed resistance through a high eIF4E/4EBP ratio [86] or a switch to mTORC1-independent translation [87] (Figure 2(a)). Inhibitors that degrade Mnk1 kinase and prevent eIF4E phosphorylation have shown promise in breast cancer cell lines [88] (Figure 2(a)). Many efforts are ongoing to directly target eIF4E or the assembly of the eIF4F complex in various preclinical and clinical trials (reviewed in [19]). The most promising therapeutics includes eIF4E suppression via

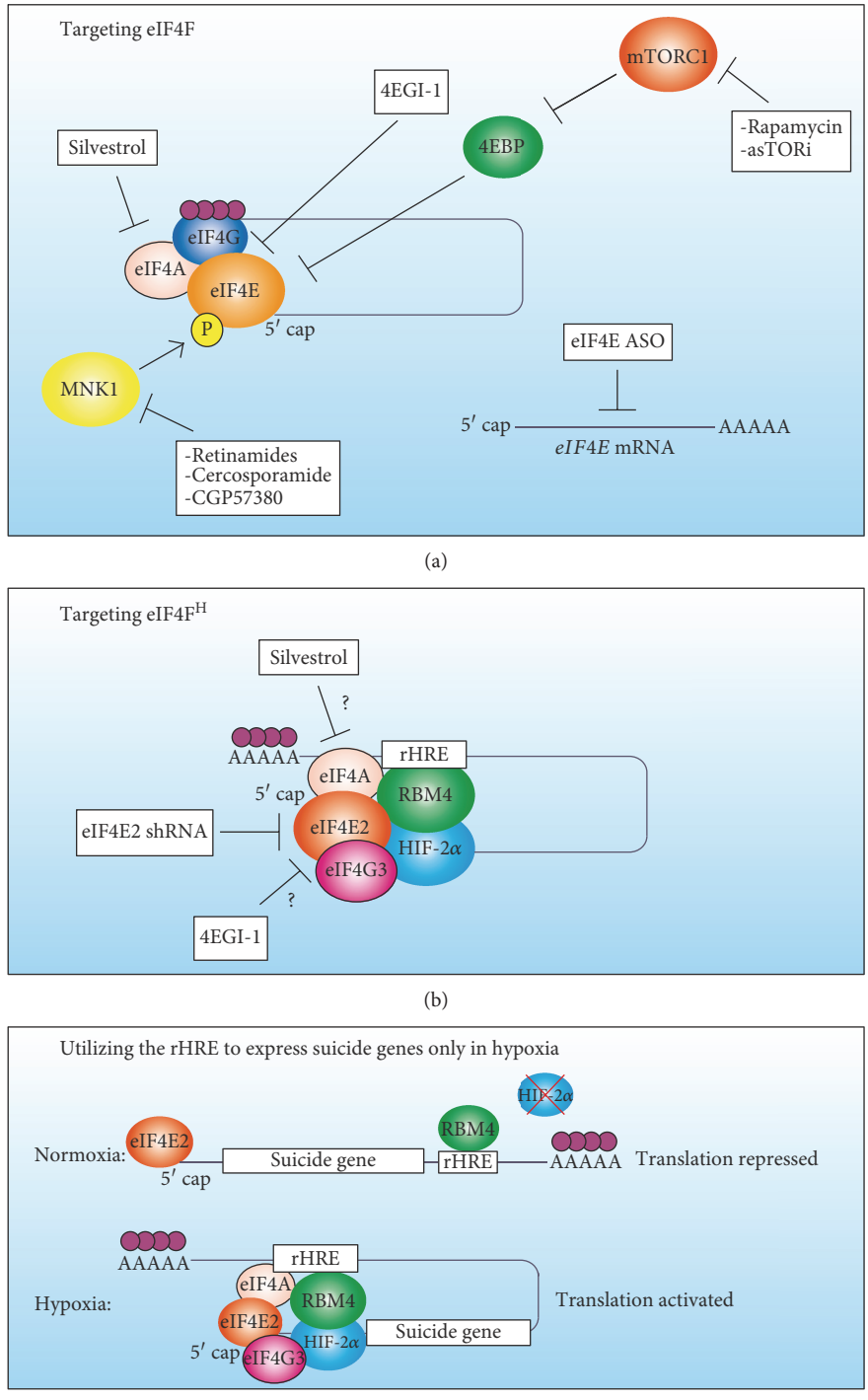

Figure 2: Summary of current therapeutic strategies targeting eIF4F and possible therapeutic interventions for eIF4F^H. (a) Rapamycin and asTORi inhibit mTORC1, allowing hypophosphorylated 4E-binding protein (4EBP) to block the eukaryotic initiation factor 4E (eIF4E) binding site from eIF4G. Inhibitors that degrade Mnk1 kinase prevent eIF4E phosphorylation, which reduces tumor growth. The most promising therapeutics includes eIF4E suppression via antisense oligonucleotides (ASOs) and disrupting the eIF4E-eIF4G interaction with drugs such as 4EGI-1. Inhibiting the eIF4A RNA helicase has displayed high preclinical potency, especially silvestrol, in mouse models of tumor progression. (b) Current evidence demonstrates that suppression of eIF4E2 via lentiviral-delivered shRNAs is effective at stalling or reversing tumor growth in mouse xenografts of several different cancer cell lines. Drugs used to target eIF4F such as 4EGI-1 and silvestrol could potentially also inhibit eIF4F^H through blocking the eIF4E2-eIF4G3 interaction or inhibiting eIF4A, respectively. (c) The 3′ UTR RNA hypoxia response element (rHRE) that is found in eIF4E2-dependent transcripts could be exploited as a hypoxia-inducible RNA sequence. The rHRE would repress synthesis until the therapeutic RNA reaches the hypoxic tumor cells. This would be especially useful when paired with a suicide gene, for example.

antisense oligonucleotides [89, 90] and disrupting the eIF4E-eIF4G interaction with drugs such as 4EGI-1 [91, 92] (Figure 2(a)). Targeting translation has the same rationale as the classic target of cancer therapeutics and cell proliferation: cancer cells proliferate more, therefore requiring more mRNA translation. However, proliferation and translation are fundamental processes that normal healthy cells utilize. The dosage for therapeutics targeting these pathways must be carefully considered as there could be a fine line between killing a cancer cell and a healthy cell. Targeting eIF4E2-driven translation could be more selective to cancer cells, or at least hypoxic tumor cells, rather than healthy cells because chronic hypoxia is associated with disease.

Development of therapeutics targeting eIF4E2 is in their infancy as this cap-binding protein has only recently been linked to tumor growth and its mechanisms of initiation and regulation are only beginning to be elucidated. Current evidence demonstrates that suppression of eIF4E2 via lentiviral-delivered shRNAs is effective at stalling or reversing tumor growth in mouse xenografts of several different cancer cell lines [22] (Figure 2(b)). Importantly, oxygenated cells are unaffected while hypoxic cells display widespread cell death. It will be a priority that interventions targeting eIF4E2 hit the metastatic and/or progressive phenotype, and not just cancer cells. Therefore, while eIF4E2 is involved in tumor growth [22] and several cancer cell hallmarks *in vitro* [22, 62], future studies should aim to more tightly link eIF4E2 to high-risk, metastatic cancer disease.

The eIF4E2 is part of the $eIF4F^H$ complex that includes an eIF4G homolog, eIF4G3 [53]. Therefore, effective strategies that disrupt eIF4E-eIF4G interactions could be employed in a similar fashion with eIF4E2-eIF4G3 (Figure 2(b)). Interestingly, eIF4A is also part of $eIF4F^H$, and drugs inhibiting this RNA helicase have displayed high preclinical potency, especially silvestrol, in mouse models of tumor progression [93]. Part of the reason that this drug is so effective could be that it disrupts both eIF4E- and eIF4E2-dependent translations (Figure 2(b)). Because of the high sequence homology between *EIF4E* and *EIF4E2*, some posttranslational regulatory pathways could be shared and therapeutically exploited such as phosphorylation.

Besides disrupting eIF4E2 activity or complex formation, the 3′ UTR rHRE that is found in eIF4E2-dependent transcripts could be exploited as a hypoxia-inducible RNA sequence. The hypoxia response elements found within the promoters of HIF target genes have been used in gene therapy for cancer treatment [94, 95], but RNA has emerged as an attractive source of gene products in place of DNA [96]. mRNA has several advantages including a lack of requirement for nuclear entry, which poses a barrier to plasmid DNA delivery, especially in nondividing or slowly dividing hypoxic cells. mRNA also has a negligible chance of integrating into the host genome avoiding aberrant transcription of oncogenes. A major limitation of gene therapy is selective expression, and an rHRE fusion could achieve this. There is also evidence that the rHRE is not only strictly an activator of hypoxic translation but also a repressor of translation in oxygenated conditions [23]. Therefore, the rHRE could repress synthesis until the therapeutic RNA reaches the hypoxic tumor region. This would be especially useful when paired with a suicide gene, for example (Figure 2(c)). Whether developing a small molecule inhibitor of eIF4E2 or an rHRE-RNA fusion, targeting hypoxia has its challenges such as accessing hypoxic areas that are remote from blood vessels and impaired uptake in hypoxic cells (reviewed in [97]). Constant improvements are being made in nanomedicine and drug design to generate tumor-reaching vehicles [98] and hypoxia-activated bioreductive prodrugs (reviewed in [97]), respectively.

6. Physioxia

Another important factor to consider when investigating cellular responses to hypoxia and targeting them with drugs is physiological oxygen levels (physioxia). The partial oxygen pressure within various human organs *in vivo* is much lower than it is in the atmosphere [99, 100]. By the time oxygen enters the lungs and is distributed throughout the various tissues, its availability is well below 21% (160 mmHg). Each tissue has its own "normoxia," and for this reason, the term "physioxia" is used to more effectively describe the *in vivo* partial oxygen pressure. The mean partial pressure of oxygen range reported by Carreau et al. is 29.2 ± 1.8 mmHg in the muscle to 72 ± 20 mmHg in the kidney (or the equivalent of $3.8 \pm 0.2\%$ O_2 to $9.5 \pm 2.6\%$ O_2) [99]. The oxygen within cells and organelles could be even lower due to consumption rates. In human cell culture, measures are taken to control the cellular environment to better reflect physiological conditions such as temperature and pH. Oxygen is a surprisingly neglected variable as cells are routinely cultured in ambient air (21% O_2). Furthermore, it is important to consider that 24 h is required for the dissolved oxygen in culture media to equilibrate with the ambient air [101]. Therefore, cell culture studies in low oxygen incubators should be performed after a 24 h exposure of either the cells or the media alone (before adding it to the cells) to the new oxygen environment.

HIF-2α, but not HIF-1α, is stabilized under chronic 5% O_2 [68], which overlaps with the mean tissue oxygenation of several organs. Indeed, HIF-2α activates eIF4E2-directed translation in several primary cell lines at oxygen levels as high as 5–8% O_2 evidenced by eIF4E2 and rHRE-containing transcripts associated with polysomes [102] (Figure 3). The eIF4E and some of its most dependent transcripts (e.g., TOP-containing mRNAs [103]) are associated with polysomes at oxygen levels as low as 1–3% O_2 in primary cells [102]. This suggests that eIF4E2 is actively participating in translation in the low range of physioxia, while eIF4E is active throughout the entire range. Moreover, this provides the intriguing possibility that there is a window within the physiological range of oxygen availability where both eIF4E and eIF4E2 are contributing to the cellular proteome through interactions with distinct mRNAs. Cancer cells displayed a shifted window of dual eIF4E and eIF4E2 usage (3–12% O_2) suggesting that eIF4E2 is activated and eIF4E is sequestered at higher oxygen levels relative to primary cells [102]. Perhaps during gradual tumor hypoxification, there is selective pressure on hypoxic cells to repress eIF4E-dependent translation early

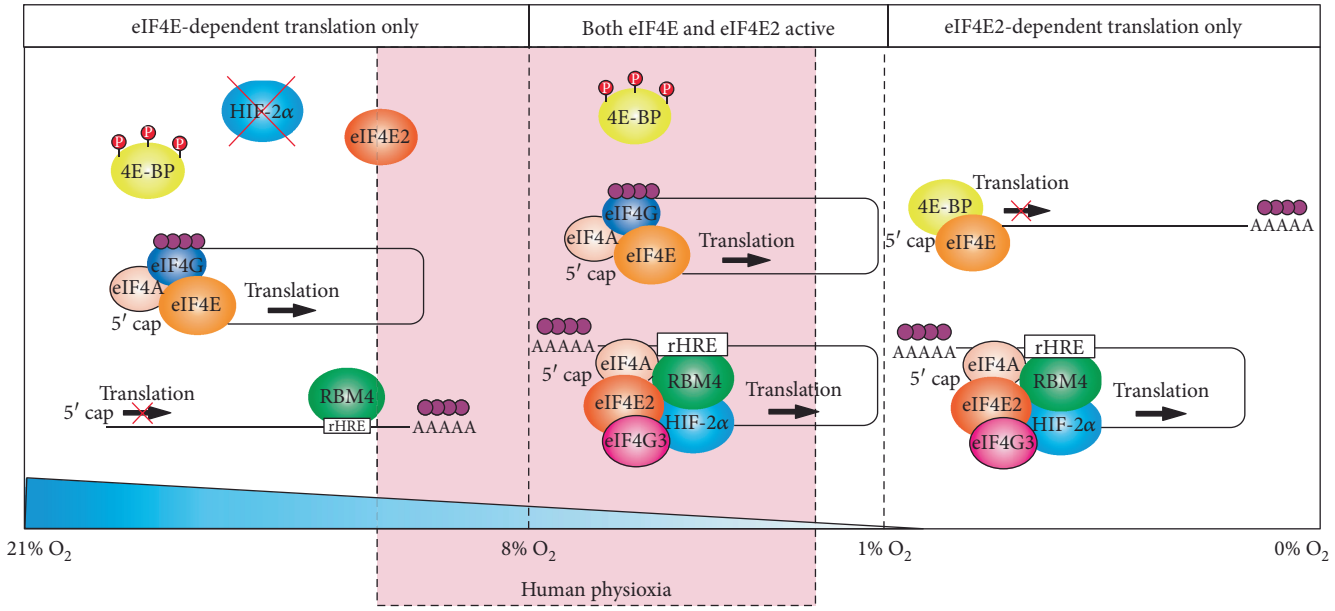

FIGURE 3: Both eIF4E- and eIF4E2-dependent translation initiations are active in the range of human physiological tissue oxygenation. The mean partial pressure of oxygen in human tissues (physioxia) ranges from 29.2 ± 1.8 mmHg in the muscle to 72 ± 20 mmHg in the kidney (or the equivalent of $3.8 \pm 0.2\%$ O_2 to $9.5 \pm 2.6\%$ O_2). The ability of mTORC1 to phosphorylate and inactivate the eIF4E repressor 4EBP decreases significantly between 1 and 3% O_2. This allows eIF4E-dependent translation to remain active between 1 and 21% O_2. Furthermore, the eIF4E2 hypoxic activator HIF-2α is stabilized below 8% O_2, allowing eIF4E2-dependent translation to be active in the low to midrange of human physioxia. Therefore, there is a window during physiological tissue oxygenation where eIF4E and eIF4E2 are cooperating to produce the cellular proteome. It is important to note that to achieve the indicated oxygen concentrations in cell culture media, 24 h is required for the dissolved oxygen to equilibrate with the ambient air.

and activate eIF4E2 early. Indeed, studies have shown that overexpressing eIF4E selectively disables hypoxic tumor cells [104] and eIF4E2 mRNA targets are enriched in cancer-driving genes [22, 23, 53, 62, 102].

The implications of the above studies are twofold. First, eIF4E2-dependent translation may be important in the normal physiology of human tissues with mean partial oxygen pressures in the low range of physioxia such as the brain and muscle. Several classic and modern cancer therapeutics target essential processes such as cell proliferation and protein synthesis, but eIF4E2 initially emerged as a potential drug target that could be more selective to cancer cells. Therefore, the possibility that small molecule targeting of eIF4E2 and fusing rHRE sequences to suicide genes are toxic to at least some tissues must be noted. Second, if a fundamental process like protein synthesis is differentially regulated in physioxia relative to the common cell culture condition of normoxia (21% O_2), then perhaps, cancer therapeutics in general should be tested in conditions of lower oxygen.

7. Conclusions

We present a summary of evidence leading to the discovery and ongoing characterization of noncanonical cap-dependent hypoxic translation and its involvement in tumor growth. This review consolidates studies using several different eIF4E2 aliases to highlight that it is conserved across eukaryotes and could have a role in advanced cancer stage in humans. The role of eIF4E2 in various model organisms suggests that it participates in the general stress response with perhaps stress-specific activators. In human cells, eIF4E2 is part of a hypoxic eIF4F complex ($eIF4F^H$) with eIF4G3 and eIF4A that increases the translation efficiency of mRNAs irrespective of their abundance. However, further efforts are needed to fully elucidate the mechanism of initiation through interactions with either canonical initiation factors or their homologs and to more tightly link eIF4E2 to high-risk, metastatic cancer disease. The recent successes of disabling canonical translation and eIF4E with drugs should highlight the novel therapeutic potential of targeting the homologous eIF4E2 in the treatment of hypoxic solid tumors.

Conflicts of Interest

The authors declare that they have no conflicts of interest.

Authors' Contributions

Gaelan Melanson and Sara Timpano contributed equally to this work.

Acknowledgments

The work in James Uniacke's laboratory is supported by the Cancer Research Society, Canadian Cancer Society (Grant no. 703327), Canadian Institutes of Health Research (PJT 152925), Natural Sciences and Engineering Council of Canada, and Ontario Ministry of Research and Innovation. Sara Timpano was supported by an Ontario Graduate Scholarship.

References

[1] F. Gebauer and M. W. Hentze, "Molecular mechanisms of translational control," *Nature Reviews Molecular Cell Biology*, vol. 5, no. 10, pp. 827–835, 2004.

[2] R. J. Dowling, I. Topisirovic, T. Alain et al., "mTORC1-mediated cell proliferation, but not cell growth, controlled by the 4E-BPs," *Science*, vol. 328, no. 5982, pp. 1172–1176, 2010.

[3] S. Wullschleger, R. Loewith, and M. N. Hall, "TOR signaling in growth and metabolism," *Cell*, vol. 124, no. 3, pp. 471–484, 2006.

[4] N. Sonenberg and A. G. Hinnebusch, "Regulation of translation initiation in eukaryotes: mechanisms and biological targets," *Cell*, vol. 136, no. 4, pp. 731–745, 2009.

[5] A. Pause, G. J. Belsham, A. C. Gingras et al., "Insulin-dependent stimulation of protein synthesis by phosphorylation of a regulator of 5′-cap function," *Nature*, vol. 371, no. 6500, pp. 762–767, 1994.

[6] G. J. Brunn, C. C. Hudson, A. Sekulić et al., "Phosphorylation of the translational repressor PHAS-I by the mammalian target of rapamycin," *Science*, vol. 277, no. 5322, pp. 99–101, 1997.

[7] T. A. Lin, X. Kong, T. Haystead et al., "PHAS-I as a link between mitogen-activated protein kinase and translation initiation," *Science*, vol. 266, no. 5185, pp. 653–656, 1994.

[8] S. Braunstein, K. Karpisheva, C. Pola et al., "A hypoxia-controlled cap-dependent to cap-independent translation switch in breast cancer," *Molecular Cell*, vol. 28, no. 3, pp. 501–512, 2007.

[9] J. Brugarolas, K. Lei, R. L. Hurley et al., "Regulation of mTOR function in response to hypoxia by REDD1 and the TSC1/TSC2 tumor suppressor complex," *Genes & Development*, vol. 18, no. 23, pp. 2893–2904, 2004.

[10] L. Liu, T. P. Cash, R. G. Jones, B. Keith, C. B. Thompson, and M. C. Simon, "Hypoxia-induced energy stress regulates mRNA translation and cell growth," *Molecular Cell*, vol. 21, no. 4, pp. 521–531, 2006.

[11] J. Pelletier and N. Sonenberg, "Internal initiation of translation of eukaryotic mRNA directed by a sequence derived from poliovirus RNA," *Nature*, vol. 334, no. 6180, pp. 320–325, 1988.

[12] S. Weingarten-Gabbay, S. Elias-Kirma, R. Nir et al., "Systematic discovery of cap-independent translation sequences in human and viral genomes," *Science*, vol. 351, no. 6270, p. aad4939, 2016.

[13] L. PD, H. P. Harding, and D. Ron, "Translation reinitiation at alternative open reading frames regulates gene expression in an integrated stress response," *The Journal of Cell Biology*, vol. 167, no. 1, pp. 27–33, 2004.

[14] K. M. Vattem and R. C. Wek, "Reinitiation involving upstream ORFs regulates *ATF4* mRNA translation in mammalian cells," *Proceedings of the National Academy of Sciences of the United States of America*, vol. 101, no. 31, pp. 11269–11274, 2004.

[15] J. D. Carpten, A. L. Faber, C. Horn et al., "A transforming mutation in the pleckstrin homology domain of AKT1 in cancer," *Nature*, vol. 448, no. 7152, pp. 439–444, 2007.

[16] J. Li, C. Yen, D. Liaw et al., "*PTEN*, a putative protein tyrosine phosphatase gene mutated in human brain, breast, and prostate cancer," *Science*, vol. 275, no. 5308, pp. 1943–1947, 1997.

[17] Y. Samuels, Z. Wang, A. Bardelli et al., "High frequency of mutations of the *PIK3CA* gene in human cancers," *Science*, vol. 304, no. 5670, p. 554, 2004.

[18] S. A. Forbes, N. Bindal, S. Bamford et al., "COSMIC: mining complete cancer genomes in the catalogue of somatic mutations in cancer," *Nucleic Acids Research*, vol. 39, Supplement 1, pp. D945–D950, 2011.

[19] M. Bhat, N. Robichaud, L. Hulea, N. Sonenberg, J. Pelletier, and I. Topisirovic, "Targeting the translation machinery in cancer," *Nature Reviews. Drug Discovery*, vol. 14, no. 4, pp. 261–278, 2015.

[20] E. Rom, H. C. Kim, A. C. Gingras et al., "Cloning and characterization of 4EHP, a novel mammalian eIF4E-related cap-binding protein," *The Journal of Biological Chemistry*, vol. 273, no. 21, pp. 13104–13109, 1998.

[21] S. Ramaswamy, K. N. Ross, E. S. Lander, and T. R. Golub, "A molecular signature of metastasis in primary solid tumors," *Nature Genetics*, vol. 33, no. 1, pp. 49–54, 2003.

[22] J. Uniacke, J. K. Perera, G. Lachance, C. B. Francisco, and S. Lee, "Cancer cells exploit eIF4E2-directed synthesis of hypoxia response proteins to drive tumor progression," *Cancer Research*, vol. 74, no. 5, pp. 1379–1389, 2014.

[23] J. Uniacke, C. E. Holterman, G. Lachance et al., "An oxygen-regulated switch in the protein synthesis machinery," *Nature*, vol. 486, no. 7401, pp. 126–129, 2012.

[24] D. R. Gallie, "The cap and poly(A) tail function synergistically to regulate mRNA translational efficiency," *Genes & Development*, vol. 5, no. 11, pp. 2108–2116, 1991.

[25] A. J. Shatkin, "Capping of eucaryotic mRNAs," *Cell*, vol. 9, no. 4, pp. 645–653, 1976.

[26] Y. V. Svitkin, B. Herdy, M. Costa-Mattioli, A. C. Gingras, B. Raught, and N. Sonenberg, "Eukaryotic translation initiation factor 4E availability controls the switch between cap-dependent and internal ribosomal entry site-mediated translation," *Molecular and Cellular Biology*, vol. 25, no. 23, pp. 10556–10565, 2005.

[27] S. K. Jang, H. G. Kräusslich, M. J. Nicklin, G. M. Duke, A. C. Palmenberg, and E. Wimmer, "A segment of the 5′ nontranslated region of encephalomyocarditis virus RNA directs internal entry of ribosomes during in vitro translation," *Journal of Virology*, vol. 62, no. 8, pp. 2636–2643, 1988.

[28] M. Kozak, "New ways of initiating translation in eukaryotes?," *Molecular and Cellular Biology*, vol. 21, no. 6, pp. 1899–1907, 2001.

[29] M. Kozak, "Alternative ways to think about mRNA sequences and proteins that appear to promote internal initiation of translation," *Gene*, vol. 318, pp. 1–23, 2003.

[30] K. J. Lang, A. Kappel, and G. J. Goodall, "Hypoxia-inducible factor-1α mRNA contains an internal ribosome entry site that allows efficient translation during normoxia and hypoxia," *Molecular Biology of the Cell*, vol. 13, no. 5, pp. 1792–1801, 2002.

[31] I. Stein, A. Itin, P. Einat, R. Skaliter, Z. Grossman, and E. Keshet, "Translation of vascular endothelial growth factor mRNA by internal ribosome entry: implications for translation under hypoxia," *Molecular and Cellular Biology*, vol. 18, no. 6, pp. 3112–3119, 1998.

[32] M. Holcik and N. Sonenberg, "Translational control in stress and apoptosis," *Nature Reviews Molecular Cell Biology*, vol. 6, no. 4, pp. 318–327, 2005.

[33] R. M. Young, S. J. Wang, J. D. Gordan, X. Ji, S. A. Liebhaber, and M. C. Simon, "Hypoxia-mediated selective mRNA translation by an internal ribosome entry site-independent mechanism," *The Journal of Biological Chemistry*, vol. 283, no. 24, pp. 16309–16319, 2008.

[34] B. Joshi, A. Cameron, and R. Jagus, "Characterization of mammalian eIF4E-family members," *European Journal of Biochemistry*, vol. 271, no. 11, pp. 2189–2203, 2004.

[35] J. Zuberek, D. Kubacka, A. Jablonowska et al., "Weak binding affinity of human 4EHP for mRNA cap analogs," *RNA*, vol. 13, no. 5, pp. 691–697, 2007.

[36] A. R. Tee, J. A. Tee, and J. Blenis, "Characterizing the interaction of the mammalian eIF4E-related protein 4EHP with 4E-BP1," *FEBS Letters*, vol. 564, no. 1-2, pp. 58–62, 2004.

[37] P. F. Cho, F. Poulin, Y. A. Cho-Park et al., "A new paradigm for translational control: inhibition via $5'$-$3'$ mRNA tethering by Bicoid and the eIF4E cognate 4EHP," *Cell*, vol. 121, no. 3, pp. 411–423, 2005.

[38] A. Yarunin, R. E. Harris, M. P. Ashe, and H. L. Ashe, "Patterning of the Drosophila oocyte by a sequential translation repression program involving the d4EHP and Belle translational repressors," *RNA Biology*, vol. 8, no. 5, pp. 904–912, 2011.

[39] P. F. Cho, C. Gamberi, Y. A. Cho-Park, I. B. Cho-Park, P. Lasko, and N. Sonenberg, "Cap-dependent translational inhibition establishes two opposing morphogen gradients in *Drosophila* embryos," *Current Biology*, vol. 16, no. 20, pp. 2035–2041, 2006.

[40] C. A. Weidmann and A. C. Goldstrohm, "*Drosophila* Pumilio protein contains multiple autonomous repression domains that regulate mRNAs independently of Nanos and brain tumor," *Molecular and Cellular Biology*, vol. 32, no. 2, pp. 527–540, 2012.

[41] J. C. Villaescusa, C. Buratti, D. Penkov et al., "Cytoplasmic Prep1 interacts with 4EHP inhibiting *Hoxb4* translation," *PLoS One*, vol. 4, no. 4, article e5213, 2009.

[42] M. Morita, L. W. Ler, M. R. Fabian et al., "A novel 4EHP-GIGYF2 translational repressor complex is essential for mammalian development," *Molecular and Cellular Biology*, vol. 32, no. 17, pp. 3585–3593, 2012.

[43] R. Fu, M. T. Olsen, K. Webb, E. J. Bennett, and J. Lykke-Andersen, "Recruitment of the 4EHP-GYF2 cap-binding complex to tetraproline motifs of tristetraprolin promotes repression and degradation of mRNAs with AU-rich elements," *RNA*, vol. 22, no. 3, pp. 373–382, 2016.

[44] L. von Stechow, D. Typas, J. Carreras Puigvert et al., "The E3 ubiquitin ligase ARIH1 protects against genotoxic stress by initiating a 4EHP-mediated mRNA translation arrest," *Molecular and Cellular Biology*, vol. 35, no. 7, pp. 1254–1268, 2015.

[45] C. Chapat, S. M. Jafarnejad, E. Matta-Camacho et al., "Cap-binding protein 4EHP effects translation silencing by microRNAs," *Proceedings of the National Academy of Sciences of the United States of America*, vol. 114, no. 21, pp. 5425–5430, 2017.

[46] D. Kubacka, A. Kamenska, H. Broomhead, N. Minshall, E. Darzynkiewicz, and N. Standart, "Investigating the consequences of eIF4E2 (4EHP) interaction with 4E-transporter on its cellular distribution in HeLa cells," *PLoS One*, vol. 8, no. 8, article e72761, 2013.

[47] N. G. Tan, H. C. Ardley, G. B. Scott, S. A. Rose, A. F. Markham, and P. A. Robinson, "Human homologue of ariadne promotes the ubiquitylation of translation initiation factor 4E homologous protein, 4EHP," *FEBS Letters*, vol. 554, no. 3, pp. 501–504, 2003.

[48] F. Okumura, W. Zou, and D. E. Zhang, "ISG15 modification of the eIF4E cognate 4EHP enhances cap structure-binding activity of 4EHP," *Genes & Development*, vol. 21, no. 3, pp. 255–260, 2007.

[49] G. E. Parker, B. A. Pederson, M. Obayashi, J. M. Schroeder, R. A. Harris, and P. J. Roach, "Gene expression profiling of mice with genetically modified muscle glycogen content," *Biochemical Journal*, vol. 395, no. 1, pp. 137–145, 2006.

[50] Y. Liu and E. Wang, "Transcriptional analysis of normal human fibroblast responses to microgravity stress," *Genomics, Proteomics & Bioinformatics*, vol. 6, no. 1, pp. 29–41, 2008.

[51] T. Nagata, Y. Takahashi, M. Sugahara et al., "Profiling of genes associated with transcriptional responses in mouse hippocampus after transient forebrain ischemia using high-density oligonucleotide DNA array," *Brain Research. Molecular Brain Research*, vol. 121, no. 1-2, pp. 1–11, 2004.

[52] L. Valzania, H. Ono, M. Ignesti et al., "*Drosophila* 4EHP is essential for the larval-pupal transition and required in the prothoracic gland for ecdysone biosynthesis," *Developmental Biology*, vol. 410, no. 1, pp. 14–23, 2016.

[53] J. J. Ho, M. Wang, T. E. Audas et al., "Systemic reprogramming of translation efficiencies on oxygen stimulus," *Cell Reports*, vol. 14, no. 6, pp. 1293–1300, 2016.

[54] Y. Sato, N. Yamamoto, H. Kunitoh et al., "Genome-wide association study on overall survival of advanced non-small cell lung cancer patients treated with carboplatin and paclitaxel," *Journal of Thoracic Oncology*, vol. 6, no. 1, pp. 132–138, 2011.

[55] T. D. Dinkova, B. D. Keiper, N. L. Korneeva, E. J. Aamodt, and R. E. Rhoads, "Translation of a small subset of *Caenorhabditis elegans* mRNAs is dependent on a specific eukaryotic translation initiation factor 4E isoform," *Molecular and Cellular Biology*, vol. 25, no. 1, pp. 100–113, 2005.

[56] M. Ptushkina, K. Berthelot, T. von der Haar, L. Geffers, J. Warwicker, and J. E. McCarthy, "A second eIF4E protein in *Schizosaccharomyces pombe* has distinct eIF4G-binding properties," *Nucleic Acids Research*, vol. 29, no. 22, pp. 4561–4569, 2001.

[57] M. Ptushkina, N. Malys, and J. E. McCarthy, "eIF4E isoform 2 in *Schizosaccharomyces pombe* is a novel stress-response factor," *EMBO Reports*, vol. 5, no. 3, pp. 311–316, 2004.

[58] K. A. Ruud, C. Kuhlow, D. J. Goss, and K. S. Browning, "Identification and characterization of a novel cap-binding protein from *Arabidopsis thaliana*," *The Journal of Biological Chemistry*, vol. 273, no. 17, pp. 10325–10330, 1998.

[59] M. J. Osborne, L. Volpon, J. A. Kornblatt, B. Culjkovic-Kraljacic, A. Baguet, and K. L. B. Borden, "eIF4E3 acts as a tumor suppressor by utilizing an atypical mode of methyl-7-guanosine cap recognition," *Proceedings of the National Academy of Sciences of the United States of America*, vol. 110, no. 10, pp. 3877–3882, 2013.

[60] A. L. Landon, P. A. Muniandy, A. C. Shetty et al., "MNKs act as a regulatory switch for eIF4E1 and eIF4E3 driven mRNA translation in DLBCL," *Nature Communications*, vol. 5, p. 5413, 2014.

[61] J. S. Brody and A. Spira, *Detection Methods for Disorders of the Lung*, Google Patents, Boston, MA, USA, 2005, WO 2005000098 A2 PCT/UST2004/018460.

[62] N. J. Kelly, J. F. A. Varga, E. J. Specker, C. M. Romeo, B. L. Coomber, and J. Uniacke, "Hypoxia activates cadherin-22 synthesis via eIF4E2 to drive cancer cell migration, invasion and adhesion," *Oncogene*, 2017.

[63] A. J. Majmundar, W. J. Wong, and M. C. Simon, "Hypoxia-inducible factors and the response to hypoxic stress," *Molecular Cell*, vol. 40, no. 2, pp. 294–309, 2010.

[64] L. Schito and G. L. Semenza, "Hypoxia-inducible factors: master regulators of cancer progression," *Trends Cancer*, vol. 2, no. 12, pp. 758–770, 2016.

[65] A. Loboda, A. Jozkowicz, and J. Dulak, "HIF-1 and HIF-2 transcription factors—similar but not identical," *Molecules and Cells*, vol. 29, no. 5, pp. 435–442, 2010.

[66] P. J. Ratcliffe, "HIF-1 and HIF-2: working alone or together in hypoxia?," *The Journal of Clinical Investigation*, vol. 117, no. 4, pp. 862–865, 2007.

[67] R. R. Raval, K. W. Lau, M. G. B. Tran et al., "Contrasting properties of hypoxia-inducible factor 1 (HIF-1) and HIF-2 in von Hippel-Lindau-associated renal cell carcinoma," *Molecular and Cellular Biology*, vol. 25, no. 13, pp. 5675–5686, 2005.

[68] L. Holmquist-Mengelbier, E. Fredlund, T. Löfstedt et al., "Recruitment of HIF-1α and HIF-2α to common target genes is differentially regulated in neuroblastoma: HIF-2α promotes an aggressive phenotype," *Cancer Cell*, vol. 10, no. 5, pp. 413–423, 2006.

[69] C. M. Wiener, G. Booth, and G. L. Semenza, "*In vivo*expression of mRNAs encoding hypoxia-inducible factor 1," *Biochemical and Biophysical Research Communications*, vol. 225, no. 2, pp. 485–488, 1996.

[70] H. Tian, S. L. McKnight, and D. W. Russell, "Endothelial PAS domain protein 1 (EPAS1), a transcription factor selectively expressed in endothelial cells," *Genes & Development*, vol. 11, no. 1, pp. 72–82, 1997.

[71] M. S. Wiesener, J. S. Jürgensen, C. Rosenberger et al., "Widespread hypoxia-inducible expression of HIF-2α in distinct cell populations of different organs," *The FASEB Journal*, vol. 17, no. 2, pp. 271–273, 2003.

[72] G. L. Semenza, "Targeting HIF-1 for cancer therapy," *Nature Reviews. Cancer*, vol. 3, no. 10, pp. 721–732, 2003.

[73] M. E. Hubbi, D. M. G. Kshitiz, S. Rey et al., "A nontranscriptional role for HIF-1α as a direct inhibitor of DNA replication," *Science Signaling*, vol. 6, no. 262, article ra10, 2013.

[74] S. K. Park, A. M. Dadak, V. H. Haase, L. Fontana, A. J. Giaccia, and R. S. Johnson, "Hypoxia-induced gene expression occurs solely through the action of hypoxia-inducible factor 1α (HIF-1α): role of cytoplasmic trapping of HIF-2α," *Molecular and Cellular Biology*, vol. 23, no. 14, pp. 4959–4971, 2003.

[75] K. L. Talks, H. Turley, K. C. Gatter et al., "The expression and distribution of the hypoxia-inducible factors HIF-1α and HIF-2α in normal human tissues, cancers, and tumor-associated macrophages," *The American Journal of Pathology*, vol. 157, no. 2, pp. 411–421, 2000.

[76] T. D. Baird and R. C. Wek, "Eukaryotic initiation factor 2 phosphorylation and translational control in metabolism," *Advances in Nutrition*, vol. 3, no. 3, pp. 307–321, 2012.

[77] M. Koritzinsky, M. G. Magagnin, T. van den Beucken et al., "Gene expression during acute and prolonged hypoxia is regulated by distinct mechanisms of translational control," *The EMBO Journal*, vol. 25, no. 5, pp. 1114–1125, 2006.

[78] I. Topisirovic, Y. V. Svitkin, N. Sonenberg, and A. J. Shatkin, "Cap and cap-binding proteins in the control of gene expression," *Wiley Interdiscip Rev RNA*, vol. 2, no. 2, pp. 277–298, 2011.

[79] E. Connolly, S. Braunstein, S. Formenti, and R. J. Schneider, "Hypoxia inhibits protein synthesis through a 4E-BP1 and elongation factor 2 kinase pathway controlled by mTOR and uncoupled in breast cancer cells," *Molecular and Cellular Biology*, vol. 26, no. 10, pp. 3955–3965, 2006.

[80] D. Silvera, S. C. Formenti, and R. J. Schneider, "Translational control in cancer," *Nature Reviews. Cancer*, vol. 10, no. 4, pp. 254–266, 2010.

[81] S. Pyronnet, H. Imataka, A. C. Gingras, R. Fukunaga, T. Hunter, and N. Sonenberg, "Human eukaryotic translation initiation factor 4G (eIF4G) recruits mnk1 to phosphorylate eIF4E," *The EMBO Journal*, vol. 18, no. 1, pp. 270–279, 1999.

[82] L. Furic, L. Rong, O. Larsson et al., "eIF4E phosphorylation promotes tumorigenesis and is associated with prostate cancer progression," *Proceedings of the National Academy of Sciences of the United States of America*, vol. 107, no. 32, pp. 14134–14139, 2010.

[83] N. Robichaud, S. V. del Rincon, B. Huor et al., "Phosphorylation of eIF4E promotes EMT and metastasis via translational control of SNAIL and MMP-3," *Oncogene*, vol. 34, no. 16, pp. 2032–2042, 2015.

[84] I. Topisirovic, M. Ruiz-Gutierrez, and K. L. Borden, "Phosphorylation of the eukaryotic translation initiation factor eIF4E contributes to its transformation and mRNA transport activities," *Cancer Research*, vol. 64, no. 23, pp. 8639–8642, 2004.

[85] D. Benjamin, M. Colombi, C. Moroni, and M. N. Hall, "Rapamycin passes the torch: a new generation of mTOR inhibitors," *Nature Reviews. Drug Discovery*, vol. 10, no. 11, pp. 868–880, 2011.

[86] T. Alain, N. Sonenberg, and I. Topisirovic, "mTOR inhibitor efficacy is determined by the eIF4E/4E-BP ratio," *Oncotarget*, vol. 3, no. 12, pp. 1491-1492, 2012.

[87] T. Muranen, L. M. Selfors, D. T. Worster et al., "Inhibition of PI3K/mTOR leads to adaptive resistance in matrix-attached cancer cells," *Cancer Cell*, vol. 21, no. 2, pp. 227–239, 2012.

[88] S. Ramalingam, L. Gediya, A. K. Kwegyir-Afful et al., "First MNKs degrading agents block phosphorylation of eIF4E, induce apoptosis, inhibit cell growth, migration and invasion in triple negative and Her2-overexpressing breast cancer cell lines," *Oncotarget*, vol. 5, no. 2, pp. 530–543, 2014.

[89] R. J. DeFatta, C. O. Nathan, and A. De Benedetti, "Antisense RNA to eIF4E suppresses oncogenic properties of a head and neck squamous cell carcinoma cell line," *Laryngoscope*, vol. 110, no. 6, pp. 928–933, 2000.

[90] J. R. Graff, B. W. Konicek, T. M. Vincent et al., "Therapeutic suppression of translation initiation factor eIF4E expression reduces tumor growth without toxicity," *The Journal of Clinical Investigation*, vol. 117, no. 9, pp. 2638–2648, 2007.

[91] L. Chen, B. H. Aktas, Y. Wang et al., "Tumor suppression by small molecule inhibitors of translation initiation," *Oncotarget*, vol. 3, no. 8, pp. 869–881, 2012.

[92] N. J. Moerke, H. Aktas, H. Chen et al., "Small-molecule inhibition of the interaction between the translation initiation factors eIF4E and eIF4G," *Cell*, vol. 128, no. 2, pp. 257–267, 2007.

[93] R. Cencic, M. Carrier, G. Galicia-Vázquez et al., "Antitumor activity and mechanism of action of the cyclopenta[*b*]benzofuran, silvestrol," *PLoS One*, vol. 4, no. 4, article e5223, 2009.

[94] K. Binley, S. Iqball, A. Kingsman, S. Kingsman, and S. Naylor, "An adenoviral vector regulated by hypoxia for the treatment of ischaemic disease and cancer," *Gene Therapy*, vol. 6, no. 10, pp. 1721–1727, 1999.

[95] H. Ruan, J. Wang, L. Hu, C. S. Lin, K. R. Lamborn, and D. F. Deen, "Killing of brain tumor cells by hypoxia-responsive element mediated expression of BAX," *Neoplasia*, vol. 1, no. 5, pp. 431–437, 1999.

[96] M. S. Kormann, G. Hasenpusch, M. K. Aneja et al., "Expression of therapeutic proteins after delivery of chemically modified mRNA in mice," *Nature Biotechnology*, vol. 29, no. 2, pp. 154–157, 2011.

[97] W. R. Wilson and M. P. Hay, "Targeting hypoxia in cancer therapy," *Nature Reviews. Cancer*, vol. 11, no. 6, pp. 393–410, 2011.

[98] J. Shi, P. W. Kantoff, R. Wooster, and O. C. Farokhzad, "Cancer nanomedicine: progress, challenges and opportunities," *Nature Reviews. Cancer*, vol. 17, no. 1, pp. 20–37, 2017.

[99] A. Carreau, B. El Hafny-Rahbi, A. Matejuk, C. Grillon, and C. Kieda, "Why is the partial oxygen pressure of human tissues a crucial parameter? Small molecules and hypoxia," *Journal of Cellular and Molecular Medicine*, vol. 15, no. 6, pp. 1239–1253, 2011.

[100] D. K. Harrison and P. Vaupel, "Heterogeneity in tissue oxygenation: from physiological variability in normal tissues to pathophysiological chaos in malignant tumours," *Advances in Experimental Medicine and Biology*, vol. 812, pp. 25–31, 2014.

[101] D. Newby, L. Marks, and F. Lyall, "Dissolved oxygen concentration in culture medium: assumptions and pitfalls," *Placenta*, vol. 26, no. 4, pp. 353–357, 2005.

[102] S. Timpano and J. Uniacke, "Human cells cultured under physiological oxygen utilize two cap-binding proteins to recruit distinct mRNAs for translation," *The Journal of Biological Chemistry*, vol. 291, no. 20, pp. 10772–10782, 2016.

[103] C. C. Thoreen, L. Chantranupong, H. R. Keys, T. Wang, N. S. Gray, and D. M. Sabatini, "A unifying model for mTORC1-mediated regulation of mRNA translation," *Nature*, vol. 485, no. 7396, pp. 109–113, 2012.

[104] K. M. Rouschop, L. Dubois, M. B. E. Schaaf et al., "Deregulation of cap-dependent mRNA translation increases tumour radiosensitivity through reduction of the hypoxic fraction," *Radiotherapy and Oncology*, vol. 99, no. 3, pp. 385–391, 2011.

Hindawi
Oxidative Medicine and Cellular Longevity
Volume 2017, Article ID 2908039, 9 pages
https://doi.org/10.1155/2017/2908039

Clinical Study

The Role of Redox-Regulating Enzymes in Inoperable Breast Cancers Treated with Neoadjuvant Chemotherapy

Nelli Roininen,[1,2] Kirsi-Maria Haapasaari,[2] and Peeter Karihtala[1]

[1]*Department of Oncology and Radiotherapy, Medical Research Center Oulu, Oulu University Hospital and University of Oulu, Oulu, Finland*
[2]*Department of Pathology, Medical Research Center Oulu, Oulu University Hospital and University of Oulu, Oulu, Finland*

Correspondence should be addressed to Peeter Karihtala; peeter.karihtala@oulu.fi

Received 2 March 2017; Revised 14 August 2017; Accepted 5 September 2017; Published 19 November 2017

Academic Editor: Peng Huang

Although validated predictive factors for breast cancer chemoresistance are scarce, there is emerging evidence that the induction of certain redox-regulating enzymes may contribute to a poor chemotherapy effect. We investigated the possible association between chemoresistance and cellular redox state regulation in patients undergoing neoadjuvant chemotherapy (NACT) for breast cancer. In total, 53 women with primarily inoperable or inflammatory breast cancer who were treated with NACT were included in the study. Pre-NACT core needle biopsies and postoperative tumor samples were immunohistochemically stained for nuclear factor erythroid 2-related factor 2 (Nrf2), Kelch-like ECH-associated protein 1 (Keap1), thioredoxin (Trx), and peroxiredoxin I (Prx I). The expression of all studied markers increased during NACT. Higher pre-NACT nuclear Prx I expression predicted smaller size of a resected tumor ($p = 0.00052$; $r = -0.550$), and higher pre-NACT cytoplasmic Prx I expression predicted a lower amount of evacuated nodal metastasis ($p = 0.0024$; $r = -0.472$). Pre-NACT nuclear Trx expression and pre-NACT nuclear Keap1 expression had only a minor prognostic significance as separate factors, but when they were combined, low expression for both antibodies before NACT predicted dismal disease-free survival (log-rank $p = 0.0030$). Our results suggest that redox-regulating enzymes may serve as potential prognostic factors in primarily inoperable breast cancer patients.

1. Introduction

Breast cancer is the most common cancer among women worldwide, and it is the fifth most common cause of death from cancer overall [1]. In Finland, 31% of the all invasive cancers in women were breast cancers causing 16% of all female cancer deaths during the years 2008–2012 (Association of the Nordic Cancer Registries). If the cancer is already widely locally advanced at the time of diagnosis and thus cannot be safely removed surgically, presurgical neoadjuvant chemotherapy (NACT) to shrink the primary tumor can be administered. The current Finnish breast cancer guidelines restrict NACT mainly to the patients with primarily inoperable disease due to inflammatory or widely locally advanced breast cancer. These cancers usually have an aggressive biological profile, and without efficient predictive factors, valuable time may be spent on ineffective chemotherapy. On the other hand, the breast cancer patients getting a complete response for NACT have usually an excellent outcome [2]. To save time and avoid ineffective chemotherapy regimens, more accurate prognostic factors for the chemotherapy responsiveness and aggressiveness of the breast cancer are needed.

Reactive oxygen species (ROS) are involved in cellular processes that favor cell migration and adhesion [3, 4]. Moderate oxidative stress accelerates carcinogenesis [5], while high ROS concentration leads to apoptosis and senescence [6]. Oxidative stress markers and antioxidant enzyme levels may therefore be useful predictive and prognostic biomarkers in cancer. Among the most potent antioxidant enzymes are peroxiredoxins (Prx) I–VI. Prxs are highly conserved through the living organisms from bacteria to human, indicating the importance of these enzymes [7, 8]. Although Prxs contribute to doxorubicin resistance of breast cancer cells *in vitro*, they have also breast cancer-suppressive properties via p53 and c-Myc inhibition [9, 10]. Similarly, human

thioredoxin (Trx, cytoplasmic and nuclear) is involved in many physiological redox reactions but is also associated with increased hypoxia-induced factor 1α and vascular endothelial growth factor production and also chemoresistance *in vitro* [11–13].

Nrf2 (nuclear factor erythroid 2-related factor 2) belongs to the cap'n'collar (CNC) bZIP transcription factors [14]. Under normoxia, Nrf2 is constitutively driven to proteosomal degradation by its proximal regulator, Keap1 (Kelch-like ECH-associated protein 1). When the cell is exposed to oxidative stress, Nrf2-Keap1 interaction is disturbed and Nrf2 relocates from the cytoplasm to the nucleus where it complexes with small maf proteins and upregulates genes with an antioxidant response element (ARE) in their regulatory regions. Nrf2 has been suggested to play an essential role in the development of chemoresistance [15]. Therefore, Prx enzymes, Nrf2 transcription factor, Trx, and Keap1 are all markers that should be studied for predictive and prognostic use in malignancies.

Most chemotherapy agents act directly or indirectly on the excessive production of ROS [8, 16]. Anthracyclines (such as epirubicin and doxorubicin) and taxanes (usually docetaxel and paclitaxel) are the standard of care in breast cancer chemotherapy, including the neoadjuvant setting. Anthracyclines bind to metals, such as iron, and form drug-metal complexes. This kind of a complex is capable of producing iron-mediated oxidative stress reaction in the cell that leads to covalent modification of guanine bases of DNA [17]. The main mechanism of action of taxanes is based on the disruption of microtubule function, but they also exert at least their adverse effects via increased ROS production [18, 19].

The aim of the current study was to evaluate the possible association between major redox-regulating proteins and chemoresistance in a cohort of patients with primarily inoperable breast cancers treated with NACT. The prognostic value of the studied proteins was also assessed, both in pre-NACT and postoperative samples. As the main finding, immunohistochemical pre-NACT Keap1 and Trx expressions appear to predict especially poor outcome in these patients.

2. Materials and Methods

2.1. Patients and Samples. The study included 53 breast cancer patients, who at the time of diagnosis were inoperable due to local invasion or inflammatory breast cancer. The patients were treated with NACT in Oulu University Hospital, Finland, during the years 2000–2015. All the patients received a minimum of two NACT cycles (ranging from 2 to 16 cycles, median 6 cycles) (Table 1). All patients underwent mastectomy and axillary evacuation with radical intention after NACT. The response for NACT was classified as a complete response (no viable cancer cells in breast or lymph nodes after surgery), a partial response, a stable disease (no radiological change in tumor size during the NACT), or a progressive disease. The mean age at diagnosis was 56.4 (32–77), and the mean follow-up time was 43.8 months (3–112). None of the patients had earlier diagnosis of invasive breast cancer.

Table 1: Patient characteristics.

	Number of patients	Percentage or range
Mean years of age at diagnosis	56.4	32–77
Menopausal status	**53**	**100**
Premenopausal	17	32.1
Postmenopausal	28	52.8
Not known	8	15.1
Bilateral breast cancer	**53**	**100**
Bilateral breast cancer	4	7.5
Unilateral breast cancer	49	92.5
NACT received	**53**	**100**
Docetaxel + doxorubicin	20	37.7
Docetaxel + trastuzumab	14	26.4
Docetaxel + epirubicin	3	5.7
Other chemotherapy	16	30.2
Median number of neoadjuvant cycles	6.0	2–16
Surgical procedure	**53**	**100**
Mastectomy and axillary evacuation	53	100
Adjuvant chemotherapy	**53**	**100**
Cyclophosphamide + epirubicin + fluorouracil	11	20.8
Other chemotherapy	18	34
No adjuvant chemotherapy	24	45.3
Radiotherapy	**53**	**100**
Yes	52	98.1
No	1	1.9
Adjuvant endocrine therapy	**53**	**100**
Tamoxifen	10	18.9
Aromatase inhibitor	23	43.4
GnRH analogue + tamoxifen	5	9.4
GnRH analogue + aromatase inhibitor	1	1.9
Tamoxifen and aromatase inhibitor (sequentially)	2	3.8
No adjuvant hormonal therapy	12	22.6
Recurrence status	**53**	**100**
Distant	20	37.7
Local	3	5.6
No recurrence	30	56.6

Tumor properties and patient data were collected from medical records and are presented in Tables 2 and 3.

A core needle biopsy sample before NACT and a resected tumor sample after NACT were obtained from each patient in the study. Pre-NACT tumor sizes were available from magnetic resonance imaging in 38 (71.7%) patients and from ultrasound in 13 (24.5%) patients and were unmeasurable in 2 (3.8%; tumor filled the whole breast) patients. The mean tumor size based on imaging at the time of diagnosis was 54.6 mm (10–140 mm), and after NACT, it was 31.2 mm (0–90 mm). The average postoperative tumor size measured from the resected tumor sample was 39.1 mm (0–150 mm).

Table 2: Pre- and postoperative tumor sizes.

	Mean size (mm) and number of patients	Range
Tumor size at the time of diagnosis	54.6 (50)	10–140 mm
Preoperative tumor size	31.2 (47)	0–90 mm
Postoperative tumor size	39.1 (52)	0–150 mm

Patients were classed after the TNM classification, and the histopathology was evaluated according to the current WHO classification [20]. Estrogen receptor (ER), progesterone receptor (PR), and Ki-67 expressions were analyzed by immunohistochemistry as described previously [7]. HER2 expression was determined by immunohistochemistry, and when an HER2-positive result appeared, gene amplification status was determined using chromogenic in situ hybridization. Cancers with six or more gene copies were considered *HER2* positive [21].

2.2. Immunohistochemistry. Staining was performed following the routine protocol in the Department of Pathology, Oulu University Hospital. Tissue sections (4 μm) were cut from the paraffin-embedded blocks. After deparaffinization in xylene and rehydration in graded alcohol solutions, the sections were heated in a microwave oven for 2 min (800 W) + 10 min (150 W) in citrate buffer (pH 6.0) and incubated in room temperature for 20 min. Immunostaining for Nrf2 was done the same, but the heating time at 150 W was 15 min in Tris-EDTA buffer (pH 9.0). The sections were then rinsed in distilled water and phosphate-buffered saline with TWEEN (PBS-TWEEN), incubated in endogenous peroxidase-neutralizing solution (Dako S2023, Dako A/S, Glostrup, Denmark) for 5 min, and washed twice for 5 min in PBS-TWEEN. The Keap1 and Prx I sections were incubated in protein block solution for 5 min.

The preprocessed slides were then incubated for 1 hr at room temperature with the monoclonal anti-Nrf2 (ab62352, EnVision detection system, Dako A/S, Glostrup, Denmark), anti-Keap1 (ab66620, Novolink Polymer Detection System, Leica Biosystems Newcastle Ltd., Newcastle, UK), anti-Trx (#2429, Cell Signaling Technology, Dako A/S, Glostrup, Denmark), and anti-Prx I (LF-PA0095, Novolink Polymer Detection System, Leica Biosystems Newcastle Ltd., Newcastle, UK) antibodies (dilutions 1 : 400, 1 : 800, 1 : 600, and 1 : 150, resp.). The Keap1 and Prx I slides were then incubated for 30 min in antibody-blocking solution. All the slides were finally incubated with a biotinylated secondary antibody and avidin-biotin-peroxidase complex (Novolink polymer for Prx I and Keap1, Envision polymer K5007 for Trx and Nrf2). Two rinses (5 min each) were performed with PBS following each step of the immunostaining procedure. The color was developed with incubation of 3 min with diaminobenzidine tetrahydrochloride (K5007, EnVision detection system, Dako A/S, Glostrup, Denmark). The slides were rinsed in distilled water, counterstained with Mayer's hematoxylin, washed, dehydrated, cleared, and mounted with Depex (BDH, Poole, UK). In negative controls, the primary antibody was omitted. Samples unrelated to the study material that were known to react with the various indicator antibodies were used as positive controls.

Two of the authors (NR and KMH) performed the evaluation of immunostaining for the tumor cell cytoplasm and nuclei. The intensity of the staining of both cell compartments was evaluated as 0 (negative), 1 (weakly positive), 2 (moderately positive), or 3 (strongly positive). The amount

Table 3: Tumor properties. Estrogen receptor (ER), progesterone receptor (PR), Ki-67, and HER2 expressions and grade are reported as in postoperative PAD. If unavailable in postoperative PPS, the assessment from the core needle biopsy is reported.

	Number of patients	Percentage or range
Response to NACT	**52***	**100**
Complete response	6	11.3
Partial response	44	83.0
Stable disease	2	3.8
Progression	0	0
Histopathological grade	**53**	**100**
Grade 1	1	1.9
Grade 2	19	35.8
Grade 3	19	35.8
No information or no viable cancer cells	14	26.4
ER status	**53**	**100**
Negative (0%)	9	17.0
Weak (1–9%)	8	15.1
Moderate (10–59%)	2	3.8
High (>59%)	34	64.2
PR status	**53**	**100**
Negative (0%)	23	43.4
Weak (1–9%)	5	9.4
Moderate (10–59%)	3	5.6
High (>59%)	22	41.5
Ki-67 status	**53**	**100**
Negative (<5%)	6	11.3
Weak (5–14%)	12	22.6
Moderate (15–30%)	12	22.6
High positive (>30%)	22	41.5
No information or no viable cancer cells	1	1.9
HER2 status	**53**	**100**
Negative	37	69.8
Positive (confirmed with CISH)	16	30.2
Median number of metastatic lymph nodes	**2.0**	**0–20**
Distant metastases at the time of diagnosis	**53**	**100**
Absent	43	81.1
Present	10	18.9

*The information of pre-NACT tumor size was missing from one patient.

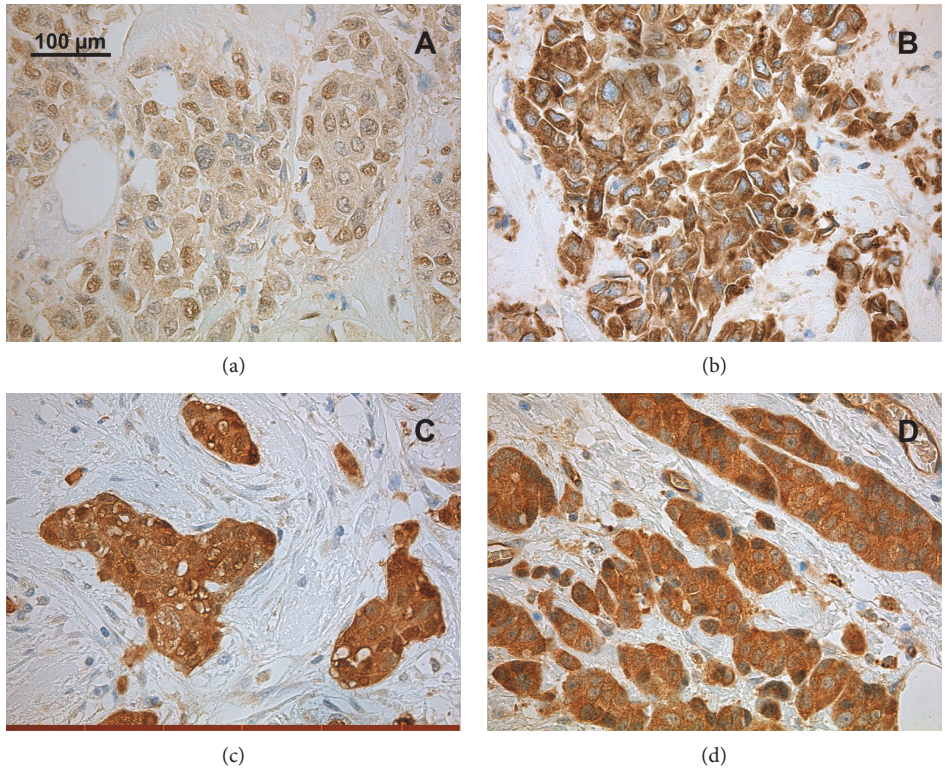

Figure 1: Immunohistochemical detection of protein levels of Keap1 (a), Nrf2 (b), Trx (c), and Prx I (d) in postoperative samples of NACT-treated patients. The figures represent samples with weakly positive (a), moderately/strongly positive (b), and strongly positive (c, d) cytoplasmic staining. None of the tumor samples were totally negative, but negative staining can be seen in connective tissue (c, d). Nuclear staining is negative in figures (b) and (d) and partly moderately positive in (a) and (c).

of stained cells was reported as percentages (0–100) out of all malignant cells. A histological sum score, H score, was computed by multiplying the intensity and staining percentage scores resulting in scale of 0–300 [22]. The H score allows areas with different intensities to be taken into account. Separate H scores were created for both nuclear and cytoplasmic immunostaining. Raw H scores were used in statistical analyses, with the exception of Kaplan-Meier analysis, where two-classed variable was created based on the receiver operating characteristic (ROC) analysis of the H score.

2.3. Statistical Analyses. For statistical analyses, ER, PR, Ki-67, and HER2 expressions and grade were recorded as mentioned in the postoperative pathoanatomical diagnosis (PAD). If unavailable in postoperative PAD, the assessments from the preoperative core needle biopsy were used. ER and PR expressions were classified into either negative (<1% of positivity) or positive (1–100% of tumor cells positive). Ki-67 was divided into either negative to moderate (0–30%) or high (>30%). Grade was divided into either I-II or III for statistical analyses. Tumor size was processed as millimeters, and the number of nodal metastases was also treated as a continuous variable.

IBM SPSS Statistics version 22.0.0.0 for Mac (IBM Corporation, Armonk, NY, USA) was used for statistical analysis. Two-classed variables (ER, PR, Ki-67 grade; the presence of multifocal disease; and bilateral breast cancer) were tested against H scores with the independent samples Mann-Whitney U test. Continuous variables were correlated with two-tailed Spearman's test, with the correlation coefficient. The Wilcoxon test was applied when comparing core needle biopsy H scores to postoperative H scores. Survival was analyzed by using the Kaplan-Meier method with the log-rank and Breslow tests. The endpoint in breast cancer-specific survival (BCSS) was the confirmed death due to metastatic breast cancer while in disease-free survival (DFS), the endpoint was either local relapse or distant metastasis, whichever occurred earlier. Reliable multivariate analysis could not be performed due to a low number of samples. p values < 0.05 were considered significant.

2.4. Ethical Considerations. This study was approved by the Local Ethics Committee of the Ostrobothnia Hospital District (114/2011, amendment 23.2.2015) and the National Supervisory Authority for Welfare and Health (1339/05.01.00.06/2009).

3. Results

In pretreatment samples, some positive cytoplasmic immunostaining for all antibodies was detected in almost all the samples (Figure 1). Due to exhaustion of blocks or occurrence of nonrepresentative areas, especially in core needle biopsies, the immunostaining for some patients could not be reliably evaluated. Keap1 and Prx I showed at least some cytoplasmic expression in all pretreatment samples, and for

Table 4: Antigen staining in different cell compartments. The percentages represent cases showing any immunopositivity.

Target protein	Cytoplasmic staining, pretreatment (%)	Cytoplasmic staining, posttreatment (%)	Nuclear staining, pretreatment (%)	Nuclear staining, posttreatment (%)
Keap1	100.0	100.0	45.3	88.9
Nrf2	94.6	100.0	0	0
Prx I	100.0	100.0	45.9	100.0
Trx	94.6	100.0	64.9	81.8

Nrf2 and Trx, 94.6% of the samples showed at least some positivity (Table 4). Preoperative nuclear expression was detected in 45.3%, 45.9%, and 64.9% of the samples for Keap1, Prx I, and Trx, respectively (Table 4). Nrf2 was negative for nuclear staining in all samples.

Both the cytoplasmic ($p = 0.0015$) and nuclear ($p = 0.0013$) expressions of Trx were increased during the NACT. High cytoplasmic Trx expression in postoperative samples was associated with negative ER expression ($p = 0.027$). Elevated pretreatment cytoplasmic Nrf2 expression was associated with HER2 negativity ($p = 0.036$) and ER positivity ($p = 0.032$).

Nuclear, but not cytoplasmic, Keap1 expression was increased during the NACT ($p = 0.022$). Pre-NACT nuclear Keap1 expression was also connected with better tumor differentiation ($p = 0.029$). Higher nuclear Keap1 expression in postoperative samples was associated with the presence of bilateral breast cancer ($p = 0.026$). Furthermore, expressions of Keap1 and Trx were strongly connected with each other in postoperative cytoplasmic ($p = 0.00048$; $r = 0.504$) and nuclear ($p = 0.0024$; $r = 0.446$) staining. Pre-NACT and postoperative nuclear Keap1 H scores also showed a positive correlation ($p = 0.011$; $r = 0.376$).

Nuclear Prx I expression was highly increased during NACT ($p = 0.00028$), with all samples postoperatively showing some Prx I expression. The nuclear staining of Prx I in core needle biopsies correlated inversely with the size of a resected tumor ($p = 0.00052$; $r = -0.550$). Also, cytoplasmic staining of the Prx I in resected tumor samples had an inverse correlation with the amount of nodal metastasis ($p = 0.0024$; $r = -0.472$).

We also examined whether the change in antibody H scores between core needle biopsy and postoperative expression was associated with clinicopathological parameters. Increased cytoplasmic Trx expression was associated with larger primary tumor size preoperatively ($p = 0.037$; $r = 0.396$) and postoperatively ($p = 0.029$; $r = 0.389$).

3.1. Survival Analysis. In ROC analysis, the optimal cut-off H score of 15.0 was defined for pre-NACT nuclear Trx expression with regard to DFS. Likewise, ROC analysis confirmed an optimal cut-off H score of 22.5 for pre-NACT nuclear Keap1 in terms of DFS.

Higher pre-NACT nuclear Trx and nuclear Keap1 expressions predicted better DFS (log-rank $p = 0.064$; Breslow $p = 0.038$ and log-rank $p = 0.056$; Breslow $p = 0.018$, resp.) (Figure 2). When pre-NACT nuclear Trx expression and pre-NACT nuclear Keap1 expression were combined as a single factor (0 = low expression for both, 1 = high expression for Trx and/or Keap1), low expression of both Trx and Keap1 predicted poor DFS highly significantly (log-rank $p = 0.0030$; Breslow $p = 0.00082$). No significant associations between the studied markers and BCSS were found.

4. Discussion

Predictive factors for breast cancer chemotherapy are scarce, to date including mainly immunohistochemical surrogates, such as ER negativity and high Ki-67 for the identification of more chemosensitive luminal B-type breast cancer [23]. Our goal was to determine if the main regulators of the cellular redox state would have an impact on neoadjuvant chemotherapy effectiveness or patient outcome in the patients with locally advanced, primarily inoperable breast cancer.

The Trx system, including Trx, thioredoxin reductase (TrxR), and thioredoxin-interacting protein (TxNIP), not only participates to the early phases of breast carcinogenesis but is also connected to ER negativity, high proliferation, and poor survival in breast cancer and is involved in chemotherapy resistance *in vitro* [24, 25]. In lymphomas, siRNA targeted against Trx led to the sensitization of the tumor to doxorubicin which resulted in cell growth inhibition while in stomach cancer, Trx expression has been linked to multidrug resistance [26, 27]. Woolston et al. previously assessed the predictive and prognostic value of Trx family proteins in anthracycline-based NACT-treated breast cancer patients. Although predictive markers were not recognized, patients with high immunohistochemically determined TxNIP or TrxR expression had dismal outcomes [28].

In our patients, both nuclear and cytoplasmic Trx expressions increased in tumor tissue during the NACT. Increased cytoplasmic Trx expression during NACT also associated with a larger primary tumor size. This may reflect Trx-mediated chemoresistance during the therapy; alternatively, Trx induction may contribute to the increased proliferation and apoptosis resistance in various cancers [12]. Furthermore, pre-NACT nuclear Trx expression was associated with the prolonged DFS, but only with borderline significance. Trx enhances anthracycline-mediated apoptosis in breast cancer MCF-7 cells, and, again, TrxR predicts better distant metastasis-free survival in clinical breast cancer material [28, 29], although the prognostic role of Trx has been less clear.

Keap1 is a cytosolic or nuclear cysteine-rich protein, which in unstressed conditions targets newly synthesized Nrf2 to proteosomal degradation [30]. Under oxidative

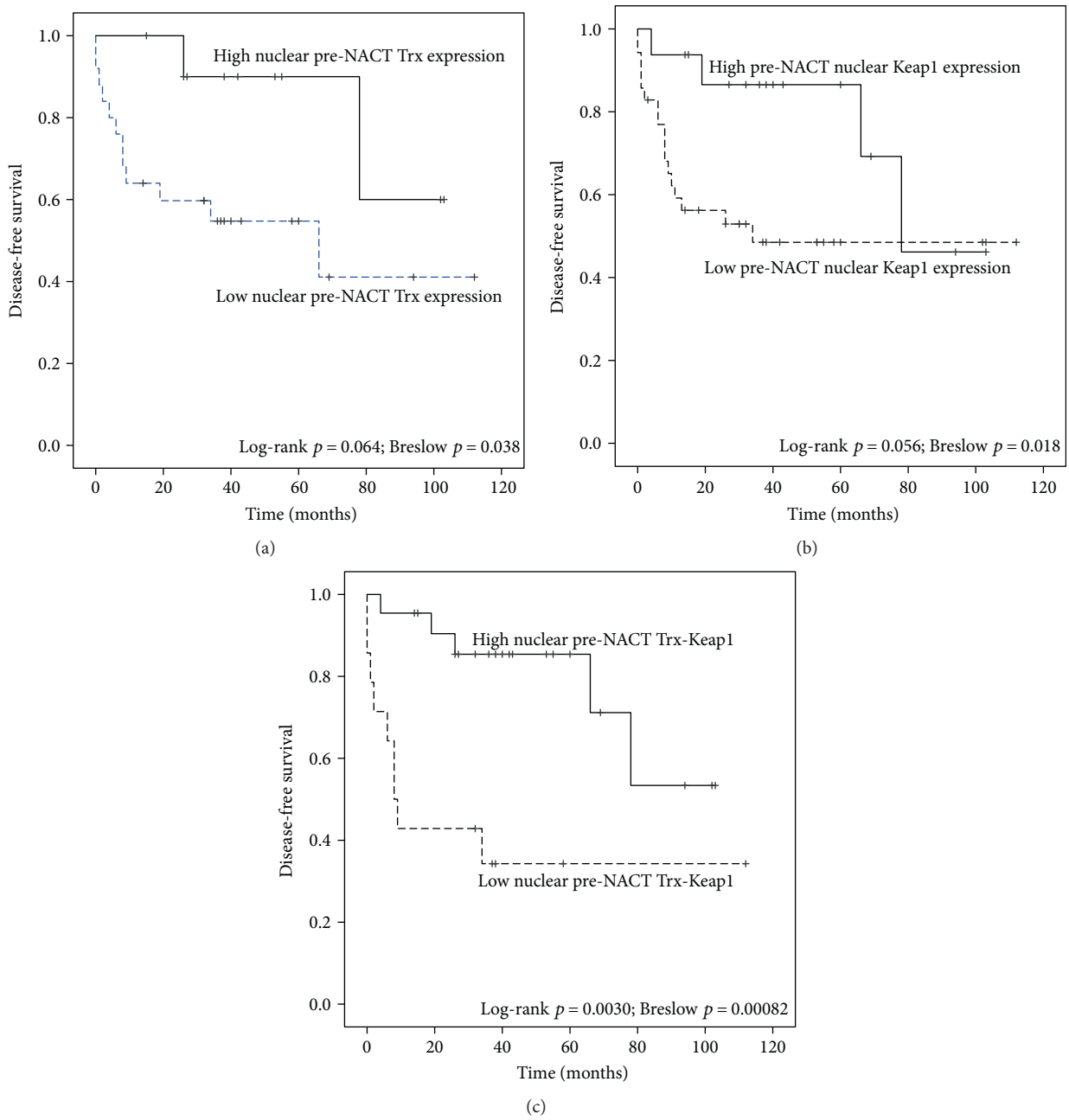

Figure 2: Kaplan-Meier curves comparing preneoadjuvant chemotherapy (NACT) expression of Trx (a) and Keap1 (b). Cut-offs for low and high expression have been generated with ROC analysis. In part (c), cases with both low nuclear pre-NACT Keap1 and low nuclear pre-NACT Keap1 have been set against other patients. Crosses indicate censored cases.

stress, several Cys residues in Keap1 are oxidized; consequently, Nrf2 becomes stable and bypasses degradation which ultimately results in widespread expression of antioxidant proteins [31]. Keap1 somatic mutations have been linked to chemoresistance in various carcinomas, although Keap1 protein expression in this context is less studied [32–35]. Higher nuclear Keap1 expression in pre-NACT samples predicted prolonged DFS in our patients, suggesting the block of excess Nrf2 function and the suppression of subsequent antioxidant induction. Rather surprisingly, no nuclear Nrf2 expression was noted in the current study, which may at least partially be linked with technical reasons. Analogous observations of Keap1 protein overexpression and better survival have been reported from pancreatic cancer and from squamous non-small-cell lung carcinoma [36, 37].

In the context of breast cancer, aberrant Keap1 methylation was found as an independent prognostic factor of better DFS (HR = 0.082), specifically in the patients treated with anthracycline/taxane-based chemotherapy [38]. In the same paper, Keap1 methylation associated with an increased risk of BCSS in the subset of patients with triple-negative breast

cancer. We have earlier reported that stronger immunohistochemical Keap1 expression is a poor prognostic factor for BCSS [39]. The current results therefore differ from our earlier observations. However, in the patients comprising this study, the prognostic value of Keap1 expression was noted for untreated preoperative samples, which, according to our knowledge, has not been explored previously. Notably, the number of samples showing nuclear Keap1 positivity nearly doubled during NACT, which suggests a role for Keap1 as a gatekeeper for Nrf2 as a response to cytotoxic therapy. The same phenomenon of markedly elevated Keap1 levels during the NACT was recently detected in ovarian cancer patients [40].

There was a strong positive correlation between Keap1 and Trx in our study, which supports the recent hypothesis that Trx as highly redox-reactive protein also maintains the active state of cysteine-rich Keap1 [41]. Patients with both low Trx and Keap1 expressions had a dismal prognosis in our current patients, with 53% having either distant or local relapse during the first nine months after diagnosis. Although there were no progressive diseases during NACT in our study cohort, the high proportion of early relapses in low-Keap1/Trx patients suggests a negative impact for the simultaneous loss of Trx and Keap1 due to chemosensitivity. Nevertheless, the low number of patients with both Keap1 and Trx core needle biopsy immunostainings available ($n = 36$) limits the power of the analysis making multivariate analysis unreliable. Another potential limitation of the study may be that due to limited sample size, we were unable to assess biological subgroups separately.

The role of Prx I in cancer development is considerably studied but to date not yet fully defined. Knockdown/knockout mice with Prx I deficiency are prone to elevated ROS amounts and development of cancer [42]. Thus, high Prx levels may protect DNA against mutations and carcinogenesis. On the other hand, Prx I gene expression induction in MCF-7 cells has been linked to the platinum resistance, which is likely due to the elimination of chemotherapy-induced ROS [43]. Furthermore, Prx I knockdown in HeLa cells induces the efficacy of beta-lapachone, an ROS-generating experimental chemotherapeutic agent [44]. In clinical samples, Prx I appears to associate with worse prognosis in pancreatic cancer, cholangiocarcinoma, hepatocellular carcinoma, and early-stage non-small-cell lung cancer [45–48]. In contrast to this, Prx I was an independent predictor of improved outcomes in a large set of ER-positive breast cancers [49]. Breast cancer-suppressive properties of Prx I have been proposed to be mediated via the inhibition of c-Myc activation and p53-dependent cytotoxicity [9, 10]. Supporting this cancer-specific role of Prx I, we observed that elevated Prx I expression was associated with both smaller primary tumor size and lower number of lymph node metastases. Additionally, we noted a significant induction of Prx I during NACT, which may reflect cancer cell adaptation to oxidative conditions [50, 51]. This would be in line with the previous mouse model data showing that doxorubicin increases the mRNA and protein expressions of Prx I, II, III, V, and VI through metallothionein activation [52].

5. Conclusions

There appears to be significant antioxidant enzyme upregulation during breast cancer NACT. Due to the restricted sample size, the current study is mainly hypothesis generating and applies only to patients with primary inoperable breast cancer. If confirmed in larger and preferably in prospective settings, especially Keap1 and Trx expression in chemotherapy-naïve patients may serve as predictive or prognostic biomarkers.

Conflicts of Interest

The authors declare that they have no conflicts of interest.

Acknowledgements

The authors thank Barry Ziola for giving comments and for proofreading the manuscript and Riitta Vuento for the outstanding technical assistance. The Heikki Ruotsalainen and Thelma Mäkikyrö Foundations provided funding for the study.

References

[1] M. Ervik, F. Lam, J. Ferlay, L. Mery, I. Soerjomataram, and F. Bray, *Cancer Today*, International Agency for Research on Cancer. Cancer Today, Lyon, France, 2016, http://gco.iarc.fr/today.

[2] P. Cortazar, L. Zhang, M. Untch et al., "Pathological complete response and long-term clinical benefit in breast cancer: the CTNeoBC pooled analysis," *The Lancet*, vol. 384, no. 9938, pp. 164–172, 2014.

[3] T. R. Hurd, M. Degennaro, and R. Lehmann, "Redox regulation of cell migration and adhesion," *Trends in Cell Biology*, vol. 22, no. 2, pp. 107–115, 2012.

[4] L. Tochhawng, S. Deng, S. Pervaiz, and C. T. Yap, "Redox regulation of cancer cell migration and invasion," *Mitochondrion*, vol. 13, no. 3, pp. 246–253, 2013.

[5] J. E. Klaunig, Y. Xu, J. S. Isenberg et al., "The role of oxidative stress in chemical carcinogenesis," *Environmental Health Perspectives*, vol. 106, Supplement 1, pp. 289–295, 1998.

[6] L. Sena and N. Chandel, "Physiological roles of mitochondrial reactive oxygen species," *Molecular Cell*, vol. 48, no. 2, pp. 158–167, 2012.

[7] P. Karihtala, A. Mäntyniemi, S. W. Kang, V. L. Kinnula, and Y. Soini, "Peroxiredoxins in breast carcinoma," *Clinical Cancer Research*, vol. 9, no. 9, pp. 3418–3424, 2003.

[8] B. Kalyanaraman, "Teaching the basics of redox biology to medical and graduate students: oxidants, antioxidants and disease mechanisms," *Redox Biology*, vol. 1, no. 1, pp. 244–257, 2013.

[9] R. A. Egler, E. Fernandes, K. Rothermund et al., "Regulation of reactive oxygen species, DNA damage, and c-Myc function by peroxiredoxin 1," *Oncogene*, vol. 24, no. 54, pp. 8038–8050, 2005.

[10] A. Morinaka, Y. Funato, K. Uesugi, and H. Miki, "Oligomeric peroxiredoxin-I is an essential intermediate for p53 to activate MST1 kinase and apoptosis," *Oncogene*, vol. 30, no. 40, pp. 4208–4218, 2011.

[11] J. Hwang, L. T. Nguyen, Y. H. Jeon, C. Y. Lee, and M. H. Kim, "Crystal structure of fully oxidized human thioredoxin," *Biochemical and Biophysical Research Communications*, vol. 467, no. 2, pp. 218–222, 2015.

[12] G. Powis and D. L. Kirkpatrick, "Thioredoxin signaling as a target for cancer therapy," *Current Opinion in Pharmacology*, vol. 7, no. 4, pp. 392–397, 2007.

[13] S. J. Welsh, W. T. Bellamy, M. M. Briehl, T. Angiogenesis, and G. Powis, "The redox protein thioredoxin-1 (Trx-1) increases hypoxia-inducible factor 1α protein expression: Trx-1 overexpression results in increased vascular endothelial growth factor production and enhanced tumor angiogenesis," *Cancer Research*, vol. 62, no. 17, pp. 5089–5095, 2002.

[14] K. Itoh, J. Mimura, and M. Yamamoto, "Discovery of the negative regulator of Nrf2, Keap1: a historical overview," *Antioxidants & Redox Signaling*, vol. 13, no. 11, pp. 1665–1678, 2010.

[15] J. H. No, Y.-B. Kim, and Y. S. Song, "Targeting Nrf2 signaling to combat chemoresistance," *Journal of Cancer Prevention*, vol. 19, no. 2, pp. 111–117, 2014.

[16] P. Karihtala and U. Puistola, "Hypoxia and oxidative stress in the pathogenesis of gynecological cancers and in therapeutical options," *Current Cancer Therapy Reviews*, vol. 7, no. 1, pp. 37–55, 2011.

[17] A. Rabbani, R. M. Finn, and J. Ausió, "The anthracycline antibiotics: antitumor drugs that alter chromatin structure," *BioEssays*, vol. 27, no. 1, pp. 50–56, 2005.

[18] V. A. Carozzi, A. Canta, and A. Chiorazzi, "Chemotherapy-induced peripheral neuropathy: what do we know about mechanisms?," *Neuroscience Letters*, vol. 596, pp. 90–107, 2015.

[19] J.-H. Hung, C.-Y. Chen, H. A. Omar et al., "Reactive oxygen species mediate terbufos-induced apoptosis in mouse testicular cell lines via the modulation of cell cycle and pro-apoptotic proteins," *Environmental Toxicology*, vol. 31, no. 12, pp. 1888–1898, 2016.

[20] S. R. Lakhani, I. O. Ellis, S. J. Schnitt, P. H. Tan, and M. J. van der Vijver, *WHO Classification of Tumours*, International Agency for Research on Cancer, Lyon, 4 edition, 2012.

[21] J. Isola, M. Tanner, A. Forsyth, T. G. Cooke, A. D. Watters, and J. M. S. Bartlett, "Interlaboratory comparison of *HER-2* oncogene amplification as detected by chromogenic and fluorescence *in situ* hybridization," *Clinical Cancer Research*, vol. 10, no. 14, pp. 4793–4798, 2004.

[22] E. Specht, D. Kaemmerer, J. Sänger, R. M. Wirtz, S. Schulz, and A. Lupp, "Comparison of immunoreactive score, HER2/*neu* score and H score for the immunohistochemical evaluation of somatostatin receptors in bronchopulmonary neuroendocrine neoplasms," *Histopathology*, vol. 67, no. 3, pp. 368–377, 2015.

[23] E. Senkus, S. Kyriakides, S. Ohno et al., "Primary breast cancer: ESMO clinical practice guidelines for diagnosis, treatment and follow-up," *Annals of Oncology*, vol. 26, Supplement 5, pp. v8–v30, 2015.

[24] M. Bhatia, K. L. Mcgrath, G. Di et al., "The thioredoxin system in breast cancer cell invasion and migration," *Redox Biology*, vol. 8, pp. 68–78, 2016.

[25] N. Turunen, P. Karihtala, A. Mantyniemi et al., "Thioredoxin is associated with proliferation, p53 expression and negative estrogen and progesterone receptor status in breast carcinoma," *APMIS*, vol. 112, no. 2, pp. 123–132, 2004.

[26] C. Li, M. A. Thompson, A. T. Tamayo et al., "Over-expression of thioredoxin-1 mediates growth, survival, and chemoresistance and is a druggable target in diffuse large B-cell lymphoma," *Oncotarget*, vol. 33, no. 3, pp. 314–326, 2012.

[27] P. Sinha, G. Hutter, E. Kottgen, M. Dietel, D. Schadendorf, and H. Lage, "Increased expression of annexin I and thioredoxin detected by two-dimensional gel electrophoresis of drug resistant human stomach cancer cells," *Journal of Biochemical and Biophysical Methods*, vol. 37, no. 3, pp. 105–116, 1998.

[28] C. M. Woolston, L. Zhang, S. J. Storr et al., "The prognostic and predictive power of redox protein expression for anthracycline-based chemotherapy response in locally advanced breast cancer," *Modern Pathology*, vol. 25, no. 8, pp. 1106–1116, 2012.

[29] D. Ravi, H. Muniyappa, and K. C. Das, "Endogenous thioredoxin is required for redox cycling of anthracyclines and p53-dependent apoptosis in cancer cells," *The Journal of Biological Chemistry*, vol. 280, no. 48, pp. 40084–40096, 2005.

[30] Z. Sun, S. Zhang, J. Y. Chan, and D. D. Zhang, "Keap1 controls postinduction repression of the Nrf2-mediated antioxidant response by escorting nuclear export of Nrf2," *Molecular and Cell Biology*, vol. 27, no. 18, pp. 6334–6349, 2007.

[31] M. G. P. van der Wijst, R. Brown, and M. G. Rots, "Nrf2, the master redox switch: the Achilles' heel of ovarian cancer?," *Biochimica et Biophysica Acta (BBA) - Reviews on Cancer*, vol. 1846, no. 2, pp. 494–509, 2014.

[32] T. Ohta, K. Iijima, M. Miyamoto et al., "Loss of Keap1 function activates Nrf2 and provides advantages for lung cancer cell growth," *Cancer Research*, vol. 68, no. 5, pp. 1303–1309, 2008.

[33] T. Shibata, A. Kokubu, M. Gotoh et al., "Genetic alteration of *Keap1* confers constitutive Nrf2 activation and resistance to chemotherapy in gallbladder cancer," *Gastroenterology*, vol. 135, no. 4, pp. 1358–1368.e4, 2008.

[34] T. Jiang, N. Chen, F. Zhao et al., "High levels of Nrf2 determine chemoresistance in type II endometrial cancer," *Cancer Research*, vol. 70, no. 13, pp. 5486–5496, 2010.

[35] P. A. Konstantinopoulos, D. Spentzos, E. Fountzilas et al., "Keap1 mutations and Nrf2 pathway activation in epithelial ovarian cancer," *Cancer Research*, vol. 71, no. 15, pp. 5081–5089, 2011.

[36] J. Isohookana, K.-M. Haapasaari, Y. Soini, and P. Karihtala, "Keap1 expression has independent prognostic value in pancreatic adenocarcinomas," *Diagnostic Pathology*, vol. 10, no. 1, p. 28, 2015.

[37] L. M. Solis, C. Behrens, W. Dong et al., "Nrf2 and Keap1 abnormalities in non-small cell lung carcinoma and association with clinicopathologic features," *Clinical Cancer Research*, vol. 16, no. 14, pp. 3743–3753, 2010.

[38] R. Barbano, L. A. Muscarella, B. Pasculli et al., "Aberrant *Keap1* methylation in breast cancer and association with clinicopathological features," *Epigenetics*, vol. 8, no. 1, pp. 105–112, 2013.

[39] P. Karihtala, S. Kauppila, Y. Soini, and V. Arja-Jukkola, "Oxidative stress and counteracting mechanisms in hormone receptor positive, triple-negative and basal-like breast carcinomas," *BMC Cancer*, vol. 11, no. 1, p. 262, 2011.

[40] M. Pylvas-Eerola, A. Liakka, U. Puistola, J. Koivunen, and P. Karihtala, "Cancer stem cell properties as factors predictive of chemoresistance in neoadjuvantly-treated patients with ovarian cancer," *Anticancer Research*, vol. 36, no. 7, pp. 3425–3431, 2016.

[41] E. E. Schmidt, "Interplay between cytosolic disulfide reductase systems and the Nrf2/Keap1 pathway," *Biochemical Society Transactions*, vol. 43, no. 4, pp. 632–638, 2015.

[42] V. Rani, C. A. Neumann, C. Shao, and J. A. Tischfield, "Prdx1 deficiency in mice promotes tissue specific loss of heterozygosity mediated by deficiency in DNA repair and increased oxidative stress," *Mutation Research/Fundamental and Molecular Mechanisms of Mutagenesis*, vol. 735, no. 1-2, pp. 39–45, 2012.

[43] E. V. Kalinina, T. T. Berezov, A. A. Shtil' et al., "Expression of peroxiredoxin 1, 2, 3, and 6 genes in cancer cells during drug resistance formation," *Bulletin of Experimental Biology and Medicine*, vol. 153, no. 6, pp. 878–881, 2012.

[44] T. He, A. Banach-Latapy, L. Vernis, M. Dardalhon, R. Chanet, and M.-E. Huang, "Peroxiredoxin 1 knockdown potentiates β-lapachone cytotoxicity through modulation of reactive oxygen species and mitogen-activated protein kinase signals," *Carcinogenesis*, vol. 34, no. 4, pp. 760–769, 2013.

[45] A. P. D. Demasi, E. F. Martinez, M. H. Napimoga et al., "Expression of peroxiredoxins I and IV in multiple myeloma: association with immunoglobulin accumulation," *Virchows Archiv*, vol. 463, no. 1, pp. 47–55, 2013.

[46] Q.-K. Sun, J.-Y. Zhu, W. Wang et al., "Diagnostic and prognostic significance of peroxiredoxin 1 expression in human hepatocellular carcinoma," *Medical Oncology*, vol. 31, no. 1, p. 786, 2014.

[47] C.-Y. Cai, L.-L. Zhai, Y. Wu, and Z.-G. Tang, "Expression and clinical value of peroxiredoxin-1 in patients with pancreatic cancer," *European Journal of Surgical Oncology*, vol. 41, no. 2, pp. 228–235, 2015.

[48] J. Zhou, W. Shen, X. He, J. Qian, S. Liu, and G. Yu, "Overexpression of Prdx1 in hilar cholangiocarcinoma: a predictor for recurrence and prognosis," *International Journal of Clinical and Experimental Pathology*, vol. 8, no. 9, pp. 9863–9874, 2015.

[49] P. C. O'Leary, M. Terrile, M. Bajor et al., "Peroxiredoxin-1 protects estrogen receptor α from oxidative stress-induced suppression and is a protein biomarker of favorable prognosis in breast cancer," *Breast Cancer Research*, vol. 16, no. 4, p. R79, 2014.

[50] A. J. Wadley, S. Aldred, and S. J. Coles, "An unexplored role for peroxiredoxin in exercise-induced redox signalling?," *Redox Biology*, vol. 8, pp. 51–58, 2016.

[51] M. Zhang, M. Hou, L. Ge et al., "Induction of peroxiredoxin 1 by hypoxia regulates heme oxygenase-1 via NF-κB in oral cancer," *PLoS One*, X.-Y. Guan, Ed., vol. 9, no. 8, article e105994, 2014.

[52] L. Jing, Y. Wu, J. Wu, J. Zhao, D. Zuo, and S. Peng, "Peroxiredoxins are involved in metallothionein protection from doxorubicin cardiotoxicity," *European Journal of Pharmacology*, vol. 659, no. 2-3, pp. 224–232, 2011.

Hindawi
Oxidative Medicine and Cellular Longevity
Volume 2017, Article ID 2734976, 16 pages
https://doi.org/10.1155/2017/2734976

Research Article

Cytotoxicity, Oxidative Stress, Cell Cycle Arrest, and Mitochondrial Apoptosis after Combined Treatment of Hepatocarcinoma Cells with Maleic Anhydride Derivatives and Quercetin

Gabriela Carrasco-Torres,[1] Rafael Baltiérrez-Hoyos,[2] Erik Andrade-Jorge,[1] Saúl Villa-Treviño,[3] José Guadalupe Trujillo-Ferrara,[1] and Verónica Rocío Vásquez-Garzón[2]

[1]*Departamento de Bioquímica y Sección de Graduados, Escuela Superior de Medicina del IPN, Ciudad de México, Mexico*
[2]*CONACYT, Facultad de Medicina y Cirugía, Universidad Autónoma Benito Juárez de Oaxaca, Oaxaca de Juárez, OAX, Mexico*
[3]*Departamento de Biología Celular, Centro de Investigación y de Estudios Avanzados del Instituto Politécnico Nacional, Ciudad de México, Mexico*

Correspondence should be addressed to José Guadalupe Trujillo-Ferrara; jtrujillo@ipn.mx and Verónica Rocío Vásquez-Garzón; vrvasquezga@conacyt.mx

Received 22 February 2017; Revised 12 June 2017; Accepted 18 July 2017; Published 10 October 2017

Academic Editor: Christian Widmann

The inflammatory condition of malignant tumors continually exposes cancer cells to reactive oxygen species, an oxidizing condition that leads to the activation of the antioxidant defense system. A similar activation occurs with glutathione production. This oxidant condition enables tumor cells to maintain the energy required for growth, proliferation, and evasion of cell death. The objective of the present study was to determine the effect on hepatocellular carcinoma cells of a combination treatment with maleic anhydride derivatives (prooxidants) and quercetin (an antioxidant). The results show that the combination of a prooxidant/antioxidant had a cytotoxic effect on HuH7 and HepG2 liver cancer cells, but not on either of two normal human epithelial cell lines or on primary hepatocytes. The combination treatment triggered apoptosis in hepatocellular carcinoma cells by activating the intrinsic pathway and causing S phase arrest during cell cycle progression. There is also clear evidence of a modification in cytoskeletal actin and nucleus morphology at 24 and 48 h posttreatment. Thus, the current data suggest that the combination of two anticarcinogenic drugs, a prooxidant followed by an antioxidant, can be further explored for antitumor potential as a new treatment strategy.

1. Introduction

The increase in the growth, proliferation, and survival of cancer cells is due to genetic and epigenetic changes that result in the modification of hundreds of genes that finally induce aberrations in multiple pathways. One of these alterations includes the reprogramming of metabolism due to the requirement of high levels of energy, nucleotides, amino acids, and lipids for rapid cell growth and proliferation [1]. The increased requirement for ATP by mitochondrial oxidative phosphorylation generates free oxygen radicals that induce oxidative stress, and under hypoxic or anoxic conditions, cancer cells resolve their energy demand by utilizing glucose as a source of energy [2, 3]. Metabolic adaptations are critical for the capability of cancer cells to sustain proliferation. Reactive oxygen species (ROS) are produced due to the increase in metabolic activity and due to the activation of oncogenes and functional loss of p53. To modulate the disturbance in redox balance during the process of carcinogenesis, cancer cells increase antioxidant defenses and upregulate prosurvival molecules [4, 5]. Cancer cells exhibit enhanced intracellular levels of glutathione (GSH) and

gamma-glutamylcysteine synthetase and activate the transcription factors NfkB, HIF, p53, and FoxM1 [5, 6]. GSH is one of the principal antioxidants involved in many cellular processes. Nrf2, an oncogenic transcription factor, regulates intracellular stress and plays a key role in the environmental control of the abundant cellular antioxidant systems responsible for GSH production [7]. The modulation of antioxidative defense systems allows tumor cells to bypass cell death caused by excessive levels of ROS. However, excessive ROS production can affect cancer cells, resulting in cell cycle arrest and apoptosis [8].

Chemotherapy is considered a promising way of treating cancer. In addition, selective targeting of cancer cells by the modulation of ROS production has been proposed as an excellent therapeutic alternative. Chemotherapeutic drugs such as amino benzenesulfonamide induce apoptosis, increase ROS, and reduce GSH levels [8]. Novel drugs have been identified, which increase ROS levels and modulate the mitochondrial membrane potential, making tumor cells susceptible to cell death. Many reports have indicated that antitumor agents exert their effects by inducing ROS, but the exact mechanism of ROS generation is not known [9]. Cancer-related multidrug resistance is associated with elevated GSH levels [10]. One of the principal criteria for potential anticancer drugs is the maximum effect on cancer cells with minimum damage to adjacent normal cells. Additionally, in recent years, there has been an increase in the demand for the development of new and effective antitumor drugs at affordable prices. The use of antitumor compounds with oxidative capacity does not harm normal cells because these drugs amplify the levels of reactive oxygen species, but the production of ROS in normal cells is regulated efficiently by the antioxidant defense system. The production of endogenous ROS in cells is regulated by enzymatic reactions mainly in the mitochondria. Flavonoids have emerged as alternative cancer treatment agents because of their multiple mechanisms of action and limited toxicity. Some flavonoids have antioxidant properties, and some induce oxidative stress, but flavonoids are less toxic than conventional therapies [10].

Quercetin is one of the most abundant flavonoids found in vegetables and fruits [11]. The cancer preventive mechanisms of quercetin include antioxidation and promotion of cell cycle arrest and cell death [12]. The anticancer effect of quercetin is mediated through their free radical-scavenging activity. Quercetin has been found to induce apoptosis via the inhibition of the Akt-CSN6-Myc signaling axis in colon cancer cells [13]. Likewise, the anticarcinogenic action of quercetin has been observed to be mediated by the downregulation of phosphatidylinositol 3-kinase (PI3K) and protein kinase C (PKC) via the induction of p53 in hepatocellular carcinoma [14]. It has been reported that quercetin delivered in the form of nanoparticles induces ROS production and p53 loss, arrests the cell cycle in the sub-G phase, and induces apoptosis by mitochondrial pathways in HepG2 cells [15]. Despite the various mechanisms of quercetin in eliminating tumor cells and its numerous effects, several studies have reported that it does not harm normal cells [16, 17]. Nevertheless, contradicting reports exist regarding the exact mechanism of action of quercetin. However, *in vitro* and *in vivo* studies have shown that quercetin potentiates the anticancer effect of some anticancer drugs, and in addition to being chemically synthesized and commercially sold, it has the advantage of being a component of diet [11].

Quercetin is effective against multiple targets involved in cancer development and progression. The goal of this study was to combine quercetin with maleic anhydride derivatives to enhance their ability to selectively kill tumor cells but not normal cells. Maleic anhydride derivatives have anticancer effects, and they are strong prooxidant compounds with a preference for cysteine [18].

2. Materials and Methods

2.1. Synthesis of Maleic Anhydride Derivatives. Synthesis was performed according to the method described in Trujillo-Ferrara et al. (1994) [19]. Briefly, 0.050 moles of maleic anhydride was dissolved in 75 mL of tetrahydrofuran at a 1 : 2 molar ratio. The exothermic reaction was maintained under vigorous stirring at room temperature for 60 minutes. The compound was separated by filtration and washed with cold ethanol (4°C), followed by incubation at 40°C in a vacuum oven for drying. The $3'5'$-dimaleimylbenzoic acid product was obtained in 98% yield. Next, maleimide was obtained by cyclization of its 3,5-dimaleamylbenzoic acid intermediate precursor through the dehydration of the maleamide group by mixing 0.028 moles of 3,5-dimaleamylbenzoic acid with 0.056 moles of anhydrous sodium acetate in a 1 : 2 molar ratio catalyst in 60 mL of acetic anhydride. The mixture was maintained under vigorous stirring in a water bath at 85°C and at reflux for 4 hours. The reaction was filtered under vacuum, followed by incubation under gentle agitation at 4°C. Then, 60 mL of acidified water (pH 3) was added, and the mixture was then incubated for 24 hours and then filtered, washed with doubly distilled water, and dried at 40°C. The 3,5-dimaleimylbenzoic acid product was obtained in 80% yield. The purity of the synthesized compounds was verified using thin layer chromatography, melting point measurement, infrared spectrometry, and nuclear magnetic resonance spectroscopy.

2.2. In Silico Analysis. Characterization of the local and global reactivity indexes of the derived maleic anhydride and quercetin was performed by Gaussian version 09 and AIM2000. For molecular structures and properties, analyses were performed using Gaussian version 09, MarvinView, and Structure Checker. Molecular modeling was carried out based on the method reported by Andrade et al. using the GaussView 5.0 computational package and Gaussian version 09 [18]. Briefly, the method used in the optimization was B3LYP, which is based on the density functional theory; then, the frequencies were calculated using the same level of theory to confirm that the conformation has been found at a minimum local energy [18]. The wave function was calculated using the optimized Z matrix of each molecule; the input file for each molecule was generated using the B3LYP method. The ionic structures were determined using the theoretical model UB3LYP/6-31G. All analyses were performed with the

Gaussian package version 09. Then, the generated files provided the value of the energy for each of the structures to calculate the global reactivity indexes. Afterward, the charges of each atom in all the neutral molecules and the respective ions were calculated. Finally, the local reactivity indexes were calculated according to the formulae described. The electronic population for the calculation of Fukui functions was based on the formulation of the quantum theory of atoms in molecules.

2.3. Cell Culture and Treatment. Human cancer cell lines (HuH7 provided by Dr. Zentella Dehesa and HepG2 obtained from American Type Culture Collection, ATCC) were maintained in Dulbecco's Modified Eagle's Medium (DMEM; Gibco, 12800-017) containing 1% L-glutamine, 10% fetal bovine serum, 100 U/mL penicillin, and 100 μg/mL streptomycin in 5% CO_2 at 37°C. As a control, we used two human epithelial cell lines (HaCaT provided by Dr. Enrique Perez and THLE-3 obtained from ATCC) and primary hepatocytes of male rat Fischer-344 were isolated following the method described by Berry and Friend with modifications (1969). HaCaT cells were cultured under the same condition as that of cancer cells. THLE-3 cells were maintained in BEGM (BEGM Bullet kit; Lonza, C3170) on plates coated with type I collagen under the conditions recommended by ATCC. Cells were grown until they reached 70% confluence in specific medium supplemented with 10% FBS; then, the cells were starved for 12 hours with 2% FBS. Compounds were immediately added, and the cells were incubated for 12, 24, and 48 hours. The group without treatment was considered negative control (NC). We used an aqueous solution containing 0.2% dimethyl sulfoxide (DMSO) as the vehicle for the compounds. The optimal dose for quercetin (Q, Sigma-Aldrich, 32,782) was 50 mM, and that for 3′5′-dimaleamylbenzoic acid (C1) and 3′5′-dimaleimylbenzoic acid (C2) was 0.01 mM. The optimal dose of each compound was used for each of the combination treatments, with the compounds administered 30 minutes apart.

2.4. Cell Viability and Cell Cycle Assays. The effect of the treatments on the viability of cells was determined using the MTT (3-(4, 5-dimethylthiazol-2-yl)-2,5-diphenyl tetrazolium bromide, Thermo Fisher Scientific, M6494) assay. Briefly, ELISA plates with each treatment groups were washed with fresh culture medium and then incubated in fresh medium containing MTT (0.5 mg/mL) for 3 hours at 37°C. The MTT-containing medium was discarded, and the cells were incubated in DMSO to dissolve the formazan aggregates. The intensity of the product was read at 570 nm using an ELISA microplate reader. For cell cycle analysis by flow cytometry, the cells were washed with PBS and incubated at 37°C with 0.25% trypsin and inactivated by adding conditioned medium with 10% FBS. Subsequently, the cells were centrifuged at 1000g for 5 minutes, and the pellet was resuspended in 1x PBS. The suspension was centrifuged again under the same conditions, the supernatant was discarded, and the cell pellet was fixed with EtOH (−20°C) added dropwise with slow stirring. Subsequently, the samples were centrifuged, 1x PBS was added, and the cell pellet was dissociated by pipetting, and the mixture was centrifuged again. Finally, the supernatant was discarded, and the cell pellet was resuspended in the staining solution (176 μL of PBS, 4 μL of 10 mg/mL RNase and 20 μL of 1 mg/μL IP, 200 μL per sample) for 40 minutes at 37°C. Then, the cell cycle distribution was analyzed using a FACSCalibur system.

2.5. Fluorescent Staining and TUNEL Assay. After treatment, the cells were fixed with 4% paraformaldehyde at room temperature (RT) under gentle agitation. Subsequently, the cells were washed with 1x PBS and permeabilized with 0.1% Triton X-100-PBS. The cells were washed again with 1x PBS and stained with the nuclear fluorescent dye Hoechst (H3570 350/461) 1 : 5000 in 1x PBS for 5 minutes in the dark. It was washed, and the second fluorescent label phalloidin (Thermo Fischer, A12379) was added at 1 : 1000 in 1x PBS. The cells were washed again, and mounted with Vectashield mounting media on conventional slides. The samples were stored in a humid chamber at 4°C for no more than 2 weeks. They were finally observed under a confocal microscope. For TUNEL assay, cells were fixed with 4% paraformaldehyde at RT covered with aluminum foil with gentle shaking for 1 hour and subsequently washed with 1x PBS and permeabilized with 0.1% Triton X-100 and 0.1% sodium citrate with shaking for 2 minutes at 4°C. Then, the cells were washed with 1x PBS, and the reaction was carried out in accordance with the instructions of the manufacturer (In Situ Cell Death Detection (fluorescein), Sigma-Aldrich; 1,684,795). The samples were then incubated at 37°C in complete darkness for 1 hour and then washed with 1x PBS and stained with Hoechst nuclear fluorescent dye (H3570 350/461) at 1 : 5000 in 1x PBS for 5 minutes. The cells were washed with 1x PBS and mounted with Vectashield mounting media on conventional slides and stored in a humid chamber at 4°C for no more than 2 weeks. Finally, they were observed under a confocal microscope.

2.6. Immunoblotting. After the respective treatments, the cells were washed two times with 1x PBS, scraped, and lysed in RIPA buffer containing a cocktail of protease inhibitors. The cell lysates were centrifuged for 10 minutes at 16000g. The supernatant was collected, and the protein content in the samples was determined using Bio-Rad protein assay reagent (Bio-Rad, 500-0113-14-15). The samples were mixed with 2x sample buffer (100 Mm TRIS-HCL pH 6.8, 4% SDS, 0.2% bromophenol blue, 5% β-mercaptoethanol, and 20% glycerol) and boiled at 95°C for 5 minutes. Proteins from the samples were resolved on 10–12% SDS-PAGE gels and then transferred to PVDF membranes for immunoblotting analysis. The membranes were blocked in 5% nonfat dried milk or 1% BSA in PBS-t (PBS-0.1% Tween 20) for one hour. Then, the membranes were incubated with the respective primary antibodies (caspase-9, sc-8355; caspase-8, sc-7890; and caspase-3, cell signaling #9662) overnight at 4°C. After that, the membranes were washed and incubated with HRP-conjugated secondary antibodies for two hours at RT and developed using chemiluminescent solution (Millipore, WBKLSO100).

2.7. Migration Assay. Cells were pretreated with 12 μM mitomycin C to inhibit cell proliferation during the assay. Subsequently, a scratch was made on the cell layer with a 200 μL micropipette tip. Cells were washed with 1x PBS, and DMEM without fetal bovine serum was added with the appropriate compounds corresponding to each of the treatment groups. The cells were incubated at 37°C with 5% CO_2 for 24 and 48 hours, washed with 1x PBS, and fixed with 4% paraformaldehyde. Subsequently, the cells were stained with 0.5% violet crystal. The cells were then washed again with 1x PBS to remove excess dye.

2.8. Measurement of Reactive Oxygen Species and Glutathione Levels. The ROS assay was performed as described earlier (Chandel et al. [20]). Briefly, approximately 10,000 cells were seeded in 96-well plates in DMEM with 10% FBS and incubated at 37°C in 5% CO_2 until they reached 80% confluence. The cells were then washed with Hank's saline solution (HBSS 1X) and cultured with 2% FBS for 12 hours. After serum starvation, they were again washed with 1X HBSS and conditioned medium with 2% SFB was added with the compounds corresponding to each of the study groups, and the cells were incubated for 24 hours. Subsequently, they were washed, and DCFDA working solution was added for 30 minutes at 37°C. Then, the fluorescence of DCFDA was measured using a Fluoroskan Ascent (Thermo Electron Corporation) fluorometer at ʎex: 480 nm and ʎem: 515 nm. The data were analyzed using GraphPad Prism. For the determination of glutathione concentration, cells were washed with Hank's saline solution and starved in DMEM with 2% FBS for 12 hours, followed by the corresponding treatments for 24 hours. Then, the cells were washed with Hank's saline solution. Trypsin was then then added for specific times for each type of cell line. Protein extraction from each of the experimental groups was then performed. The cell pellets were suspended in FEDTA (phosphate-buffered EDTA; 0.1 M monobasic sodium phosphate, 0.005 M EDTA pH 8.0) plus 25% phosphoric acid, followed by centrifugation at 16000g for 30 minutes. For the determination of reduced glutathione, 125 μL of the above supernatant was taken and mixed with 1125 mL FEDTA, and 25 μL was taken and mixed with 450 μL of FEDTA and 25 μL of O-phthaldialdehyde. For the determination of oxidized glutathione, 125 μL of the above supernatant was taken and suspended in 50 μL of 0.04 M N-ethylmaleimide and incubated for 30 minutes at RT. Subsequently, 1.07 mL of 0.1 N NaOH was added, and 25 μL of the above mixture was added to it with 450 μL of NaOH plus 25 μL of O-phthaldialdehyde. This was mixed and left at RT for 15 minutes in complete darkness. The results were obtained using a fluorometer at ʎex: 350 nm and ʎem: 420 nm. The data were analyzed using GraphPad Prism.

2.9. Statistical Analysis. The data were expressed as the mean ± SEM for each analysis. Statistical analyses were performed by one-way ANOVA and Tukey's multiple comparison tests using GraphPad Prism 7.0 software. Values were considered significant when $P < 0.05$.

3. Results

3.1. In Silico Analysis and In Vitro Assay of the Compounds. After completion of the synthesis of maleic anhydride derivatives, they were identified using infrared spectroscopy and ^{1}H nuclear magnetic resonance spectrometry, where the displacements exhibited a clear correspondence between the spectra and the composition and structure of the molecules, indicating a purity of 99%: C1, IR (ATR, cm-1) ύ: 3281.6 (NH), 1702.91 (C=O), 2800 (C-H, aromatic), C=C (1625.5) and ^{1}H NMR (CDCl3, 400 MHz) δ 10.80 (s, H-NH), 8.30 (s, H-6), 7.97 (s, H-2′), 7.97 (s, H-4′), 6.32 (dd, H-2), 6.42 (dd, H-3), C2, IR (ATR, cm-1) ύ: 1722.8 (C=O), 3100 (C-H, aromatic), C=C (1600) and ^{1}H NMR (CDCl3, 400 MHz) δ 7.66 (s, H-6), 7.99 (s, H-2′), 7.99 (s, H-4′), 7.59 (s, H-3), 7.59 (s, H-4).

In maleic anhydride derivatives, there are two places in each molecule that are susceptible to nucleophilic attack—the carbonyl carbon (by 1,2-addition) and the olefinic carbons (by Michael 1,4-addition), which are both electrophiles. However, the susceptibility of these carbons depends on their chemical softness or hardness. We carried out theoretical calculations in order to explore susceptibility, including global and local reactivity and consequent selectivity. In Figure 1(a), the geometric optimization is schematized under the same level of theory B3LYP/6-31G for compounds C1, C2, and Q. Chemical-quantum descriptors enable us to know the nucleophilic or electrophilic nature of a molecule globally or locally on a relative scale [96, 97 g]. The energies corresponding to the ionic structures (anion and cation) were calculated under the same level of theory using the UB3LYP/6-31G basis to prevent spin contamination (Figure 1(b)). The global parameters described are chemical potential (μ (eV)), donor potential μ^- (eV), acceptor potential μ^+ (eV), global hardness η (eV), global softness S (1/eV), electrophilicity index ω (eV), electron-donating power ω^- (eV), and electron-accepting power ω^+ (eV). GSH has a higher chemical potential, while the maleic anhydride derivatives have lower chemical potential. These results enabled us to predict that the electrons flow from GSH to α, β-unsaturated compounds, which is confirmed by the donor and acceptor potential where the electron flow occurs. For the case of Q, there was no representative difference in μ (eV) with respect to GSH. According to the hardness, η, interpretation, within the context of DFT, higher values of η indicate harder molecules, which are less reactive. GSH has a η value of 4.39, whereas C1, C2, and Q have values of 3.01, 3.39, and 3.37, respectively. Therefore, GSH is harder than the molecules studied. Likewise, the values of global softness, calculated as half of the reciprocal of hardness, show the same results as those of the hardness. In other words, lower softness corresponds to greater hardness. The results regarding the electrophilic index clearly show that the molecules C1, C2, and Q have values of 3.41, 3.84, and 1.97 s_x^+, respectively, maintaining an electrophilic behavior compared with the value of GSH. Electron-donating power and electron-accepting power are measurements of the ability of a chemical system to donate or accept a small fraction of the charge, respectively. The compounds C1, C2, and Q are acceptors, whereas

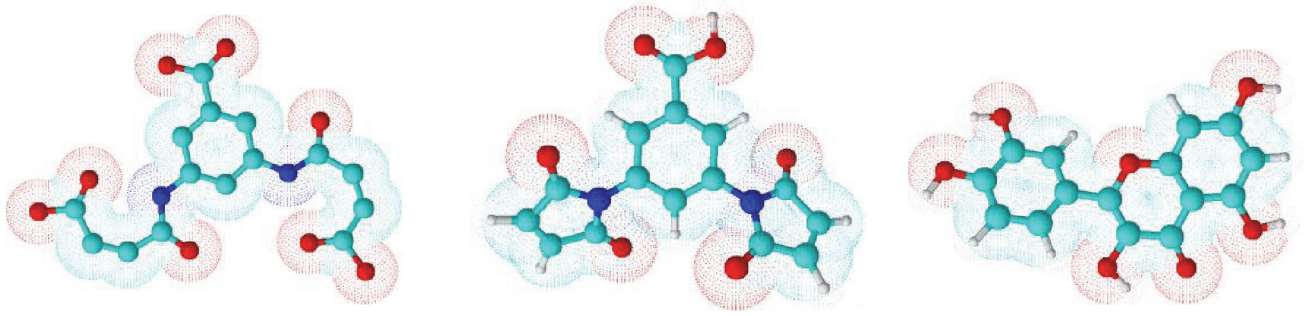

C1 C2 Q

(a)

Compounds	μ (eV)	μ^- (eV)	μ^+ (eV)	η (eV)	S (1/eV)	ω (eV)	ω^- (eV)	ω^+ (eV)
C1	−4.5433	−6.0523	−3.0343	3.0180	0.1657	3.4198	6.0687	1.5254
C2	−5.1062	−6.8024	−3.4100	3.3923	0.1474	3.8430	6.8201	1.7139
Q	−3.6495	−5.3369	−1.9620	3.3749	0.1482	1.9732	4.2198	0.5703
GSH	−3.6253	−5.8221	−1.4286	4.3936	0.1138	1.4957	3.8576	0.2322

(b)

C1

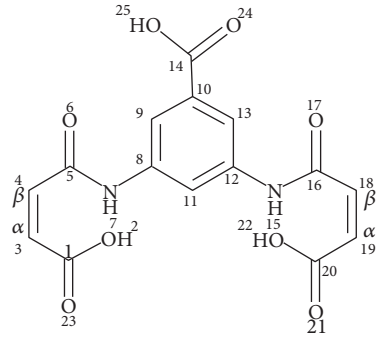

C2

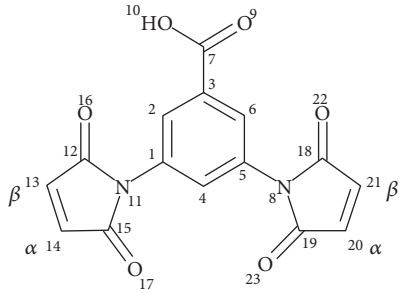

GSH

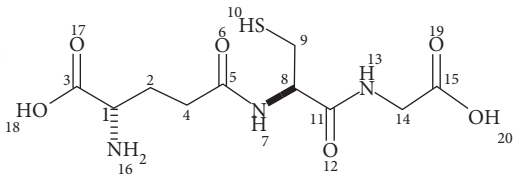

(c)

Local softness s_x^+		Local softness s_x^-
C=C	C=O	group SH
C1 C_3-C_4 0.0056	C1 C_5-C_{16} 0.0019	GSH S_{10} 0.0246
C2 C_{13}-C_{14} 0.0066	C2 C_{12}-C_{15} 0.0046	

(d)

Figure 1: In silico analysis. (a) Geometric optimization of 3′5-dimaleamylbenzoic acid, C1, 3′5-dimaleimylbenzoic acid, C2, and quercetin, Q. (b) Global chemical and quantum reactivity descriptors: chemical potential, μ^- (eV); donor chemical potential, μ^- (eV); and acceptor potential, μ^+ (eV); global hardness, η (eV); global softness (1/eV); electrophile index, ω(eV); electron-donating power, ω^- (eV); and electron-accepting power, ω^+ (eV) under the same theory level B3LYP with the 6-31G basis. (c) IUPAC-based numerical assignment. (d) Local softness, s_x^+, of olefinic carbons and carbonyl carbon of C1 and C2 versus local softness, s_x^-, of the sulfur atom (S) of glutathione (GSH) assessed using Fukui condensed function.

the GSH molecule is a donor. The chemical structures for the compounds C1, C2, and Q are represented in Figure 1(c). In the local softness analysis, the olefinic carbons of C1 and C2 are more susceptible to thiol attack than the carbonyl carbons because they are highly electrophilic. On the other hand, the thiol group of GSH has a local softness, s_x^-, value of 0.024 at the sulfur atom (S) corresponding to the sulfhydryl group (SH), which has a nucleophilic behavior, so it can be an electron donor. Sulfur is the most suitable atom to carry out this attack against the olefinic carbons of C1 and C2, as it is a soft nucleophile (Figures 1(c) and 1(d)).

3.2. Synergistic Effects of the Combination of C1 and C2 with Q on Cell Viability. One of the principal traits of cancer cells is their ability to sustain proliferation. The viability of cultured cells can be determined by the MTT assay. Metabolically active cells reduce the pale yellow tetrazolium salt (MTT) to purple-colored formazan. The absorbance of formazan correlates directly with the number of viable cells. Cytotoxic effects of Q, C1, and C2 were clearly observed in HuH7 and HepG2 at 12 hours after treatment (data not show). The results at 24 and 48 hours posttreatment indicated significantly higher toxicity in all the cancer cell lines tested. C1 had the strongest effect by itself with a 66.19% reduction in HuH7 cells and 80.2% in HepG2 cells at 48 hours (Figures 2(c) and 2(d)). The effect of the combination of Q with prooxidant compounds was not significantly different from the effect of each treatment alone. However, when the prooxidant compounds were administered prior to quercetin, the antiproliferative effect was significantly different (Figures 2(e) and 2(f)). The greatest effect was observed at 48 hours for the HepG2 cells. Interestingly, the C1 + Q treatment was the most effective combination exhibiting a reduction of 80.3% and 90.1% in the number of HuH7 and HepG2 cells, respectively, at 48 hours posttreatment (Figures 2(c) and 2(d)). The noncancerous human hepatocytes and epithelial cells, as well as the primary culture of hepatocytes from healthy rats, did not show significant changes at 12 and 24 hours posttreatment (data not shown). Subtle changes in HaCaT (Q and C2 + Q groups) and HepG2 (Q, Q + C1, and Q + C2 groups) cells were observed at 48 hours posttreatment (Figures 2(g) and 2(h)). The primary culture of hepatocytes was more sensitive to Q, Q + C1, and Q + C2 (Figure 2(i)). It is important to note that the most effective treatments (C1 + Q and C2 + Q) against the cancer cell lines did not have a significant toxic effect on noncancer cell lines in terms of compromised cell viability.

3.3. Synergistic Induction of S Phase Arrest during Cell Cycle Progression by the Combination of C1 and C2 with Q. Cancer cells have the capability to continually respond to positively acting growth stimulatory signals. HuH7 and HepG2 cells were subjected to flow cytometric analyses following treatment. The results showed an S phase arrest following 24 hours of Q + C2, C1 + Q, and C2 + Q treatments in both cell lines (Figure 3). Quercetin by itself induced cell cycle arrest at the G0/G1 phase with 68.49% and 63.01% arrested HuH7 and HepG2 cells, respectively (Figure 3(b)). Additionally, C1 treatment induced G0/G1 phase arrest during cell cycle progression. The greatest effect was induced by treatment with C1 + Q, C1 + Q, and Q + C2 ($P < 0.0001$) with a 100% decrease in the fraction of cells in G2/M phase. Thus, the results show that the compound by themselves induce cell cycle arrest at G0/G1 phase, and in combination, the compounds arrest cells at S phase.

3.4. Effects of the Combination of C1 and C2 with Q on ROS Generation and Oxidative Stress. To evaluate the possible cytotoxic effects of the combination of C1 and C2 with Q on the extent of oxidative stress, ROS generation and redox state of glutathione were determined by fluorometric analysis. Cancer cells subjected to the antioxidant treatment (Q) exhibited significantly reduced ($P < 0.0001$) ROS levels of 73.1% and 68.9% in HuH7 and HepG2 cells, respectively (Figure 4(a)). Treatment with Q + C1 and Q + C2 had a weak effect on decreasing the ROS levels in both cell lines. Treatment with the prooxidants (C1 and C2) increased ROS levels by 38.9% and 75.26%, respectively, in HuH7 cells. The compounds had a similar effect on HepG2 cells. Treatment with Q in combination with the prooxidant compounds tended to decrease ROS levels in both cell lines. The results show that the combination of the prooxidant compounds followed by quercetin increases the level of ROS. The antioxidant effect of quercetin was clearly demonstrated by the redox state of GSH, as there was a significant increase in the level of reduced glutathione and the GSH/GSSG index in addition to a decrease in the level of oxidized glutathione in both cell lines. Compounds C1 and C2 decreased the levels of reduced and oxidized glutathione by decreasing the GSH/GSSG index as well as the de novo synthesis of glutathione in both cell lines (Figure 4(b)). The application of quercetin followed by the oxidative compounds did not result in significant changes in the levels of reduced and oxidized glutathione in the HuH7 cells. However, the same treatments in the HepG2 line increased the level of reduced glutathione and the de novo synthesis of glutathione. In addition, when the prooxidant compounds were administered first, followed by treatment with quercetin, a significant decrease was observed in the levels of reduced and oxidized glutathione as well as in the de novo synthesis of glutathione and the GSH/GSSG index. These results demonstrate the modification of the redox state by prooxidant treatments and the effect of quercetin when it is administered before or after oxidative compounds.

3.5. Synergistic Effects of the Combination of C1 and C2 with Q in Cytoskeletal Actin and Nuclear Morphology. Cancer cells are known to be exceptionally resistant to apoptosis. Hoechst H3570 is often used to distinguish condensed pyknotic nuclei in apoptotic cells, as it has the ability to easily cross the cell membrane due to its lipophilic nature. Actin was stained with phalloidin A12379 to observe if there were any changes. We observed nuclear condensation in all experimental groups at 24 hours posttreatment (Supplementary Material 1A and 1B available online at https://doi.org/10.1155/2017/2734976). The degradation of actin and DNA was observed mainly in the groups treated with combinations, and a stronger effect was observed on the HepG2 cells (Figure 5). At 48 hours posttreatment, we

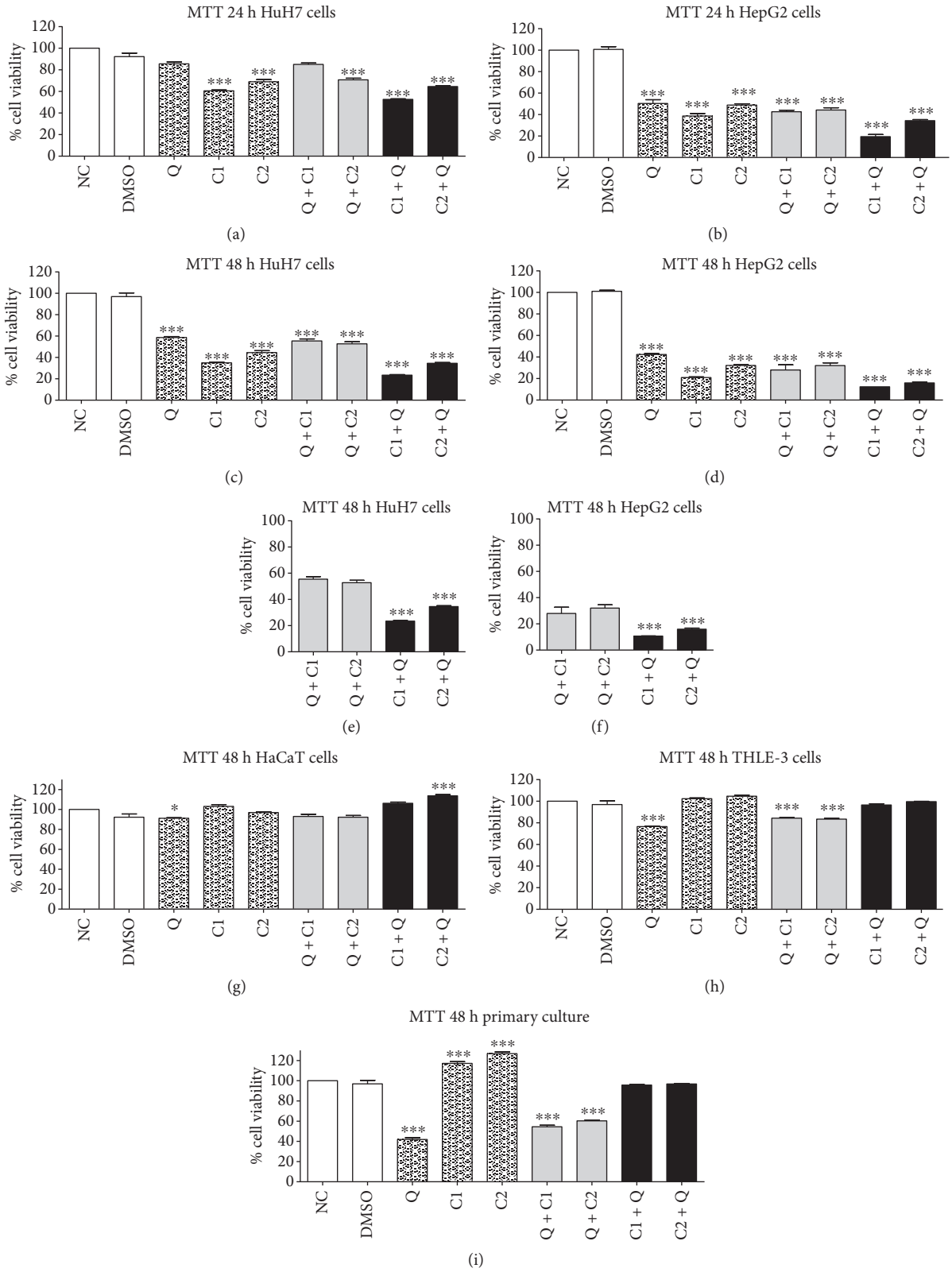

Figure 2: Effect on the viability of human liver cancer cells determined using MTT assay. (a), (c) HuH7 cells, (b), (d) HepG2 cells at 24 and 48 hours posttreatment. Effect on the viability of noncancerous human epithelial cells. (g) HaCaT cells, (h) THLE-3 cells, (i) primary culture of Fischer-344 rat hepatocytes at 48 hours posttreatment. (e), (f) Significant differences of the pleiotropic synergistic effect on cancer cells by Q + C1 and Q + C2 versus C1 + Q and C2 + Q. All data are presented as the mean ± SEM of 4 experiments; statistical evaluations were performed using Tukey's one-way ANOVA to obtain significant differences ($^{*}P < 0.05$, $^{***}P < 0.001$) with normalization based on the vehicle group. NC, normal control; DMSO, vehicle; Q, quercetin; C1, 3′5-dimaleamylbenzoic acid; C2, 3′5-dimaleimylbenzoic acid.

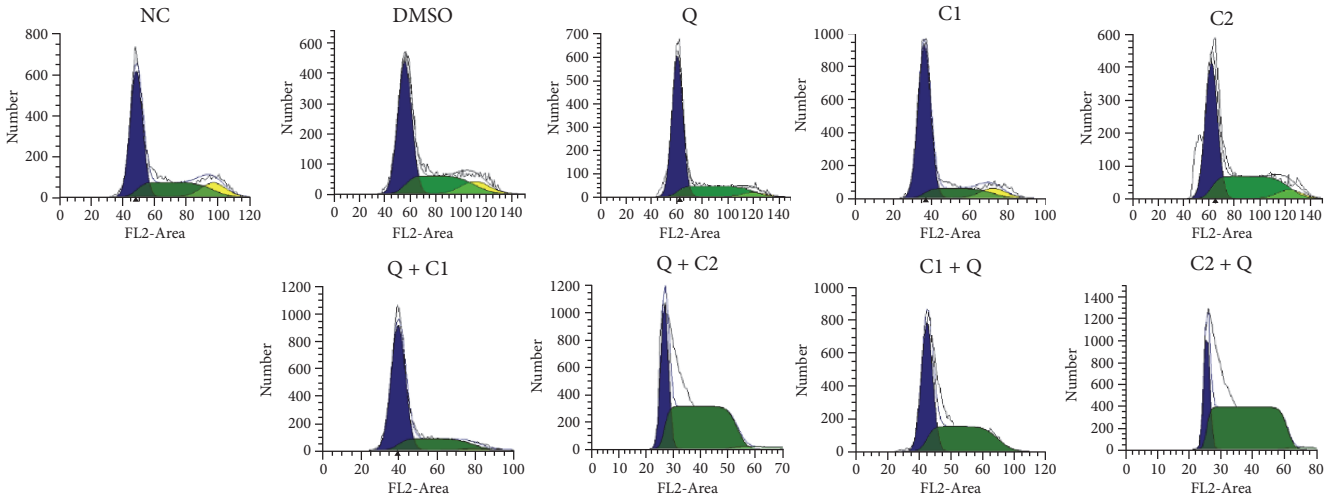

(a)

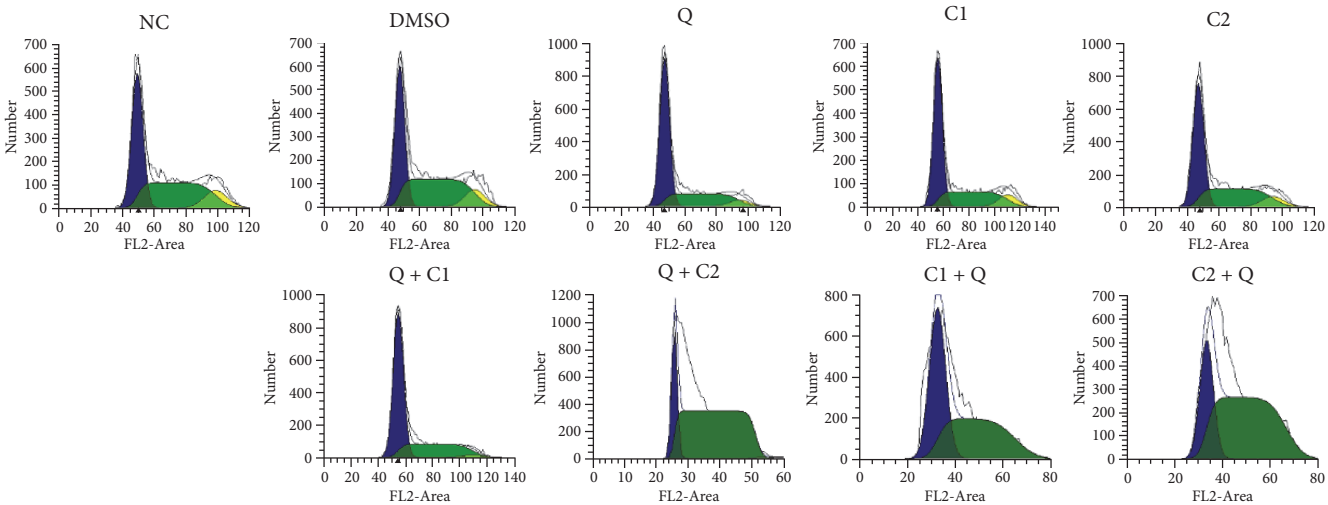

(b)

	HuH7			HepG2		
Groups	G0/G1	S	G2/M	G0/G1	S	G2/M
NC	57.30	30.98	11.72	44.61	44.63	10.75
DMSO	56.50	31.10	12.40	43.92	44.75	11.34
Q	68.49***	27.36	4.14***	63.01***	31.64	5.34***
C1	71.34***	19.49	9.17***	57.73***	32.37	9.89***
C2	51.50	36.68***	9.81***	51.65***	39.76	8.59***
Q + C1	71.38***	27.66	0.96***	65.82***	33.18	0.99***
Q + C2	31.91	68.09***	0.00***	20.10	79.90***	0.00***
C1 + Q	51.01	48.99***	0.00***	49.82	50.18***	0.00***
C2 + Q	40.01	59.99***	0.00***	29.20	70.80***	0.00***

(c)

Figure 3: Cell cycle progression by flow cytometry in cells. (a) HuH7 and (b) HepG2 cells at 24 hours posttreatment; (c) treatment with Q, C1, C2, and Q + C1 arrests cells in the G0/G1 phase of the cell cycle, and treatment with Q + C2, C1 + Q, and C2 + Q arrests cells in the S phase of the cell cycle; the G2/M phase is affected by all treatments. All data are presented as the mean ± SEM of 4 experiments; statistical evaluations were performed using Tukey's one-way ANOVA to obtain significant differences (***$P < 0.001$) with normalization based on the vehicle group treated with DMSO.

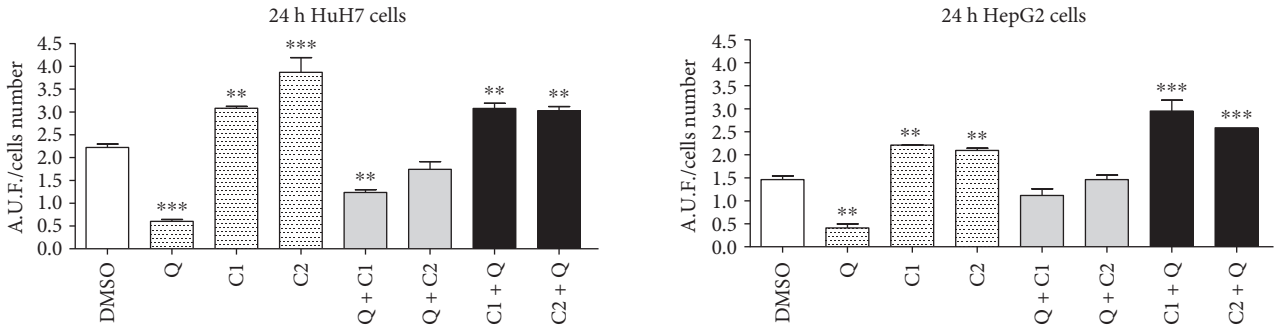

(a)

Groups	HuH7				HepG2			
mmol/mg Cell protein	GSH	GSSG	GSH + GSSG	GSH /GSSG	GSH	GSSG	GSH + GSSG	GSH /GSSG
DMSO	2.08	0.90	2.91	0.68	1.98	0.98	2.97	0.66
Q	2.29**	0.73**	3.02	0.75***	2.42***	0.80**	3.22**	0.75***
C1	1.13***	0.62***	1.75***	0.64*	1.21***	0.71***	1.93***	0.62
C2	1.31***	0.50***	1.82***	0.72	1.40***	0.56***	1.97***	0.71
Q + C1	2.22	0.95	3.18*	0.69	2.33***	1.03	3.36***	0.69
Q + C2	2.16	0.84	3.01	0.71	2.25***	0.92	3.18**	0.70
C1 + Q	0.88***	0.63***	1.52***	0.58***	0.94***	0.71***	1.66***	0.56***
C2 + Q	0.93***	0.68***	1.61***	0.57***	1.02***	0.76***	1.78***	0.57***

(b)

Figure 4: Effect of the treatments on ROS production assessed from the oxidation of DCFDA by hydrogen peroxide using fluorometric assay on HuH7 and HepG2 cells at 24 hours posttreatment; (b) determination of GSH and GSSG levels by fluorometric assay per mmol/mg protein at 24 hours posttreatment in HuH7 and HepG2 cells. All data are presented as the mean ± SEM of 3 experiments; statistical evaluations were performed using Tukey's one-way ANOVA to obtain significant differences ($^{*}P < 0.05$, $^{**}P < 0.01$, and $^{***}P < 0.001$) with normalization based on the vehicle group treated with DMSO.

found more marked morphological change characteristic of apoptosis, with the treatment with C1 followed by quercetin being the most efficient (Figure 6). The apoptotic effect of the single administration of C1 was not significantly different in terms of toxicity in comparison to that observed when it was combined with quercetin (Supplementary Material 1). No effect was observed on cytoskeletal actin and nuclear morphology when quercetin was administered alone. The cell line HepG2 was the most susceptible to the apoptotic effects of the treatments.

3.6. Anticarcinogenesis Treatment Induces Apoptosis. The number of pyknotic nuclei (which correspond to fragmented DNA) were quantified at 24 and 48 hours posttreatment (Figures 7(a), 7(b), 7(c), 7(d), 7(e), and 7(f); Supplementary Materials 1E–H). There were statistically significant changes ($P < 0.001$) in most groups; the highest number of pyknotic nuclei was observed in the C1 + Q (48.3%) and C2 + Q (44.22%) treatment groups at 24 hours posttreatment, with an average of 75.1% in HuH7 cells at 48 hours posttreatment (Figures 7(a) and 7(c)). We observed the strongest effect in the HepG2 cells in response to C1 + Q (89.13) and C2 + Q (84%) at 24 hours posttreatment (Figures 7(b) and 7(d)). In general, single treatment with C1 was the most effective in inducing pyknotic nuclei with the maximum effect at 48 hours posttreatment (Supplementary Materials 1G and 1H). No significant changes were observed for each of the treatment groups at 12 and 24 hours in the noncancerous human cells that were stained with Hoechst and phalloidin. However, after prolonged exposure and starvation for more than 48 hours, some pyknotic nuclei were observed in the control cells. Figures 7(e) and 7(f) represent the quantified results for the apoptotic nuclei at 24 and 48 hours posttreatment, and the effect was minimal in the control groups. The number of cells positive for TUNEL (cells stained in green) was increased in response to treatment with C1 + Q and C2 + Q compared to those in response to the treatment with each of the compounds alone at 24 hours after treatment. This same behavior was observed at 48 hours posttreatment; however, the number of living cells was already lower at that time point than at 24 hours, which is why the number of fragmented nuclei was smaller. This assay demonstrated that the administration of the compounds individually leads to a lower extent of cell death.

3.7. Synergistic Effects of the Combination of C1 and C2 with Q on Activating the Intrinsic Pathway of Apoptosis. To determine the mechanism of apoptosis induced by the administration of C1 and C2 in combination with Q, Western blotting was performed. Cell lysates were prepared and analyzed for caspase-8, caspase-9, and caspase-3 expressions at 12, 24, 36, and 48 hours posttreatment. The results showed an increase in the level of procaspase-9 in all groups posttreatment (Figures 8(a), 8(b), 8(c), and 8(d)). The cleavage of

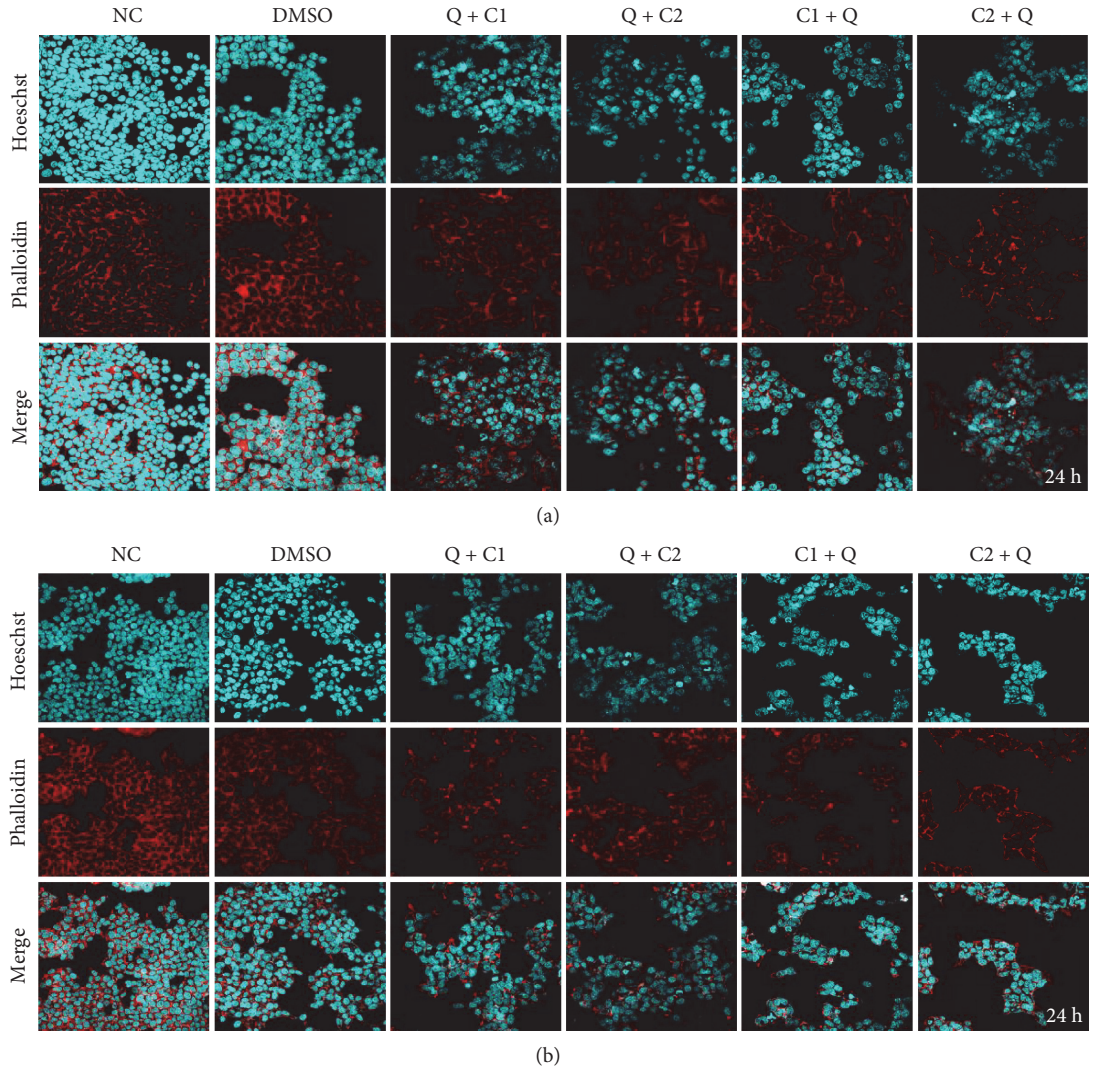

Figure 5: Synergistic effects of C1 and C2 in combination with Q on cytoskeletal actin and nuclear morphology in human liver cancer cells (a) HuH7 and (b) HepG2 at 24 hours posttreatment. Hoechst nuclear staining is shown in cyan, and F actin staining by phalloidin is shown in red at a magnification of 40x.

caspase-9, an apoptotic marker, increased in all treatment groups, although the highest level was observed in the C1 + Q- and C2 + Q-treated HuH7 cells, and C2 + Q also strongly activated caspase-9 in HepG2 cells at 24 hours posttreatment (Figures 8(e) and 8(f)). The level of activated caspase-3 was confirmed in all treatment groups, although the highest level was observed in the C1 + Q and C2 + Q treatments in both cell lines at 36 h posttreatment (Figures 8(g), 8(h), 8(i), and 8(j)). The expression of procaspase-8 was observed from 12 hours onwards posttreatment in all experimental groups, and active caspase-8 was not observed (data not show).

4. Discussion

Hepatocellular carcinoma (HCC) is one of the most common causes of cancer-related death worldwide [21]. Similar to other types of cancers, HCC arises from a multistep and multifactorial process. Different risk factors determine the progression of HCC malignancy, and treatments are not efficient when it is detected. Although the relationship is not clear, diet has an important role in the development of HCC [22, 23]. This has led to the use of chemopreventive substances as alternative treatments. Antioxidants in the diet, such as flavonoids contained in several fruits and vegetables, have been used in animal models to show beneficial effects against liver tumors to induce apoptosis, and they have been shown to cause death in cancer cell lines [22, 24, 25]. Quercetin, a flavonoid widely studied as a chemopreventive agent in different types of cancer, is considered an excellent antioxidant [25]. It has been proven that quercetin inhibits metabolic activities and induces cell death by apoptosis in HCC cell lines such as HepG2, HuH7, and Hep3B2 [26]. Additionally, quercetin has been associated with the inhibition of enzymes that activate carcinogens and the suppression of key signal transduction pathways and receptor interactions. However, several studies have indicated that the anticancer activities and efficacy of quercetin can be further enhanced

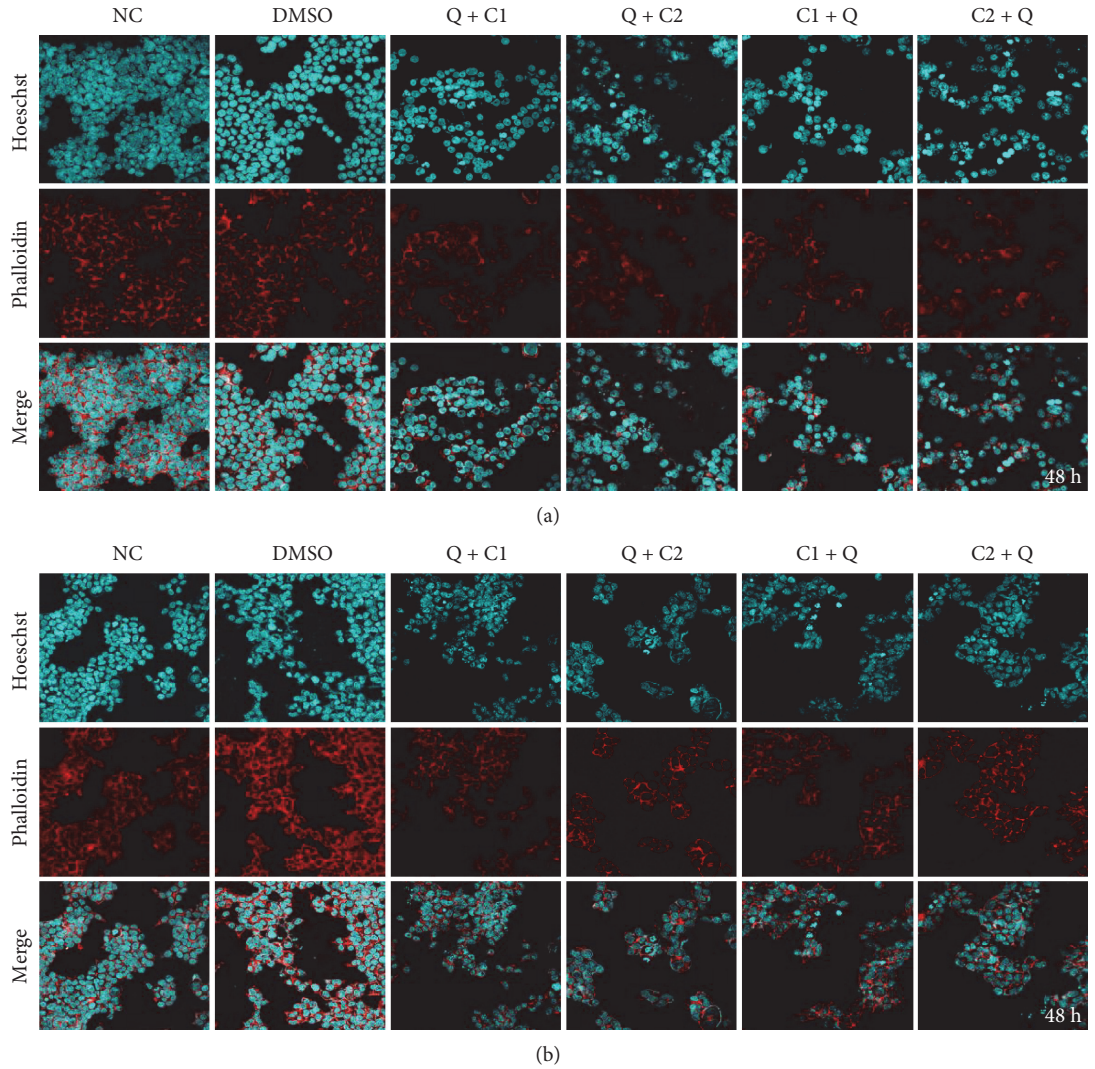

Figure 6: Synergistic effect of the combination of Q with C1 and C2 versus C1 and C2 with Q on cytoskeletal actin and nuclear morphology in (a) HuH7 and (b) HepG2 cells at 48 hours posttreatment. Hoechst nuclear staining is shown in cyan, and F actin staining by phalloidin is shown in red at a magnification of 40x.

by combining it with other compounds [27–29]. The discovery of new drugs and novel therapeutic approaches for hepatocellular carcinoma opens the possibility of developing more effective strategies against various human cancers. In this regard, maleic anhydride derivatives have been shown to have anti-inflammatory and antiproliferative effects and to interfere with different cellular signaling pathways that depend on the availability of reduced thiols [30].

For the first time, our study demonstrates the cytotoxic effects of maleic anhydride derivatives (C1 and C2) on HuH7 and HepG2 cells (Figure 2). C1 and C2 can synergize with quercetin to inhibit cell viability. Additionally, we demonstrate the cancer preventive effect of quercetin and show that even when administered alone, C1 and C2 can exert cytotoxic effects on HuH7 and HepG2 cells at 24 and 48 hours after treatment. C1 and C2 were more cytotoxic against tumor cells compared to quercetin. The maximum of cytotoxic effect was observed when the compounds C1 and C2 were administered before quercetin. Interestingly, this effect was not observed in noncarcinogenic cell lines. These results suggest the selectivity of antitumor effect exerted by the compounds and indicate the possibility of a treatment approach that does not result in harmful effects on normal cells. However, the ability of quercetin to avert damage to normal cells has been previously reported [31]. The primary culture of hepatocytes was more sensitive to quercetin and the rest of the agents, except for the combinations C1 + Q and C2 + Q until 48 hours posttreatment. The noncancerous cells HaCaT and THLE-3 cells did not display drastic cytotoxic effects after 48 hours of treatment. Extensive studies have been conducted to determine the optimal antitumor dose of quercetin and other flavonoids, and the experimental results indicate that cell viability is inhibited by quercetin in a time- and dose-dependent manner [13, 32]. We observed that the combination of maleic anhydride derivatives followed by quercetin decreased cell viability with a specific and almost selective effect on tumor cells.

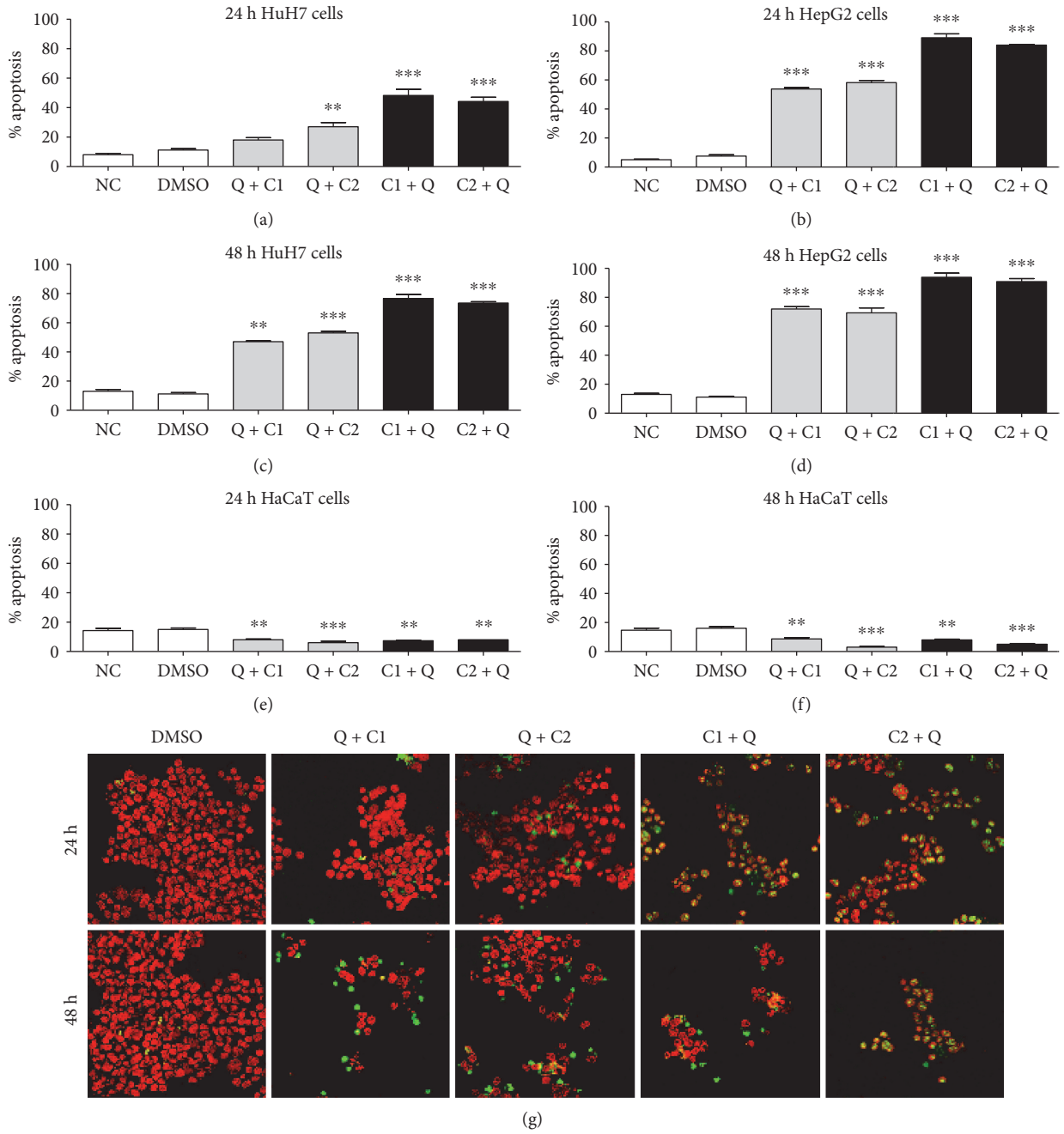

Figure 7: Quantification of pyknotic nuclei by staining with Hoechst in cells (a), (c) HuH7 cells, (b) (d) HepG2 cells, and (e), (f) HaCaT cells at 24 hours and 48 hours posttreatment. All data are presented as the mean ± SEM of 3 experiments; statistical evaluations were performed using Tukey's one-way ANOVA to obtain significant differences ($^{**}P < 0.01$, $^{***}P < 0.001$) with normalization based on the vehicle group treated with DMSO. (g) TUNEL assay in HepG2 cells; nuclear staining of Hoechst is shown in red, and TUNEL is shown in green at a magnification of 40x.

The transformation changes occurring during carcinogenesis include the ability to respond to growth factors and produce mitogenic signals [33]. The progression of the cell cycle implies a sequential activation of CDKs. To test the mechanism of antitumor effect in this respect, we analyzed cell cycle progression. Our data in HuH7 and HepG2 cells revealed that treatment with Q + C2, C1 + Q, and C2 + Q resulted in S phase arrest concomitantly with a reduction in the proportion of cells in the G2/M phase. Individual treatment with Q and C1 and combined treatment with Q + C1 induced arrest in the G0/G1 phase. A similar G0/G1 phase arrest by quercetin has been observed in HL-60, U937, and OE33 cells, resulting in caspase-dependent cell death [12, 34, 35]. These results demonstrate specific responses depending on the administration schedule of the compounds and the type of cells used. Quercetin induces cytotoxicity in cancer cell lines in a dose-dependent manner and activates the mitochondrial pathway of apoptosis [36].

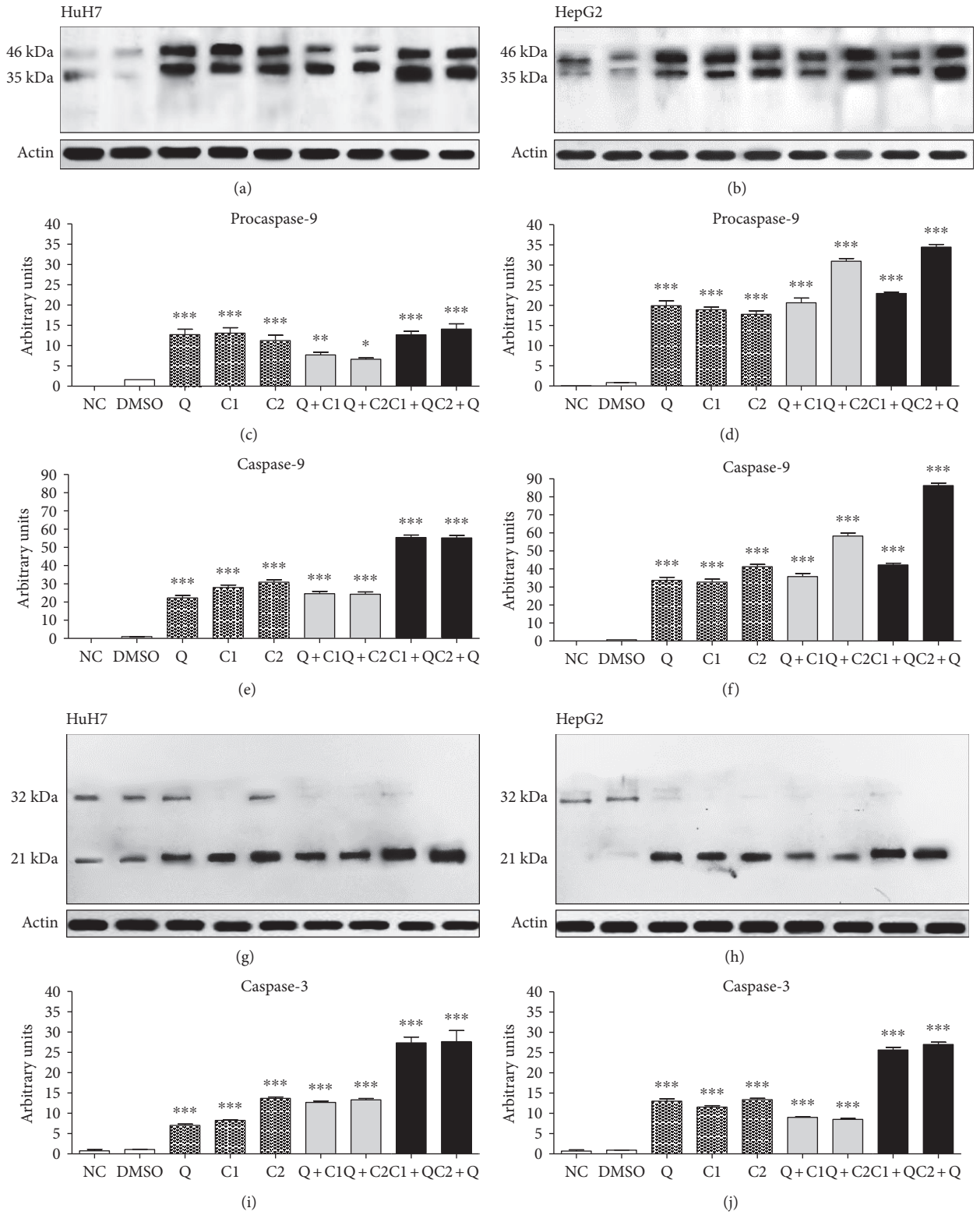

Figure 8: Activation of the intrinsic pathway of apoptosis after the effect induced by individual and combination treatments. Expression of procaspase-9 at 46 kDa and activation of caspase-9 at 35 kDa in (a) HuH7 and (b) HepG2 cells at 24 h posttreatment. Expression of procaspase-3 at 32 kDa and activation of caspase-3 at 21 kDa were observed at 36 hours posttreatment in (g) HuH7 and (h) HepG2 cells. For all cases, actin was used as a control of protein loading. (c), (d), (e), (f), (i), and (j) graphs corresponding to the colorimetric quantification by ImageJ. All data are presented as the mean ± SEM of 4 experiments; statistical evaluations were performed using one-way ANOVA with Tukey's test to obtain significant differences ($^{*}P < 0.05$, $^{**}P < 0.01$, and $^{***}P < 0.001$) with normalization based on the vehicle group treated with DMSO.

In leukemic cell lines, quercetin induces S phase arrest during cell cycle progression in a dose-dependent manner, although Nalm6 cells exhibit maximum sensitivity to the cytotoxic effects of quercetin at relatively low doses (10 μM). Breast cancer cell lines display limited sensitivity to quercetin; in T47D cells IC50 value was 160 μM [36]. Quercetin was shown to induce cytotoxicity and lead to G2/M phase arrest in a dose-dependent manner in ovarian cancer cells. The G2/M phase arrest increased after treatment with 100 μg/mL quercetin aglycone [37]. Interestingly, when quercetin was tested in ovarian cancer cells, the cells showed much less sensitivity, and at high doses of quercetin, the viability of normal ovarian cells was not significantly affected [32].

Cancer cells generate ROS due to their increased requirement for ATP; the imbalance between antioxidants and prooxidants results in oxidative stress that eventually promotes cell death [38]. However, due to deregulated redox balance, cancer cells escape programmed cell death regardless of the persistently higher ROS, in a more efficient manner than normal cells, while the higher intracellular levels of reduced glutathione promote cell survival in tumors. Additionally, anticancer drugs have been shown to exert apoptotic effects based on GSH depletion [39]. Our results showed that treatment of HuH7 and HepG2 cells with C1, C2, C1 + Q, and C2 + Q results in an increase in ROS levels and concomitant decrease in GSH. The combination of maleic anhydride derivatives and quercetin has a greater effect on the GSH/GSSH index. The *in vitro* analysis of maleic anhydride derivatives clearly showed a selective reaction with the thiol group of glutathione [18]. Our findings show that C1 and C2 decrease the levels of reduced glutathione in HuH7 and HepG2 cells. According to the results of our in silico analysis, maleic anhydride derivatives are electron acceptors and therefore have an electrophilic behavior. In addition, the oxidative effects of C1 and C2 are limited by quercetin. When quercetin is administered before the maleic anhydride derivatives, the depletion of ROS and reduced glutathione by C1 and C2 is restricted. However, the combination of maleic anhydride derivatives and quercetin resulted in a greater decrease in the level of reduced glutathione. Surprisingly, with this combination and order of administration, high ROS levels were observed despite the presence of quercetin. According to the results obtained, it is possible to conclude that changes in glutathione and ROS levels might account for the greater antitumor effect of the administration of C1 and C2 before quercetin. Quercetin and its potentially toxic oxidation products (semiquinone and quinone radicals) exert prooxidant effects within cells as a consequence of persistent exposure to persistent high ROS levels, and these radicals, with high reactivity toward thiols, react with GSH [24, 40, 41]. The other ways in which quercetin acts as a prooxidant may be by altering ROS metabolism due to the decrease in intracellular GSH or by downregulating heat shock protein (Hsp)-90 and inhibiting TRX reductase.

Since GSH is one of the main cellular free radical scavengers in addition to thioredoxin family members, a high glutathione index indicates redox balance and appropriate intracellular redox homeostasis. ROS are implicated in cell invasion and migration. Further, we show that antitumor compounds inhibit the migration of HuH7 and HepG2 cells (Supplementary 2A and 2B). It has been shown that quercetin can prevent cell migration and epithelial-mesenchymal transition by suppressing the expression of N-cadherin and vimentin in prostate cancer cell lines with no cytotoxic effect on normal prostate epithelial cells. The combination of antioxidants has shown potent and significant induction of apoptosis and suppression of cell proliferation, MMP secretion, cell invasion, cell migration, and angiogenesis. Similarly, quercetin has been shown to synergize with epigallocatechin gallate to inhibit stemness, invasion, and migration of prostate cancer cells [29].

Our results, therefore, show that concomitant effects of maleic anhydride derivatives and quercetin in HCC cell lines induced cytotoxicity by a deregulation in the adaptive stress responses (ROS increase and diminish reduced glutathione) reflected in cell cycle arrest at S phase. To confirm that the cytotoxicity effects induced by treatment with antitumor agents resulted in apoptosis, Hoechst staining and TUNEL assay were performed. Our data have validated the apoptotic effects of treatment with antitumor agents, with the highest effects with the administration of maleic anhydride derivatives before quercetin. Consistent with our findings, it has been previously reported that the decrease in intracellular-reduced glutathione and increase of reactive oxygen species trigger apoptosis. Additionally, several reports have demonstrated that increased ROS act upstream of caspase-3 activation. Accumulation of ROS after treatment with antitumor agents was shown to induce DNA damage and apoptosis by decreasing the mitochondrial membrane potential resulting in the release of cytochrome C [42]. To determine the mechanisms by which treatment with antitumor agents induce apoptosis, Western blotting was performed. The results showed an increase in the levels of procaspase-9 and caspase-9; however, no significant effects were observed in the activation of caspase-8. The observed increase in the level of activated caspase-3 and cleaved caspase-9 confirmed the activation of the intrinsic pathway of apoptosis. Our findings indicate that quercetin alone clearly decreases the reactive oxygen species and increases the levels of reduced glutathione, the GSH/GSSG index, and the de novo synthesis of glutathione, and despite this, it induces mitochondrial apoptosis. The effect of quercetin on HCC cells can be explained based on the previous studies that have attributed this effect to the direct interaction of quercetin with DNA, which enables it to modulate proapoptotic and antiapoptotic proteins, inhibit the PI3K/Akt pathway, and thus decrease survival.

5. Conclusions

The present study indicated that treatment with C1, C2, or Q individually exerts cytotoxic effect on tumor cell lines, but the combination of maleic anhydride derivatives and quercetin exacerbates the cytotoxic effects. HuH7 and HepG2 cell are highly sensitive to growth inhibition by treatment with C1 + Q and C2 + Q. The combination treatment can block cell cycle progression at the S phase, whereas the individual treatments inhibit the cell cycle at the G0/G1 phase. The cytotoxic

treatment triggers the mitochondrial apoptotic pathway by regulating the expression of caspase-9 and activating caspase-3. C1 and C2 increased ROS levels, and quercetin depleted ROS production. The combination treatments C1 + Q and C2 + Q increased ROS levels and depleted GSH in HuH7 and HepG2 cells at 24 and 48 hours. These findings demonstrate the pleiotropic effects of the combination of maleic anhydride derivatives and quercetin on liver cancer cells and open the possibility of using their effective chemopreventive effects in hepatocellular carcinoma.

Abbreviations

Q: Quercetin
C1: 3′5′-dimaleamylbenzoic acid
C2: 3′5′-dimaleimylbenzoic acid
HCC: Hepatocellular carcinoma
ROS: Reactive oxygen species
GSH: L-c-glutamyl-L-cysteinyl-glycine
GSSG: Oxidized glutathione
DCFDA: 2′,7′-dichlorodihydrofluorescein diacetate
DFT: Density functional level of theory
MTT: 3-(4,5-dimethylthiazol-2-yl)-2,5-diphenyl tetrazolium bromide
DMEM: Dulbecco's Modified Eagle's medium
FBS: Fetal bovine serum
PI: Propidium iodide
CDKs: Cyclin-dependent kinases.

Conflicts of Interest

The authors declare that they have no conflicts of interest.

Acknowledgments

This work was supported by CONACYT Grant 178558 which was given to Saúl Villa-Treviño, 270189 to Rafael Baltiérrez-Hoyos, 2014-2499 to Verónica Rocío Vásquez-Garzón, and Scholarship A150273 CONACYT to Gabriela Carrasco-Torres and by the CINVESTAV. The authors thank Eunice Romo Medina, Sergio Hernández García, Leobardo Molina García, Ma. Del Carmen Namorado Tonix, and Jaime Escobar Herrera for their technical support and thank the research assistant Samia Fattel-Fazenda for having given great teaching to this research group and for their unconditional support for the development of this project.

References

[1] N. Hay, "Reprogramming glucose metabolism in cancer: can it be exploited for cancer therapy?," *Nature Reviews Cancer*, vol. 16, no. 10, pp. 635–649, 2016.

[2] Y. D. Bhutia, E. Babu, S. Ramachandran, and V. Ganapathy, "Amino acid transporters in cancer and their relevance to "glutamine addiction": novel targets for the design of a new class of anticancer drugs," *Cancer Research*, vol. 75, no. 9, pp. 1782–1788, 2015.

[3] O. Warburg, "On the origin of cancer cells," *Science*, vol. 123, no. 3191, pp. 309–314, 1956.

[4] S. Perez, R. Taléns-Visconti, S. Rius-Pérez, I. Finamor, and J. Sastre, "Redox signaling in the gastrointestinal tract," *Free Radical Biology and Medicine*, vol. 104, pp. 75–103, 2017.

[5] C. V. Recktenwald, R. Kellner, R. Lichtenfels, and B. Seliger, "Altered detoxification status and increased resistance to oxidative stress by K-ras transformation," *Cancer Research*, vol. 68, no. 24, pp. 10086–10093, 2008.

[6] B. Benassi, M. Fanciulli, F. Fiorentino et al., "C-Myc phosphorylation is required for cellular response to oxidative stress," *Molecular Cell*, vol. 21, no. 4, pp. 509–519, 2006.

[7] J. L. Roh, E. H. Kim, H. Jang, and D. Shin, "Nrf2 inhibition reverses the resistance of cisplatin-resistant head and neck cancer cells to artesunate-induced ferroptosis," *Redox Biology*, vol. 11, pp. 254–262, 2016.

[8] H. Pelicano, L. Feng, Y. Zhou et al., "Inhibition of mitochondrial respiration: a novel strategy to enhance drug-induced apoptosis in human leukemia cells by a reactive oxygen species-mediated mechanism," *The Journal of Biological Chemistry*, vol. 278, no. 39, pp. 37832–37839, 2003.

[9] J. R. Kirshner, V. Balasubramanyam, J. Kepros et al., "Elesclomol induces cancer cell apoptosis through oxidative stress," *Molecular Cancer Therapeutics*, vol. 7, no. 8, pp. 2319–2327, 2008.

[10] C. Chen, J. Zhou, and C. Ji, "Quercetin: a potential drug to reverse multidrug resistance," *Life Sciences*, vol. 87, no. 11-12, pp. 333–338, 2010.

[11] A. Niedzwiecki, M. W. Roomi, T. Kalinovsky, and M. Rath, "Anticancer efficacy of polyphenols and their combinations," *Nutrients*, vol. 8, no. 9, 2016.

[12] J. A. Choi, J. Y. Kim, J. Y. Lee et al., "Induction of cell cycle arrest and apoptosis in human breast cancer cells by quercetin," *International Journal of Oncology*, vol. 19, no. 4, pp. 837–844, 2001.

[13] L. Yang, Y. Liu, M. Wang et al., "Quercetin-induced apoptosis of HT-29 colon cancer cells via inhibition of the Akt-CSN6-Myc signaling axis," *Molecular Medicine Reports*, vol. 14, no. 5, pp. 4559–4566, 2016.

[14] A. K. Maurya and M. Vinayak, "Anticarcinogenic action of quercetin by downregulation of phosphatidylinositol 3-kinase (PI3K) and protein kinase C (PKC) via induction of p53 in hepatocellular carcinoma (HepG2) cell line," *Molecular Biology Reports*, vol. 42, no. 9, pp. 1419–1429, 2015.

[15] K. Bishayee, A. R. Khuda-Bukhsh, and S. O. Huh, "PLGA-loaded gold-nanoparticles precipitated with quercetin downregulate HDAC-Akt activities controlling proliferation and activate p53-ROS crosstalk to induce apoptosis in hepatocarcinoma cells," *Molecules and Cells*, vol. 38, no. 6, pp. 518–527, 2015.

[16] P. Plackova, M. Šála, M. Šmídková et al., "9-norbornyl-6-chloropurine (NCP) induces cell death through GSH depletion-associated ER stress and mitochondrial dysfunction," *Free Radical Biology and Medicine*, vol. 97, pp. 223–235, 2016.

[17] R. A. Rafiq, A. Quadri, L. A. Nazir, K. Peerzada, B. A. Ganai, and S. A. Tasduq, "A potent inhibitor of phosphoinositide 3-kinase (PI3K) and mitogen activated protein (MAP) kinase signalling, quercetin (3, 3′, 4′, 5, 7-pentahydroxyflavone) promotes cell death in ultraviolet (UV)-B-irradiated B16F10 melanoma cells," *PLoS One*, vol. 10, no. 7, article e0131253, 2015.

[18] E. Andrade-Jorge, M. Godínez-Victoria, L. E. Sánchez-Torres, L. H. Fabila-Castillo, and J. G. Trujillo-Ferrara, "Aryl

maleimides as apoptosis inducers on L5178-Y murine leukemia cells (in silico, in vitro and ex vivo study)," *Anti-Cancer Agents in Medicinal Chemistry*, vol. 16, no. 12, pp. 1615–1621, 2016.

[19] J. Trujillo-Ferrara, R. Santillan, H. I. Beltrán, N. Farfán, and H. Höpfl, "^{1}H and ^{13}C NMR spectra for a series of arylmaleamic acids, arylmaleimides, arylsuccinamic acids and arylsuccinimides," *Magnetic Resonance in Chemistry*, vol. 37, no. 9, pp. 682–686, 1999.

[20] N. S. Chandel, P. T. Schumacker, and R. H. Arch, "Reactive oxygen species are downstream products of TRAF-mediated signal transduction," *The Journal of Biological Chemistry*, vol. 276, no. 46, pp. 42728–42736, 2001.

[21] J. Ferlay, I. Soerjomataram, R. Dikshit et al., "Cancer incidence and mortality worldwide: sources, methods and major patterns in GLOBOCAN 2012," *International Journal of Cancer*, vol. 136, no. 5, pp. E359–E386, 2015.

[22] H. B. El-Serag and K. L. Rudolph, "Hepatocellular carcinoma: epidemiology and molecular carcinogenesis," *Gastroenterology*, vol. 132, no. 7, pp. 2557–2576, 2007.

[23] C. Y. Liao, C. C. Lee, C. C. Tsai et al., "Novel investigations of flavonoids as chemopreventive agents for hepatocellular carcinoma," *BioMed Research International*, vol. 2015, Article ID 840542, 26 pages, 2015.

[24] J. H. Jeong, J. Y. An, Y. T. Kwon, J. G. Rhee, and Y. J. Lee, "Effects of low dose quercetin: cancer cell-specific inhibition of cell cycle progression," *Journal of Cellular Biochemistry*, vol. 106, no. 1, pp. 73–82, 2009.

[25] A. M. Seufi, S. S. Ibrahim, T. K. Elmaghraby, and E. E. Hafez, "Preventive effect of the flavonoid, quercetin, on hepatic cancer in rats via oxidant/antioxidant activity: molecular and histological evidences," *Journal of Experimental & Clinical Cancer Research*, vol. 28, p. 80, 2009.

[26] A. F. Brito, M. Ribeiro, A. M. Abrantes et al., "New approach for treatment of primary liver tumors: the role of quercetin," *Nutrition and Cancer*, vol. 68, no. 2, pp. 250–266, 2016.

[27] C. Deng, B. Zhang, S. Zhang et al., "Low nanomolar concentrations of cucurbitacin-I induces G2/M phase arrest and apoptosis by perturbing redox homeostasis in gastric cancer cells in vitro and in vivo," *Cell Death and Disease*, vol. 7, article e2106, 2016.

[28] F. D. Meng, Y. Li, X. Tian et al., "Synergistic effects of snail and quercetin on renal cell carcinoma Caki-2 by altering AKT/mTOR/ERK1/2 signaling pathways," *International Journal of Clinical and Experimental Pathology*, vol. 8, no. 6, pp. 6157–6168, 2015.

[29] S. N. Tang, C. Singh, D. Nall, D. Meeker, S. Shankar, and R. K. Srivastava, "The dietary bioflavonoid quercetin synergizes with epigallocathechin gallate (EGCG) to inhibit prostate cancer stem cell characteristics, invasion, migration and epithelial-mesenchymal transition," *Journal of Molecular Signaling*, vol. 5, p. 14, 2010.

[30] A. S. Kalgutkar, B. C. Crews, and L. J. Marnett, "Design, synthesis, and biochemical evaluation of N-substituted maleimides as inhibitors of prostaglandin endoperoxide synthases," *Journal of Medicinal Chemistry*, vol. 39, no. 8, pp. 1692–1703, 1996.

[31] Y. O. Son, K. Y. Lee, S. H. Kook et al., "Selective effects of quercetin on the cell growth and antioxidant defense system in normal versus transformed mouse hepatic cell lines," *European Journal of Pharmacology*, vol. 502, no. 3, pp. 195–204, 2004.

[32] L. Yi, Y. Zongyuan, G. Cheng, Z. Lingyun, Y. Guilian, and G. Wei, "Quercetin enhances apoptotic effect of tumor necrosis factor-related apoptosis-inducing ligand (TRAIL) in ovarian cancer cells through reactive oxygen species (ROS) mediated CCAAT enhancer-binding protein homologous protein (CHOP)-death receptor 5 pathway," *Cancer Science*, vol. 105, no. 5, pp. 520–527, 2014.

[33] T. K. MacLachlan, N. Sang, and A. Giordano, "Cyclins, cyclin-dependent kinases and cdk inhibitors: implications in cell cycle control and cancer," *Critical Reviews in Eukaryotic Gene Expression*, vol. 5, no. 2, pp. 127–156, 1995.

[34] Z. Yuan, C. Long, T. Junming, L. Qihuan, Z. Youshun, and Z. Chan, "Quercetin-induced apoptosis of HL-60 cells by reducing PI3K/Akt," *Molecular Biology Reports*, vol. 39, no. 7, pp. 7785–7793, 2012.

[35] Q. Zhang, X. H. Zhao, and Z. J. Wang, "Flavones and flavonols exert cytotoxic effects on a human oesophageal adenocarcinoma cell line (OE33) by causing G2/M arrest and inducing apoptosis," *Food and Chemical Toxicology*, vol. 46, no. 6, pp. 2042–2053, 2008.

[36] S. Srivastava, R. R. Somasagara, M. Hegde et al., "Quercetin, a natural flavonoid interacts with DNA, Arrests Cell Cycle and Causes Tumor Regression by Activating Mitochondrial Pathway of Apoptosis," *Scientific Reports*, vol. 6, article 24049, 2016.

[37] Y. Wang, A. Han, E. Chen et al., "The cranberry flavonoids PAC DP-9 and quercetin aglycone induce cytotoxicity and cell cycle arrest and increase cisplatin sensitivity in ovarian cancer cells," *International Journal of Oncology*, vol. 46, no. 5, pp. 1924–1934, 2015.

[38] F. Dajas, "Life or death: neuroprotective and anticancer effects of quercetin," *Journal of Ethnopharmacology*, vol. 143, no. 2, pp. 383–396, 2012.

[39] T. Schnelldorfer, S. Gansauge, F. Gansauge, S. Schlosser, H. G. Beger, and A. K. Nussler, "Glutathione depletion causes cell growth inhibition and enhanced apoptosis in pancreatic cancer cells," *Cancer*, vol. 89, no. 7, pp. 1440–1447, 2000.

[40] A. W. Boots, N. Kubben, G. R. Haenen, and A. Bast, "Oxidized quercetin reacts with thiols rather than with ascorbate: implication for quercetin supplementation," *Biochemical and Biophysical Research Communications*, vol. 308, no. 3, pp. 560–565, 2003.

[41] D. Metodiewa, A. K. Jaiswal, N. Cenas, E. Dickancaité, and J. Segura-Aguilar, "Quercetin may act as a cytotoxic prooxidant after its metabolic activation to semiquinone and quinoidal product," *Free Radical Biology and Medicine*, vol. 26, no. 1-2, pp. 107–116, 1999.

[42] K. Al-Khayal, A. Alafeefy, M. A. Vaali-Mohammed et al., "Novel derivative of aminobenzenesulfonamide (3c) induces apoptosis in colorectal cancer cells through ROS generation and inhibits cell migration," *BMC Cancer*, vol. 17, no. 1, p. 4, 2017.

Hindawi
Oxidative Medicine and Cellular Longevity
Volume 2017, Article ID 3749157, 8 pages
https://doi.org/10.1155/2017/3749157

Review Article

Lysosomes as Oxidative Targets for Cancer Therapy

Rebecca F. Dielschneider,[1] Elizabeth S. Henson,[2] and Spencer B. Gibson[3]

[1]*Providence University College, Otterburne, MB, Canada*
[2]*Research Institute in Oncology and Hematology, CancerCare Manitoba, 675 McDermot Ave., Winnipeg, MB, Canada*
[3]*Department of Biochemistry and Medical Genetics, Faculty of Health Sciences, University of Manitoba, Winnipeg, MB, Canada*

Correspondence should be addressed to Spencer B. Gibson; spencer.gibson@umanitoba.ca

Received 10 March 2017; Accepted 31 May 2017; Published 5 July 2017

Academic Editor: Felipe Dal Pizzol

Lysosomes are membrane-bound vesicles that contain hydrolases for the degradation and recycling of essential nutrients to maintain homeostasis within cells. Cancer cells have increased lysosomal function to proliferate, metabolize, and adapt to stressful environments. This has made cancer cells susceptible to lysosomal membrane permeabilization (LMP). There are many factors that mediate LMP such as Bcl-2 family member, p53; sphingosine; and oxidative stress which are often altered in cancer. Upon lysosomal disruption, reactive oxygen species (ROS) levels increase leading to lipid peroxidation, mitochondrial dysfunction, autophagy, and reactive iron. Cathepsins are also released causing degradation of macromolecules and cellular structures. This ultimately kills the cancer cell through different types of cell death (apoptosis, autosis, or ferroptosis). In this review, we will explore the contributions lysosomes play in inducing cell death, how this is regulated by ROS in cancer, and how lysosomotropic agents might be utilized to treat cancers.

1. Introduction

Lysosomes are membrane-enclosed vesicles that contain at least 60 hydrolases within an acidic environment. These hydrolases, which include the cathepsin family of proteases, are responsible for degradation, recycling, and disposal of cellular macromolecules [1]. Lysosomes are often termed the garbage disposal of the cell, but as our knowledge and understanding increase, the roles lysosomes play in other cellular functions expand [2]. The lysosomal degradation pathway regulates a variety of cellular functions such as autophagy, endocytosis, and phagocytosis to maintain cellular homeostasis [1]. In addition, this pathway directly or indirectly regulates cell signaling, metabolism, and degradation of protein aggregates and damaged organelles [3–5]. When the degradative pathway is dysregulated, diseases such as cancer can progress. This makes lysosomes a potential target for cancer therapy.

2. Lysosomal Biology

Lysosomes are the most acidic vesicles within the cell. This acidic pH is maintained by the action of a proton pump which hydrolyzes ATP to ADP in order to pump an H^+ ion into the lumen of the lysosome [6]. The lysosomal membrane consists of a lipid bilayer and membrane proteins. The most abundant lysosomal membrane proteins are lysosome-associated membrane proteins 1 and 2 (LAMP-1 and LAMP-2). The inner lumen of these proteins is highly glycosylated and protects the lysosomal membrane from the digestive enzymes [7, 8]. These enzymes can digest DNA, RNA, sugars, lipids, and proteins. Among these enzymes is the diverse cathepsin protease family. Cathepsins A and G are serine proteases, meaning that their active site contains a vital serine. Cathepsins B, C, F, H, K, L, O, S, V, X, and W are cysteine proteases. Cathepsins D and E are aspartic proteases. Cysteine cathepsins are the most stable and active at an acidic

pH. Like caspases, cathepsins have a wide range of cellular substrates. Cystatins, thyropins, and serpins prevent cathepsin substrates from binding and are thus endogenous inhibitors of cathepsins [9].

Lysosomal biogenesis is controlled by master regulators transcription factor EB (TFEB) and microphthalmia-associated transcription factor (MITF). These proteins receive cues in the cytoplasm and translocate into the nucleus to induce the transcription of lysosomal biogenesis network of genes [5, 10, 11]. TFEB and MITF are phosphorylated by mTOR in the cytoplasm and retained there by binding to 14-3-3 proteins [10]. Upon inhibition of the mTOR pathway under stress conditions, lysosomal biogenesis could be activated.

3. Lysosomes in Cancer

Lysosomes have been associated with diseases such as lysosomal storage disorders, neurodegenerative disorders, and cardiovascular disease [12, 13]. In cancer, lysosomal function is also altered. Many cancer cells have increased the number of lysosomes to maintain homeostasis by the increased degradation and recycling macromolecules to maintain cell proliferation and survive under stress condition in the microenvironment [4, 14, 15]. Indeed, increased expression of cathepsin B has been associated with increased cancer invasion [16]. Despite the ubiquitous nature of lysosomes in all mammalian cell types, cancer cells have been shown to increase lysosomal biogenesis [14, 17] and alter cellular biology [18, 19], thus affecting lysosomes. One such biological process that impacts lysosomes is sphingolipid metabolism. Altered sphingolipid metabolism has been found in many cancers [20–22]. Different cancer cell types overexpress sphingosine kinase (SK) [23–25] and downregulate acidic sphingomyelinase (ASM) [19]. These changes affect lysosomal membrane structure and function in cancer cells.

Lysosomes also play an important role in drug resistance in cancer by sequestering weak-base chemotherapeutic drugs within the cell. This increases lysosomal biogenesis resulting in enlargement of the lysosomal compartment in cells [15]. The enlarged compartment allows significant concentration of chemotherapeutic drugs to be stored in lysosomes and blocks these drugs from reaching their cellular targets. In addition, lysosomes provide a mechanism for exocytosis of drugs from the cancer cells [15]. These mechanisms render cancer cells drug-resistant, thus highlighting lysosomes as a target for cancer therapy.

4. Lysosomal Membrane Permeabilization (Figure 1)

Lysosomal membrane permeabilization (LMP) has been shown to be an effective therapeutic strategy in many cancer models [26]. LMP involves either the slight or the complete permeabilization of the lysosome. This permeabilization can cause lipid peroxidation and a partial or complete release of lysosomal contents. Cell death can be mediated by the reactive oxygen species (ROS) and/or lysosomal cathepsins [3, 4, 26]. In addition, sphingolipids can contribute to LMP [27]. Sphingosine has been shown to induce LMP when added to cells [27]. Upon TNFα, radiation, and DNA-damaging drug treatments, p53 is phosphorylated and translocates to lysosomes where it induces LMP [5]. Various cellular components can protect the lysosome from permeabilization such as cholesterol [28], lysosomal localization of heat shock protein 70 [29], and lipid peroxidation scavengers. Tocopherols are endogenous inhibitors of lipid peroxidation. Among tocopherols is α-tocopherol, otherwise known as vitamin E [30, 31]. Thus, there are many factors regulating LMP in cancer cells.

Cancer cells are sensitive to LMP by a variety of mechanisms. Cell lines transformed with oncogenic Src and Ras display altered lysosomal localization and decrease in LAMP-1 and LAMP-2 [18]. Decreases in the LAMP proteins prime cells for LMP. Other cancer cells increase lysosomal biogenesis [14, 17], increase lysosomal size, and alter heat shock protein 70 (HSP-70) localization creating destabilized lysosomes [29]. Cancer cells have altered sphingolipid metabolism which increases the amount of sphingosine and renders lysosomes sensitive to LMP [22, 27, 32]. Finally, many cancer cells have altered metabolism that increases ROS leading to destabilization of lysosomes leading to LMP [3, 23]. Thus, cancer cells might be sensitive to lysosome-mediated cell death.

5. Lysosome-Mediated Cell Death (LCD)

Since their discovery as the suicide bags of the cell, lysosomes have been explored as therapeutic targets in cancer. Due to these numerous alterations to this pathway, LMP is an effective way to kill many different cancer cell types. These include breast cancer [19, 30, 33], ovarian cancer [19], cervical cancer [19], colon cancer [18, 34, 35], prostate cancer [19], lung cancer [35–37], bone cancer [19], skin cancer [35], and AML [14]. Cancer cells are susceptible to lysosome-mediated cell death through increased ROS and lipid peroxidation leading to mitochondrial dysfunction and plasma membrane permeabilization [38]. Furthermore, the release of cathepsins caused cleavage and degradation of proteins leading to cell death [3]. The relations of lysosome-mediated cell death with other forms of cell death will be discussed below.

6. Lysosomes and Apoptosis

Apoptosis is a form of program cell death involving mitochondrial dysfunction and activation of cysteine proteases called caspases. It leads to DNA condensation and membrane blebbing and eventually to the formation of apoptotic bodies that are phagocytosed by the surrounding cells. Mitochondrial dysfunction is triggered by the translocation of the Bcl-2 family member Bax to the mitochondria where it interacts with Bak and other BH3-only Bcl-2 family members such as Bid to form a pore allowing cytochrome c to be released and loss of membrane potential to occur. This leads to an increase in ROS and activation of caspase 9 and caspase 3 leading to cell death [39].

Lysosomes could play important roles in regulating apoptosis upstream of mitochondrial function and after caspase

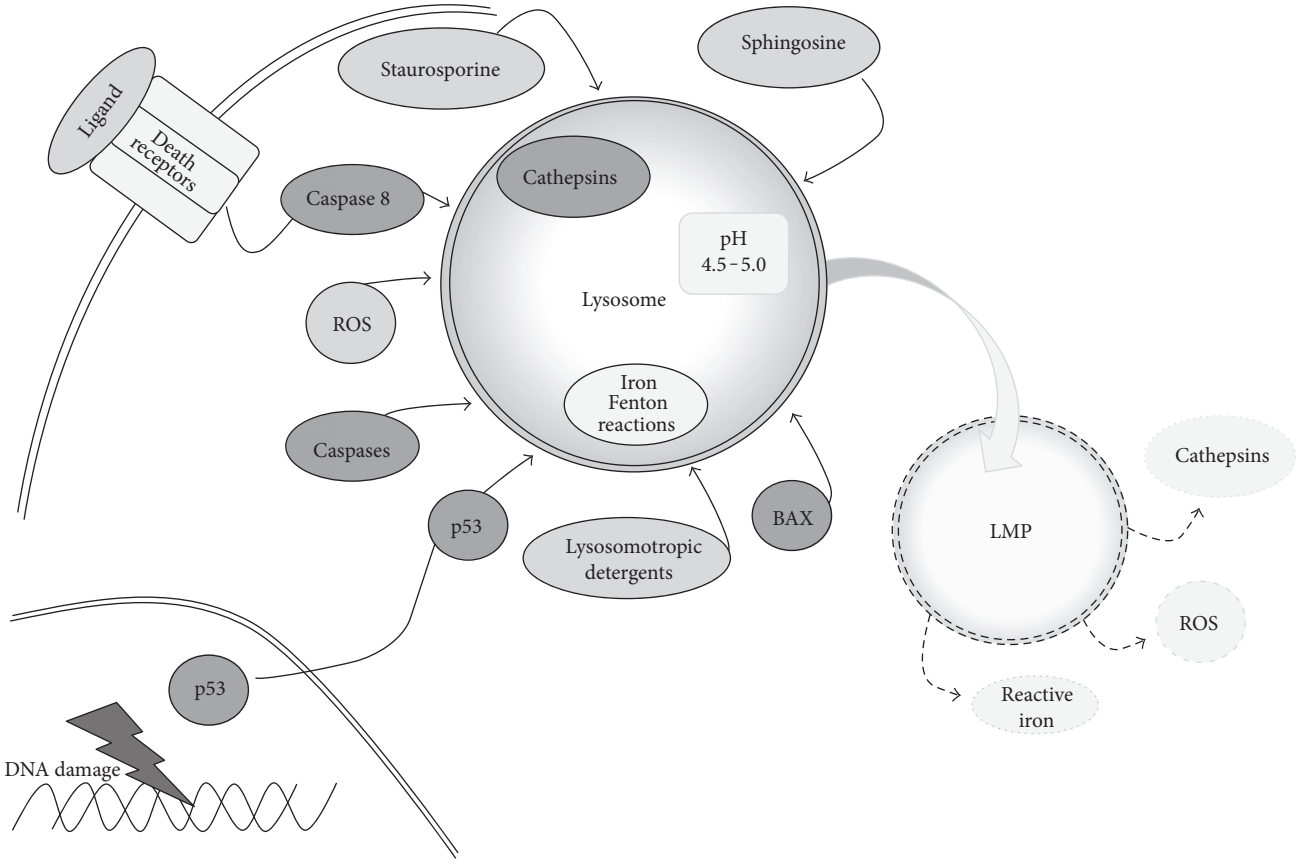

Figure 1: Regulation of lysosomal membrane permeabilization (LMP). There are many factors that regulate lysosomal membrane permeabilization (LMP). These include increased levels of sphingosine, cathepsins, and ROS. The activation of caspase, Bax, and p53 and treatment with staurosporine, or lysosomotropic agents, also lead to LMP. This results in the release of ROS, cathepsins, and reactive iron from lysosomes.

activation. Following oxidative stress, it was shown that low concentrations of hydrogen peroxide cause LMP before mitochondrial dysfunction and caspase activation [40]. Blocking cathepsin D activation also prevented the release of mitochondrial cytochrome c and caspase activation [41]. Moreover, ultraviolent radiation induces LMP under conditions of oxidative stress before mitochondrial release of cytochrome c [42]. Bax interacts with other BH3-only Bcl-2 family members such as BIM and BID at lysosomes contributing to LMP independent of its mitochondrial functions. BID is also a target of cathepsins allowing its translocation to the mitochondria to interact with Bax and Bak [42]. Similar to mitochondrial regulation, antiapoptotic Bcl-2 family members can prevent LMP [26]. This suggests that lysosomal disruption can lead to mitochondrial dysfunction.

Lysosomal disruption can also occur after mitochondrial dysfunction. Following loss of membrane potential, ROS production is increased. ROS destabilizes lysosomal membranes through lipid peroxidation leading to rupture [14, 27]. Activation of caspase 8 by death receptors or activation of caspase 9 has been associated with LMP [36, 43]. Overall lysosomes can play a role in either initiating or executing apoptosis.

7. Lysosome and Autophagy

Lysosomes fuse with autophagosomes forming an autolysosome to degrade extracellular or intracellular material [44]. Autophagy plays important roles in cancer cell adaptation to stress where it protects cancer cells from death during development and where its induction is limited to further progression of the disease [45]. Lysosomes function in autophagy regulation in three main areas: (i) lysosomal restoration, (ii) lysophagy, and (iii) autolysosomal degradation. Under normal conditions, lysosomal biogenesis occurs through biosynthesis and endocytic pathways to maintain homeostasis. Under stress conditions, the number of lysosomes decreased due to their role in degrading macromolecules for recycling or removing damaged organelles. Lysosomal levels are restored through a process called autophagic lysosomal reformation (ALR) [46]. This process can be prevented by autophagy inhibitors such as rapamycin and cathepsin inhibitors [46]. The second way autophagy regulates lysosomes is when lysosomes themselves become damaged such as through LMP. The damaged lysosomes are engulfed by autophagosomes which then fuse with functional lysosomes to remove them from the cells [47]. The levels of lysosomes are then restored by lysosomal biogenesis.

Table 1: The use of lysosomotropic agents as therapeutics in cancer.

Lysosomotropic Agent		Model	Effective doses	Reference
Siramesine	In vitro	Breast cancer lines: Mcf-7, Mcf-10A, and MDA-MB-468	1–10 μM	[18, 19, 30]
		Cervix carcinoma cell lines: HeLa and ME-180	1–10 μM	
		Colorectal cancer cell lines: Hkh2 and HCT116	8 μM	
		Fibroblast cell line: NIH3&3-SrcY527F	4–10 μM	
		Fibrosarcoma cell lines: WEHI-S and R4	5 μM	
		Mast cells (primary)	2–20 μM	
		Osteosarcoma cell line: U2OS	1–10 μM	
		Ovarian carcinoma cell line: SKOV3	8–10 μM	
		Prostate cancer cell lines: PC3 and Du145-P	5–10 μM	
	In vivo	WEHI-R4 in BALB-c mice	25–100 mg/kg/d	
		Mcf-7 in SCID mice	30–100 mg/kg/d	
		PC3-MDR in SCID mice	30 mg/kg	
Desipramine	In vitro	Breast cancer lines: Mcf-7 and Mcf-10A	25 μM	[19]
		Cervix carcinoma cell line: HeLa	25–50 μM	
		Colorectal cancer cell lines: Hkh2 and HCT116	8 μM	
		Fibroblast cell line: NIH3&3-SrcY527F	8–25 μM	
		Osteosarcoma cell line: U2OS	25–50 μM	
		Ovarian carcinoma cell line: SKOV3	75–100 μM	
		Prostate cancer cell lines: PC3 and Du145-P	5–10 μM	
	In vivo	Mcf-7 in SCID mice	30 mg/kg, 2×/wk	
Nortriptyline	In vitro	Breast cancer line: Mcf-7	25–50 μM	[19]
		Cervix carcinoma cell line: HeLa	25–50 μM	
		Colorectal cancer cell lines: Hkh2 and HCT116	8 μM	
		Fibroblast cell line: NIH3&3-SrcY527F	10–25 μM	
		Osteosarcoma cell line: U2OS	25–50 μM	
		Ovarian carcinoma cell line: SKOV3	40–60 μM	
		Prostate cancer cell lines: PC3 and Du145-P	40–80 μM	
Amlodipine	In vitro	Breast cancer line: Mcf-7	25–50 μM	[19]
		Fibroblast cell line: NIH3&3-SrcY527F	10–30 μM	
		Ovarian carcinoma cell line: SKOV3	37.5–50 μM	
		Prostate cancer cell lines: PC3 and Du145-P	40–50 μM	
Terfenadine	In vitro	Breast cancer line: Mcf-7	25–50 μM	[19]
		Colorectal cancer cell lines: Hkh2 and HCT116	8 μM	
		Fibroblast cell line: NIH3&3-SrcY527F	2.5–5 μM	
		Ovarian carcinoma cell line: SKOV3	6–8 μM	
		Prostate cancer cell lines: PC3 and Du145-P	1–10 μM	
	In vivo	Mcf-7 in SCID mice	10 mg/kg, 2×/wk	
Mefloquine	In vitro	AML cells (primary)	5–15 μM	[14]
		AML cell lines: HL60, KG1A OCI-AML2, and TEX	1–10 μM	
		APL cell line: NB4	5–7 μM	
		CML cell line: K562	6–10 μM	
		Dendritic cells (primary)	25–50 μM	
		Erythroleukemic cell line: OCI-M2	7–9 μM	
		Gastric cancer cell lines: AGS, Hs746T, MKN45, MKN74, NCI-N87, SNU1, SNU16, TCC1, YCC10, and YCC11	0.5–5 μM	
		Lymphosarcoma cell line: MDAY-D2	3–5 μM	
		Macrophage/monocyte cell lines: THP-1 and U937	5–18 μM	
		Oral cancer cell line: KVP20C	5 μM	

Table 1: Continued.

Lysosomotropic Agent		Model	Effective doses	Reference
	In vivo	Prostate cancer cell line: PC3	5–40 μM	
		K562, MDAY-D2, and OCI-AML2 in NOD-SCID mice	50 mg/kg	
		Primary AML cells in NOD-SCID mice	100 mg/kg/d	
		YCC or SNU1 in SCID mice	Unknown	
		PC3 in C57B1/6J mice	200 μg/25 mg	
Primaquine	In vitro	Breast cancer cell line: Mcf-7	7 μM	[58]
		Colon cancer cell lines: Caco-2 and HT-29	40–70 μM	
		Oral cancer cell line: KVB20C	50–75 μM	
Atovaquone	In vitro	Oral cancer cell line: KVB20C	2–12.5 μM	[59]
Ciprofloxacin	In vitro	Cervix carcinoma cell line: HeLa	10 μg/ml	[34]
		Colorectal cancer cell line HCT116	1–5 μM	
Pterostilbene	In vitro	AML cell lines: HL-60, MV4-11, and OCI-AML2	25–75 μM	[58]
		Macrophage cell lines: THP-1 and U937	25–75 μM	
		Melanoma cell line: A375	10–50 μM	

Finally, the fusion of lysosomes and autophagosomes provides essential amino acids and nutrients to the cell and degrades damaged organelles [48]. If this process was left unchecked, the destruction of intracellular structures will lead to cellular collapse and a form of cell death called autosis [49]. This is dependent on functional lysosomes.

8. Lysosome and Ferroptosis

Ferroptotic cell death is a type of cell death that is distinct from apoptosis and autophagy [50, 51]. It is characterized by iron-dependent accumulation of ROS. Several proteins responsible for the regulation of iron such as ferritin and transferrin and the cysteine antiporter receptor have implicated the regulation of ferroptosis [52, 53]. One of the major storage sites for iron is lysosomes. In the presence of hydrogen peroxide, free iron undergoes a Fenton reaction creating reactive iron and increasing ROS [38]. The lysosomal disruptor siramesine induces a rapid rise in the lysosomal pH followed by lysosomal leakage mediated in part by inhibiting sphingomyelinase (ASM) [19]. This destabilization of lysosomal membranes leads to increased reactive iron and increased ROS causing cell death [30]. We found that the combination with a dual tyrosine kinase inhibitor of ErbB1 and ErbB2 tyrosine kinase receptors called lapatinib with siramesine could induce ferroptosis through blocking iron transport allowing the iron released by lysosomal disruption to accumulate and increase ROS [54]. The role lysosomes play in regulating ferroptosis through increased active iron and ROS requires future investigations.

9. Lysosomotropic Agents

LMP can be induced by numerous different stimuli that are collectively called lysosomotropic agents. Lysosomotropic agents are weak-base lipophilic or cationic amphiphilic drugs that accumulate in lysosomes. This occurs through diffusion across the lysosomal membrane where the agents become protonated and become trapped in the lysosome [26]. This causes damage to the lysosomal membranes leading to LMP. Lysosomotropic agents include metal nanoparticles [55], kinase inhibitor ML-9 [56], and numerous different types of pharmaceuticals. Pharmaceutical lysosomotropic agents include the antidepressants siramesine, nortriptyline, desipramine, imipramine, and clomipramine [19]. These have shown effectiveness in breast cancer, colon cancer, and CLL cells. Antimalarials mefloquine and chloroquine have shown effectiveness in breast cancer, lymphoma, and leukemia cells [14, 57–59]. Chloroquine has been investigated in clinical trials with only partial activity in lymphoma reported. There is, however, no evidence in these trails that chloroquine is acting through LMP. Antiallergy drugs terfenadine and loratadine [19] were effective at inducing cell death in breast and lung cancer cells. The treatments of stilbenoid antioxidant pterostilbene [35, 60] and antipsychotics chlorpromazine, thioridazine, and aripiprazole [19] showed efficacy in breast and leukemia cells. The use of these agents is summarized in Table 1. Many of these agents are FDA-approved or have been extensively studied in clinical trials but, with the exception of chloroquine, not in cancer patients [61]. This provides the foundation for many of these lysosomotropic agents to be clinically investigated for their efficacy in a variety of cancers in the near future.

10. Conclusion

Lysosomes play a dynamic role in cells and are altered in cancer. The initiation of LMP in cancer cells is a novel mechanism to engage the different cell death mechanisms selective for cancer. LMP is induced by lysosomotropic agents through increased ROS, lipid peroxidation, and activation of cathepsins. Many of these lysosomotropic agents are FDA-approved and could be moved rapidly to the clinic. Targeting lysosomes to induce oxidative stress will be

dependent on the context of other therapies and drug resistance mechanisms found in cancer cells. Further investigation is needed to understand the regulation of lysosome-mediated cell death and the use of lysosomotropic agents in combination with other standard chemotherapy drugs or novel targeted anticancer drugs. Nevertheless, targeting lysosomes provides hope that effective treatment against drug-resistant cancers could be developed.

Conflicts of Interest

There is no conflict of interest in publishing this manuscript.

References

[1] P. Saftig and J. Klumperman, "Lysosome biogenesis and lysosomal membrane proteins: trafficking meets function," *Nature Reviews Molecular Cell Biology*, vol. 10, no. 9, pp. 623–635, 2009.

[2] C. Settembre and A. Ballabio, "Lysosomal adaptation: how the lysosome responds to external cues," *Cold Spring Harbor Perspectives in Biology*, vol. 6, no. 6, 2014.

[3] S. Aits and M. Jaattela, "Lysosomal cell death at a glance," *Journal of Cell Science.*, vol. 126, Part 9, pp. 1905–1912, 2013.

[4] G. Kroemer and M. Jaattela, "Lysosomes and autophagy in cell death control," *Nature Reviews Cancer*, vol. 5, no. 11, pp. 886–897, 2005.

[5] C. Settembre, A. Fraldi, D. L. Medina, and A. Ballabio, "Signals from the lysosome: a control centre for cellular clearance and energy metabolism," *Nature Reviews Molecular Cell Biology*, vol. 14, no. 5, pp. 283–296, 2013.

[6] V. Bouche, A. P. Espinosa, L. Leone, M. Sardiello, A. Ballabio, and J. Botas, "Drosophila Mitf regulates the V-ATPase and the lysosomal-autophagic pathway," *Autophagy*, vol. 12, no. 3, pp. 484–498, 2016.

[7] J. W. Chen, T. L. Murphy, M. C. Willingham, I. Pastan, and J. T. August, "Identification of two lysosomal membrane glycoproteins," *The Journal of Cell Biology*, vol. 101, no. 1, pp. 85–95, 1985.

[8] R. Kundra and S. Kornfeld, "Asparagine-linked oligosaccharides protect Lamp-1 and Lamp-2 from intracellular proteolysis," *The Journal of Biological Chemistry*, vol. 274, no. 43, pp. 31039–31046, 1999.

[9] V. Stoka, V. Turk, and B. Turk, "Lysosomal cathepsins and their regulation in aging and neurodegeneration," *Ageing Research Reviews*, vol. 32, pp. 22–37, 2016.

[10] A. Roczniak-Ferguson, C. S. Petit, F. Froehlich et al., "The transcription factor TFEB links mTORC1 signaling to transcriptional control of lysosome homeostasis," *Science Signaling*, vol. 5, no. 228, article ra42, 2012.

[11] M. Sardiello, M. Palmieri, A. di Ronza et al., "A gene network regulating lysosomal biogenesis and function," *Science*, vol. 325, no. 5939, pp. 473–477, 2009.

[12] J. J. Maciejko, "Managing cardiovascular risk in lysosomal acid lipase deficiency," *American Journal of Cardiovascular Drugs*, vol. 17, pp. 217–231, 2017.

[13] C. S. Pereira, H. Ribeiro, and M. F. Macedo, "From lysosomal storage diseases to NKT cell activation and back," *International Journal of Molecular Sciences*, vol. 18, no. 3, 2017.

[14] M. A. Sukhai, S. Prabha, R. Hurren et al., "Lysosomal disruption preferentially targets acute myeloid leukemia cells and progenitors," *The Journal of Clinical Investigation*, vol. 123, no. 1, pp. 315–328, 2013.

[15] B. Zhitomirsky and Y. G. Assaraf, "Lysosomes as mediators of drug resistance in cancer," *Drug Resistance Updates : Reviews and Commentaries in Antimicrobial and Anticancer Chemotherapy*, vol. 24, pp. 23–33, 2016.

[16] S. A. Ibrahim, E. A. El-Ghonaimy, H. Hassan et al., "Hormonal-receptor positive breast cancer: IL-6 augments invasion and lymph node metastasis via stimulating cathepsin B expression," *Journal of Advanced Research*, vol. 7, no. 5, pp. 661–670, 2016.

[17] R. M. Perera, S. Stoykova, B. N. Nicolay et al., "Transcriptional control of autophagy-lysosome function drives pancreatic cancer metabolism," *Nature*, vol. 524, no. 7565, pp. 361–365, 2015.

[18] N. Fehrenbacher, L. Bastholm, T. Kirkegaard-Sorensen et al., "Sensitization to the lysosomal cell death pathway by oncogene-induced down-regulation of lysosome-associated membrane proteins 1 and 2," *Cancer Research*, vol. 68, no. 16, pp. 6623–6633, 2008.

[19] N. H. Petersen, O. D. Olsen, L. Groth-Pedersen et al., "Transformation-associated changes in sphingolipid metabolism sensitize cells to lysosomal cell death induced by inhibitors of acid sphingomyelinase," *Cancer Cell*, vol. 24, no. 3, pp. 379–393, 2013.

[20] A. S. Don, J. H. Hsiao, J. M. Bleasel, T. A. Couttas, G. M. Halliday, and W. S. Kim, "Altered lipid levels provide evidence for myelin dysfunction in multiple system atrophy," *Acta Neuropathologica Communications*, vol. 2, p. 150, 2014.

[21] L. K. Ryland, T. E. Fox, X. Liu, T. P. Loughran, and M. Kester, "Dysregulation of sphingolipid metabolism in cancer," *Cancer Biology & Therapy*, vol. 11, no. 2, pp. 138–149, 2011.

[22] J. P. Truman, M. Garcia-Barros, L. M. Obeid, and Y. A. Hannun, "Evolving concepts in cancer therapy through targeting sphingolipid metabolism," *Biochimica et Biophysica Acta*, vol. 1841, no. 8, pp. 1174–1188, 2014.

[23] T. Kawamori, W. Osta, K. R. Johnson et al., "Sphingosine kinase 1 is up-regulated in colon carcinogenesis," *FASEB Journal*, vol. 20, no. 2, pp. 386–388, 2006.

[24] E. Le Scolan, D. Pchejetski, Y. Banno et al., "Overexpression of sphingosine kinase 1 is an oncogenic event in erythroleukemic progression," *Blood*, vol. 106, no. 5, pp. 1808–1816, 2005.

[25] V. E. Nava, J. P. Hobson, S. Murthy, S. Milstien, and S. Spiegel, "Sphingosine kinase type 1 promotes estrogen-dependent tumorigenesis of breast cancer MCF-7 cells," *Experimental Cell Research*, vol. 281, no. 1, pp. 115–127, 2002.

[26] P. Boya and G. Kroemer, "Lysosomal membrane permeabilization in cell death," *Oncogene*, vol. 27, no. 50, pp. 6434–6451, 2008.

[27] R. F. Dielschneider, H. Eisenstat, S. Mi et al., "Lysosomotropic agents selectively target chronic lymphocytic leukemia cells due to altered sphingolipid metabolism," *Leukemia*, vol. 30, no. 6, pp. 1290–1300, 2016.

[28] H. Appelqvist, L. Sandin, K. Bjornstrom et al., "Sensitivity to lysosome-dependent cell death is directly regulated by lysosomal cholesterol content," *PloS One*, vol. 7, no. 11, article e50262, 2012.

[29] M. Gyrd-Hansen, J. Nylandsted, and M. Jaattela, "Heat shock protein 70 promotes cancer cell viability by safeguarding lysosomal integrity," *Cell Cycle*, vol. 3, no. 12, pp. 1484-1485, 2004.

[30] M. S. Ostenfeld, N. Fehrenbacher, M. Hoyer-Hansen, C. Thomsen, T. Farkas, and M. Jaattela, "Effective tumor cell death by sigma-2 receptor ligand siramesine involves lysosomal leakage and oxidative stress," *Cancer Research*, vol. 65, no. 19, pp. 8975–8983, 2005.

[31] H. Zalkin, A. L. Tappel, and J. P. Jordan, "Studies of the mechanism of vitamin E action. V. Selenite and tocopherol inhibition of lipid peroxidation in the chick," *Archives of Biochemistry and Biophysics*, vol. 91, pp. 117–122, 1960.

[32] P. Xia, J. R. Gamble, L. Wang et al., "An oncogenic role of sphingosine kinase," *Current Biology : CB*, vol. 10, no. 23, pp. 1527–1530, 2000.

[33] D. L. Medina, A. Fraldi, V. Bouche et al., "Transcriptional activation of lysosomal exocytosis promotes cellular clearance," *Developmental Cell*, vol. 21, no. 3, pp. 421–430, 2011.

[34] H. Erdal, M. Berndtsson, J. Castro, U. Brunk, M. C. Shoshan, and S. Linder, "Induction of lysosomal membrane permeabilization by compounds that activate p53-independent apoptosis," *Proceedings of the National Academy of Sciences of the United States of America*, vol. 102, no. 1, pp. 192–197, 2005.

[35] S. Mena, M. L. Rodriguez, X. Ponsoda, J. M. Estrela, M. Jaattela, and A. L. Ortega, "Pterostilbene-induced tumor cytotoxicity: a lysosomal membrane permeabilization-dependent mechanism," *PloS One*, vol. 7, no. 9, article e44524, 2012.

[36] Q. Y. Chen, J. G. Shi, Q. H. Yao et al., "Lysosomal membrane permeabilization is involved in curcumin-induced apoptosis of A549 lung carcinoma cells," *Molecular and Cellular Biochemistry*, vol. 359, no. 1-2, pp. 389–398, 2012.

[37] T. Mijatovic, V. Mathieu, J. F. Gaussin et al., "Cardenolide-induced lysosomal membrane permeabilization demonstrates therapeutic benefits in experimental human non-small cell lung cancers," *Neoplasia*, vol. 8, no. 5, pp. 402–412, 2006.

[38] F. Yu, Z. Chen, B. Wang et al., "The role of lysosome in cell death regulation," *Tumour Biology : The Journal of the International Society for Oncodevelopmental Biology and Medicine*, vol. 37, no. 2, pp. 1427–1436, 2016.

[39] D. R. Green and F. Llambi, "Cell death signaling," *Cold Spring Harbor Perspectives in Biology*, vol. 7, no. 12, 2015.

[40] C. O. Eno, G. Zhao, A. Venkatanarayan, B. Wang, E. R. Flores, and C. Li, "Noxa couples lysosomal membrane permeabilization and apoptosis during oxidative stress," *Free Radical Biology & Medicine*, vol. 65, pp. 26–37, 2013.

[41] H. Appelqvist, A. C. Johansson, E. Linderoth et al., "Lysosome-mediated apoptosis is associated with cathepsin D-specific processing of bid at Phe24, Trp48, and Phe183," *Annals of Clinical and Laboratory Science*, vol. 42, no. 3, pp. 231–242, 2012.

[42] C. Oberle, J. Huai, T. Reinheckel et al., "Lysosomal membrane permeabilization and cathepsin release is a Bax/Bak-dependent, amplifying event of apoptosis in fibroblasts and monocytes," *Cell Death and Differentiation*, vol. 17, no. 7, pp. 1167–1178, 2010.

[43] Y. Akazawa, J. L. Mott, S. F. Bronk et al., "Death receptor 5 internalization is required for lysosomal permeabilization by TRAIL in malignant liver cell lines," *Gastroenterology*, vol. 136, no. 7, pp. 2365–2376, 2009, e2361-2367.

[44] M. B. Azad, Y. Chen, and S. B. Gibson, "Regulation of autophagy by reactive oxygen species (ROS): implications for cancer progression and treatment," *Antioxidants & Redox Signaling*, vol. 11, no. 4, pp. 777–790, 2009.

[45] Y. Chen, E. S. Henson, W. Xiao et al., "Tyrosine kinase receptor EGFR regulates the switch in cancer cells between cell survival and cell death induced by autophagy in hypoxia," *Autophagy*, vol. 12, no. 6, pp. 1029–1046, 2016.

[46] J. Zhang, W. Zhou, J. Lin et al., "Autophagic lysosomal reformation depends on mTOR reactivation in H2O2-induced autophagy," *The International Journal of Biochemistry & Cell Biology*, vol. 70, pp. 76–81, 2016.

[47] J. Hasegawa, I. Maejima, R. Iwamoto, and T. Yoshimori, "Selective autophagy: lysophagy," *Methods*, vol. 75, pp. 128–132, 2015.

[48] D. J. Klionsky, F. C. Abdalla, H. Abeliovich et al., "Guidelines for the use and interpretation of assays for monitoring autophagy," *Autophagy*, vol. 8, no. 4, pp. 445–544, 2012.

[49] Y. Liu, S. Shoji-Kawata, R. M. Sumpter Jr. et al., "Autosis is a Na+,K+-ATPase-regulated form of cell death triggered by autophagy-inducing peptides, starvation, and hypoxia-ischemia," *Proceedings of the National Academy of Sciences of the United States of America*, vol. 110, no. 51, pp. 20364–20371, 2013.

[50] S. J. Dixon, K. M. Lemberg, M. R. Lamprecht et al., "Ferroptosis: an iron-dependent form of nonapoptotic cell death," *Cell*, vol. 149, no. 5, pp. 1060–1072, 2012.

[51] N. Yagoda, M. von Rechenberg, E. Zaganjor et al., "RAS-RAF-MEK-dependent oxidative cell death involving voltage-dependent anion channels," *Nature*, vol. 447, no. 7146, pp. 864–868, 2007.

[52] J. D. Mancias, X. Wang, S. P. Gygi, J. W. Harper, and A. C. Kimmelman, "Quantitative proteomics identifies NCOA4 as the cargo receptor mediating ferritinophagy," *Nature*, vol. 509, no. 7498, pp. 105–109, 2014.

[53] D. L. Schonberg, T. E. Miller, Q. Wu et al., "Preferential iron trafficking characterizes glioblastoma stem-like cells," *Cancer Cell*, vol. 28, no. 4, pp. 441–455, 2015.

[54] E. R. Wood, A. T. Truesdale, O. B. McDonald et al., "A unique structure for epidermal growth factor receptor bound to GW572016 (lapatinib): relationships among protein conformation, inhibitor off-rate, and receptor activity in tumor cells," *Cancer Research*, vol. 64, no. 18, pp. 6652–6659, 2004.

[55] S. Sabella, R. P. Carney, V. Brunetti et al., "A general mechanism for intracellular toxicity of metal-containing nanoparticles," *Nanoscale*, vol. 6, no. 12, pp. 7052–7061, 2014.

[56] A. Kondratskyi, M. Yassine, C. Slomianny et al., "Identification of ML-9 as a lysosomotropic agent targeting autophagy and cell death," *Cell Death & Disease*, vol. 5, article e1193, 2014.

[57] A. R. Choi, J. H. Kim, Y. H. Woo, H. S. Kim, and S. Yoon, "Anti-malarial drugs primaquine and chloroquine have different sensitization effects with anti-mitotic drugs in resistant cancer cells," *Anticancer Research*, vol. 36, no. 4, pp. 1641–1648, 2016.

[58] I. Fernandes, N. Vale, V. de Freitas, R. Moreira, N. Mateus, and P. Gomes, "Anti-tumoral activity of imidazoquines, a new class of antimalarials derived from primaquine," *Bioorganic & Medicinal Chemistry Letters*, vol. 19, no. 24, pp. 6914–6917, 2009.

[59] Y. Zhang, Y. Li, Y. Li et al., "Chloroquine inhibits MGC803 gastric cancer cell migration via the toll-like receptor 9/nuclear factor kappa B signaling pathway," *Molecular Medicine Reports*, vol. 11, no. 2, pp. 1366–1371, 2015.

[60] P. C. Hsiao, Y. E. Chou, P. Tan et al., "Pterostilbene simultaneously induced G0/G1-phase arrest and MAPK-mediated mitochondrial-derived apoptosis in human acute myeloid leukemia cell lines," *PloS One*, vol. 9, no. 8, article e105342, 2014.

[61] Y. Zhang, Z. Liao, L. J. Zhang, and H. T. Xiao, "The utility of chloroquine in cancer therapy," *Current Medical Research and Opinion*, vol. 31, no. 5, pp. 1009–1013, 2015.

Hindawi
Oxidative Medicine and Cellular Longevity
Volume 2017, Article ID 1485283, 11 pages
https://doi.org/10.1155/2017/1485283

Review Article

Reactive Oxygen Species-Mediated Mechanisms of Action of Targeted Cancer Therapy

Hanna-Riikka Teppo,[1] Ylermi Soini,[1] and Peeter Karihtala[2]

[1]*Department of Pathology, Medical Research Center Oulu, Oulu University Hospital and University of Oulu, Oulu, Finland*
[2]*Department of Oncology and Radiotherapy, Medical Research Center Oulu, Oulu University Hospital and University of Oulu, Oulu, Finland*

Correspondence should be addressed to Peeter Karihtala; peeter.karihtala@oulu.fi

Received 10 March 2017; Revised 15 May 2017; Accepted 21 May 2017; Published 18 June 2017

Academic Editor: Spencer Gibson

Targeted cancer therapies, involving tyrosine kinase inhibitors and monoclonal antibodies, for example, have recently led to substantial prolongation of survival in many metastatic cancers. Compared with traditional chemotherapy and radiotherapy, where reactive oxygen species (ROS) have been directly linked to the mediation of cytotoxic effects and adverse events, the field of oxidative stress regulation is still emerging in targeted cancer therapies. Here, we provide a comprehensive review regarding the current evidence of ROS-mediated effects of antibodies and tyrosine kinase inhibitors, use of which has been indicated in the treatment of solid malignancies and lymphomas. It can be concluded that there is rapidly emerging evidence of ROS-mediated effects of some of these compounds, which is also relevant in the context of drug resistance and how to overcome it.

1. Introduction

There has been significant progress in the development of novel oncological treatments during the last decade. However, radiotherapy and traditional chemotherapy still form the backbone of treatment in most malignancies. The importance of conventional cytotoxic chemotherapy is underlined in adjuvant treatments, where only trastuzumab and imatinib are currently approved in HER2- (human epidermal growth factor receptor 2-) positive early breast cancer and Kit-positive gastrointestinal stromal tumour (GIST) treatments, respectively. In metastatic disease, nevertheless, targeted cancer therapy has prolonged survival significantly. This has been observed especially in HER2-overexpressing breast cancer, renal cell carcinoma (RCC), GISTs, melanoma, and colorectal cancer (CRC) [1–5]. In several metastatic cancer trials, there have been plateaus in survival curves in patients treated with targeted therapies, even after relatively long follow-up periods. The current paradigm still suggests that metastatic cancer is curable extremely rarely and that drug resistance ultimately develops [6].

Reactive oxygen species (ROS) are a set of highly reactive molecules comprising singlet oxygen ($^1O_2$), superoxide ($O_2^{\bullet-}$), hydroxyl radical ($OH^{\bullet}$), and hydrogen peroxide (H_2O_2). They have crucial roles in both physiological functions and tumour development [7]. Production of ROS is elevated in malignant compared with benign tissues as a result, for example, of increased metabolic rate, oncogene activation, and defective vasculature, leading to hypoxic areas, but several lines of evidence suggest that cancer tissues may upregulate levels of antioxidant enzymes to counteract increased oxidative stress, as reviewed elsewhere [8–10]. Excess ROS are quenched by enzymatic antioxidants such as superoxide dismutase (SOD), catalase, glutathione (GSH), and peroxiredoxins (Prxs) and nonenzymatic antioxidants such as vitamins E and A [8]. In addition, enzymes such as thioredoxin-1 (Trx-1) and GSH are able to restore REDOX-sensitive proteins to their proper function by reducing the cysteine residues within these proteins [10]. The expression of antioxidant proteins is controlled by the major antioxidant response regulator nuclear factor erythroid 2-related factor 2 (NFE2L2). NFE2L2 is activated during oxidative and

electrophilic stress and released from its inhibitory molecule Kelch-like ECH-associated protein 1 regulator (Keap1) [10].

The effectiveness of traditional cancer chemotherapy is largely based on the generation of ROS and consequently on the increase of oxidative stress that exceeds the reduction capacity of cancerous tissue, leading ultimately to apoptosis or necrosis [10]. Also, many adverse effects of chemotherapy are due to excess ROS production in healthy tissues, such as anthracycline-mediated cardiotoxicity, and nephrotoxicity triggered by platinum compounds [11, 12]. Up to 50% of patients with cancer receive radiotherapy at some stage of their illness [13]. Both therapeutic and side effects of ionizing radiation during radiotherapy are mainly based on the interaction of $OH^{\bullet}$ with target tissue DNA [14].

Targeted cancer therapy mostly involves monoclonal antibodies, small-molecule tyrosine kinase inhibitors (TKIs) and, more recently, immunotherapies. In a broad context, some hormonal therapies such as tamoxifen therapy [15] can also be included in this category, but they are not discussed in this review. The rationale for targeted cancer therapies is to specifically disrupt certain upregulated pathways in malignant cells. Theoretically, this could lead to more effective cancer cell death, with less harmful effects. However, the compounds concerned have drug-specific and sometimes life-threatening adverse effects, and therefore, combinations of these treatments are often limited in a clinical setting [16]. At first, targeted cancer therapies were considered to be promising magic bullets with single targets [17, 18], but their wider clinical use has produced much information about their diverse mechanisms of action and development of drug resistance, where also ROS could have a substantial role.

In this paper, we will review the current evidence of ROS-mediated effects of antibodies and tyrosine kinase inhibitors that have European Medicines Agency (EMA) approval as regards the treatment of solid malignancies or lymphomas. Originally, we also aimed to address oncoimmunological compounds, but the ROS-mediated effects of these compounds are still largely unknown. Since most of the drugs discussed in this review are novel, the research field has so far been uncoordinated and somewhat sporadic. However, regarding some of the compounds concerned, there is rapidly emerging evidence of ROS-mediated effects and adverse effects. As far as we know, no previous reviews on this topic exist.

2. Tyrosine Kinase Inhibitors

Tyrosine kinase inhibitors are compounds of small molecular weight. Their small size enables oral administration of the drugs and effective penetrance through cell membranes, after which they exert their functions intracellularly. The main mechanism of action of all TKIs is competitive adenosine triphosphate inhibition at the catalytic binding site of tyrosine kinase, but TKIs differ considerably in their specificity against different kinases [19]. There are currently nearly 20 EMA-approved TKIs for the treatment of solid tumours or lymphomas, and the list is expanding rapidly (http://ema.europa.eu).

2.1. Sunitinib, Pazopanib, and Sorafenib. Sunitinib was the first TKI approved for the treatment of advanced/metastatic RCC (in 2006), and currently, there are also indications for its use in the treatment of imatinib-resistant GISTs and pancreatic neuroendocrine carcinomas. Sunitinib is one of the most commonly administered TKIs in clinical practice. The main mechanism of action is mediated by effective blocking of vascular endothelial growth factor receptors (VEGFRs) 1–3, platelet-derived growth factor receptor-α (PDGFR-α) and PDGFR-β, and c-Kit [20]. Possible ROS-mediated cytotoxic effects of sunitinib have been evaluated, but results consistently demonstrate that there is no connection between ROS and cytotoxic effects, nor an association with sunitinib-induced vasoconstriction [21–23]. Indeed, there is evidence that sunitinib may even act as an antioxidant by ameliorating lipid peroxidation and increasing GSH levels in cisplatin-treated mice (Figure 1). This not only reduces oxidative stress-triggered side effects but also improves chemotherapy efficacy [24] (Table 1). Sunitinib also inhibits the activity and expression of neuronal nitric oxide synthase (NOS), which has been associated with the neuroprotective effects of sunitinib in vitro and also with reduced vasodilation in animal experiments [25, 26]. Sunitinib combined with chloroquine increases inducible NOS, leading to an increase in reactive nitrogen species and apoptosis while, on the other hand, the increased level of GSH abrogates apoptosis [27]. Whether these effects are relevant as regards tumour growth remains unclear on the basis of the current literature. Interestingly, sunitinib induces incomplete autophagy in bladder-cancer cell lines but does not induce mitochondrial depolarization or the induction of ROS and rather targets lysosomes and induces lysosome-dependent cell death [22].

Pazopanib is also a wide-range TKI, which blocks not only VEGFRs, PDGFRs, and c-Kit, like sunitinib, but also targets fibroblast growth factor receptors-1 (FGFRs-1) and FGFRs-3, IL-2-inducible T-cell kinase, lymphocyte-specific protein tyrosine kinase, and macrophage colony-stimulating factor 1 receptor (c-Fms). Pazopanib is less well studied as regards the topic of this review, but at least pazopanib-triggered erythrocyte apoptosis has been suggested to be dependent on oxidative stress [28]. Another TKI, axitinib, has been indicated for the treatment of RCC. Besides its VEGFR-targeted effects, it also induces oxidative DNA damage, leading to mitotic catastrophe and a cellular senescence program. This further promotes natural killer (NK) cell-mediated recognition and elimination of RCC through the regulation NK-activating ligand expression [29]. This data has linked axitinib-mediated oxidative stress to its immunomodulatory effects, which is especially relevant in RCC, one of the most immunogenic cancers [30].

Sorafenib is multikinase inhibitor that blocks VEGFR-2 and VEGFR-3, PDGFR-β, and RAF-kinases, for example, consequently inhibiting proliferation and angiogenesis. Sorafenib is currently indicated for the treatment of metastatic RCC, hepatocellular carcinoma (HCC), and radioiodine refractory, differentiated thyroid cancer. Interestingly, the effectiveness of sorafenib is widely reliant on kinase-independent, ROS-mediated mechanisms, especially in mitochondria. In HCC HepG2 cell lines, sorafenib induces a significant

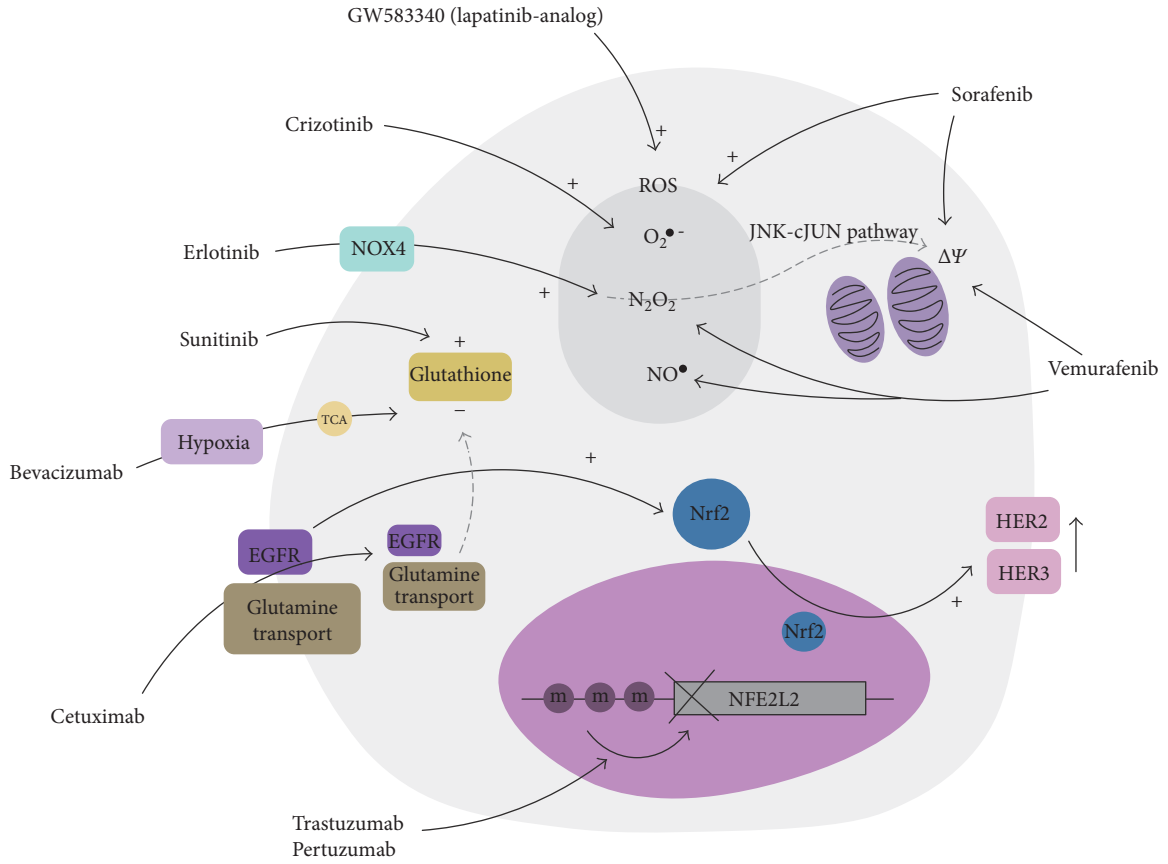

Figure 1: Expected ROS-mediated effects of targeted therapies. In addition to the respective signalling pathway that a targeted agent affects, the diagram represents their putative ROS-related effects. CRC: colorectal cancer; GISTs: gastrointestinal stromal tumours; RCC: renal cell carcinoma; ROS: reactive oxygen species; $O_2^{\bullet -}$: superoxide; H_2O_2: hydrogen peroxide; NO•: nitric oxide; ΔΨ: mitochondrial membrane polarity; TCA: tricarboxylic acid cycle; m: methylation; NFE2L2: nuclear factor erythroid 2-related factor 2.

increase in the production of ROS, mainly in mitochondria, which is followed by a rapid and deep depletion of GSH in the mitochondria, cytoplasm, and nuclei [31]. Coriat et al. demonstrated later that sorafenib particularly induces the production of H_2O_2, $O_2^{\bullet -}$, and nitric oxide in HepG2 cells [32]. Superoxide dismutase (SOD) mimics efficiently inhibited the antiproliferative and cytotoxic effects of sorafenib and increased tumour growth in mice, while H_2O_2 and NO• inhibitors had no effect on sorafenib cytotoxicity. Intriguingly, the authors consequently confirmed, in the series of HCC patients, that higher serum levels of advanced oxidation production proteins were predictive of prolonged relapse-free survival and overall survival. In another recent paper, it was suggested that sorafenib brought about elevated ROS production and inhibited mitochondrial respiration, and gene expression profiling also revealed that sorafenib led to a substantial change toward aerobic glycolysis [33]. In line with this, glucose withdrawal or glycolytic inhibitor dramatically improved sorafenib cytotoxicity. It thus appears that mitochondrial dysfunction and $O_2^{\bullet -}$ production play a significant role in sorafenib treatment, facts that allow possible predictive biomarkers and combination treatments to be assessed in future clinical trials. Indeed, in a recent article, sorafenib was shown to disrupt the mitochondrial membrane potential in RCC, leading to increased ROS and thus breaking resistance to TRAIL-induced apoptosis [34]. Some compounds such as melatonin may increase the therapeutic action of sorafenib and induce further ROS increase during administration of both compounds [35].

2.2. Crizotinib. Recent landmark trials showed a huge improvement in progression-free survival of crizotinib-treated patients with anaplastic lymphoma kinase (ALK) translocation, metastatic non-small-cell lung cancer (NSCLC) and thereafter changed the treatment of this disease [36, 37]. Although the efficacy of crizotinib is thought to be specific to ALK inhibition, crizotinib also exerts its functions via the generation of $O_2^{\bullet -}$ and activation of an apoptotic cascade that contributes to cardiomyocyte toxicity in vitro [23]. Accumulation of ROS after crizotinib treatment, somewhat nonspecifically measured by using the general oxidative stress indicator H_2DCFDA, has been also been reported in human alveolar rhabdomyosarcoma cells [38]. The established cancer stem-cell marker, aldehyde lactate dehydrogenase (ALDH), protected TKI (crizotinib and erlotinib)-resistant cells from TKI-derived ROS toxicity in cell lines [39]. Again, pharmacological disruption of ALDH activity with disulfiram led to accumulation of ROS to toxic

Table 1: The most important redox-associated targeted cancer therapy compounds with EMA-approved indications for the treatment of solid tumours or lymphomas. All indications are for metastatic or inoperable carcinomas if not otherwise mentioned.

Drug	EMA-approved indication in solid tumours	Main targets	Role in redox system
Afatinib	EGFR-mutated NSCLC	EGFR	Chronic oxidative stress associated with resistance.
Axitinib	RCC	VEGFR1–3, PDGFR, c-Kit	Oxidative stress-mediated genotoxic effects.
Bevacizumab	CRC Breast cancer NSCLC Ovarian cancer Peritoneal cancer RCC	VEGF	Increases ROS levels. Combined with autophagy inhibitor enhances ROS levels and apoptosis.
Cetuximab	HNSCC CRC	EGFR	Reduces the amount of GSH by internalizing EGFR and glutamine transport. Decreases Nox1 and Nox1-related effect of oxaliplatin.
Crizotinib	ALK-positive NSCLC	ALK, c-MET	Increased $O_2^{\bullet-}$ production linked with cardiotoxicity. Prx II up-regulation associated with resistance.
Erlotinib	EGFR-mutated NSCLC Pancreatic cancer	EGFR	Increases ROS-mediated apoptosis in HNSCC and NSCLC.
Gefitinib	EGFR-mutated NSCLC	EGFR	Increases oxidative stress linked to EMT and cardiotoxicity. NFE2L2/Keap1-axis related to treatment resistance.
Imatinib	GISTs	PDGFRα, KIT, ABL, CSF-1 receptor	Induces ROS-dependent apoptosis in melanoma.
Lapatinib	HER2-positive breast cancer	HER1, HER2	Increases ROS; low ROS levels linked with resistance, which may be overcome with antioxidant mimics.
Pazopanib	RCC, sarcomas	Various kinases, for example, VEGFR1–3, (PDGFR-α and PDGFR-β), c-Kit, FGFR-1, and FGFR-3	May induce oxidative DNA damage-mediated erythrocyte apoptosis.
Rituximab	Non-Hodgkin's lymphoma	CD-20	CD20 stimulation leads to the production of $O_2^{\bullet-}$.
Sorafenib	HCC, RCC, radioiodine-refractory thyroid cancer	Various kinases, for example, VEGFR-2 and VEGFR-3, PDGFR-β, and RAF-kinases	Increases oxidative stress, which possibly is a predictive factor for sorafenib
Sunitinib	GISTs, pancreatic NET, RCC	Various kinases, for example, VEGFR1–3, (PDGFR-α and PDGFR-β), c-Kit	Enhances antioxidant defence, decreases NOS activity and expression.
Trastuzumab	HER2-positive breast cancer and HER2-positive gastric cancer	HER2 dimerization	Regulatory loop with *NFE2L2* NFE2L2 increases trastuzumab resistance.
Vemurafenib	BRAF (V600E) mutated melanoma	BRAF V600E	Increases $NO^{\bullet}$ and $O_2^{\bullet-}$ production increases depolarization of mitochondrial membranes. Induces PGC1α

levels, consequent DNA damage, and apoptosis. These results have not been tested yet in vivo, but if confirmed, modulation of ROS levels could boost the therapeutic effects of crizotinib.

2.3. Erlotinib, Gefitinib, and Afatinib. Gefitinib and erlotinib are TKIs targeted against epidermal growth factor receptor (EGFR) and are approved for the treatment of NSCLC in the first and subsequent lines of therapy. The mechanism of action allows drugs to act only in tumours with activating EGFR mutations, which are found in 10–15% of Caucasian patients. Afatinib is another EGFR-targeted TKI, which has also proven to have activity against T790 M EGFR mutation [40]. Although targeted specifically against EGFR, EGFR-independent mechanisms of action of these drugs have also been reported. Of these three compounds, erlotinib and gefitinib in particular have been linked to oxidative stress in recent literature.

As mentioned above, ALDH-mediated protection against ROS has been connected with erlotinib resistance [39]. In those experiments, erlotinib indeed enhanced ROS production even more considerably than crizotinib. In NSCLC A549 cell lines, erlotinib induced ROS-mediated apoptosis via activation of the c-Jun N-terminal kinase (JNK) pathway, leading ultimately to EGFR inhibition and a therapeutic response. As expected, it was possible to reverse this

phenomenon by way of administration of the ROS scavenger N-acetyl cysteine [41, 42].

In recent papers, gefitinib has also been demonstrated to produce a dose-dependent increase in oxidative stress, which has been associated with induced epithelial-mesenchymal transition and cardiotoxicity of this EGFR-targeted TKI [43, 44]. In gefitinib-resistant A549 cells, Prx II was highly upregulated via demethylation of the Prx II gene when compared with the gefitinib-sensitive A549 cell line [45]. Elevated Prx II expression resulted in downregulation of ROS, attenuated apoptosis, increased colony formation, and cell cycle progression in gefitinib-resistant cells, factors that were recovered with Prx II mRNA knockdown. Prx II thus emerges as a potentially targetable factor for overcoming gefitinib resistance. In theory, this may also apply to other EGFR-targeted TKIs, although they have not yet been assessed from this perspective.

Abnormal NFE2L2-Keap1regulation has been associated with the acquisition of resistance to traditional chemotherapy and also to poor prognosis in NSCLC [46, 47]. Recently, NFE2L2 has been characterized as being essentially important in EGFR TKI resistance. In a study by Leone et al. [48], a strong synergistic effect of the histone deacetylate inhibitor vorinostat and EGFR TKIs led to remarkably enhanced antiproliferative and proapoptotic effects of EGFR TKIs, possibly due to underlying changes in REDOX homeostasis. When vorinostat was administered with erlotinib or gefitinib, NFE2L2 levels were notably attenuated via c-Myc downregulation, and simultaneously, Keap1 upregulation was observed.

The EGFR pathway is able to activate NFE2L2 in EGFR wild-type NSCLC after ligand-receptor binding. Also, activation of downstream signalling of the mutated EGFR pathway leads to constitutive expression of NFE2L2. Exposure to oxidative stress in the form of cigarette smoke extract was found to attenuate EGFR-TKI cytotoxicity in EGFR-mutated NSCLC due to oxidative stress-related NFE2L2 activation. Based on their experiments, the authors also hypothesized that inactivating Keap1 mutations could be used as predictive factors of EGFR TKI resistance, which is also supported by very recent results in a paper by Krall et al. [49, 50]. If this could be confirmed in a prospective clinical trial, it would allow more optimal selection of patients for these costly and potentially toxic treatments and development of more specific molecular targets to overcome resistance.

In line with results concerning other EGFR-targeted TKIs in NSCLC, erlotinib also elicits cytotoxicity via oxidative stress generation in head and neck squamous cell carcinoma (HNSCC) cell lines, again being reversible with N-acetyl cysteine [51]. In these experiments, the source of oxidative stress was reported as NADPH oxidase 4-induced H_2O_2 production. Afatinib is a less well studied EGFR-targeted TKI, but chronic oxidative stress has been connected to the development of afatinib resistance [52].

2.4. Vemurafenib. Vemurafenib was the first BRAF inhibitor to be used in the treatment of inoperable or metastatic melanoma. Despite the overall survival benefit when set against dabrafenib [53], acquired resistance is also a major clinical problem with this drug, and it occurs in virtually all patients sooner or later. Vemurafenib acts by targeting the most common genetic alteration in melanomas, BRAF V600E, and thus it suppresses the RAS/MEK/ERK signalling pathway and accordingly cell proliferation and adhesion. As an additional mechanism of action, vemurafenib stimulates $NO^{\bullet}$ and $O_2^{\bullet -}$ production and it also induces depolarization of mitochondrial membranes in BRAF V600E-mutated melanoma cells, potentially initiating apoptosis and growth inhibition [54, 55]. Intrinsic high rates of mitochondrial respiration and oxidative stress of vemurafenib-resistant melanomas have been harnessed to overcome resistance to prooxidants, the administration of which leads to notably increased cell death in these already oxidatively stressed cells [56]. On the other hand, in a recent paper by Luo and colleagues [57], vemurafenib was neatly demonstrated to suppress the metastatic potential of melanoma by inducing the oxidative stress regulator PGC1α (peroxisome proliferator-activated receptor-gamma coactivator-1α) and further suppressing the expression of most integrins. The phenomenon was independent of the cytostatic effect of vemurafenib. All in all, vemurafenib appears to have notable and partly ROS-dependent therapeutic effects, which are independent of BRAF V600E inhibition. As far as we know, no data currently exists about another approved BRAF V600E inhibitor, dabrafenib, and ROS-mediated effects.

2.5. Lapatinib. Lapatinib is the only TKI approved for treatment of breast cancer, more specifically its HER2-overexpressing subtype. HER2 is an acquired oncogene that is overexpressed in 20–30% of breast cancer patients. This receptor tyrosine kinase (RTK) drives prosurvival and proliferation signalling, and HER2 expression in breast cancer is associated with aggressive disease and resistance to chemotherapy. Increased ROS levels have been reported after treatment with a lapatinib analogue (GW583340) in inflammatory breast cancer models. In contrast, extremely low ROS levels have been observed in GW583340-resistant models, probably resulting from increased SOD1, SOD2, and GSH expression in lapatinib-resistant breast cancer cells. Elevated antioxidant expression also correlated with decreased lapatinib-analogue efficacy and, most interestingly, from a therapeutic point of view, a SOD mimic was able to overcome resistance in GW583340-sensitive cells [58]. Similarly, Zhang and colleagues [59] demonstrated NFE2L2-mediated ROS suppression in another lapatinib-resistant breast cancer cell line. Also in this work, lapatinib resistance was overcome with ROS level downregulation. In theory, these results could potentially provide a basis for reversing lapatinib resistance by way of ROS level suppressors.

2.6. Imatinib. Up to 90% of GISTs harbour activating mutations in platelet-derived growth factor receptor-α (PDGFR-α) or KIT (CD117) genes. Besides these, imatinib also targets other tyrosine kinases such as ABL and colony-stimulating factor-1 receptor. Imatinib has EMA approval for the treatment of KIT-positive GISTs (in both adjuvant and metastatic settings), inoperable dermatofibrosarcoma protuberans, and chronic myeloid leukaemia (CML). Most of the data relating

to the ROS-mediated mechanisms of imatinib are based on leukaemia material, but this is not in the scope of this review. However, auranofin, a gold-containing chemical applied for treatment of rheumatoid arthritis, inhibits thioredoxin reductase, inducing ROS formation and in this way dramatically inhibiting GIST cell growth, and it also induces apoptosis in imatinib-resistant cells [60]. ROS-dependent apoptosis has also been reported in melanoma cell lines after imatinib treatment [61].

3. mTOR Inhibitors

Two mammalian target of rapamycin (mTOR) inhibitors, everolimus and temsirolimus, have been approved for treatment of cancer. The oncological indications for everolimus are rapidly widening, and currently, it is used in the treatment of advanced/metastatic breast cancer, RCC, and neuroendocrine carcinomas of lung, pancreatic, or gastrointestinal origin. mTOR inhibitors are also applied in the treatment of graft-versus-host reactions after organ transplants. The available evidence of ROS-mediated effects of mTOR inhibitors is derived solely in connection with everolimus, virtually only concentrating on it as an immunosuppressant, not as an oncological compound. Animal and patient studies are still contradictory in this field. Decreased serum and plasma concentrations of malondialdehyde, protein carbonyls, and oxidized LDL have been reported after both short- and long-term everolimus dosing [62, 63], while after kidney ischaemia/reperfusion injury everolimus was noted to promote both oxidative and nitrosative stress [64]. Thus, based on current information, mTOR inhibitors do not appear to have substantial ROS-mediated roles in the treatment of malignancies, but the field is still understudied.

4. Monoclonal Antibodies

4.1. Trastuzumab and Pertuzumab. Trastuzumab is a monoclonal antibody that blocks HER2 dimerization with other HER partners, evokes antibody-dependent cellular cytotoxicity, and inhibits MAPK and PI3K/Akt pathways (Vu et al. 2012). Pertuzumab, another humanized monoclonal antibody, inhibits HER2 dimerization with other HER family receptors and significantly enhances the cytotoxicity mediated by trastuzumab in a clinical setting [1]. Trastuzumab is indicated in the (neo) adjuvant therapy of breast cancer and it also has approval in a metastatic setting in HER2-positive gastric and breast cancer. Pertuzumab is indicated in combination with trastuzumab to enhance the anti-HER efficacy, both in neoadjuvant and metastatic settings.

NFE2L2 regulation has a relevant role in RTK signalling and in anti-HER therapies. It has been demonstrated that NFE2L2 positively regulates HER2 and HER3 gene transcription and protein expression, and further, pAKT levels in an ovarian cancer cell line. SiRNA inhibition of NFE2L2 directly inhibited the transcription of HER2 [65, 66]. To further support the crosstalk between these two players, combination treatment with trastuzumab and pertuzumab led to the inhibition of NFE2L2 by promoter methylation. Pharmacological activation of NFE2L2 protected cells from the cytotoxic effect of trastuzumab-pertuzumab treatment and resulted in antioxidant induction. This further emphasizes the notion that NFE2L2 functions as an oncogene and has a major part in evolving drug resistance, even in antibody-based treatment.

Despite the fact that tumour cells and tissue have an increased antioxidant capacity [10], primary and metastatic HER2-positive breast cancer patients have a decreased antioxidant status in their blood, which is restored with trastuzumab combined with chemotherapy up to the levels of healthy controls [67]. On the flip side of (highly effective) trastuzumab treatment, deleterious effects on cardiomyocytes have been widely reported in the literature. Blocking HER2 receptors induces cardiomyocyte death through a mitochondrial pathway that is dependent on ROS and can be reversed by inhibiting Bax and Bac proteins that mediate cell death through this pathway [68].

Just as in any other anticancer therapy, resistance to trastuzumab treatment frequently occurs. One of the putative mechanisms that involves oxidative stress regulation behind trastuzumab resistance is loss of function of the tumour suppressor PTEN due to increased levels of reduced Trx-1 protein. Trx-1 binds to PTEN, enabling full AKT signalling and cell growth, and trastuzumab-resistant cells gained drug sensitivity after treatment with the Trx-1 inhibitor 1-methylpropyl 2-imidazolyl disulphide (PX-12) [69]. Trastuzumab resistance is an immense clinical problem, especially in HER2-positive metastatic breast cancer and in vivo studies with PX-12 to overcome this resistance represent a reasonable step in the future.

Reactive oxygen species also seem to be involved in the regulation HER2 expression after radiation, at least in vitro. Wattenberg and colleagues [70] recently reported that radiation exposure increased cell surface and total protein expression of HER2, EGFR, and CD20 in breast cancer, HNSCC, and non-Hodgkin lymphoma (NHL) cell lines, respectively. HER2 upregulation was mediated for the most part via intracellular production of ROS. Radiation-induced expression led to enhanced antibody-dependent cell-mediated cytotoxicity (ADCC) when breast cancer cells were treated with trastuzumab.

4.2. Rituximab. Rituximab is a chimeric humanized monoclonal antibody specific to CD20. CD20 is an integral transmembrane phosphoprotein present on the surface of precursor B-cells, maturing B-cells, and differentiated plasma cells. It is described to be a calcium-channel protein, and binding of rituximab to CD20 causes subsequent calcium influx and downstream apoptotic signalling [71].

Rituximab is indicated in the treatment of NHL and other B-cell malignancies. It sensitizes B-cell lymphoma cells to standard anticancer drugs and restores drug sensitivity of NHL cells via downregulation of antiapoptotic factors, such as Bcl-2, and inhibition of survival signalling of the p38 MAPK signal pathway [72]. In addition, combining irradiation with rituximab to treat a Burkitt's lymphoma cell line was shown to be effective in triggering cell-cycle arrest and apoptosis and bringing about an increase in intracellular ROS levels [72]. Thus, the efficacy of rituximab-combination therapies is often due to the synergy of oxidative stress damage

caused by traditional anticancer strategies and the proapoptotic process triggered by rituximab.

In addition to the proapoptotic features of anti-CD20 treatment, rituximab-mediated complement-dependent cytotoxicity involves ROS production, more specifically $O_2^{\bullet-}$ [73]. Wang et al. studied a highly conserved antiapoptotic molecule, phosphatidylethanolamine-binding protein (hPEBP) and its role in rituximab resistance. It was shown that hPEBP4 was overexpressed in the majority of NHL patients and it inhibited rituximab-mediated complement-dependent cytotoxicity, calcium influx, and ROS generation. Knockdown of hPEBP4 potentiated the chemosensitization effect of rituximab during topoisomerase I inhibitor treatment [74].

In a study by Alinari et al. [75], rituximab was combined with the anti-CD74 antiproliferative agent milatuzumab to test their potential efficacy on mantle cell lymphoma cells isolated from patients. CD74 is a glycoprotein associated with major histocompatibility complex (MHC) class II and functions as an accessory signalling and survival molecule. The study showed that the cytotoxicity of the combination treatment was partially dependent on ROS formation and mitochondrial membrane dysfunction. The results showed that cell death was not due to classic apoptosis nor autophagic mechanisms, and they suggest that cytoskeletal features and antibody capping might be influential factors in increasing the intracellular ROS burst and the loss of mitochondrial membrane polarity. This drug combination was later tested in a phase I/II trial, showing activity in heavily pretreated patients with relapsed or refractory indolent NHL [76].

4.3. Bevacizumab. Bevacizumab is a recombinant, humanized monoclonal antibody that targets VEGF, inhibiting ligand binding to VEGFR and ultimately inhibiting neoangiogenesis and vascular leakiness. Bevacizumab is approved for the treatment of CRC and NSCLC, for example. However, the results of antiangiogenic treatment have been disappointing in many cases. Fack and colleagues [77] studied the adaptation of glioblastoma to bevacizumab treatment. Researchers observed that while bevacizumab causes hypoxia in tumours, on the downside, cell metabolism is reprogrammed toward anaerobic metabolism, favouring lactate production. L-cysteine, l-cystathione, and GSH levels were reduced, indicating that oxidative stress levels increased after bevacizumab treatment. This is also expectable in tumours with insufficient vascularization.

Metabolic stress under hypoxia caused by antiangiogenic treatment also upregulates autophagy, which is a means to escape from metabolic stress. There is some evidence that inhibition of autophagy enhances the efficacy of bevacizumab via alteration of the redox balance. In a human HCC study [78], autophagy inhibition led to increased apoptosis and elevated ROS levels during nutrient starvation and hypoxia. Combined treatment with autophagy inhibitor and bevacizumab led to enhanced reduction of xenograft tumour growth. Researchers observed that bevacizumab- and chloroquine-treated cells expressed more 8-hydroxydeoxyguanosine, a marker of DNA oxidative stress damage, than either agent alone. The main conclusion was that autophagy modulates ROS levels, and this could be an efficient way to enhance antiangiogenic treatment. In retinal cells exposed to H_2O_2 and bevacizumab, increased bevacizumab concentrations decreased bcl-2 mRNA and increased apoptosis, implying that oxidative stress levels influence the effect of bevacizumab on apoptosis [79].

4.4. Cetuximab. EMA-approved indications for cetuximab are CRC and HNSCC. Cetuximab is a recombinant monoclonal antibody designed to target EGFR and is applicable if the downstream signalling pathway does not harbour activating mutations, such as Ras, which are frequent in colorectal cancer. EGFR is overexpressed in 90% of cases of HNSCC.

In addition to MAPK signalling blockade, EGFR inhibition might lead to additional mechanisms that affect cell survival. Lu and colleagues [80] described how cetuximab downregulated a complex in the cell cytoplasmic membrane formed by a glutamine transport protein, ASCT2, and EGFR via endocytosis in HNSCC cell lines. Internalization of glutamine receptor led to decreased glutamine, which is necessary for GSH synthesis, and resulted in decreased ROS-reducing capacity. Increased oxidative stress via this mechanism induced apoptosis independent of EGFR-pathway downregulation. Combined use of oridonine and cetuximab suppressed phosphorylated EGFR formation, increasing ROS and apoptosis in laryngeal carcinoma cells [81].

Conflicting data exists regarding the efficacy of oxaliplatin, one of the most applied chemotherapeutic agents in CRC, and cetuximab, when they are used in combination treatments. Results favouring this combination suggest that cetuximab inhibits DNA repair mechanisms to support oxaliplatin efficacy [82, 83]. In contrast to this, several phase III randomized clinical trials have revealed that despite a survival benefit when cetuximab or oxaliplatin are added to chemotherapy backbones as single agents, their combination does not increase survival [84–86]. An experimental study by Dahan and colleagues [87] showed that cetuximab has an antagonizing effect on oxaliplatin in CRC. The effect of oxaliplatin is dependent on Nox1-evoked ROS formation. When EGFR and the downstream Ras/Nox1 cascade were inhibited by cetuximab, ROS formation decreased and oxaliplatin efficacy was lost. Similar results not favouring the combination were reported by Santoro and colleagues [88]. The efficacy of oxaliplatin in causing apoptosis was ROS-dependent and occurred via signal transducer and activator of transcription 1 (STAT1) and dual oxidase 2 (DUOX2), but cetuximab caused DUOX2 inhibition and p38 activation, reducing the cytotoxicity of oxaliplatin.

5. Conclusions

Although new targeted treatments have produced significant leaps ahead in the treatment of solid malignancies and lymphomas, their prolonged use is often limited due to the acquisition of resistance, contributing eventually to treatment failure in metastatic disease. There is a significant clinical need for more accurate predictive factors as regards these drugs, to avoid both clinical and financial toxicity [89].

Based on this review of the literature, monoclonal antibodies and TKIs seem to have many ROS-mediated

mechanisms of action, which may be related to their efficacy and also to toxicity. The majority of the reviewed targeted therapy agents increase the oxidative stress burden up to a level that is likely to surpass the reduction capacity of cancerous cells. In this way, they possess antitumour efficacy in addition to their targeted impact. Such agents were anti-VEGFR-PDGFR TKIs (axitinib, pazopanib, and sorafenib), anti-EGFR TKIs (afatinib, erlotinib, and gefitinib), anti-ALK (crizotinib), anti-HER2 TKI (lapatinib), anti-BRAF TKI (vemurafenib), and anti-VEGFR antibody (bevacizumab). They all target cell membrane-related protein structures, RTKs, or associated proteins, with the purpose of conveying external messages into the cell. Not surprisingly, they are also associated with reactive oxygen molecules that can function as second messengers [90].

Some agents such as trastuzumab and pertuzumab inhibit the major redox response regulator NFE2L2. In contrast, increased levels of NFE2L2 and upregulation of other antioxidants lead to tolerance to oxidative stress, a sign that is also related to therapy resistance. Such cases are noted in anti-EGFR and anti-HER2 therapies (trastuzumab, lapatinib), while in the case of vemurafenib, antioxidant upregulation seems to have therapeutic effects. Sunitinib and cetuximab might also have beneficial effects for cancerous tissue via upregulated GSH levels.

On the other hand, as regards many drugs such as the TKIs regorafenib, lenvatinib, and dabrafenib and the monoclonal EGFR inhibitor panitumumab, there is a total lack of evidence of ROS-mediated actions, or these agents remain unstudied from this perspective. The efficacy of the monoclonal anti-CD20 antibody rituximab has been widely studied in non-Hodgkin's lymphoma and leukaemia models in combination with traditional cytotoxic agents and irradiation. Its additive effect is often mediated via the Bcl-2-related mitochondrial apoptotic pathway, enhancing ROS-related cytotoxicity of conventional antitumour therapies [91, 92], but it also increases intracellular oxidative stress and results in a loss of mitochondrial membrane potential.

Rather surprisingly, we did not find any original articles describing ROS-mediated effects of novel oncoimmunological agents such as the CTLA-4 inhibitor ipilimumab or programmed death (PD-1) antibodies such as pembrolizumab or nivolumab. However, a reasonable amount of data exists to point out that an oxidative milieu has an enormous impact on tumour cells, tumour-infiltrating lymphocytes, and other immune cells (and their interactions). It is plausible that these agents have direct ROS-dependent mechanisms arising from interactions between PD-1 antibodies and ROS generation [93]. Since ROS levels and redox status have potential as prognostic or predictive factors of immunotherapy, studies addressing these issues are eagerly awaited.

In conclusion, many TKIs and monoclonal antibodies seem to mediate their effects (and adverse effects) via ROS, and therefore, it is essential to accelerate more systematic studies in this field. In addition, we should further study the potential antagonizing effects of targeted therapies when they are combined with traditional chemotherapeutic agents, as discussed in the context of cetuximab.

Conflicts of Interest

The authors declare that there are no conflicts of interest regarding the publication of this article.

References

[1] S. M. Swain, J. Baselga, S. B. Kim et al., "Pertuzumab, Trastuzumab, and docetaxel in HER2-positive metastatic breast cancer," *The New England Journal of Medicine*, vol. 372, pp. 724–734, 2015.

[2] C. Brown, "Targeted therapy: an elusive cancer target," *Nature*, vol. 537, pp. S106–S108, 2016.

[3] S. Bauer and H. Joensuu, "Emerging agents for the treatment of advanced, imatinib-resistant gastrointestinal stromal tumors: current status and future directions," *Drugs*, vol. 75, pp. 1323–1334, 2015.

[4] C. Franklin, E. Livingstone, A. Roesch, B. Schilling, and D. Schadendorf, "Immunotherapy in melanoma: recent advances and future directions," *European Journal of Surgical Oncology*, vol. 43, pp. 604–611, 2017.

[5] S. Y. Lee and S. C. Oh, "Advances of targeted therapy in treatment of unresectable metastatic colorectal cancer," *BioMed Research International*, vol. 2016, Article ID 7590245, 14 pages, 2016.

[6] A. M. Tsimberidou, A. M. Eggermont, and R. L. Schilsky, "Precision cancer medicine: the future is now, only better," *American Society of Clinical Oncology Educational Book*, pp. 61–69, 2014.

[7] F. Weinberg and N. S. Chandel, "Reactive oxygen species-dependent signaling regulates cancer," *Cellular and Molecular Life Sciences*, vol. 66, no. 23, pp. 3663–3673, 2009.

[8] P. Karihtala and Y. Soini, "Reactive oxygen species and antioxidant mechanisms in human tissues and their relation to malignancies," *APMIS*, vol. 115, pp. 81–103, 2007.

[9] P. Karihtala and U. Puistola, "Hypoxia and oxidative stress in the pathogenesis of gynecological cancers and in therapeutical options," *Current Cancer Therapy Reviews*, vol. 7, pp. 37–55, 2011.

[10] S. A. Castaldo, J. R. Freitas, N. V. Conchinha, and P. A. Madureira, "The tumorigenic roles of the cellular REDOX regulatory systems," *Oxidative Medicine and Cellular Longevity*, vol. 2016, Article ID 8413032, 17 pages, 2016.

[11] P. Angsutararux, S. Luanpitpong, and S. Issaragrisil, "Chemotherapy-induced cardiotoxicity: overview of the roles of oxidative stress," *Oxidative Medicine and Cellular Longevity*, vol. 2015, Article ID 795602, 13 pages, 2015.

[12] T. Karasawa and P. S. Steyger, "An integrated view of cisplatin-induced nephrotoxicity and ototoxicity," *Toxicology Letters*, vol. 237, pp. 219–227, 2015.

[13] A. C. Begg, F. A. Stewart, and C. Vens, "Strategies to improve radiotherapy with targeted drugs," *Nature Reviews. Cancer*, vol. 11, pp. 239–253, 2011.

[14] E. C. Halperin, L. W. Brady, C. A. Perez, and D. E. Wazer, "Perez & Brady's principles and practice of radiation oncology, 6th edition," *LWW*, 2013.

[15] M. P. Cole, C. T. Jones, and I. D. Todd, "A new anti-oestrogenic agent in late breast cancer. An early clinical appraisal of ICI46474," *British Journal of Cancer*, vol. 25, pp. 270–275, 1971.

[16] H. Gharwan and H. Groninger, "Kinase inhibitors and monoclonal antibodies in oncology: clinical implications," *Nature Reviews Clinical Oncology*, vol. 13, pp. 209–227, 2016.

[17] V. Raso, "Antibodies in diagnosis and therapy. The magic bullet—nearing the century mark," *Seminars in Cancer Biology*, vol. 1, pp. 227–242, 1990.

[18] D. S. Dimitrov and J. D. Marks, "Therapeutic antibodies: current state and future trends—is a paradigm change coming soon?" *Methods in Molecular Biology*, vol. 525, pp. 1–27, 2009, xiii.

[19] J. T. Hartmann, M. Haap, H. G. Kopp, and H. P. Lipp, "Tyrosine kinase inhibitors - a review on pharmacology, metabolism and side effects," *Current Drug Metabolism*, vol. 10, pp. 470–481, 2009.

[20] D. B. Mendel, A. D. Laird, X. Xin et al., "In vivo antitumor activity of SU11248, a novel tyrosine kinase inhibitor targeting vascular endothelial growth factor and platelet-derived growth factor receptors: determination of a pharmacokinetic/pharmacodynamic relationship," *Clinical Cancer Research*, vol. 9, no. 1, pp. 327–337, 2003.

[21] M. H. Kappers, V. J. de Beer, Z. Zhou et al., "Sunitinib-induced systemic vasoconstriction in swine is endothelin mediated and does not involve nitric oxide or oxidative stress," *Hypertension*, vol. 59, pp. 151–157, 2012.

[22] M. Santoni, C. Amantini, M. B. Morelli et al., "Pazopanib and sunitinib trigger autophagic and non-autophagic death of bladder tumour cells," *British Journal of Cancer*, vol. 109, pp. 1040–1050, 2013.

[23] K. R. Doherty, R. L. Wappel, D. R. Talbert et al., "Multi-parameter in vitro toxicity testing of crizotinib, sunitinib, erlotinib, and nilotinib in human cardiomyocytes," *Toxicology and Applied Pharmacology*, vol. 272, pp. 245–255, 2013.

[24] G. M. Suddek, "Sunitinib improves chemotherapeutic efficacy and ameliorates cisplatin-induced nephrotoxicity in experimental animals," *Cancer Chemotherapy and Pharmacology*, vol. 67, pp. 1035–1044, 2011.

[25] W. Cui, Z. J. Zhang, S. Q. Hu et al., "Sunitinib produces neuroprotective effect via inhibiting nitric oxide overproduction," *CNS Neuroscience & Therapeutics*, vol. 20, pp. 244–252, 2014.

[26] A. M. Thijs, C. M. van Herpen, V. Verweij et al., "Impaired endothelium-dependent vasodilation does not initiate the development of sunitinib-associated hypertension," *Journal of Hypertension*, vol. 33, pp. 2075–2082, 2015.

[27] A. K. Abdel-Aziz, S. Shouman, E. El-Demerdash, M. Elgendy, and A. B. Abdel-Naim, "Chloroquine synergizes sunitinib cytotoxicity via modulating autophagic, apoptotic and angiogenic machineries," *Chemico-Biological Interactions*, vol. 217, pp. 28–40, 2014.

[28] E. Signoretto, J. Zierle, R. Bissinger, M. Castagna, E. Bossi, and F. Lang, "Triggering of suicidal erythrocyte death by pazopanib," *Cellular Physiology and Biochemistry*, vol. 38, pp. 926–938, 2016.

[29] M. B. Morelli, C. Amantini, M. Santoni et al., "Axitinib induces DNA damage response leading to senescence, mitotic catastrophe, and increased NK cell recognition in human renal carcinoma cells," *Oncotarget*, vol. 6, pp. 36245–36259, 2015.

[30] M. Itsumi and K. Tatsugami, "Immunotherapy for renal cell carcinoma," *Clinical & Developmental Immunology*, vol. 2010, Article ID 284581, 8 pages, 2010.

[31] J. F. Chiou, C. J. Tai, Y. H. Wang, T. Z. Liu, Y. M. Jen, and C. Y. Shiau, "Sorafenib induces preferential apoptotic killing of a drug- and radio-resistant Hep G2 cells through a mitochondria-dependent oxidative stress mechanism," *Cancer Biology & Therapy*, vol. 8, pp. 1904–1913, 2009.

[32] R. Coriat, C. Nicco, C. Chéreau et al., "Sorafenib-induced hepatocellular carcinoma cell death depends on reactive oxygen species production in vitro and in vivo," *Molecular Cancer Therapeutics*, vol. 11, pp. 2284–2293, 2012.

[33] V. Tesori, A. C. Piscaglia, D. Samengo et al., "The multikinase inhibitor sorafenib enhances glycolysis and synergizes with glycolysis blockade for cancer cell killing," *Scientific Reports*, vol. 5, p. 9149, 2015.

[34] B. Gillissen, A. Richter, A. Richter et al., "Bax/Bak-independent mitochondrial depolarization and reactive oxygen species induction by sorafenib overcome resistance to apoptosis in renal cell carcinoma," *The Journal of Biological Chemistry*, vol. 292, no. 16, pp. 6478–6492, 2017.

[35] N. Prieto-Domínguez, R. Ordóñez, A. Fernández et al., "Melatonin-induced increase in sensitivity of human hepatocellular carcinoma cells to sorafenib is associated with reactive oxygen species production and mitophagy," *Journal of Pineal Research*, vol. 61, pp. 396–407, 2016.

[36] A. T. Shaw, D. W. Kim, K. Nakagawa et al., "Crizotinib versus chemotherapy in advanced ALK-positive lung cancer," *The New England Journal of Medicine*, vol. 368, pp. 2385–2394, 2013.

[37] B. J. Solomon, T. Mok, D. W. Kim et al., "First-line crizotinib versus chemotherapy in ALK-positive lung cancer," *The New England Journal of Medicine*, vol. 371, pp. 2167–2177, 2014.

[38] F. Megiorni, H. P. McDowell, S. Camero et al., "Crizotinib-induced antitumour activity in human alveolar rhabdomyosarcoma cells is not solely dependent on ALK and MET inhibition," *Journal of Experimental & Clinical Cancer Research*, vol. 34, p. 112, 2015.

[39] D. Raha, T. R. Wilson, J. Peng et al., "The cancer stem cell marker aldehyde dehydrogenase is required to maintain a drug-tolerant tumor cell subpopulation," *Cancer Research*, vol. 74, pp. 3579–3590, 2014.

[40] K. S. Nguyen, J. W. Neal, and H. Wakelee, "Review of the current targeted therapies for non-small-cell lung cancer," *World Journal of Clinical Oncology*, vol. 5, pp. 576–587, 2014.

[41] X. Qian, J. Li, J. Ding, Z. Wang, W. Zhang, and G. Hu, "Erlotinib activates mitochondrial death pathways related to the production of reactive oxygen species in the human non-small cell lung cancer cell line A549," *Clinical and Experimental Pharmacology & Physiology*, vol. 36, pp. 487–494, 2009.

[42] F. Shan, Z. Shao, S. Jiang, and Z. Cheng, "Erlotinib induces the human non-small-cell lung cancer cells apoptosis via activating ROS-dependent JNK pathways," *Cancer Medicine*, vol. 5, pp. 3166–3175, 2016.

[43] H. M. Korashy, I. M. Attafi, M. A. Ansari et al., "Molecular mechanisms of cardiotoxicity of gefitinib in vivo and in vitro rat cardiomyocyte: role of apoptosis and oxidative stress," *Toxicology Letters*, vol. 252, pp. 50–61, 2016.

[44] I. S. Okon, K. A. Coughlan, M. Zhang, Q. Wang, and M. H. Zou, "Gefitinib-mediated reactive oxygen specie (ROS) instigates mitochondrial dysfunction and drug resistance in lung cancer cells," *The Journal of Biological Chemistry*, vol. 290, pp. 9101–9110, 2015.

[45] T. Kwon, J. K. Rho, J. C. Lee et al., "An important role for peroxiredoxin II in survival of A549 lung cancer cells resistant to gefitinib," *Experimental & Molecular Medicine*, vol. 47, article e165, 2015.

[46] M. C. Jaramillo and D. D. Zhang, "The emerging role of the Nrf2-Keap1 signaling pathway in cancer," *Genes & Development*, vol. 27, pp. 2179–2191, 2013.

[47] J. D. Hayes and M. McMahon, "NRF2 and KEAP1 mutations: permanent activation of an adaptive response in cancer," *Trends in Biochemical Sciences*, vol. 34, pp. 176–188, 2009.

[48] A. Leone, M. S. Roca, C. Ciardiello et al., "Vorinostat synergizes with EGFR inhibitors in NSCLC cells by increasing ROS via up-regulation of the major mitochondrial porin VDAC1 and modulation of the c-Myc-NRF2-KEAP1 pathway," *Free Radical Biology & Medicine*, vol. 89, pp. 287–299, 2015.

[49] T. Yamadori, Y. Ishii, S. Homma et al., "Molecular mechanisms for the regulation of Nrf2-mediated cell proliferation in non-small-cell lung cancers," *Oncogene*, vol. 31, pp. 4768–4777, 2012.

[50] E. B. Krall, B. Wang, D. M. Munoz et al., "KEAP1 loss modulates sensitivity to kinase targeted therapy in lung cancer," *eLife*, vol. 1, p. 6, 2017 Feb.

[51] K. P. Orcutt, A. D. Parsons, Z. A. Sibenaller et al., "Erlotinib-mediated inhibition of EGFR signaling induces metabolic oxidative stress through NOX4," *Cancer Research*, vol. 71, pp. 3932–3940, 2011.

[52] T. H. Truong, P. M. Ung, P. B. Palde, C. E. Paulsen, A. Schlessinger, and K. S. Carroll, "Molecular basis for redox activation of epidermal growth factor receptor kinase," *Cell Chemical Biology*, vol. 23, pp. 837–848, 2016.

[53] P. B. Chapman, A. Hauschild, C. Robert et al., "BRIM-3 study group. Improved survival with vemurafenib in melanoma with BRAF V600E mutation," *The New England Journal of Medicine*, vol. 364, pp. 2507–2516, 2011.

[54] L. Yu, L. X. Gao, X. Q. Ma, F. X. Hu, C. M. Li, and Z. Lu, "Involvement of superoxide and nitric oxide in BRAF(V600E) inhibitor PLX4032-induced growth inhibition of melanoma cells," *Integrative Biology*, vol. 6, no. 12, pp. 1211–1217, 2014.

[55] D. Bauer, F. Werth, H. A. Nguyen, F. Kiecker, and J. Eberle, "Critical role of reactive oxygen species (ROS) for synergistic enhancement of apoptosis by vemurafenib and the potassium channel inhibitor TRAM-34 in melanoma cells," *Cell Death & Disease*, vol. 8, no. article e2594, 2017.

[56] P. Corazao-Rozas, P. Guerreschi, M. Jendoubi et al., "Mitochondrial oxidative stress is the Achille's heel of melanoma cells resistant to Braf-mutant inhibitor," *Oncotarget*, vol. 4, pp. 1986–1998, 2013.

[57] C. Luo, J. H. Lim, Y. Lee et al., "A PGC1α-mediated transcriptional axis suppresses melanoma metastasis," *Nature*, vol. 537, pp. 422–426, 2016.

[58] K. M. Aird, J. L. Allensworth, I. Batinic-Haberle, H. K. Lyerly, M. W. Dewhirst, and G. R. Devi, "ErbB1/2 tyrosine kinase inhibitor mediates oxidative stress-induced apoptosis in inflammatory breast cancer cells," *Breast Cancer Research and Treatment*, vol. 132, pp. 109–119, 2012.

[59] R. Zhang, H. Qiao, S. Chen et al., "Berberine reverses lapatinib resistance of HER2-positive breast cancer cells by increasing the level of ROS," *Cancer Biology & Therapy*, vol. 17, pp. 925–934, 2016.

[60] Z. Y. Pessetto, S. J. Weir, G. Sethi, M. A. Broward, and A. K. Godwin, "Drug repurposing for gastrointestinal stromal tumor," *Molecular Cancer Therapeutics*, vol. 12, pp. 1299–1309, 2013.

[61] S. P. Chang, S. C. Shen, W. R. Lee, L. L. Yang, and Y. C. Chen, "Imatinib mesylate induction of ROS-dependent apoptosis in melanoma B16F0 cells," *Journal of Dermatological Science*, vol. 62, pp. 183–191, 2011.

[62] E. Suyani, U. B. Derici, T. Sahin et al., "Effects of everolimus on cytokines, oxidative stress, and renal histology in ischemia-reperfusion injury of the kidney," *Renal Failure*, vol. 31, pp. 698–703, 2009.

[63] K. Rosing, M. Fobker, F. Kannenberg et al., "Everolimus therapy is associated with reduced lipoprotein-associated phospholipase A2 (Lp-Pla2) activity and oxidative stress in heart transplant recipients," *Atherosclerosis*, vol. 230, pp. 164–170, 2013.

[64] A. Kezic, F. Thaiss, J. U. Becker, T. Y. Tsui, and M. Bajcetic, "Effects of everolimus on oxidative stress in kidney model of ischemia/reperfusion injury," *American Journal of Nephrology*, vol. 37, pp. 291–301, 2013.

[65] H. S. Khalil, S. P. Langdon, I. H. Kankia, J. Bown, and Y. Y. Deeni, "NRF2 regulates HER2 and HER3 signaling pathway to modulate sensitivity to targeted immunotherapies," *Oxidative Medicine and Cellular Longevity*, vol. 2016, Article ID 4148791, 22 pages, 2016.

[66] H. S. Khalil, S. P. Langdon, A. Goltsov et al., "A novel mechanism of action of HER2 targeted immunotherapy is explained by inhibition of NRF2 function in ovarian cancer cells," *Oncotarget*, vol. 7, pp. 75874–75901, 2016.

[67] L. G. Lemos, V. J. Victorino, A. C. Herrera et al., "Trastuzumab-based chemotherapy modulates systemic redox homeostasis in women with HER2-positive breast cancer," *International Immunopharmacology*, vol. 27, pp. 8–14, 2015.

[68] L. I. Gordon, M. A. Burke, A. T. Singh et al., "Blockade of the erbB2 receptor induces cardiomyocyte death through mitochondrial and reactive oxygen species-dependent pathways," *The Journal of Biological Chemistry*, vol. 284, pp. 2080–2087, 2009.

[69] A. Sadeghirizi, R. Yazdanparast, and S. Aghazadeh, "Combating trastuzumab resistance by targeting thioredoxin-1/PTEN interaction," *Tumour Biology*, vol. 37, pp. 6737–6747, 2016.

[70] M. M. Wattenberg, A. R. Kwilas, S. R. Gameiro, A. P. Dicker, and J. W. Hodge, "Expanding the use of monoclonal antibody therapy of cancer by using ionising radiation to upregulate antibody targets," *British Journal of Cancer*, vol. 110, pp. 1472–1480, 2014.

[71] E. Janas, R. Priest, J. I. Wilde, J. H. White, and R. Malhotra, "Rituxan (anti-CD20 antibody)-induced translocation of CD20 into lipid rafts is crucial for calcium influx and apoptosis," *Clinical and Experimental Immunology*, vol. 139, pp. 439–446, 2005.

[72] S. Alas, C. P. Ng, and B. Bonavida, "Rituximab modifies the cisplatin-mitochondrial signaling pathway, resulting in apoptosis in cisplatin-resistant non-Hodgkin's lymphoma," *Clinical Cancer Research*, vol. 8, pp. 836–845, 2002.

[73] B. Bellosillo, N. Villamor, A. López-Guillermo et al., "Complement-mediated cell death induced by rituximab in B-cell lymphoproliferative disorders is mediated in vitro by a caspase-independent mechanism involving the generation of reactive oxygen species," *Blood*, vol. 98, pp. 2771–2777, 2001.

[74] K. Wang, Y. Jiang, W. Zheng et al., "Silencing of human phosphatidylethanolamine-binding protein 4 enhances rituximab-induced death and chemosensitization in B-cell lymphoma," *PloS One*, vol. 8, no. article e56829, 2013.

[75] L. Alinari, B. Yu, B. A. Christian et al., "Combination anti-CD74 (milatuzumab) and anti-CD20 (rituximab) monoclonal antibody therapy has in vitro and in vivo activity in mantle cell lymphoma," *Blood*, vol. 117, pp. 4530–4541, 2011.

[76] B. A. Christian, M. Poi, J. A. Jones et al., "The combination of milatuzumab, a humanized anti-CD74 antibody, and veltuzumab, a humanized anti-CD20 antibody, demonstrates activity in patients with relapsed and refractory B-cell non-Hodgkin lymphoma," *British Journal of Haematology*, vol. 169, pp. 701–710, 2015.

[77] F. Fack, H. Espedal, O. Keunen et al., "Bevacizumab treatment induces metabolic adaptation toward anaerobic metabolism in glioblastomas," *Acta Neuropathologica*, vol. 129, pp. 115–131, 2015.

[78] X. L. Guo, D. Li, K. Sun et al., "Inhibition of autophagy enhances anticancer effects of bevacizumab in hepatocarcinoma," *Journal of molecular medicine (Berlin, Germany)*, vol. 91, pp. 473–483, 2013.

[79] S. Kim, Y. J. Kim, N. R. Kim, and H. S. Chin, "Effects of bevacizumab on Bcl-2 expression and apoptosis in retinal pigment epithelial cells under oxidative stress," *Korean Journal of Ophthalmology*, vol. 29, pp. 424–432, 2015.

[80] H. Lu, X. Li, Y. Lu, S. Qiu, and Z. Fan, "ASCT2 (SLC1A5) is an EGFR-associated protein that can be co-targeted by cetuximab to sensitize cancer cells to ROS-induced apoptosis," *Cancer Letters*, vol. 381, pp. 23–30, 2016.

[81] S. Cao, M. Xia, Y. Mao et al., "Combined oridonin with cetuximab treatment shows synergistic anticancer effects on laryngeal squamous cell carcinoma: involvement of inhibition of EGFR and activation of reactive oxygen species-mediated JNK pathway," *International Journal of Oncology*, vol. 49, pp. 2075–2087, 2016.

[82] M. Prewett, D. S. Deevi, R. Bassi et al., "Tumors established with cell lines selected for oxaliplatin resistance respond to oxaliplatin if combined with cetuximab," *Clinical Cancer Research*, vol. 13, pp. 7432–7440, 2007.

[83] D. Balin-Gauthier, J. P. Delord, M. J. Pillaire et al., "Tumors established with cell lines selected for oxaliplatin resistance respond to oxaliplatin if combined with cetuximab," *British Journal of Cancer*, vol. 98, pp. 120–128, 2008.

[84] J. Taieb, J. Tabernero, E. Mini et al., "Oxaliplatin, fluorouracil, and leucovorin with or without cetuximab in patients with resected stage III colon cancer (PETACC-8): an open-label, randomised phase 3 trial," *The Lancet Oncology*, vol. 15, pp. 862–873, 2014.

[85] K. M. Tveit, T. Guren, B. Glimelius et al., "Phase III trial of cetuximab with continuous or intermittent fluorouracil, leucovorin, and oxaliplatin (Nordic FLOX) versus FLOX alone in first-line treatment of metastatic colorectal cancer: the NORDIC-VII study," *Journal of Clinical Oncology*, vol. 30, pp. 1755–1762, 2012.

[86] T. S. Maughan, R. A. Adams, C. G. Smith et al., "Addition of cetuximab to oxaliplatin-based first-line combination chemotherapy for treatment of advanced colorectal cancer: results of the randomised phase 3 MRC COIN trial," *Lancet*, vol. 377, pp. 2103–2114, 2011.

[87] L. Dahan, A. Sadok, J. L. Formento, J. F. Seitz, and H. Kovacic, "Modulation of cellular redox state underlies antagonism between oxaliplatin and cetuximab in human colorectal cancer cell lines," *British Journal of Pharmacology*, vol. 158, pp. 610–620, 2009.

[88] V. Santoro, R. Jia, H. Thompson et al., "Role of reactive oxygen species in the abrogation of oxaliplatin activity by cetuximab in colorectal cancer," *Journal of the National Cancer Institute*, vol. 108, p. djv394, 2015.

[89] S. Y. Zafar and A. P. Abernethy, "Financial toxicity, part I: a new name for a growing problem," *Oncology (Williston Park, N.Y.)*, vol. 27, pp. 80-81, 2013, 149.

[90] I. Nakashima, K. Takeda, Y. Kawamoto, Y. Okuno, M. Kato, and H. Suzuki, "Redox control of catalytic activities of membrane-associated protein tyrosine kinases," *Archives of Biochemistry and Biophysics*, vol. 434, pp. 3–10, 2005.

[91] S. Alas, C. P. Ng, and B. Bonavida, "Rituximab modifies the cisplatin-mitochondrial signaling pathway, resulting in apoptosis in cisplatin-resistant non-Hodgkin's lymphoma," *Clinical Cancer Research*, vol. 8, pp. 836–845, 2002.

[92] M. Fengling, L. Fenju, W. Wanxin et al., "Rituximab sensitizes a Burkitt lymphoma cell line to cell killing by X-irradiation," *Radiation and Environmental Biophysics*, vol. 48, pp. 371–378, 2009.

[93] V. Tkachev, S. Goodell, A. W. Opipari et al., "Programmed death-1 controls T cell survival by regulating oxidative metabolism," *Journal of Immunology*, vol. 194, pp. 5789–5800, 2015.

Hindawi
Oxidative Medicine and Cellular Longevity
Volume 2017, Article ID 7203758, 11 pages
https://doi.org/10.1155/2017/7203758

Research Article

Cellular Preoxygenation Partially Attenuates the Antitumoral Effect of Cisplatin despite Highly Protective Effects on Renal Epithelial Cells

Bahram Rasoulian,[1] Ayat Kaeidi,[2,3] Maryam Rezaei,[4] and Zahra Hajializadeh[3]

[1]*Razi Herbal Medicines Research Center and Department of Physiology, Lorestan University of Medical Sciences, Khorramabad, Iran*
[2]*Department of Physiology and Pharmacology, Rafsanjan University of Medical Sciences, Rafsanjan, Iran*
[3]*Physiology-Pharmacology Research Center, Rafsanjan University of Medical Sciences, Rafsanjan, Iran*
[4]*Razi Herbal Medicines Research Center, Lorestan University of Medical Sciences, Khorramabad, Iran*

Correspondence should be addressed to Ayat Kaeidi; a.kaeidi@rums.ac.ir

Received 17 November 2016; Accepted 15 January 2017; Published 19 February 2017

Academic Editor: Spencer Gibson

Our previous in vitro studies demonstrated that oxygen pretreatment significantly protects human embryonic renal tubular cell against acute cisplatin- (CP-) induced cytotoxicity. The present study was designed to investigate whether this protective effect is associated with decreasing therapeutic effects of cisplatin on malignant cells. For this purpose, cultured human embryonic kidney epithelial-like (AD293), cervical carcinoma epithelial-like (Hela), and ovarian adenocarcinoma epithelial-like (OVCAR-3) cells were subjected to either 2-hour pretreatment with oxygen (≥90%) or normal air and then to a previously determined 50% lethal dose of cisplatin for 24 hours. Cellular viability was evaluated via MTT and Neutral Red assays. Also, activated caspase-3 and Bax/Bcl-2 ratio, as the biochemical markers of cell apoptosis, were determined using immunoblotting. The hyperoxic preexposure protocol significantly protects renal AD293 cells against cisplatin-induced toxicity. Oxygen pretreatment also partially attenuated the cisplatin-induced cytotoxic effects on Hela and OVCAR-3 cells. However, it did not completely protect these cells against the therapeutic cytotoxic effects of cisplatin. In summary, the protective methods for reducing cisplatin nephrotoxic side effects like oxygen pretreatment might be associated with concurrent reduction of the therapeutic cytotoxic effects of cisplatin on malignant cells like cervical carcinoma (Hela) and ovarian adenocarcinoma (OVCAR-3) cells.

1. Introduction

Cisplatin (CP) (*cis*-diamminedichloroplatinum (II)) as an antineoplastic drug is a standard component in treatment regimens for many solid tumors like head and neck, ovarian, cervical, and testicular cancers. The efficacy of cisplatin is dose-dependent and the main dose-limiting side effect of cisplatin is nephrotoxicity. However, there are some other adverse effects like ototoxicity, neurotoxicity, gastrotoxicity, and myelosuppression [1, 2]. It is well known that cisplatin, depending on the dose of administration, causes renal tubular cell death at least through affecting two distinct cellular mechanisms. With higher doses, necrotic cell death is predominant, whereas lower concentrations which are most commonly used in real clinical practice primarily induce apoptosis [1, 3]. Even with hydration, as the accepted method for reducing cisplatin nephrotoxicity, about one-third of patients treated with this drug have some evidence of renal damage (such as transient elevation of blood urea nitrogen levels) within the days following cisplatin administration [4].

It has been demonstrated that oxygen pretreatment largely reduces cisplatin-induced nephrotoxicity both in vitro and in vivo [5–7] and some clinical studies have used hyperoxic pretreatment method for reducing cisplatin-induced nephropathy in cancer patients [8]. Nevertheless, it has not been revealed whether this highly protective effect of oxygen pretreatment on renal tubular cells is associated with reduced therapeutic cytotoxic effects of cisplatin on malignant cells. In fact, the present study focused on preclinical and in vitro aspects of this concern.

On the other hand, it has been proposed that normobaric or hyperbaric oxygen therapy elicits direct antitumoral effects [9] and in some cases can enhance chemotherapeutic activity of some anticancer drugs especially on hypoxic tumoral cells. For example, it has been shown that combined administration of cisplatin and hyperbaric oxygen enhances chemotherapeutic response to cisplatin in epithelial ovarian cancer cells in mice xenografts [10]. Despite the possible chemosensitizing effect of simultaneous oxygen administration, the direct effects of malignant cell "preoxygenation" on chemotherapeutic activity of anticancer drugs such as cisplatin have not been studied yet. It should be noted that, in the course of hyperbaric or hyperoxic exposure, unlike the inner cells of the tumor, superficial tumoral cells are exposed to higher tissue oxygenation. This in vitro study was designed to compare the effects of short course and single dose hyperoxic pretreatment on cytotoxic and apoptotic effects of cisplatin in normal renal tubular epithelial cells and two malignant ovarian (OVADR-3) and cervical (Hela) cell lines.

2. Materials and Methods

2.1. Materials. Cell culture reagents, fetal bovine serum (FBS), penicillin-streptomycin solution, and trypsin EDTA were purchased from Biosera Co. (East Sussex, UK). Dishes and culture flasks were obtained from SPL Lifesciences Inc. (Gyeonggi-do, South Korea). Cisplatin, 3-[4,5-dimethyl-2-thiazolyl]-2,5-diphenyl-2-tetrazolium bromide (MTT), and Neutral Red were acquired from Sigma (St. Louis, MI, USA). Primary polyclonal anti-caspase-3 and primary monoclonal anti-β-actin antibodies were purchased from Cell Signaling Technology, Inc. (Beverly, MA, USA). Primary polyclonal anti-Bax and primary monoclonal anti-Bcl-2 antibodies were purchased from Santa Cruz Biotechnology, Inc. (Delaware Ave., Santa Cruz, USA).

2.2. Cell Culture. AD293 (human embryonic kidney epithelial-like), Hela (human cervical carcinoma epithelial-like), and OVCAR-3 (human ovarian adenocarcinoma epithelial-like) cells were purchased from National Cell Bank of Iran (NCBI), Pasteur Institute of Iran (Tehran, Iran). Cells were grown on Dulbecco's modified Eagle's medium (DMEM) enhanced with 10% fetal bovine serum, penicillin (100 U/mL), and streptomycin (100 mg/mL). They were preserved at 37°C under an atmosphere of 5% CO_2.

2.3. Experimental Groups. Four experimental groups were assessed for each cell type as follows: (1) cells incubated with normal air flow and cisplatin vehicle (Air + Veh); (2) cells incubated with oxygen flow and cisplatin vehicle (O_2 + Veh); (3) cells incubated with normal air flow and cisplatin (Air + CP); (4) cells incubated with oxygen flow and cisplatin (O_2 + CP).

All three cell types (AD293, Hela, and OVCAR-3) were grown in plastic culture flasks and used in exponential growth phase or when grown to confluent monolayer. Growth medium was changed three times a week. For the MTT and Neutral Red assays, cells were plated at the density of 5000 per well in a 96-well microplate (7-8 wells were determined for each experimental group). In experiments related to each cell type, cells in "Air + Veh" and "O_2 + Veh" groups were grown in normal medium, and cells in the other 2 groups were grown in culture medium with cisplatin. For protein extraction, cells were grown in a six-well plate and allowed to attach and grow for 24 h. Cisplatin was dissolved in phosphate-buffered saline (PBS), and then the cells were incubated in a medium with cisplatin or vehicle (PBS) for 24 h. Cisplatin was used by its previously determined lethal dose 50% (LD_{50}) in experiments related to each cell type, that is, 50 μM, 35 μM, and 30 μM for AD293, Hela, and OVCAR-3 cells, respectively. LD_{50} was approved by both MTT and Neutral Red cell viability assays (Figure 1).

2.4. Hyperoxic Pretreatment and Cisplatin Administration. Prior to drug treatment, to produce hyperoxia preexposure, different cell line plates in incubator were exposed to 95% oxygen/5% CO_2 with continuously flowing humidified atmosphere for 2 h at 37°C. Parallel plates were kept in continuously flowing humidified 95% air/5% CO_2. Closely following oxygen pretreatment, cisplatin (or vehicle) was added to the culture plates. Via an oxygen meter (Lutron DO-5510, Taiwan), oxygen content of the chamber was checked throughout the preexposure period. It should be noted that, initially, there were 2 other control groups in each experimental set in which cells were simply incubated with normal air and 5% CO_2 without any flow. However, continuous air flow did not affect the cell viability or apoptotic markers. Thus, the control groups, treated with cisplatin or vehicle without any air flow, were not considered in the final analysis.

2.5. Cell Viability Analysis

Neutral Red Assay. For in vitro cellular cytotoxicity evaluation, Neutral Red assay has been widely used. This test is based on the combination of Neutral Red (3-amino-7-dimethyl-1-2-methylphenazine hydrochloride) into the lysosomes of viable cells. Neutral Red (4 mg/mL) was diluted into medium (1 : 100) and incubated overnight at 37°C and, before use, the Neutral Red solution was centrifuged. Prepared Neutral Red solution (200 μL) was added to any well and the cells were incubated for 3 h (37°C). After that, using 1% calcium chloride and 0.5% formaldehyde solution, the cells were quickly washed. After 10 min incubation of the cells (at room temperature) with a 50% ethanol and 1% acetic acid solution, the Neutral Red dye was released from the viable cell. Finally, absorbance (OD) values were measured by spectrophotometry at 540 nm. Results values were expressed as percentages of control.

MTT Assay. Cellular viability was evaluated by the 2-(4,5-dimethylthiazol-2-yl)-2,5-diphenyltetrazolium bromide (MTT) reduction to formazan. MTT was dissolved in PBS and added to the culture media at 0.5 mg/mL as a final concentration. After additional 2 h incubation at 37°C, the supernatant media were carefully removed and 100 μL DMSO was added to each plate well. Finally, wavelengths absorbance (OD) values were determined at 540 nm by spectrophotometry with a microplate reader apparatus (Eliza MAT 2000,

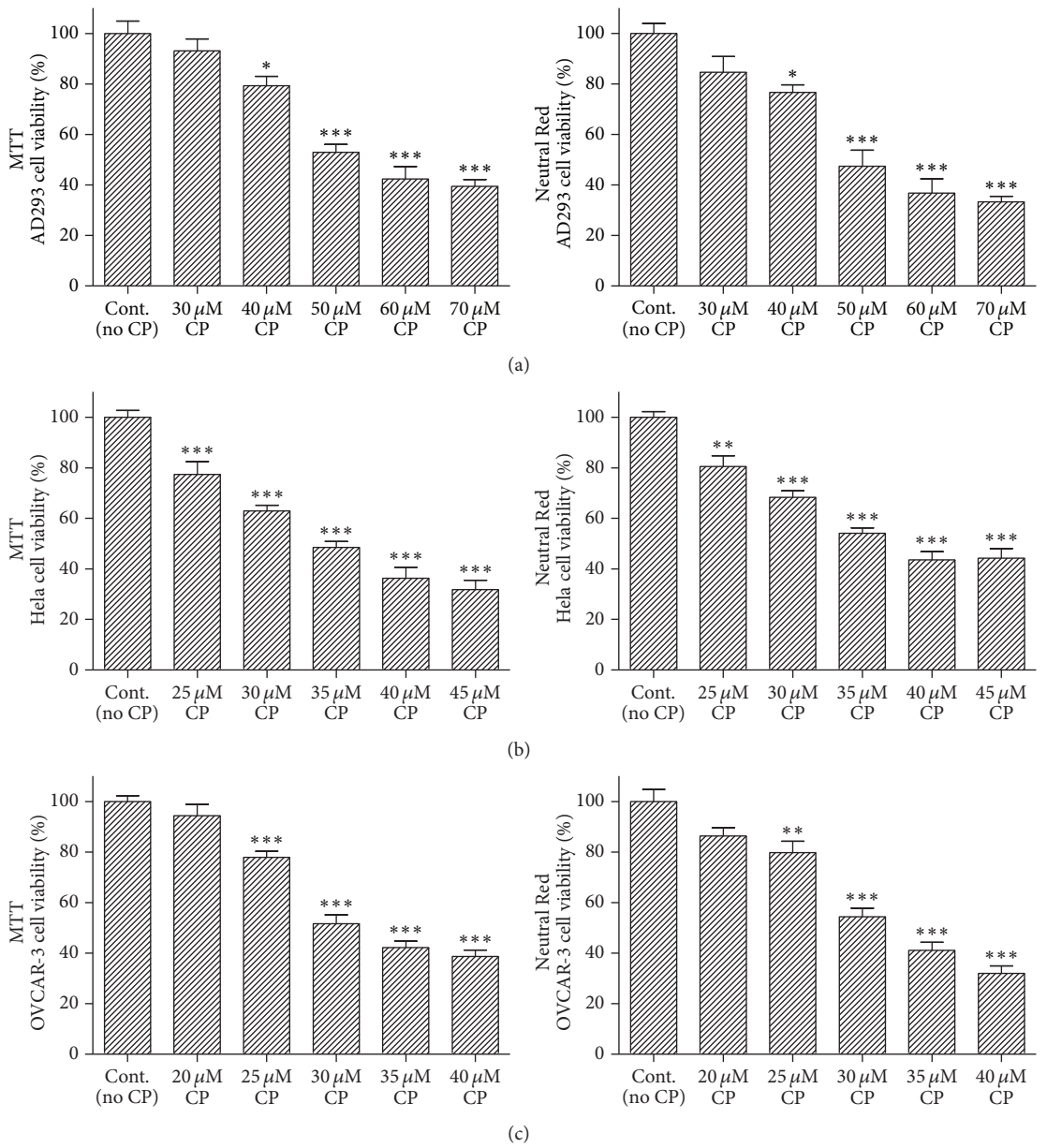

Figure 1: Effect of cisplatin on cell viability. Different cells types (AD293-(a), Hela-(b), and OVCAR-3-(c)) were incubated with variant doses of cisplatin for 24 h. Cell viability was determined by MTT and Neutral Red assays. Data are mean ± SD; $n = 6$–8 wells for each group/cell type; $^{*}p < 0.05$, $^{**}p < 0.01$, and $^{***}p < 0.001$ versus control.

DRG Instruments, GmbH). Each experiment was performed 5-6 independent times. Results were represented as percentages of control.

2.6. Western Blot Analysis. AD293, Hela, and OVCAR-3 cells were separately homogenized in ice-cold buffer containing 10 mM Tris-HCl (pH 7.4), 1 mM EDTA, 0.1% SDS, 0.1% Na-deoxycholate, and 1% NP-40 which is supplemented with protease inhibitors (1 mM sodium orthovanadate, 10 μg/mL aprotinin, 1 mM phenylmethylsulfonyl fluoride, and 2.5 μg/mL of leupeptin). The homogenate was centrifuged at 14000 rpm for 15 min at 4°C. The subsequent supernatant was preserved as the whole cell fraction. Via the Bradford method, protein concentration was evaluated. The same amounts of protein (40 μg) were resolved on a 12% SDS-PAGE gel and finally transferred to PVDF membranes (Roche, Germany) electrophoretically. After overnight blocking (4°C) with 5% nonfat dried milk (blocking buffer, TBS-T, 150 mM NaCl, 20 mM Tris-HCl, and 0.1% Tween 20, pH 7.5), the PVDF membranes were explored with rabbit monoclonal antibody to caspase-3 (Cell Signaling Technology, 1 : 1000 overnight at 4°C) and Bax and Bcl-2 (Santa Cruz Biotechnology, 1 : 1000 for 3 h at room temperature).

The blots were incubated for 60 min (room temperature) by a secondary antibody conjugated to horseradish peroxidase (1 : 15000, GE Healthcare Bio-Sciences, USA) following

washing three times in TBS-T. The blocking buffer was used as a diluent of antibodies. The complexes of antibody-antigen were indicated via the ECL system and exposed to chemiluminescent detection film (Roche, Germany). To analyze the intensity of the expression, Lab Work analyzing software (UVP, UK) was used. β-Actin immunoblotting (antibody from Cell Signaling Technology, USA; 1 : 1000) was used to control for loading. The western blot experiments for each protein were performed 4-5 independent times.

2.7. Statistical Analysis. Cell viability results were expressed as mean ± SEM. The difference in mean cell viability assays between experimental groups was examined by One-Way ANOVA, followed by Tukey's post hoc test. The values of protein band densities (Bax, Bcl-2, and caspase-3) were expressed as tested protein/β-actin ratio for each sample and were expressed as median (range) in related graphs. Different groups were compared by Kruskal-Wallis followed by Mann–Whitney U test between selected groups. GraphPad Prism (GraphPad Software, USA) and IBM SPSS Statistics (version 15) software were used for drawing graphs and statistical analysis, respectively. $p < 0.05$ was considered as significant.

3. Results

3.1. Cell Viability Results. At first, we analyzed the effects of different concentrations of cisplatin on human embryonic kidney epithelial-like (AD293), cervical carcinoma epithelial-like (Hela), and ovarian adenocarcinoma epithelial-like (OVCAR-3) cells viability using the MTT and Neutral Red assays. After the initial 24 h attachment/growth period, confluent monolayers of cultured cells were exposed to cisplatin (at the concentrations of 20 to 70 μM for 24 h). Figure 1 shows that cisplatin could decrease the viability of all cell types and this toxicity was dose-dependent. The toxic effect observed in 50, 35, and 30 μM cisplatin for AD293, Hela, and OVCAR-3, respectively, resulted in approximately 50% decrease of relative cell viability and this was used as the optimum dose for damaging the cells and evaluating the protective effects of the oxygen pretreatment (Figure 2).

As shown in Figure 2, there was no significant difference between "Air + Veh" and "O_2 + Veh" groups in any cell type indicating that 2 hours of 90% oxygen pretreatment did not have any toxic effect either on AD293 or malignant cells (Hela and OVCAR-3) (Figure 2). In AD293 cells, there was no significant difference among "O_2 + CP" group and both vehicle treated groups and there was a significant difference between "O_2 + CP" and "Air + CP" groups. Thus, MTT and Neutral Red assays showed that oxygen pretreatment largely protects human renal AD293 cells against acute single dose cisplatin-induced toxicity (Figure 2).

In contrast to normal AD293 cells, in the case of malignant Hela and OVCAR-3 cell lines, there was a significant difference between "O_2 + CP" and both "Air + CP" and "O_2 + CP" groups. This means that cisplatin cytotoxic effects on these cell lines exist despite hyperoxic pretreatment. But there was a significant reduction in the cytotoxic effects of cisplatin as determined by significant higher cell viability results in "O_2 + CP" group compared to "Air + CP" group in both MTT and Neutral Red assays of these two cell lines (Figure 2).

3.2. Western Blot Results. Figure 3 shows western blot results of renal AD293 cells. It is obvious that cisplatin led to increased expression of apoptosis markers, that is, cleaved caspase-3, Bax, and Bax/Bcl-2 ratio. Furthermore, oxygen pretreatment significantly decreased cisplatin-induced apoptosis. There was not any significant difference in the expression level of the antiapoptotic protein, Bcl-2, among various groups in all 3 cell types (Figures 3–5). Also, cisplatin led to a significant higher expression of apoptotic markers in Hela and OVCAR-3 cells and there was a significant (or marginally significant) cisplatin-induced increase in expression of apoptotic markers, despite pretreatment with oxygen, except for the cleaved caspase-3 of Hela cells ($p = 0.11$ between "O_2 + CP" and "Air + CP" groups, Figure 4(a)). There was a significant (Bax in Hela cells, Figure 4(b)), marginally significant (Bax/Bcl-2 in Hela cells, Figure 4(d)), or nonsignificant (cleaved caspase-3 in Hela cells (Figure 4(a)) and all apoptotic markers in OVCAR-3 cells (Figures 5(a)–5(d))) reduction of apoptotic markers in oxygen pretreated groups subjected to cisplatin administration.

3.3. Discussion. As mentioned in the Results, oxygen pretreatment attenuates, at least, some antitumor properties of cisplatin on Hela and OVCAR-3 cell lines; however, it is noteworthy that in this study the antitumor properties of cisplatin were not fully abolished. Cisplatin cellular toxicity on renal tubular AD93 cells was highly reduced in two control groups (with no cisplatin treatment) after oxygen preconditioning procedure. Bax and cleaved caspase-3 expiration, proteins related to apoptosis, were elevated fallowing cisplatin treatment in AD93 cells. Hyperbaric oxygen pretreatment elicited a significant inhibitory effect on elevated Bax and cleaved caspase-3 expiration on AD93 cells. It should be noted that cisplatin oxygen pretreatment before cisplatin therapy has no significant effect on Bcl-2 expiration in AD93 cells. Cisplatin increased caspase-3 activation and Bax expression as apoptosis markers in Hela cells. It should be noted that cisplatin-induced cellular toxicity, through apoptosis mechanisms, remained after oxygen preconditioning. In addition, after oxygen preconditioning, reduction in Bax expression was significant compared to cisplatin treated Hela cells (without oxygen preconditioning). But there was no significant deference in reduction of cleaved caspase-3 expressions between oxygen preconditioning + cisplatin and non-oxygen preconditioning + cisplatin treated Hela cells. Cisplatin treatment had no significant effect on Bcl-2 expression level in Hela cells. Cisplatin elevated Bax expression and caspase-3 activation in ovarian cancer cell line, OVCAR-3. Similar to Hela cells, cisplatin-induced apoptosis factors still remained following oxygen preconditioning. It should be noted that, following oxygen preconditioning + cisplatin, no significant difference was observed between the expression levels of Bax and cleaved caspase-3 compared to that of cisplatin treated OVCAR-3. Also, cisplatin therapy or oxygen preconditioning had no significant effect on Bcl-2 protein expression in OVCAR-3 cells.

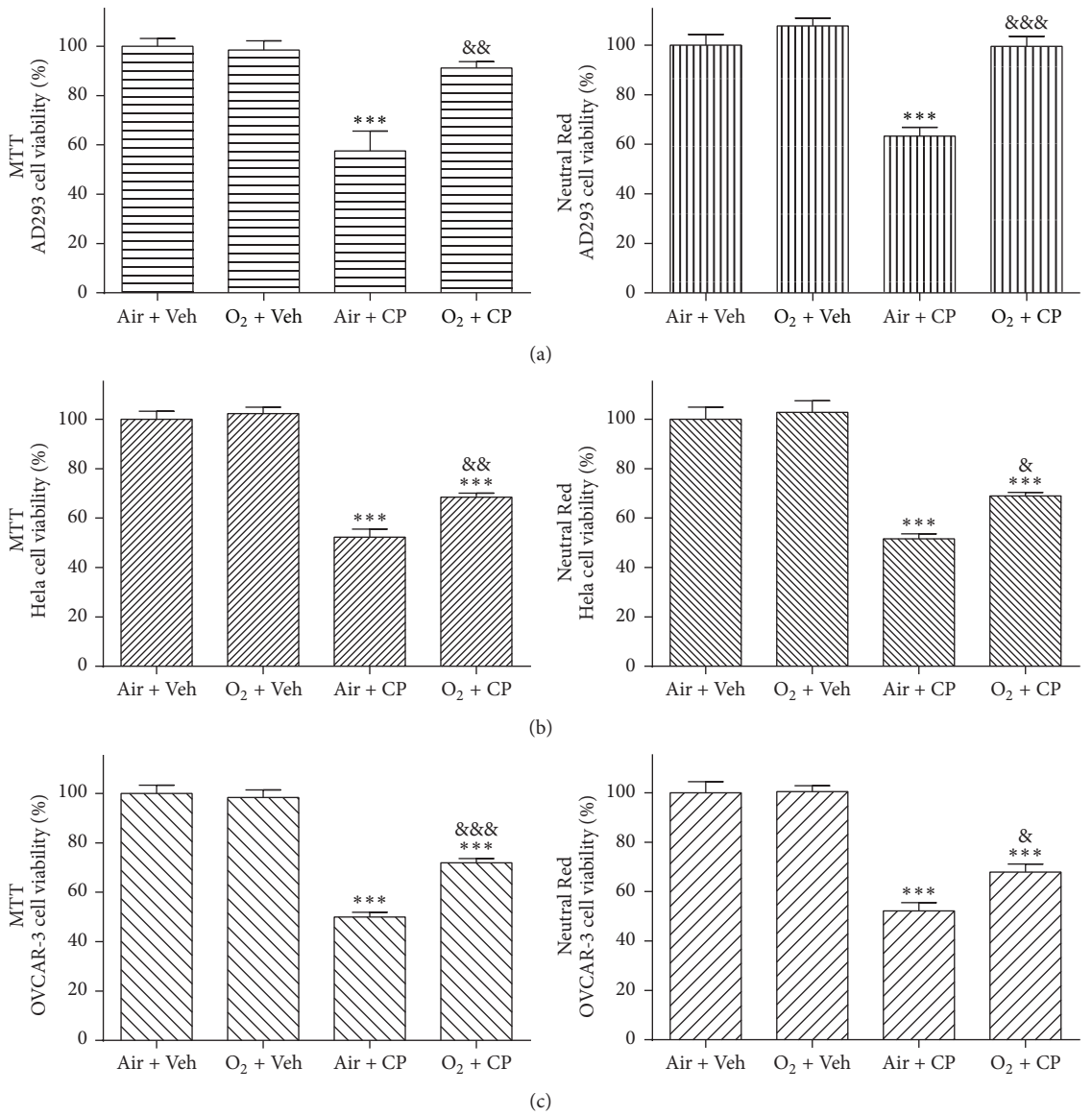

Figure 2: Hyperoxic preconditioning prevents cisplatin-induced cells death. AD293 (a), Hela (b), and OVCAR-3 (c) cells were treated with nearly pure oxygen (≥90%) preconditioning (2 h) and then cisplatin (50, 35, and 30 μM for AD293, Hela, and OVCAR-3 cells, resp.) was added for an additional 24 h. Cell viability was then determined using the MTT and Neutral Red assays. Data are mean ± SEM; $n = 6$–8 wells for each group; $^{***}p < 0.001$ versus both "Air + Veh" and "O_2 + Veh" groups (in (a), (b), and (c) parts); $^{\&}p < 0.05$, $^{\&\&}p < 0.01$, and $^{\&\&\&}p < 0.001$ versus "Air + CP" group (in (a), (b), and (c) parts).

As we know, cisplatin is one of the most potent antitumor platinum based agents. It is also a very effective compound against a wide spectrum of cancers [1]. Despite the useful properties of platinum compounds, they are toxic. Patients getting these agents experience strict side effects which in turn seriously restricts further administration. Thus, in order to achieve success in tumor chemotherapy, management of such drug-induced cytotoxicity is of critical significance. The side effects of platinum therapy include general cell-damaging effects, such as nausea, vomiting, and decreased number of blood cells and platelets, as well as reduced bone marrow production and attenuated response to infection. More specific side effects include damage to the kidney, neuronal damage, and hearing loss [11–13].

In this regard, the main controlling approaches include renoprotection and enhancing drug removal via hydration using osmotic diuretics. However, avoiding the nephrotoxic medications is crucial and additional therapies are also required.

Cisplatin causes significant oxidant loading to the renal epithelial cells through free radical production which results in damage to the antioxidant defense systems [14]. Cisplatin-induced oxidative stress has been proposed as an inducer in both Fas-mediated [15] and mitochondrial pathways [16, 17] of renal cell apoptosis [1].

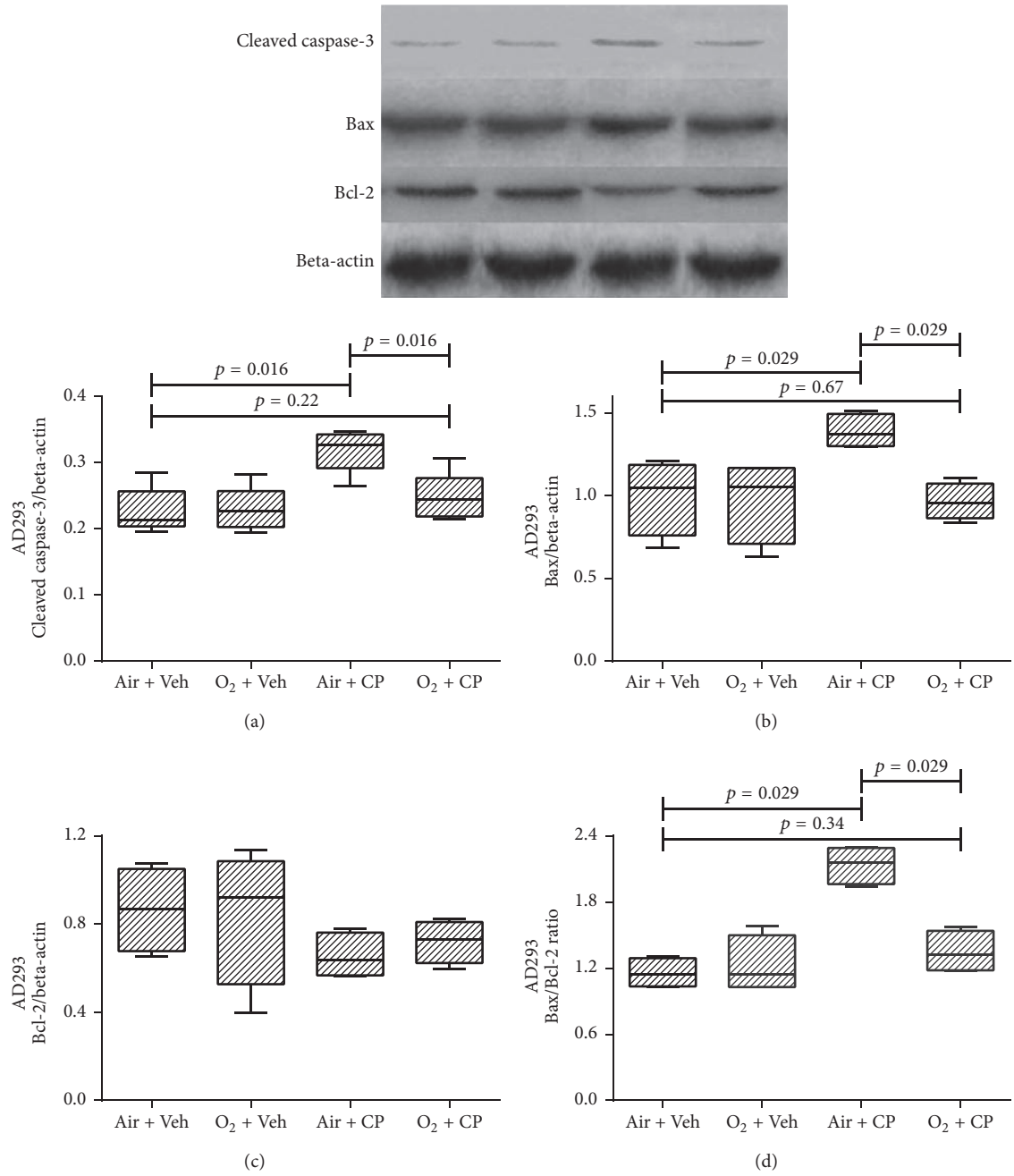

Figure 3: Western blot analysis of the caspase-3 protein activation, Bax, Bcl-2, and Bax : Bcl-2 ratio of AD293 cells. Cells were exposed to cisplatin (50, 35, and 30 μM for AD293, Hela, and OVCAR-3 cells, resp.) and cisplatin plus hyperoxic preconditioning (2 h) for 24 h. Each value in the graph represents the mean ± SEM band density ratio for each group. Beta-actin was used as an internal control ($n = 4$).

Previous studies by this group have demonstrated that pretreatment with hyperbaric oxygen could protect the rat kidney against cisplatin-induced nephropathy [7]. In addition, it has been shown that oxygen preconditioning can protect human renal tubular cells from cisplatin-induced cytotoxicity in vitro [5]. Likewise, in animal models, oxygen pretreatment reduces ischemia-reperfusion injuries in various vital organs such as the central nervous system [18–21], liver [22, 23], heart [24], and kidney [25, 26]. Moreover, it has been reported that hyperoxic preconditioning could attenuate hypoxia-induced apoptosis in cultured mesenchymal stem cells [27]. In addition, the negative properties of deceased-donor hypoxia and useful properties of living-donor hyperoxic preconditioning on kidney graft function have been demonstrated in some clinical investigations [28, 29]; however, some others failed to show such a relevance [30].

Short-term pretreatment with oxygen partially elevated ROS induction in various tissues [31]. It seems that these useful effects are associated with the upregulation of endogenous

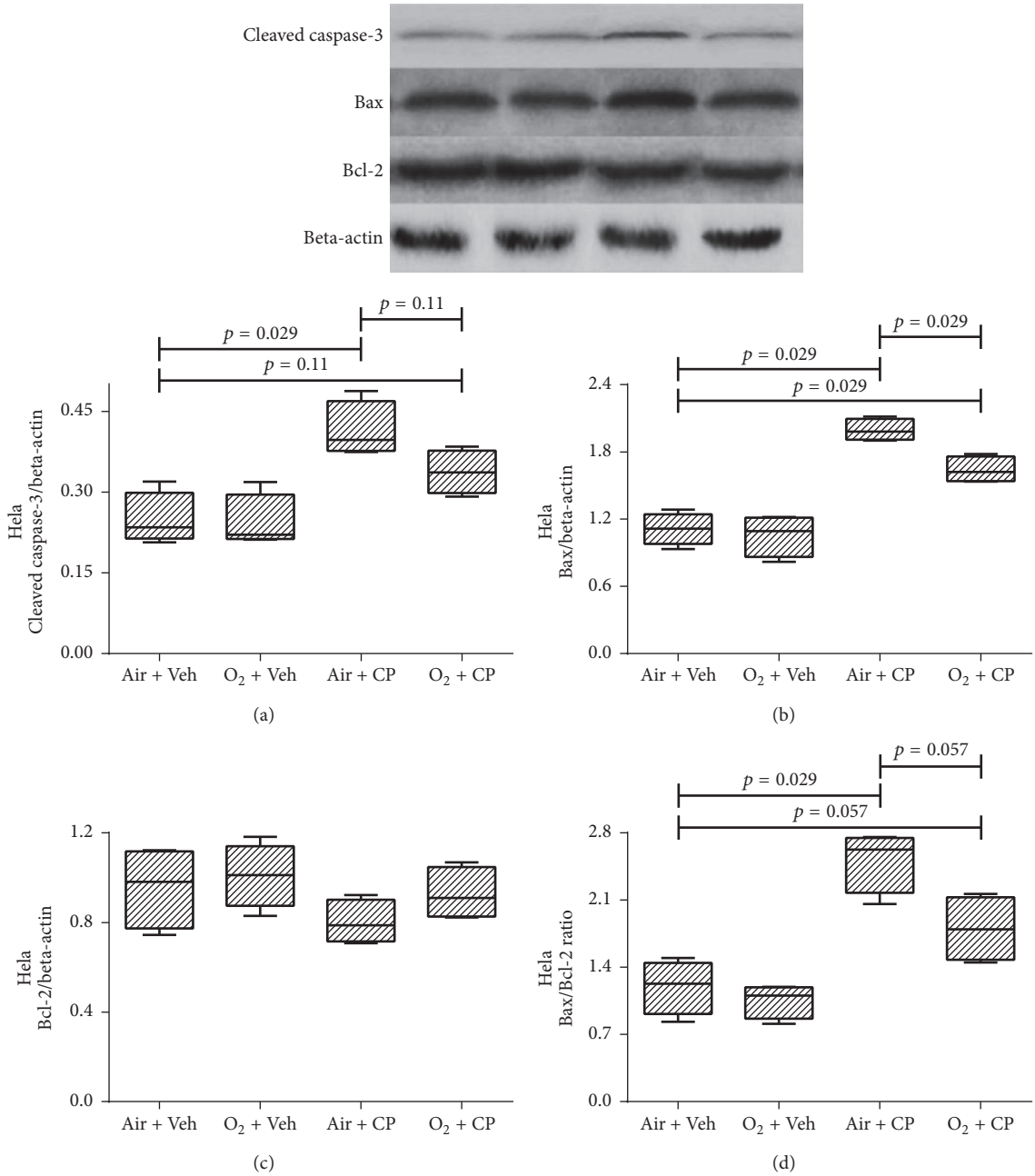

Figure 4: Western blot analysis of the caspase-3 protein activation, Bax, Bcl-2, and Bax : Bcl-2 ratio of Hela cells. Cells were exposed to cisplatin (50, 35, and 30 μM for AD293, Hela, and OVCAR-3 cells, resp.) and cisplatin plus hyperoxic preconditioning (2 h) for 24 h. Each value in the graph represents the mean ± SEM band density ratio for each group. Beta-actin was used as an internal control ($n = 4$).

mechanisms underlying cellular defense such as antioxidant systems and heat shock proteins [6, 21, 32]. On the other hand, a prior investigation revealed that intermittent oxygen exposure can induce more potent degrees of tolerance to ischemia in rat brain in comparison with continued oxygen pretreatment [19]. Furthermore, delayed cardioprotective effects of hyperoxic preconditioning against ischemia-reperfusion injury could be continued via intermittent oxygen administration [33]. Although long-term hyperoxic treatment could be toxic by itself, short-term oxygen preconditioning is a safe procedure that could be effortlessly applied in clinical practice [34].

As previously mentioned, cisplatin administration leads to significant oxidant loading to the renal epithelial cells through formation of free radicals as well as damage to cellular antioxidant defense systems. This explains, at least partially, the cellular mechanisms through which cisplatin-induced cytotoxic effects are mediated on renal tubular cells [35, 36].

Previous in vivo investigations have shown that short-term pretreatment with nearly pure oxygen causes some degrees of protection against nephrotoxicity induced by cisplatin and renal as well as cardiac ischemic injuries [5–7, 33]. These protective properties could be due to exciting the

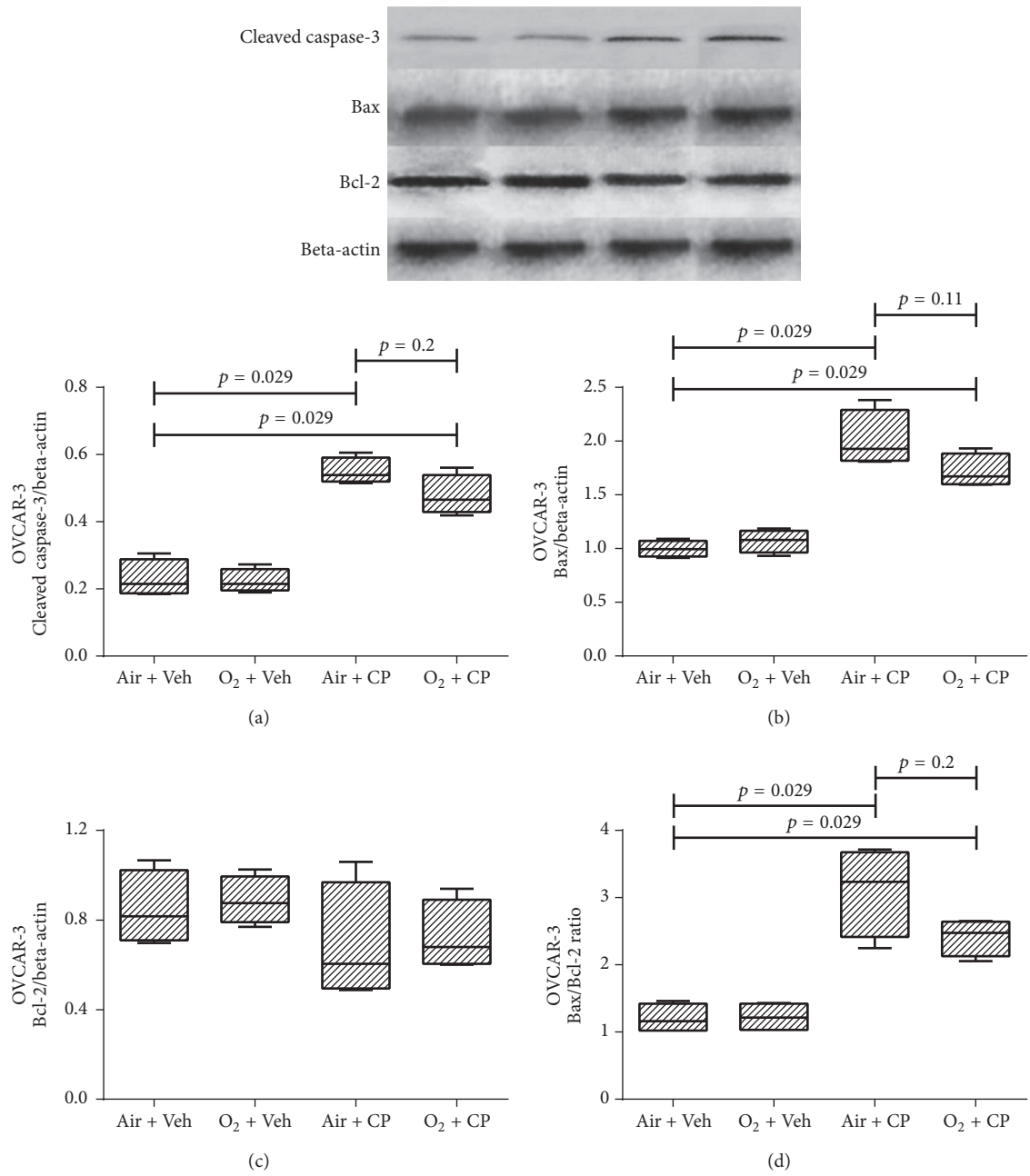

Figure 5: Western blot analysis of the caspase-3 protein activation, Bax, Bcl-2, and Bax : Bcl-2 ratio of OVCAR-3 cells. Cells were exposed to cisplatin (50, 35, and 30 μM for AD293, Hela, and OVCAR-3 cells, resp.) and cisplatin plus hyperoxic preconditioning (2 h) for 24 h. Each value in the graph represents the mean ± SEM band density ratio for each group. Beta-actin was used as an internal control ($n = 4$).

endogenous defense mechanisms such as antioxidant systems via induction of mild oxidative stress by hyperoxia [33]. However, there is no evidence in the literature in support of cisplatin-induced injury attenuation via oxygen pretreatment in human renal tubular cells.

An additional important concern is that most cisplatin cytotoxic effects are mediated via various common pathways among tumoral and renal epithelial cells. Hence, approaches that decrease cisplatin-induced nephropathy might have some unsought complications which in turn reduce the antitumor effect of this valuable drug [2].

Over the past half century, hyperbaric oxygen treatment has been used as an operative and safe cure for a variety of nonmalignant situations like decompression sickness, arterial embolism, and severe carbon monoxide poisoning [37, 38]. In addition, hyperbaric oxygen has been applied for the management of several chronic radiation injury forms [39–41]. A significant interpretation of the literature on the efficacy of hyperbaric oxygen treatment in this context is complicated by the heterogeneity of the treated disease, the various tissue damage types, and the several toxicity scoring systems used. Few randomized controlled trials using

oxygen therapy for the management of chronic radiation injury have been investigated; however, the findings appear promising for some subgroups such as head and neck patients and for those with proctitis as a result of radiation [39].

Apoptosis investigations in neoplasms treated with hyperbaric oxygen are very limited. Two in vitro investigations on oral and breast cancer cells showed no significant change in apoptosis following hyperbaric oxygen [42, 43]. In addition, another study supports the activation of the proapoptotic pathway, mitogen-activated protein kinase (MAPK), and downregulation of the antiapoptotic pathway, extracellular-signal-regulated kinases (ERK), in hematopoetic cells following hyperbaric oxygen treatment [44].

Moreover, hyperbaric oxygen treatment has been shown to induce apoptosis in osteosarcoma cells [45]. Also, two different in vivo models, gliomas and breast tumors, have reported the induction of cell death following hyperbaric oxygen treatment [46–48].

Altogether, this may suggest that changes in concentration of oxygen affected the cellular antioxidant pathways [49], leading to a change in cell survival signaling. However, the map is multifaceted and mechanistic investigations are essential before any last conclusions can be drawn. Preexposure to oxygen with optimum method has considerable results in reducing cisplatin-induced renal injury in experimental studies and the results are largely encouraging for designing additional clinical trials in cancer patients.

Additional studies are required to investigate the protective effects of oxygen pretreatment against cisplatin-induced cytotoxicity among different tumoral and renal cells.

4. Conclusion

Hyperbaric oxygen preconditioning induces potent protective effects against cisplatin-induced renal epithelial cells toxicity. This protective effect may relate, at least in part, to a reduction in cisplatin-induced cellular apoptosis mechanisms. In spite of the potent protective effects, hyperbaric oxygen preconditioning may reduce the antitumoral properties of cisplatin. The cellular mechanisms underlying these effects may relate to a reduction in apoptosis factors.

Competing Interests

The authors declare that they have no competing interests regarding the publication of this paper.

Acknowledgments

The authors wish to thank Mr. Reza Rostami from Razi Herbal Medicines Research Center, for providing some cell culture laboratory equipment. They also thank Mr. S. Mohammad Ahmadi Soleimani for English editing of this manuscript.

References

[1] M. H. Hanigan and P. Devarajan, "Cisplatin nephrotoxicity: molecular mechanisms," *Cancer Therapy*, vol. 1, pp. 47–61, 2003.

[2] R. P. Miller, R. K. Tadagavadi, G. Ramesh, and W. B. Reeves, "Mechanisms of cisplatin nephrotoxicity," *Toxins*, vol. 2, no. 11, pp. 2490–2518, 2010.

[3] W. Lieberthal, V. Triaca, and J. Levine, "Mechanisms of death induced by cisplatin in proximal tubular epithelial cells: apoptosis vs. necrosis," *American Journal of Physiology*, vol. 270, no. 4, pp. F700–F708, 1996.

[4] K. B. Meyer and N. E. Madias, "Cisplatin nephrotoxicity," *Mineral and Electrolyte Metabolism*, vol. 20, no. 4, pp. 201–213, 1994.

[5] A. Kaeidi, B. Rasoulian, Z. Hajializadeh, S. Pourkhodadad, and M. Rezaei, "Cisplatin toxicity reduced in human cultured renal tubular cells by oxygen pretreatment," *Renal Failure*, vol. 35, no. 10, pp. 1382–1386, 2013.

[6] B. Rasoulian, M. Jafari, M. Mahbod et al., "Pretreatment with oxygen protects rat kidney from cisplatin nephrotoxicity," *Renal Failure*, vol. 32, no. 2, pp. 234–242, 2010.

[7] B. Rasoulian, A. Kaeidi, S. Pourkhodadad et al., "Effects of pretreatment with single-dose or intermittent oxygen on cisplatin-induced nephrotoxicity in rats," *Nephro-Urology Monthly*, vol. 6, no. 5, Article ID e19680, 2014.

[8] A. Saadat, S. S. Shariat Maghani, Z. Rostami et al., "Normobaric hyperoxia preconditioning ameliorates cisplatin nephrotoxicity," *Renal Failure*, vol. 36, no. 1, pp. 5–8, 2014.

[9] K. Selvendiran, M. L. Kuppusamy, S. Ahmed et al., "Oxygenation inhibits ovarian tumor growth by downregulating STAT3 and cyclin-D1 expressions," *Cancer Biology and Therapy*, vol. 10, no. 4, pp. 386–390, 2010.

[10] T. Alagoz, R. E. Buller, B. Anderson et al., "Evaluation of hyperbaric oxygen as a chemosensitizer in the treatment of epithelial ovarian cancer in xenografts in mice," *Cancer*, vol. 75, no. 9, pp. 2313–2322, 1995.

[11] B. Desoize and C. Madoulet, "Particular aspects of platinum compounds used at present in cancer treatment," *Critical Reviews in Oncology/Hematology*, vol. 42, no. 3, pp. 317–325, 2002.

[12] N. Shah and D. S. Dizon, "New-generation platinum agents for solid tumors," *Future Oncology*, vol. 5, no. 1, pp. 33–42, 2009.

[13] D. Mukherjea, S. Jajoo, T. Kaur, K. E. Sheehan, V. Ramkumar, and L. P. Rybak, "Transtympanic administration of short interfering (si)rna for the nox3 isoform of NADPH oxidase protects against cisplatin-induced hearing loss in the rat," *Antioxidants and Redox Signaling*, vol. 13, no. 5, pp. 589–598, 2010.

[14] R. Çetin, E. Devrim, B. Kiliçoğlu, A. Avci, Ö. Çandir, and I. Durak, "Cisplatin impairs antioxidant system and causes oxidation in rat kidney tissues: possible protective roles of natural antioxidant foods," *Journal of Applied Toxicology*, vol. 26, no. 1, pp. 42–46, 2006.

[15] M. K. A. Bauer, M. Vogt, M. Los, J. Siegel, S. Wesselborg, and K. Schulze-Osthoff, "Role of reactive oxygen intermediates in activation-induced CD95 (APO-1/Fas) ligand expression," *The Journal of Biological Chemistry*, vol. 273, no. 14, pp. 8048–8055, 1998.

[16] M. Kruidering, B. Van De Water, E. De Heer, G. J. Mulder, and J. F. Nagelkerke, "Cisplatin-induced nephrotoxicity in porcine proximal tubular cells: mitochondrial dysfunction by inhibition of complexes I to IV of the respiratory chain," *Journal of*

Pharmacology and Experimental Therapeutics, vol. 280, no. 2, pp. 638–649, 1997.

[17] G. Nowak, "Protein kinase C-α and ERK1/2 mediate mitochondrial dysfunction, decreases in active Na^+ transport, and cisplatin-induced apoptosis in renal cells," *The Journal of Biological Chemistry*, vol. 277, no. 45, pp. 43377–43388, 2002.

[18] M. R. Bigdeli, S. Hajizadeh, M. Froozandeh et al., "Normobaric hyperoxia induces ischemic tolerance and upregulation of glutamate transporters in the rat brain and serum TNF-α level," *Experimental Neurology*, vol. 212, no. 2, pp. 298–306, 2008.

[19] M. R. Bigdeli, S. Hajizadeh, M. Froozandeh, B. Rasulian, A. Heidarianpour, and A. Khoshbaten, "Prolonged and intermittent normobaric hyperoxia induce different degrees of ischemic tolerance in rat brain tissue," *Brain Research*, vol. 1152, no. 1, pp. 228–233, 2007.

[20] H. Dong, L. Xiong, Z. Zhu, S. Chen, L. Hou, and T. Sakabe, "Preconditioning with hyperbaric oxygen and hyperoxia induces tolerance against spinal cord ischemia in rabbits," *Anesthesiology*, vol. 96, no. 4, pp. 907–912, 2002.

[21] H. Nie, L. Xiong, N. Lao, S. Chen, N. Xu, and Z. Zhu, "Hyperbaric oxygen preconditioning induces tolerance against spinal cord ischemia by upregulation of antioxidant enzymes in rabbits," *Journal of Cerebral Blood Flow and Metabolism*, vol. 26, no. 5, pp. 666–674, 2006.

[22] S.-Y. Yu, J.-H. Chiu, S.-D. Yang et al., "Preconditioned hyperbaric oxygenation protects the liver against ischemia-reperfusion injury in rats," *Journal of Surgical Research*, vol. 128, no. 1, pp. 28–36, 2005.

[23] Y. Liu, X.-J. Sun, J. Liu, Z.-M. Kang, and X.-M. Deng, "Heme oxygenase-1 could mediate the protective effects of hyperbaric oxygen preconditioning against hepatic ischemia-reperfusion injury in rats," *Clinical and Experimental Pharmacology and Physiology*, vol. 38, no. 10, pp. 675–682, 2011.

[24] M. Foadoddini, M. Esmailidehaj, H. Mehrani et al., "Pretreatment with hyperoxia reduces in vivo infarct size and cell death by apoptosis with an early and delayed phase of protection," *European Journal of Cardio-thoracic Surgery*, vol. 39, no. 2, pp. 233–240, 2011.

[25] B. Rasoulian, H. Mohammadhosseniakbari, M. Kadkhodaee et al., "Preconditioning with oxygen attenuates rat renal ischemia-reperfusion injury," *Journal of Surgical Research*, vol. 146, no. 2, pp. 282–288, 2008.

[26] H. Wahhabaghai, B. Rasoulian, M. Esmaili et al., "Hyperoxia-induced protection against rat's renal ischemic damage: relation to oxygen exposure time," *Renal Failure*, vol. 31, no. 6, pp. 514–521, 2009.

[27] U. Saini, R. J. Gumina, B. Wolfe, M. L. Kuppusamy, P. Kuppusamy, and K. D. Boudoulas, "Preconditioning mesenchymal stem cells with caspase inhibition and hyperoxia prior to hypoxia exposure increases cell proliferation," *Journal of Cellular Biochemistry*, vol. 114, no. 11, pp. 2612–2623, 2013.

[28] B. Einollahi, F. Poor-Reza-Gholi, S. Rezaeean et al., "Deceased-donor hyperoxia deteriorates kidney graft function," *Transplant International*, vol. 24, no. 2, pp. e16–e18, 2011.

[29] K. Montazeri, M. Vakily, A. Honarmand et al., "Short-time intermittent preexposure of living human donors to hyperoxia improves renal function in early posttransplant period: a double-blind randomized clinical trial," *Journal of Transplantation*, vol. 2011, Article ID 204843, 8 pages, 2011.

[30] Z. Rostami, B. Einollahi, and M. H. Ghadiani, "Does living donor hyperoxia have an impact on kidney graft function after transplantation," *Nephro-Urology Monthly*, vol. 5, no. 3, pp. 835–839, 2013.

[31] P. Tähepôld, G. Valen, J. Starkopf, C. Kairane, M. Zilmer, and J. Vaage, "Pretreating rats with hyperoxia attenuates ischemia-reperfusion injury of the heart," *Life Sciences*, vol. 68, no. 14, pp. 1629–1640, 2001.

[32] M. R. Bigdeli, B. Rasoulian, and A. A. Meratan, "In vivo normobaric hyperoxia preconditioning induces different degrees of antioxidant enzymes activities in rat brain tissue," *European Journal of Pharmacology*, vol. 611, no. 1–3, pp. 22–29, 2009.

[33] B. Baharvand, M. E. Dehaj, M. Foadaddini et al., "Delayed cardioprotective effects of hyperoxia preconditioning prolonged by intermittent exposure," *Journal of Surgical Research*, vol. 160, no. 1, pp. 53–59, 2010.

[34] P. Tinits, "Oxygen therapy and oxygen toxicity," *Annals of Emergency Medicine*, vol. 12, no. 5, pp. 321–328, 1983.

[35] N. Pabla and Z. Dong, "Cisplatin nephrotoxicity: mechanisms and renoprotective strategies," *Kidney International*, vol. 73, no. 9, pp. 994–1007, 2008.

[36] I. Arany and R. L. Safirstein, "Cisplatin nephrotoxicity," *Seminars in Nephrology*, vol. 23, no. 5, pp. 460–464, 2003.

[37] G. Gabb and E. D. Robin, "Hyperbaric oxygen: a therapy in search of diseases," *Chest*, vol. 92, no. 6, pp. 1074–1082, 1987.

[38] P. M. Tibbles and J. S. Edelsberg, "Hyperbaric-oxygen therapy," *The New England Journal of Medicine*, vol. 334, no. 25, pp. 1642–1648, 1996.

[39] M. H. Bennett, J. Feldmeier, N. Hampson, R. Smee, and C. Milross, "Hyperbaric oxygen therapy for late radiation tissue injury," *Cochrane Database of Systematic Reviews*, vol. 5, Article ID CD005005, 2012.

[40] J. J. Feldmeier, "Hyperbaric oxygen for delayed radiation injuries," *Undersea and Hyperbaric Medicine*, vol. 31, no. 1, pp. 133–145, 2004.

[41] D. Mathieu, *Handbook on Hyperbaric Medicine*, Springer, Berlin, Germany, 2006.

[42] E. V. Granowitz, N. Tonomura, R. M. Benson et al., "Hyperbaric oxygen inhibits benign and malignant human mammary epithelial cell proliferation," *Anticancer Research*, vol. 25, no. 6, pp. 3833–3842, 2005.

[43] T. B. Sun, R. L. Chen, and Y. H. Hsu, "The effect of hyperbaric oxygen on human oral cancer cells," *Undersea and Hyperbaric Medicine*, vol. 31, no. 2, pp. 251–260, 2004.

[44] Y.-C. Chen, S.-Y. Chen, P.-S. Ho et al., "Apoptosis of T-leukemia and B-myeloma cancer cells induced by hyperbaric oxygen increased phosphorylation of p38 MAPK," *Leukemia Research*, vol. 31, no. 6, pp. 805–815, 2007.

[45] Y. Kawasoe, M. Yokouchi, Y. Ueno, H. Iwaya, H. Yoshida, and S. Komiya, "Hyperbaric oxygen as a chemotherapy adjuvant in the treatment of osteosarcoma," *Oncology Reports*, vol. 22, no. 5, pp. 1045–1050, 2009.

[46] A. Raa, C. Stansberg, V. M. Steen, R. Bjerkvig, R. K. Reed, and L. E. B. Stuhr, "Hyperoxia retards growth and induces apoptosis and loss of glands and blood vessels in DMBA-induced rat mammary tumors," *BMC Cancer*, vol. 7, article 23, 2007.

[47] L. E. B. Stuhr, A. Raa, A. M. Øyan et al., "Hyperoxia retards growth and induces apoptosis, changes in vascular density and gene expression in transplanted gliomas in nude rats," *Journal of Neuro-Oncology*, vol. 85, no. 2, pp. 191–202, 2007.

[48] I. Moen, A. M. Øyan, K.-H. Kalland et al., "Hyperoxic treatment induces mesenchymal-to-epithelial transition in a rat adenocarcinoma model," *PLoS ONE*, vol. 4, no. 7, Article ID e6381, 2009.

[49] C. A. Godman, R. Joshi, C. Giardina, G. Perdrizet, and L. E. Hightower, "Hyperbaric oxygen treatment induces antioxidant gene expression," *Annals of the New York Academy of Sciences*, vol. 1197, pp. 178–183, 2010.

Hindawi
Oxidative Medicine and Cellular Longevity
Volume 2017, Article ID 3481710, 13 pages
https://doi.org/10.1155/2017/3481710

Research Article

Triethylenetetramine Synergizes with Pharmacologic Ascorbic Acid in Hydrogen Peroxide Mediated Selective Toxicity to Breast Cancer Cell

Lianlian Wang,[1,2,3] Xiaofang Luo,[2,3] Cong Li,[2] Yubing Huang,[4] Ping Xu,[2,3] Laetitia H. Lloyd-Davies,[5] Thibaut Delplancke,[3] Chuan Peng,[6] Rufei Gao,[7] Hongbo Qi,[2,3] Chao Tong,[2,3] and Philip Baker[3,5]

[1]*Department of Reproduction Health and Infertility, The First Affiliated Hospital of Chongqing Medical University, Chongqing 400016, China*
[2]*Department of Obstetrics and Gynecology, The First Affiliated Hospital of Chongqing Medical University, Chongqing 400016, China*
[3]*Canada-China-New Zealand Joint Laboratory of Maternal and Fetal Medicine, Chongqing Medical University, Chongqing 400016, China*
[4]*Molecular Medicine and Cancer Research Center, Department of Biochemistry and Molecular Biology, Chongqing Medical University, Chongqing 400016, China*
[5]*College of Medicine, University of Leicester, Leicester LE1 7RH, UK*
[6]*Laboratory of Lipid & Glucose Metabolism, The First Affiliated Hospital of Chongqing Medical University, Chongqing 400016, China*
[7]*Laboratory of Reproductive Biology, School of Public Health and Management, Chongqing Medical University, Chongqing 400016, China*

Correspondence should be addressed to Chao Tong; chaotongcqmu@163.com

Received 12 October 2016; Accepted 5 January 2017; Published 8 February 2017

Academic Editor: Lynne Postovit

Breast cancer is characterized by overexpression of superoxide dismutase (SOD) and downregulation of catalase and more resistance to hydrogen peroxide (H_2O_2) than normal cells. Thus, relatively high H_2O_2 promotes breast cancer cell growth and proliferation. However, excessive intracellular H_2O_2 leads to death of breast cancer cells. In cancer cells, high level ascorbic acid (Asc) is able to be autoxidized and thus provides an electron to oxygen to generate H_2O_2. In the present study, we demonstrated that triethylenetetramine (TETA) enhances Asc autoxidation and thus elevates H_2O_2 production in MCF-7 cells. Furthermore, Asc/TETA combination significantly impaired cancer cell viability, while having much milder effects on normal cells, indicating Asc/TETA could be a promising therapy for breast cancer. Moreover, SOD1 and N-acetyl-L-cysteine failed to improve MCF-7 cells viability in the presence of Asc/TETA, while catalase significantly inhibited the cytotoxicity of Asc/TETA to breast cancer cells, strongly suggesting that the selective cytotoxicity of Asc/TETA to cancer cells is H_2O_2-dependent. In addition, Asc/TETA induces RAS/ERK downregulation in breast cancer cells. Animal studies confirmed that Asc/TETA effectively suppressed tumor growth in vivo. In conclusion, TETA synergizes pharmacologic Asc autoxidation and H_2O_2 overproduction in breast cancer cells, which suppresses RAS/ERK pathway and results in apoptosis.

1. Introduction

Hydrogen peroxide plays an integral role in cancer cell biology. Cancer cells produce more H_2O_2 than normal cells [1], firstly due to an overreaction of enzymes in the electron transport chain that produces excessive reactive oxygen species (ROS) [2] and secondly as a consequence of the overexpression of superoxide dismutase (SOD), which converts superoxide (O_2^-) to hydrogen peroxide (H_2O_2) [3].

Breast cancer is the leading cause of cancer-related deaths in females worldwide [4]. Like many malignancies it is characterized by overexpression of SOD along with

downregulation of catalase (CAT), which converts H_2O_2 to H_2O and O_2. Thus, breast cancer cells maintain a higher intracellular H_2O_2 than normal cells [5], suggesting breast cancer cells are able to accumulate and tolerate H_2O_2 within certain range. However, mild elevating of H_2O_2 in cancer cells has been shown to arrest the cell cycle and induce apoptosis and has proven beneficial [6, 7]; this indicates selective overload of H_2O_2 in cancer cells could be a therapeutic strategy for breast cancer. Indeed, hydrogen peroxide inducible agents have shown potential as anticancer drugs [8]. However, most chemotherapeutic agents for cancer are toxic to the host. Therefore, existing medicine or natural products that selectively promote H_2O_2 production in cancer cells, sparing normal cells, are promising candidates for achieving therapeutic activity and selectivity.

Ascorbic acid (Asc), also known as vitamin C, is a well-known natural antioxidant. It has been long assumed to be essential for free radical clearance [9]. Previous studies have reported that high concentrations of Asc are able to induce autoxidation and thus reveal anticancer effects [7], while lower concentrations of Asc failed to show similar effects [10].

In sequential one-electron oxidations, the high concentration of Asc donates 2 electrons to oxygen resulting in formation of dehydroascorbic acid (DHA) and H_2O_2. The sequential one-electron oxidation of Asc can occur via the dianion Asc^{2-}, which autoxidizes in the presence of dioxide to produce the Asc^{-}, dehydroascorbic acid, and H_2O_2 [11]. This process is shown in the following formulas:

$$\begin{aligned} \text{Ascorbate} + H_2O &\longrightarrow AscH^- + Asc^{\bullet-} \\ Asc^{2-} + O_2 &\longrightarrow Asc^{\bullet-} + O_2^{\bullet-} \\ 2Asc^{\bullet-} + H^+ &\longrightarrow AscH^- + DHA \\ 2O_2^{\bullet-} + 2H^+ &\longrightarrow H_2O_2 + O_2 \end{aligned} \quad (1)$$

Therefore, it is important to investigate whether a high concentration of Asc associated autoxidation is critical for its anticancer effects. Asc is very stable and barely autoxidizes alone. However, in the presence of oxidative metal activators, such as iron, copper, and manganese, Asc autoxidation can be dramatically promoted as evidenced by the accumulation of ascorbic acid ion ($Asc^{\bullet-}$) and ultimately result in elevated $O_2^{\bullet-}$ and H_2O_2 production [12]. In addition, $O_2^{\bullet-}$ can further be reduced to H_2O_2 by accepting electron from Asc [13].

The function of catalysts for Asc autoxidation in aqueous solution mainly relies on their component groups [7], especially the amino groups, which are considered prooxidative [14]. Triethylenetetramine (TETA) is a telomerase inhibitor that has been clinically used to treat cancer for decades [15]. Previous studies demonstrate that TETA could overcome cisplatin resistance in human ovarian cancer cell cultures, via inhibition of Cu/Zn superoxide dismutase, namely, SOD1 [16, 17]. TETA is an alkali compound containing two amino groups and has a tendency to undergo redox as well as acid-base reactions in aqueous solution. Moreover, it possesses 4 nitrogen atoms, which have 1s22s22p3 electronic arrangement. Each nitrogen atom has a lone pair of electrons, which is able to pair with a proton from Asc. Therefore, we hypothesized that TETA could enhance Asc autoxidation in breast cancer cells and thus elevate intracellular H_2O_2, which will further boost Asc derived selective cytotoxicity to breast cancer cells (Figure 1). In the present study, we investigated the effect TETA has on H_2O_2 production from Asc solution. We then used in vitro models to study its role in regulating breast cancer cell apoptosis, as well as underlying molecular mechanisms, by the use of an in vivo animal model.

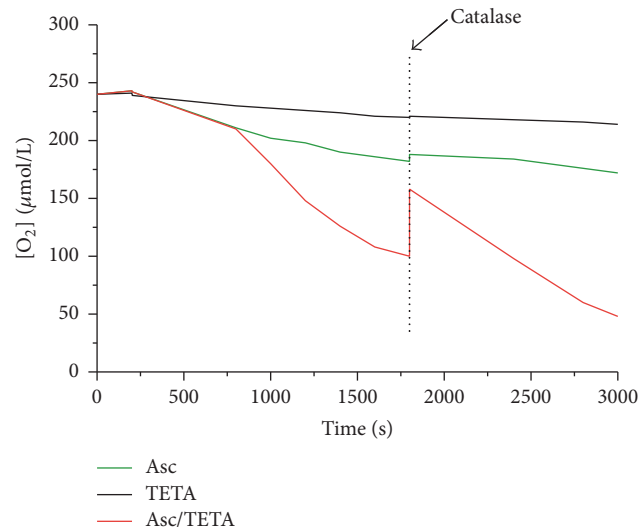

Figure 1: The effects of TETA on Asc oxidation. Oxygen consumption rate (OCR) of Asc in aqueous solution was determined by the use of an electrode oxygen monitor. 1 mM Asc alone, 30 μM TETA/1 mM Asc, or 30 μM TETA alone was added to DMEM with 10% FBS. 600 U/mL catalase was then given into each reaction to determine the return of O_2.

2. Materials and Methods

2.1. Cell Culture. All the cell lines were purchased from The Cell Bank of Chinese Academy of Sciences (Shanghai). Cells were cultured in Dulbecco's modified Eagle's medium (DMEM, HyClone, SH30022.01B, USA) supplemented with 10% Fetal Bovine Serum (FBS) (Gibco, USA) at 37°C in a humidified atmosphere with 5% CO_2.

2.2. Oxygen Consumption Assay. The rate of oxygen consumption (OCR, $d[O_2]/dt$) was determined as previously described [7]. Briefly, a Clark electrode oxygen monitor (YSI Inc.) was connected to an ESA Biostat multielectrode system in DMEM (10% FBS). The effect of TETA on the OCR of Asc was then measured and recorded. Accumulation of H_2O_2 was determined by adding catalase (Sigma, C9322-1G, Germany).

2.3. MTT Assay. MCF-7 cells were seeded in 96-well plates (3×10^3 cells/well), followed by 12 h or 24 h of treatments. The media containing Asc was removed before being subjected to MTT assay, because the oxidative products of Asc interfere with the MTT assay. 100 μL of serum-free DMEM medium

was applied into each well, and then 20 μL of 3-(4,5)-dimethylthiahiazo(-z-y1)-3,5-diphenytetrazoliumromide (MTT) (Sigma, Germany) was added to each well. Followed by 4 h of incubation at 37°C, all media were removed and then 150 μL of dimethyl sulfoxide (DMSO) (Sigma, Germany) was added to each well; after 10 min of shaking, the value of OD_{490} was recorded by a Varioskan Flash (Thermo Fisher, Finland).

2.4. ROS Measurement. The intracellular ROS was detected by using H_2DCF (Sigma, Germany) as previously reported [18]. Briefly, 10 μM of H_2DCF was added onto cells for 30 min, and then cells were harvested and analyzed by a fluorescence microscope (KEYENCE Corporation).

2.5. Western Blotting. MCF-7 cells were harvested by the use of ice-cold RIPA lysis buffer (Beyotime Biotechnology, Shanghai, China) and protein concentration was determined using the BCA protein quantification kit (Beyotime Biotechnology, Shanghai, China); western blotting was performed as previously described [19]. Primary antibodies of anti-Ac-H3, anti-SOD1, anti-CAT, anti-ERK, anti-p-ERK, anti-Cyt-C, and anti-caspase 9 were purchased from Bioworld Technology (Nanjing, China), anti-PARP, rabbit anti-caspase 3, and anti-Ac-H3 were purchased from Cell Signaling Technology, Danvers, USA, anti-RAS was purchased from BD, USA, and anti-GAPDH was purchased from Earthox, Millbrae, USA. The secondary antibodies were purchased from Biogot Biotechnology (Nanjing, China), and ECL SuperSignal West Femto Maximum Sensitivity Substrate was purchased from Thermo Fisher.

2.6. Transient Transfection. 1×10^5 cells were plated into each well of a 24-well plate 24 hours before transfection. shRNA (600 ng/well) or Plasmids (800 ng/well) were transfected with Lipofectamine 3000 (Invitrogen, USA) according to the manufacturer's protocol.

SOD1, NM_000454.3-582s1c1: CCGGGCTGTAGAAATGTATCCTGATCTCGAGATCAGGATACATTTCTACAGCTTTTTG.

CAT, NM_001752.2-1371s1c1: CCGGCGGAGATTCAACACTGCCAATCTCGAGATTGGCAGTGTTGAATCTCCGTTTTTG.

2.7. Xenograft Study. 6-week-old female nude mice (BALB/c-nu) were purchased from Vital River Laboratories (Beijing, China), the animal experiments were approved by the Medical Ethics Committee of Chongqing Medical University, and all of the procedures were in accordance with the National Institutes of Health guide for the care and use of Laboratory animals. In short, MCF-7 cells (5×10^6 in 200 μL) were subcutaneously delivered into the hind leg of mice, and a 0.72 mg 90 days' release 17β-estradiol pellet (Innovative Research of America, USA) was implanted subcutaneously into the front-back area to facilitate optimal tumor growth. The tumors were allowed to grow 14 days to reach the greatest dimension of about 3–5 mm, and treatments were initiated on the 14th day. Mice were randomly divided into 4 groups, including control (0.01 M PBS); Asc (3 g/kg body weight); TETA (30 mg/kg body weight); and Asc (3 g/kg body weight) plus TETA (30 mg/kg body weight), 10 mice in each group. Treatments were given via intraperitoneal injection daily for 25 consecutive days. Tumor size was measured every 2 days using a vernier caliper, while tumor volume was estimated based on the following formula: tumor volume (mm^3) = $L \times W^2/2$, where L is the greatest dimension of the tumor, and W means the dimension of the tumor in the perpendicular direction. Animals were sacrificed by CO_2 euthanasia when the tumor size reached 1,000 mm^3.

2.8. Statistical Analysis. Data are expressed as mean ± SD. A variety of statistical tests using GraphPad Prism 5 software were used on the basis of the design required for the specific question being asked. This meant using t-tests and 2-way ANOVA. A value of $p < 0.05$ was considered statistically significant.

3. Results

3.1. TETA Synergizes Ascorbic Acid Oxidation. To investigate the effect of TETA on promoting H_2O_2 generation from Asc, oxygen consumption of Asc in the presence and absence of TETA has been measured, respectively. As shown in Figure 1, 1 mM Asc in DMEM with 10% FBS resulted in an OCR of 55 nmol/L/s; and additional 30 μM of TETA increased OCR to 110 nmol/L/s, while 30 μM of TETA alone barely consumes O_2 and generates H_2O_2. However, in the presence of catalase (600 U/mL), H_2O_2 accumulation in Asc/TETA was dramatically suppressed compared to Asc or TETA alone. Taken together, this evidence strongly suggested that TETA enhanced Asc-dependent H_2O_2 generation.

3.2. Asc/TETA Combination Promotes Apoptosis in MCF-7 Cells. To further examine the cytotoxicity of Asc/TETA derived H_2O_2 to breast cancer cells, MCF-7 cells were treated with Asc (1 mM) along with different doses of TETA (10 μM, 30 μM, and 50 μM) for 12 hours. MTT assay results demonstrated that Asc alone resulted in a 40% reduction in MCF-7 proliferation, while TETA alone did not show any effect on cell viability. Intriguingly, the combinations of Asc and TETA significantly decreased cell viability compared to Asc alone (Figure 2(a)). Moreover, a prolonged incubation of Asc/TETA for 24 hours led to further reduction in cell viability, indicating that the anticancer effect of Asc/TETA combination is in a time-dose manner (Figure 2(b)). Further western blotting unveiled that Asc/TETA suppresses MCF-7 cell viability by elevating apoptotic signaling of caspase 9 and caspase 3 (Figure 2(c)). Morphology and cell cloning experiments confirmed that TETA synergizes Asc mediated cytotoxicity on MCF-7 cells (Figures 2(d) and 2(e)). Taken together, these results strongly suggest that TETA synergizes the anti-breast cancer effect of Asc in vitro.

3.3. Asc and TETA Synergize to Enhance Cytotoxicity In Vitro. To further validate whether the synergistic effects of Asc and TETA on cell death are specific for cancer cells, in addition to

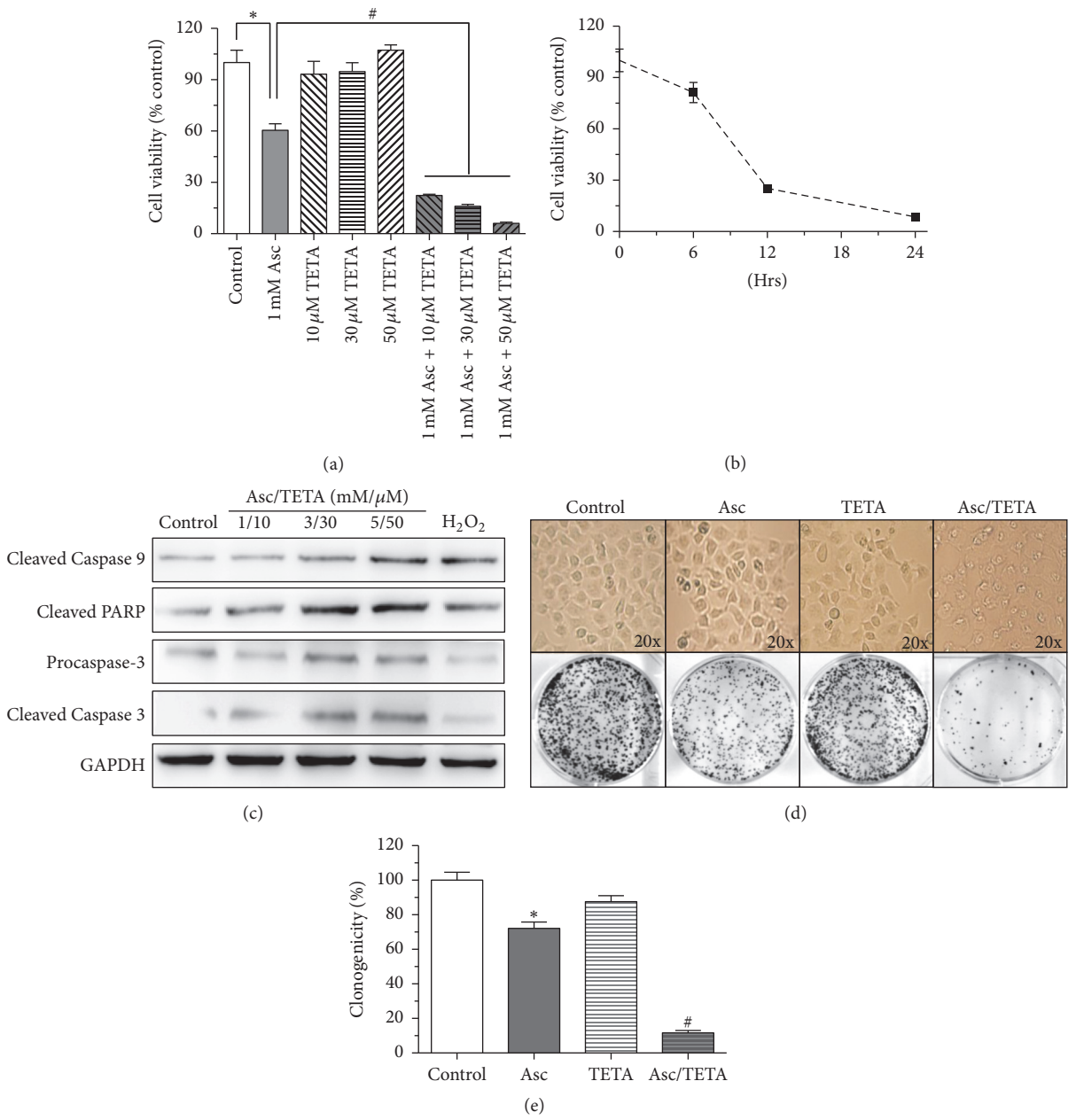

Figure 2: Asc/TETA combination induces apoptosis in MCF-7 cells. MCF-7 cells were treated with 1 mM Asc along with 10 μM, 30 μM, or 50 μM of TETA for 12 hours. (a) MTT assay was performed to assess MCF-7 viability, $^{*}p < 0.005$, $^{\#}p < 0.0001$, $n = 6$; (b) viability of MCF-7 cells was measured by MTT assay after 6, 12, and 24 hours of 1 mM Asc/10 μM TETA treatment, $n = 6$. (c) Effects of different dosage of Asc/TETA (1 : 100) on proapoptotic signaling were examined by western blotting; (d) MCF-7 cells cloning formation experiments were performed after 12 hours of 1 mM Asc/10 μM TETA treatment. (e) Statistic analysis of 3 independent experiments, $^{*}p < 0.05$ versus control, $^{\#}p < 0.01$ versus Asc, $n = 3$.

various cancer cell lines such as MCF-7, MDA-MB-157, MDA-MB-231, U87, HCC-9204, and H1299, multiple normal cell lines including Hs578Bst, HUVEC, and V79 were incubated with different concentrations of TETA (5 μM, 10 μM, 30 μM, and 50 μM) and corresponding doses of Asc (0.5 mM, 1 mM, 3 mM, and 5 mM) in accordance with the 1 : 100 TETA/Asc ratio. MTT assay results demonstrated that Asc and TETA have synergistic cytotoxicity on cancer cells but much milder effects on the viability of normal cells (Figure 3).

3.4. H_2O_2 Is Critical for Asc/TETA Induced Cytotoxicity to MCF-7 Cell. We then assessed the ROS level in MCF-7 cells. After 4 hours of incubation, Asc alone moderately elevated ROS level in MCF-7 cells, while TETA alone did not show any effect on ROS generation. However, Asc/TETA coincubation resulted in a dramatic increase of ROS compared to the other groups, while in the presence of N-acetyl-L-cysteine (NAC, Sigma, V900429, Germany), which degrade ROS except H_2O_2, Asc/TETA showed much less fluorescence staining

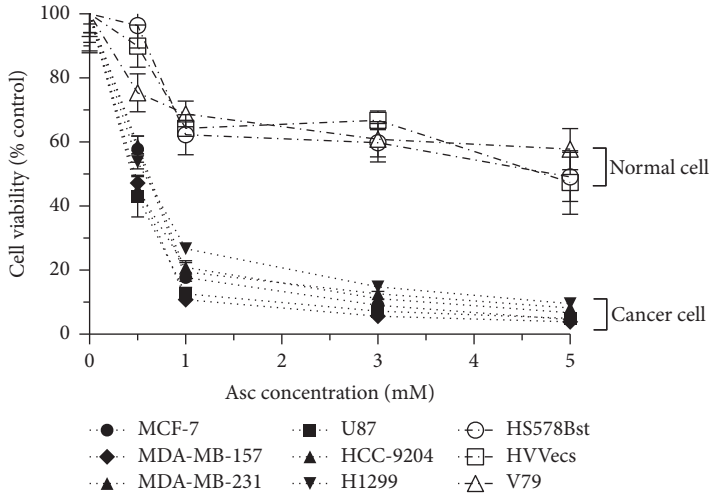

Figure 3: Selective cytotoxicity of Asc/TETA on various cell lines. MCF-7, MDA-MB-157, MDA-MB-231, U87, HCC-9204, H1299, Hs578Bst, HUVEC, or V79 cells were incubated with 1 mM, 3 mM, or 5 mM of Asc, respectively, along with 10 μM, 30 μM, or 50 μM of TETA to maintain 1 : 100 TETA-to-Asc ratio. MTT assay was performed to assess the cytotoxicity of Asc/TETA on different cell lines after 12 hours of incubation; experiment was repeated three times.

(Figure 4(a)). Taken together, these data suggested TETA potentiated not only H_2O_2 but also other types of ROS production from Asc in MCF-7 cells,

Nevertheless, ROS include hydrogen peroxide (H_2O_2), superoxide anions ($O_2^{\bullet-}$), and hydroxyl radical, to ascertain whether the cytotoxicity of Asc/TETA specifically results from H_2O_2; NAC was applied to MCF-7 cells along with Asc/TETA.

Western blotting showed that Asc/TETA combination treatment resulted in inhibition of RAS expression, which were not rescued by extra NAC treatment. Inversely, although Asc/TETA also lead to elevation of H3 acetylation in dose-dependent manner, such effect was totally reversed by 5 mM NAC (Figure 4(b)). Moreover, the effects of Asc/TETA on RAS expression and H3 acetylation demonstrated a time-dependent manner (Figure 4(c)). The data suggests that TETA/Asc suppresses RAS expression in MCF-7 cells principally through H_2O_2, while it upregulates H3 acetylation mainly through the other types of ROS. Most importantly, 5 mM NAC failed to eliminate the cytotoxicity caused by Asc/TETA. Taken together, these results indicate that H_2O_2 is the primary cytotoxic ROS induced by Asc/TETA in MCF-7 cells and possibly through the inhibition of RAS expression.

3.5. The Selective Cytotoxicity of Asc/TETA Derived H_2O_2 to MCF-7 Cells due to Compromised CAT Expression. We subsequently investigated the mechanism underlying the discrepancy of the cytotoxicity of Asc/TETA combination in cancer cells and normal cells. The effect of catalase on Asc/TETA induced cell death was examined by clone formation experiment; the data (Figure 5(a)) shows that Asc alone moderately reduced plating efficiency of MCF-7 cells, while neither TETA nor catalase shows similar effect. However, Asc/TETA combination significantly suppressed plating efficiency of MCF-7 cells, but the reduction was almost fully restored in the presence of catalase. We then determined the expression levels of CAT in MCF-7 cells and normal cells by immunoblotting. It was shown that CAT expression level is significantly compromised in MCF-7 cells compared to the normal cells (Figure 5(b)). To further determine the importance of CAT in resistance to Asc/TETA induced cell death, shCAT was transfected into the normal breast epithelial HS578Bst cells; it only dramatically repressed CAT expression in HS578Bst cells (Figure 5(c)) but also significantly impaired cell viability (Figure 5(d)). This strongly suggests that the selective toxicity to cancer cells could be attributed to CAT downregulation, and thus the cytotoxicity of combined TETA and Asc use is primarily mediated by H_2O_2.

3.6. Asc/TETA Induced Cytotoxicity to MCF-7 Cells Is Not Mediated by $O_2^{\bullet-}$. Although H_2O_2 has been found critical for TETA/Asc mediated cytotoxicity, the possibility of $O_2^{\bullet-}$ being involved in such anticancer effects has yet to be ruled out. To distinguish the roles of $O_2^{\bullet-}$ and H_2O_2 in TETA/Asc combination derived cytotoxicity, 100 U/mL SOD was applied onto MCF-7 cells with 1 mMAsc and 10 μM TETA. In contrast to CAT, SOD failed to rescue cell survival in the presence of Asc and TETA but exacerbated Asc and TETA combination induced cell death (Figure 6(a)). This indicates that $O_2^{\bullet-}$ does not contribute to TETA and Asc mediated cytotoxicity to cancer cells. Not surprisingly, SOD protein expression in MCF-7 cells was significantly higher than normal cells (Figure 6(b)). To further confirm this finding, SOD1 in MCF-7 cells was knocked down by shRNA (Figure 6(c)). In combined Asc/TETA treatment, shSOD1 did not result in enhanced viability of MCF-7 cell but led to more cell death (Figure 6(d)). This data suggests that the selective cytotoxicity of Asc/TETA to MCF-7 cells is not mediated by $O_2^{\bullet-}$.

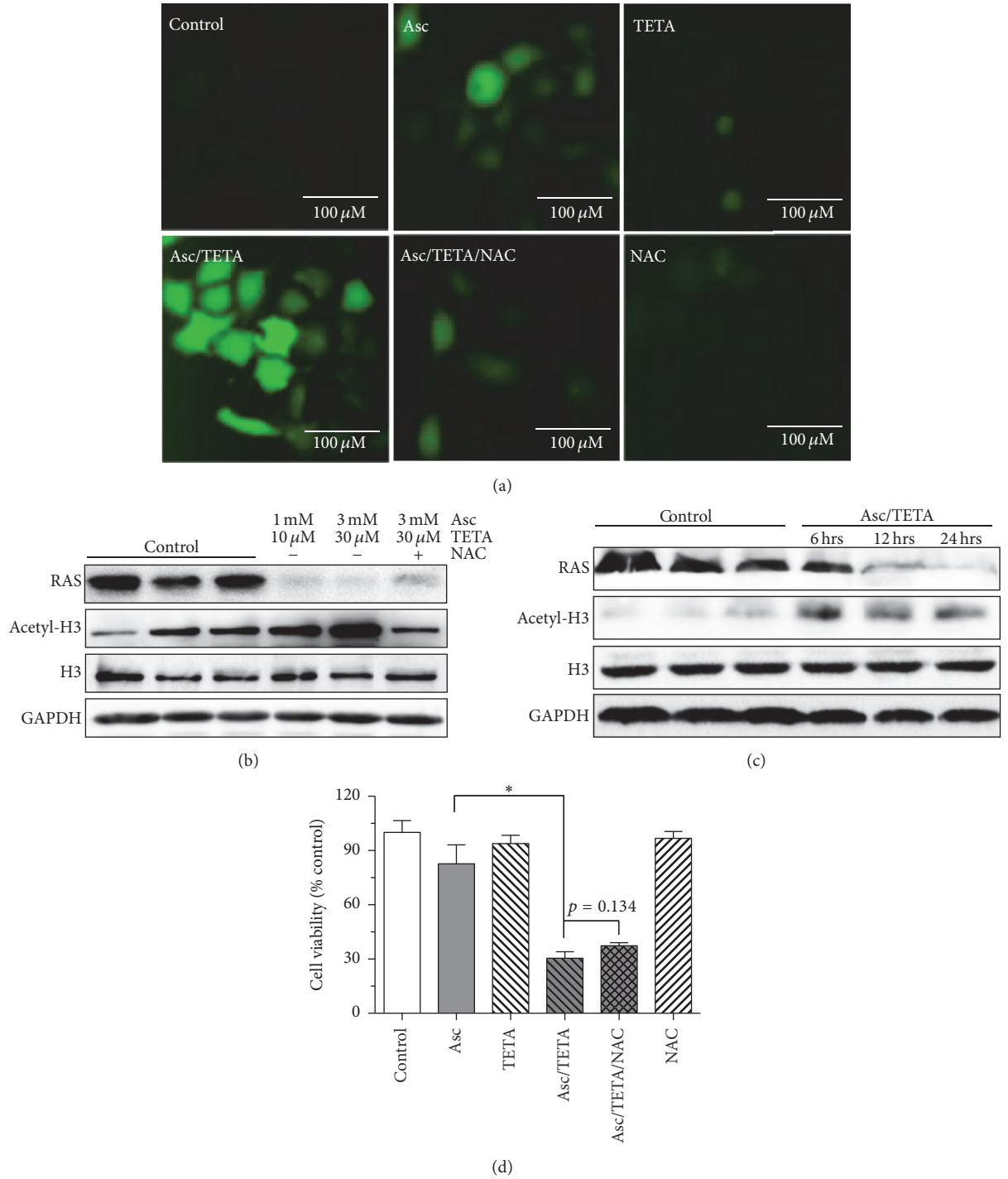

Figure 4: Asc/TETA induces H_2O_2-dependent RAS downregulation and apoptosis in MCF-7 cells. MCF-7 cells were treated with 1 mM Asc, 10 μM TETA, 1 mM Asc/10 μM TETA, 5 mM NAC, or 1 mM Asc/10 μM TETA and 5 mM NAC, respectively, for 4 hours. (a) ROS generation in MCF-7 cells was examined by H2DCF staining; (b) MCF-7 cells were treated with 1 mM Asc/10 μM TETA, 3 mM Asc/30 μM TETA, or 3 mM Asc/30 μM TETA with 5 mM NAC for 12 hours. RAS expression and H3 acetylation were assessed by western blotting; (c) MCF-7 cells were treated with 1 mM Asc/10 μM TETA for 6, 12, and 24 hours, respectively; RAS expression and H3 acetylation were assessed by western blotting; (d) MCF-7 cells were treated with 1 mM Asc, 10 μM TETA, 5 mM NAC, 1 mM Asc/10 μM TETA, or 1 mM Asc/10 μM TETA plus NAC for 12 hours; cell viability was measured with MTT assay, $^*p < 0.005$, $n = 4$. Experiment was repeated three times.

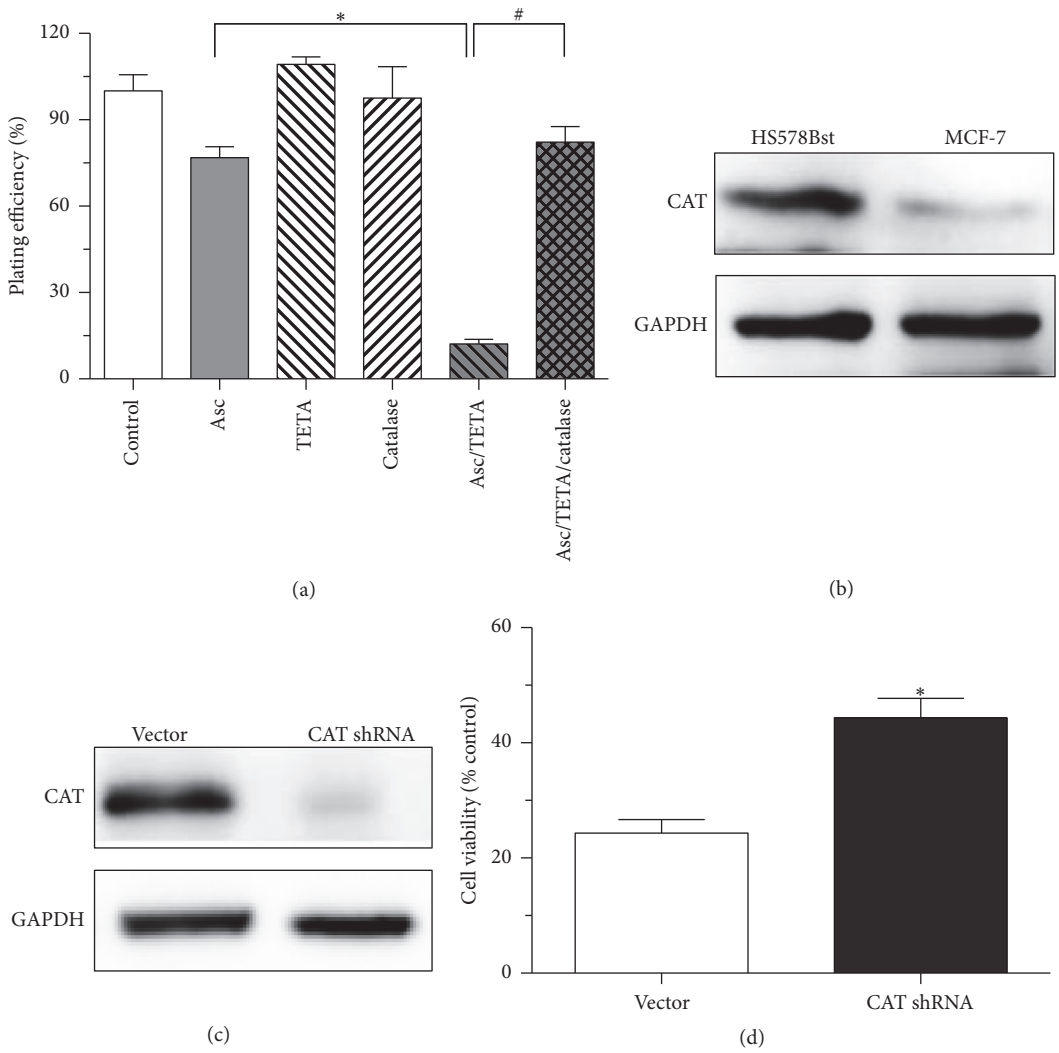

Figure 5: CAT expression levels in breast cancer cells and normal cells. (a) MCF-7 cells were treated with 1 mM Asc, 10 μM TETA, 300 U/mL catalase, 1 mM Asc/10 μM TETA, or 1 mM Asc/10 μM TETA plus catalase for 12 hours; cloning formation assay was performed, $^{*}p < 0.0001$, $^{\#}p < 0.0001$, $n = 4$; (b) CAT expression levels in HS578Bst and MCF-7 cells were determined by western blotting; (c) CAT expression in HS578Bst was suppressed by CAT shRNA; (d) HS578Bst cell viability after CAT shRNA treatment was measured by MTT assay, $p < 0.005$, $n = 4$.

3.7. The Signaling Associated with Asc/TETA Treatment in Cancer Cells. We then investigated which signaling pathways are involved in Asc/TETA induced cell death. As shown in Figure 7, western blots illustrated that Asc/TETA treatment suppressed ERK1/2 and SOD1 expression in MCF-7 cells. To further determine the type of cell death caused by Asc and TETA, Cytochrome C (Cyt-C), the key regulator of apoptosis, has been measured. Asc/TETA induced Cyt-C release was time dependent, which is consistent with previous MTT results. These data strongly suggest that Asc/TETA induced cancer cell apoptosis is probably mediated by RAS-ERK pathway.

3.8. TETA Enhances Asc-Induced Cytotoxicity In Vivo. In order to examine whether combined Asc/TETA has cytotoxicity to tumor cells in vivo, the combination was administrated into nude mice with transplanted tumors. After 25 days of treatment, there was no significant difference in viscera index between the 4 groups as has been observed (Figure 8(a)), indicating Asc/TETA has low toxicity for these organs. However, there was difference in the day 25 tumor volume between the groups, 971.1 ± 24.20 mm^3 in control group, 898.0 ± 16.03 mm^3 in TETA group, and 746.5 ± 14.44 mm^3 in Asc group, but it significantly reduced to 278.0 ± 16.42 mm^3 in Asc/TETA group. In congruence, the tumor weights were 1.276 ± 0.097 g, 0.969 ± 0.095 g, 1.226 ± 0.087 g in control, Asc, and TETA group, respectively, but dramatically declined to 0.478 ± 0.094 g by Asc/TETA treatment (Figures 8(b), 8(c), and 8(d)). These results indicate that TETA and Asc have synergistic antitumor effects in vivo, without notable toxicity to internal organs.

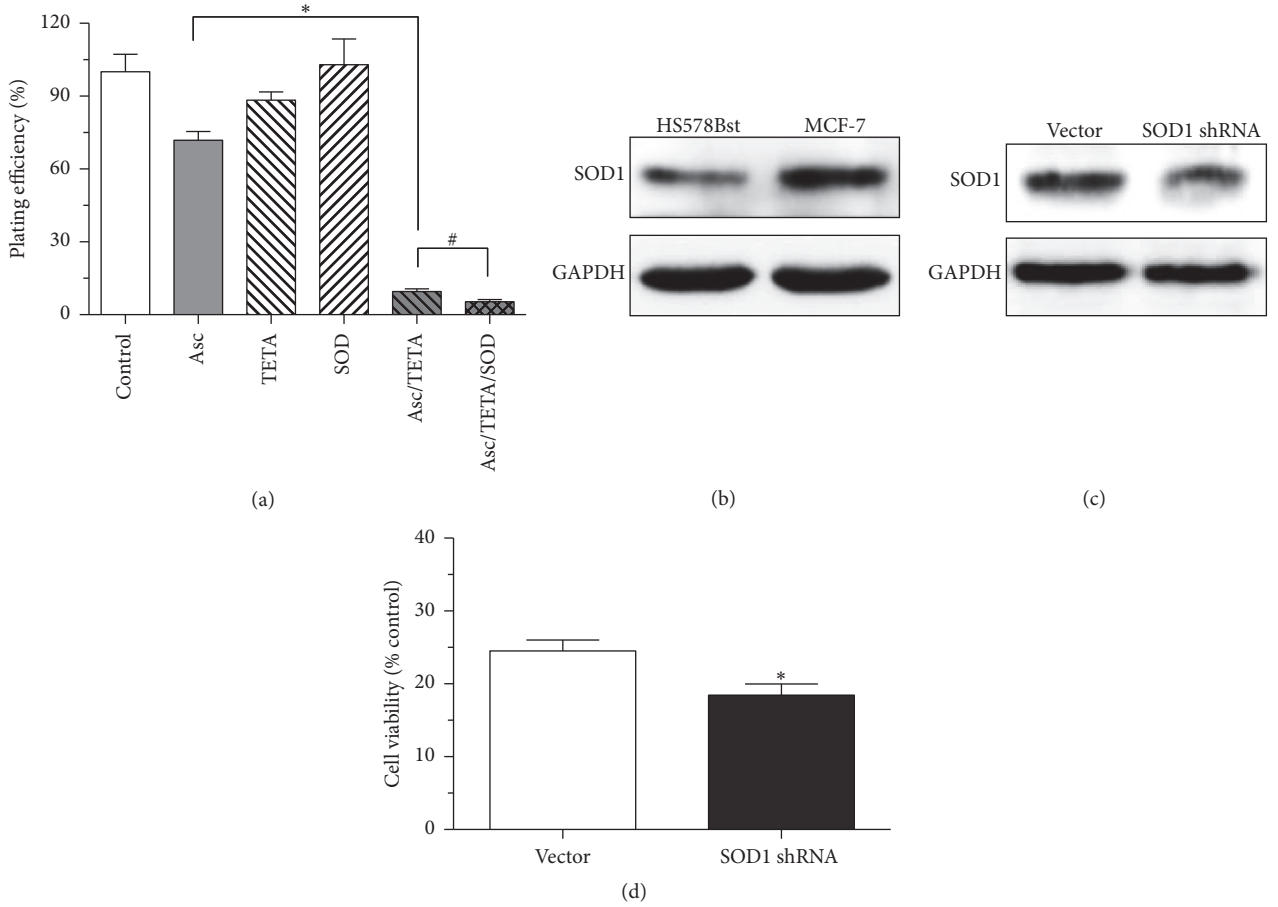

FIGURE 6: The effects of SOD on Asc/TETA induces apoptosis. (a) 1 mM Asc, 10 μM TETA, 100 U/mL SOD1, 1 mM Asc/10 μM TETA, or 1 mM Asc/10 μM TETA plus SOD was applied onto MCF-7 cells for 12 hours. Cloning formation assay was performed to determine the plating efficiency. $^{*}p < 0.0001$, $^{\#}p < 0.05$, $n = 4$; (b) SOD1 expression levels in HS578Bst and MCF-7 cells were assessed by western blotting; (c) downregulation of SOD1 expression in MCF-7 cells by SOD1 shRNA was determined by western blotting; (d) MCF-7 cell viability after SOD1 shRNA treatment was measured by MTT assay, $^{*}p < 0.05$, $n = 4$.

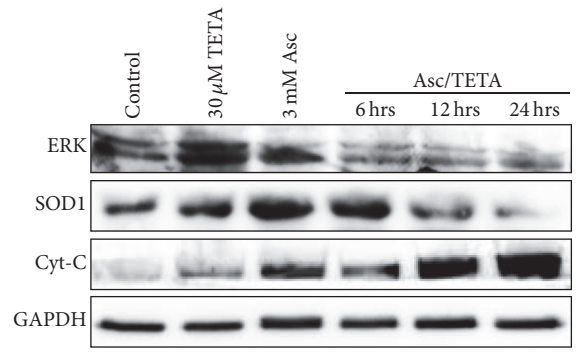

FIGURE 7: The effects of Asc/TETA on ERK and SOD expression. MCF-7 cells were incubated with 3 mM Asc, 30 μM TETA, or 3 mM Asc/30 μM TETA for various duration; ERK, RAS, and Cyt-C protein levels were assessed by western blotting.

4. Discussion

Given that one of the typical characteristics of breast cancer is SOD overexpression, along with compromised CAT expression, the intracellular oxidative stress is higher in the cancer cells compared to normal cells [20]. Wlassoff et al. have shown that hydroxyl radicals derived from H_2O_2 promote breast cancer cell apoptosis in the presence of a tamoxifen–ferrocene conjugate [21]. Other groups have demonstrated that the excessive H_2O_2 production and accumulation in cancer cells could trigger cancer cell cycle arrest and apoptosis [6], suggesting the enhancement of intracellular H_2O_2 concentration could be a promising therapy for breast cancer. Therefore, a natural compound which is able to selectively induce H_2O_2 generation in cancer cells could be an ideal therapy for breast cancer.

Asc is a potent natural antioxidant that has long been assumed to be beneficial for cancer treatment. Intriguingly, it has been reported that, in cancer cells, Asc is oxidized by donating an electron, which had an oxidation reaction with the metal ion (copper, iron, and manganese), producing the anticancer H_2O_2 [12]. Another group has also shown that 4 h of 1 mM Asc treatment on C6 cells triggers intracellular Cu release [22], which can further promote Asc oxidation, indicating H_2O_2 generated by Asc autoxidation might be beneficial for cancer treatment. However, the effectiveness of Asc derived H_2O_2 on treating cancer remains debatable.

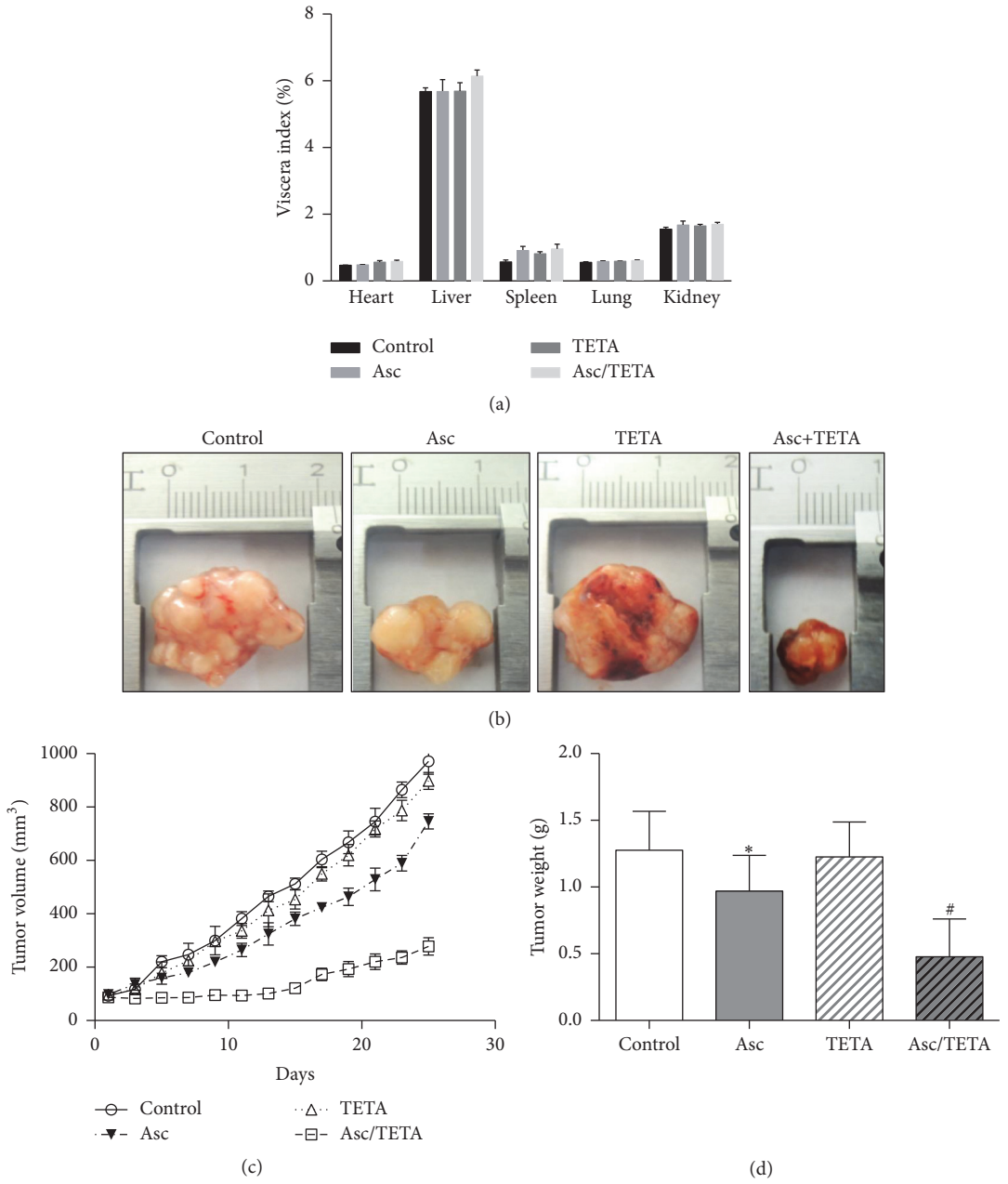

Figure 8: Asc/TETA suppresses tumorigenesis in mouse breast cancer model. 5×10^6 MCF-7 cells were subcutaneously delivered into the hind leg of female nude mice. 14 days later, mice were randomly divided into 4 groups and given vehicle (0.01 M PBS); Asc (3 g/kg body weight); TETA (30 mg/kg body weight); Asc (3 g/kg body weight) plus TETA (30 mg/kg body weight), respectively, via intraperitoneal injection once a day. On the 25th day of treatment, (a) viscera index; (b) representative pictures of tumor from different groups; (c) tumor volume, $p < 0.0001$, $n = 6$; (d) tumor weight $^{*}p < 0.05$, $^{\#}p < 0.005$, $n = 6$.

Firstly, there is no strong association between plasma Asc concentration and breast cancer risk [23]; secondly, H_2O_2 has been found to enhance growth of breast cancer [5]. Both of them indicate that not only is a high dose of Asc needed to induce a dramatic elevation of intracellular H_2O_2 flux, but also a reagent that could potentiate or promote H_2O_2 production from Asc autoxidation might be critical for Asc clinically utilized in breast cancer therapy.

Considering human circulating Asc concentration is relative high, ranging from 20 to 80 μmol/L [24, 25], and quite stable in various countries [26], it is reasonable to pursue the effects of pharmacologic Asc on breast cancer. Indeed, cumulative evidence indicates that high doses of Asc could be beneficial for breast cancer treatment. Yun et al. recently reported that high dose Asc selectively kills KRAS and BRAF mutant colorectal cancer cells [27]. Similarly, another group

has also shown that pharmacologic concentrations of Asc inhibit proliferation and induce apoptosis in various colorectal cancer lines, probably by promoting intracellular oxidative stress [28]. Asc has also exhibited anticancer properties in pancreatic cancer cells [29], providing further evidence to suggest that high dose of Asc induces H_2O_2 flux in the presence of catalytic metal ions, resulting in oxidative stress in cancer cells which ultimately leads to apoptosis. These results suggest that pharmacologic Asc may be needed to cause breast cancer cell death. Our data confirmed that a high dose of Asc is essential for inducing MCF-7 cell apoptosis in vitro and inhibiting tumorigenesis in vivo. Although many studies have shown Asc can be used as an adjuvant for breast cancer chemotherapy [30], therapy that primarily depends on Asc-induced oxidative stress in cancer cells has yet to be investigated.

TETA is a charge-deficient isosteric analogue of spermidine and a Cu (II) chelating compound. It is usually used for treating Wilson's disease. Recently, its potential in treating cancer has been unveiled; growing evidence demonstrates that TETA plays a role against cancer by inhibiting telomerase [31], in antiangiogenesis [32], and in suppressing cancer cell proliferation by modulating metabolism [33], as well as in induction of cell withered death [34]. However, none of these studies focused on the effect of TETA's chemical properties on cancer, specifically the two amino groups, and their role as a potential catalyst for Asc autoxidation. Our work is the first to report that, in aqueous solution, TETA enhances H_2O_2 production by increasing Asc oxidation. Thereafter, we examined whether Asc/TETA combination could sufficiently lead to breast cancer cell death. In vitro and in vivo experiments consistently demonstrated that high dose Asc alone only resulted in mild toxicity to cancer cells, while TETA alone barely shows any effects. However, Asc/TETA combination significantly inhibited MCF-7 cell viability, strongly suggesting that Asc/TETA combination could be a promising neoadjuvant therapy for breast cancer. Nevertheless, the underlying molecular mechanism remains to be discovered.

To examine the cytotoxicity of Asc/TETA to breast cancer cells, fluorescent staining of ROS has been performed by the use of H2DCF. The results suggested that Asc/TETA significantly promoted ROS generation in cancer cells. We then determined which type of ROS is responsible for Asc/TETA induced cancer cell death. Adding NAC does not inhibit the cytotoxicity of Asc/TETA, strongly indicating that H_2O_2 is the major type of ROS derived from Asc/TETA and the cause of the selective cytotoxicity to breast cancer cell. However, many studies have shown that chronic high extracellular H_2O_2, over several months, promotes breast cancer cell proliferation and results in an aggressive phenotype [5, 35, 36]. Nevertheless, our results are consistent with Wlassoff et al., who reported that H_2O_2 is the hydroxyl radical which stimulates apoptosis in tamoxifen–ferrocene conjugate treated MCF-7 cells [21]. This indicates that the best therapeutic window of H_2O_2-dependent breast cancer treatment would be no longer than 6 months. However, in future studies it would be pertinent to perform a real time measurement of intracellular H_2O_2 flux under Asc/TETA treatment as previously reported [37].

It is quite interesting to understand whether TETA/Asc is selectively toxic to cancer cells. It has previously been demonstrated that Asc arrested growth of some cancer cell lines, like HeLa, SK-BR-3, SK-BR-3-Dox, L929, and Mel B16, but did not influence the growth of others: Hef, OVCAR, HEp2, HEp2VA3, and V79 [38]. Our results have shown that Asc/TETA is selectively toxic to cancer cell lines, including MCF-7, MDA-MB-157, MDA-MB-231, U87, HCC-9204, and H1299, but has much milder toxicity to normal cell lines such as Hs578Bst, HUVEC, and V79. Taken together, these data suggest Asc/TETA selectively kill certain type of cancer cells, including the ER-positive MCF-7 breast cancer cells.

To investigate the mechanism of the selective cytotoxicity of Asc/TETA in breast cancer cell, the expression of SOD1 and CAT was modulated using shRNA. Interestingly, downregulation of SOD1 failed to ameliorate the cytotoxicity of Asc/TETA to cancer cells; in contrast, overexpression of catalase effectively halted the cancer cell death induced by Asc/TETA. This confirmed that H_2O_2 rather than $O_2^{\bullet-}$ is the causative factor for Asc/TETA induced cell death. In addition, to further study whether the disturbed expression pattern of SOD1 and CAT in breast cancer cell is related with cell viability, SOD1 and CAT were knocked down by shRNA, respectively. SOD1 is overexpressed in the MCF-7 cell compared to normal cells, and shSOD1RNA treatment resulted in significant reduction in viability of the MCF-7 cell, indicating endogenous SOD1 is critical for maintaining breast cancer cell physiological function. Probably a product of the SOD1, H_2O_2, is an important signaling molecule for cancer cells. It is known that certain levels of H_2O_2 promote cancer cell proliferation and growth [5]. Furthermore, due to the low levels of expression of CAT in MCF-7 cells, we then downregulated CAT in HS578Bst cells, which demonstrated augmented cell viability. This suggests low level of CAT may be beneficial for cells, possibly by blocking the removal of H_2O_2 and thus maintaining a beneficial intracellular H_2O_2 concentration.

Numerous studies have shown that RAS-ERK pathway is involved in breast cancer cell growth and metastasis [39, 40]. Our data also suggested that Asc/TETA suppressed RAS and ERK expression in a time- and dose-dependent manner. It also suppressed subsequent cancer cell apoptosis, as evidenced by release of Cyt-C and caspases cleavage, while neither TETA nor Asc alone showed similar effects. In this work, we also observed Asc/TETA treatment result in global H3 acetylation in MCF-7 cells, which is not associated with H_2O_2 production and the viability of MCF-7 cells, but evidence has shown that elevating histone acetylation by SIRT1 inhibition induces breast cancer cell apoptosis [41], possibly through the upregulation of p21 [42]. Therefore, it will be interesting to further elucidate whether histone modification in the promoter region of specific genes is involved in Asc/TETA induced breast cancer cell apoptosis. Moreover, we found that Asc/TETA treatment also leads to a downregulation of SOD1 in MCF-7 cells, which is in accordance with the SOD1 shRNA experiment result, indicating the anti-breast cancer effects of Asc/TETA combination are partially mediated by the

inhibition of SOD1. Despite other studies also suggesting Asc may be involved in regulating breast cancer cell proliferation and migration through Akt and RhoA, respectively [43, 44], it is unclear whether Asc/TETA is effective through the same pathways and warrants further investigation.

Xenograft experiments validated our findings from the cell model. Administration of Asc/TETA dramatically reduced tumor size and weight, while visceral organs in the nude mice remained unaffected. This result confirmed that TETA synergizes Asc's anti-breast cancer effects in vivo. However, the dose used in this experiment is 3 grams per kg body weight, which is a far higher dose of Asc compared to what has been used previously. Further pharmacodynamics and pharmacokinetics studies for Asc/TETA are needed to explore the optimal administrative approach and dosage for breast cancer treatment. Likewise, a treatment of Asc in combination with another natural mixture, including lysine, proline, and green tea extract, significantly reduced tumor weight and inhibited metastasis to lung, spleen, liver, kidney, and heart in a breast cancer murine model [45]. Similarly, a natural antioxidant mixture containing Asc has also been shown to effectively repress radiation-induced carcinogenesis in animal experiments [46]. It is also reported that oral administration of high dose of Asc represents strong anticarcinogenic effect and prolongs survival time of a rat cancer model induced by benzo[a]pyrene [47].

In addition to the H_2O_2 mediated apoptotic effects of Asc/TETA on cancer cells, the synergistic antioxidant properties hold potential in preventing normal cell damage from high intercellular/intracellular ROS. Findings from other groups suggest these additional antitumorigenic effects may be mediated by inhibiting HIF1 [48]. However, evidence suggests that pharmacological Asc might have side effects. Asc induced procoagulant and prothrombotic activation of RBCs, and increased thrombosis has been reported in vivo. RBCs from cancer patients exhibited increased sensitivity to the prothrombotic effects of Asc, reflecting that intravenous gram-dose vitamin C therapy needs to be carefully revisited [49]. An Asc derivative, 6-deoxy-6-chloro-ascorbic acid, exhibited more potent effects in suppressing cancer cell proliferation and is more likely to be used clinically to treat breast cancer [38].

In conclusion, the present work demonstrates that TETA synergizes with pharmacologic Asc in breast cancer to enhance hydrogen peroxide production, thus inhibiting tumorigenic RAS/ERK signaling pathways and inducing apoptosis.

Competing Interests

No potential competing interests were disclosed.

Acknowledgments

This study was supported by grants from the Natural Science Foundation of China (81100399), Yuzhong District Natural Science Foundation (20150117), Chongqing Medical University (CYYQ201507), and Chongqing Education Committee (KJ1500223).

References

[1] S. Toyokuni, K. Okamoto, J. Yodoi, and H. Hiai, "Persistent oxidative stress in cancer," *FEBS Letters*, vol. 358, no. 1, pp. 1–3, 1995.

[2] S. L. Payne, B. Fogelgren, A. R. Hess et al., "Lysyl oxidase regulates breast cancer cell migration and adhesion through a hydrogen peroxide-mediated mechanism," *Cancer Research*, vol. 65, no. 24, pp. 11429–11436, 2005.

[3] C. J. Weydert, T. A. Waugh, J. M. Ritchie et al., "Overexpression of manganese or copper-zinc superoxide dismutase inhibits breast cancer growth," *Free Radical Biology and Medicine*, vol. 41, no. 2, pp. 226–237, 2006.

[4] J. Ferlay, H.-R. Shin, F. Bray, D. Forman, C. Mathers, and D. M. Parkin, "Estimates of worldwide burden of cancer in 2008: GLOBOCAN 2008," *International Journal of Cancer*, vol. 127, no. 12, pp. 2893–2917, 2010.

[5] S. Sen, B. Kawahara, and G. Chaudhuri, "Maintenance of higher H2O2 levels, and its mechanism of action to induce growth in breast cancer cells: important roles of bioactive catalase and PP2A," *Free Radical Biology and Medicine*, vol. 53, no. 8, pp. 1541–1551, 2012.

[6] P.-J. Chua, G. W.-C. Yip, and B.-H. Bay, "Cell cycle arrest induced by hydrogen peroxide is associated with modulation of oxidative stress related genes in breast cancer cells," *Experimental Biology and Medicine*, vol. 234, no. 9, pp. 1086–1094, 2009.

[7] M. Rawal, S. R. Schroeder, B. A. Wagner et al., "Manganoporphyrins increase ascorbate-induced cytotoxicity by enhancing H_2O_2 generation," *Cancer Research*, vol. 73, no. 16, pp. 5232–5241, 2013.

[8] Y. Kuang, K. Balakrishnan, V. Gandhi, and X. Peng, "Hydrogen peroxide inducible DNA cross-linking agents: targeted anticancer prodrugs," *Journal of the American Chemical Society*, vol. 133, no. 48, pp. 19278–19281, 2011.

[9] G. R. Buettner, "The pecking order of free radicals and antioxidants: lipid peroxidation, α-tocopherol, and ascorbate," *Archives of Biochemistry and Biophysics*, vol. 300, no. 2, pp. 535–543, 1993.

[10] C. Jacobs, B. Hutton, T. Ng, R. Shorr, and M. Clemons, "Is there a role for oral or intravenous ascorbate (Vitamin C) in treating patients with cancer? A systematic review," *Oncologist*, vol. 20, no. 2, pp. 210–223, 2015.

[11] J. Du, J. J. Cullen, and G. R. Buettner, "Ascorbic acid: chemistry, biology and the treatment of cancer," *Biochimica et Biophysica Acta—Reviews on Cancer*, vol. 1826, no. 2, pp. 443–457, 2012.

[12] G. R. Buettner and B. A. Jurkiewicz, "Catalytic metals, ascorbate and free radicals: combinations to avoid," *Radiation Research*, vol. 145, no. 5, pp. 532–541, 1996.

[13] N. H. Williams and J. K. Yandell, "Reduction of oxidized cytochrome c by ascorbate ion," *Biochimica et Biophysica Acta (BBA)—Bioenergetics*, vol. 810, no. 2, pp. 274–277, 1985.

[14] A. Chakravarty, K. Bhowmik, A. Mukherjee, and G. De, "Cu(2)O nanoparticles anchored on amine-functionalized graphite nanosheet: a potential reusable catalyst," *Langmuir*, vol. 31, no. 18, pp. 5210–5219, 2015.

[15] J. Lu, "Triethylenetetramine pharmacology and its clinical applications," *Molecular Cancer Therapeutics*, vol. 9, no. 9, pp. 2458–2467, 2010.

[16] V. K. Yellepeddi, K. K. Vangara, A. Kumar, and S. Palakurthi, "Comparative evaluation of small-molecule chemosensitizers in reversal of cisplatin resistance in ovarian cancer cells," *Anticancer Research*, vol. 32, no. 9, pp. 3651–3658, 2012.

[17] D. P. G. Brown, H. Chin-Sinex, B. Nie, M. S. Mendonca, and M. Wang, "Targeting superoxide dismutase 1 to overcome cisplatin resistance in human ovarian cancer," *Cancer Chemotherapy and Pharmacology*, vol. 63, no. 4, pp. 723–730, 2009.

[18] Y. Cui, I. Parra, M. Zhang et al., "Elevated expression of mitogen-activated protein kinase phosphatase 3 in breast tumors: a mechanism of tamoxifen resistance," *Cancer Research*, vol. 66, no. 11, pp. 5950–5959, 2006.

[19] C. Tong, A. Morrison, S. Mattison et al., "Impaired SIRT1 nucleocytoplasmic shuttling in the senescent heart during ischemic stress," *FASEB Journal*, vol. 27, no. 11, pp. 4332–4342, 2013.

[20] P. T. Schumacker, "Reactive oxygen species in cancer cells: live by the sword, die by the sword," *Cancer Cell*, vol. 10, no. 3, pp. 175–176, 2006.

[21] W. A. Wlassoff, C. D. Albright, M. S. Sivashinski, A. Ivanova, J. G. Appelbaum, and R. I. Salganik, "Hydrogen peroxide overproduced in breast cancer cells can serve as an anticancer prodrug generating apoptosis-stimulating hydroxyl radicals under the effect of tamoxifen-ferrocene conjugate," *Journal of Pharmacy and Pharmacology*, vol. 59, no. 11, pp. 1549–1553, 2007.

[22] D. W. Domaille, L. Zeng, and C. J. Chang, "Visualizing ascorbate-triggered release of labile copper within living cells using a ratiometric fluorescent sensor," *Journal of the American Chemical Society*, vol. 132, no. 4, pp. 1194–1195, 2010.

[23] F. Hu, Z. Wu, G. Li et al., "The plasma level of retinol, vitamins A, C and α-tocopherol could reduce breast cancer risk? A meta-analysis and meta-regression," *Journal of Cancer Research and Clinical Oncology*, vol. 141, no. 4, pp. 601–614, 2015.

[24] L. Cahill, P. N. Corey, and A. El-Sohemy, "Vitamin C deficiency in a population of young canadian adults," *American Journal of Epidemiology*, vol. 170, no. 4, pp. 464–471, 2009.

[25] A. Jungert and M. Neuhäuser-Berthold, "The lower vitamin C plasma concentrations in elderly men compared with elderly women can partly be attributed to a volumetric dilution effect due to differences in fat-free mass," *British Journal of Nutrition*, vol. 113, no. 5, pp. 859–864, 2015.

[26] B. Olmedilla, F. Granado, S. Southon et al., "Serum concentrations of carotenoids and vitamins A, E, and C in control subjects from five European countries," *British Journal of Nutrition*, vol. 85, no. 2, pp. 227–238, 2001.

[27] J. Yun, E. Mullarky, C. Lu et al., "Vitamin C selectively kills KRAS and BRAF mutant colorectal cancer cells by targeting GAPDH," *Science*, vol. 350, no. 6266, pp. 1391–1396, 2015.

[28] A. S. Pires, C. R. Marques, J. C. Encarnação et al., "Ascorbic acid and colon cancer: an oxidative stimulus to cell death depending on cell profile," *European Journal of Cell Biology*, vol. 95, no. 6-7, pp. 208–218, 2016.

[29] J. A. Cieslak and J. J. Cullen, "Treatment of pancreatic cancer with pharmacological ascorbate," *Current Pharmaceutical Biotechnology*, vol. 16, no. 9, pp. 759–770, 2015.

[30] E. Guerriero, A. Sorice, F. Capone et al., "Vitamin C effect on mitoxantrone-induced cytotoxicity in human breast cancer cell lines," *PLoS ONE*, vol. 9, no. 12, Article ID e115287, 2014.

[31] G. Lixia, Y. Fei, J. Jiajia, and L. Jianhui, "Triethylene tetramine, a novel ligand of G-quadruplex, induces senescence of MCF-7 cells," *Biotechnology Letters*, vol. 30, no. 1, pp. 47–53, 2008.

[32] E. D. Harris, "A requirement for copper in angiogenesis," *Nutrition Reviews*, vol. 62, no. 2, pp. 60–64, 2004.

[33] M. T. Hyvönen, S. Ucal, M. Pasanen et al., "Triethylenetetramine modulates polyamine and energy metabolism and inhibits cancer cell proliferation," *Biochemical Journal*, vol. 473, no. 10, pp. 1433–1441, 2016.

[34] S. Kadowaki, D. Endoh, T. Okui, and M. Hayashi, "Trientine, a Copper-chelating agent, induced apoptosis in murine fibrosarcoma cells by activation of the p38 MAPK pathway," *Journal of Veterinary Medical Science*, vol. 71, no. 11, pp. 1541–1544, 2009.

[35] P. K. S. Mahalingaiah, L. Ponnusamy, and K. P. Singh, "Chronic oxidative stress causes estrogen-independent aggressive phenotype, and epigenetic inactivation of estrogen receptor alpha in MCF-7 breast cancer cells," *Breast Cancer Research and Treatment*, vol. 153, no. 1, pp. 41–56, 2015.

[36] P. K. Mahalingaiah and K. P. Singh, "Chronic oxidative stress increases growth and tumorigenic potential of MCF-7 breast cancer cells," *PLoS ONE*, vol. 9, no. 1, Article ID e87371, 2014.

[37] F. Liu, S. Ge, J. Yu, M. Yan, and X. Song, "Electrochemical device based on a Pt nanosphere-paper working electrode for in situ and real-time determination of the flux of H2O2 releasing from SK-BR-3 cancer cells," *Chemical Communications*, vol. 50, no. 71, pp. 10315–10318, 2014.

[38] M. Osmak, I. Kovaček, I. Ljubenkov, R. Spaventi, and M. Eckert-Maksić, "Ascorbic acid and 6-deoxy-6-chloro-ascorbic acid: potential anticancer drugs," *Neoplasma*, vol. 44, no. 2, pp. 101–107, 1997.

[39] J. Gao, X. Liu, F. Yang, T. Liu, Q. Yan, and X. Yang, "By inhibiting Ras/Raf/ERK and MMP-9, knockdown of EpCAM inhibits breast cancer cell growth and metastasis," *Oncotarget*, vol. 6, no. 29, pp. 27187–27198, 2015.

[40] N. R. Treff, D. Pouchnik, G. A. Dement, R. L. Britt, and R. Reeves, "High-mobility group A1a protein regulates Ras/ERK signaling in MCF-7 human breast cancer cells," *Oncogene*, vol. 23, no. 3, pp. 777–785, 2004.

[41] A. M. Kalle, A. Mallika, J. Badiger, Alinakhi, P. Talukdar, and Sachchidanand, "Inhibition of SIRT1 by a small molecule induces apoptosis in breast cancer cells," *Biochemical and Biophysical Research Communications*, vol. 401, no. 1, pp. 13–19, 2010.

[42] Y. Al Dhaheri, S. Attoub, K. Arafat et al., "Salinomycin induces apoptosis and senescence in breast cancer: upregulation of p21, downregulation of survivin and histone H3 and H4 hyperacetylation," *Biochimica et Biophysica Acta*, vol. 1830, no. 4, pp. 3121–3135, 2013.

[43] F. Ourique, M. R. Kviecinski, K. B. Felipe et al., "DNA damage and inhibition of akt pathway in MCF-7 cells and ehrlich tumor in mice treated with 1,4-naphthoquinones in combination with ascorbate," *Oxidative Medicine and Cellular Longevity*, vol. 2015, Article ID 495305, 10 pages, 2015.

[44] L. Ma, W.-Z. Zhu, T.-T. Liu et al., "H_2O_2 inhibits proliferation and mediates suppression of migration via DLC1/RhoA signaling in cancer cells," *Asian Pacific Journal of Cancer Prevention*, vol. 16, no. 4, pp. 1637–1642, 2015.

[45] M. W. Roomi, T. Kalinovsky, N. M. Roomi, J. Cha, M. Rath, and A. Niedzwiecki, "In vitro and in vivo effects of a nutrient mixture on breast cancer progression," *International Journal of Oncology*, vol. 44, no. 6, pp. 1933–1944, 2014.

[46] A. R. Kennedy, J. H. Ware, W. Carlton, and J. G. Davis, "Suppression of the later stages of radiation-induced carcinogenesis by antioxidant dietary formulations," *Radiation Research*, vol. 176, no. 1, pp. 62–70, 2011.

[47] K. Charalabopoulos, S. Karkabounas, P. Dimicco et al., "The role of ascorbic acid, selenium, and glutathione on benzo[a]pyrene-induced carcinogenesis in wistar rats," *Journal of BUON*, vol. 9, pp. 187–192, 2004.

[48] P. Gao, H. Zhang, R. Dinavahi et al., "HIF-dependent antitumorigenic effect of antioxidants in vivo," *Cancer Cell*, vol. 12, no. 3, pp. 230–238, 2007.

[49] K. Kim, O.-N. Bae, S.-H. Koh et al., "High-dose vitamin C injection to cancer patients may promote thrombosis through procoagulant activation of erythrocytes," *Toxicological Sciences*, vol. 147, no. 2, pp. 350–359, 2015.